2017

Potential new drug targets and therapeutic approaches for parasitic nematode infections

Melanie Abongwa
Iowa State University

Potential new drug targets and therapeutic approaches for parasitic nematode infections

by

Melanie Abongwa

A dissertation submitted to the graduate faculty

in partial fulfillment of the requirements for the degree of

DOCTOR OF PHILOSOPHY

Major: Toxicology

Program of Study Committee:
Richard J. Martin, Co-major Professor
Alan P. Robertson, Co-major Professor
Michael John Kimber
Vellareddy Anantharam
Douglas E. Jones

The student author and the program of study committee are solely responsible for the content of this dissertation. The Graduate College will ensure this dissertation is globally accessible and will not permit alterations after a degree is conferred.

Iowa State University

Ames, Iowa

2017

DEDICATION

This

dissertation research

is dedicated to

my loving and caring parents

James T. and Comfort A. Abongwa,

and my siblings

Delphine N. Terence A., and Willibrod A. Abongwa.

TABLE OF CONTENTS

Page

ACKNOWLEDGEMENTS viii

ABSTRACT xi

CHAPTER 1: GENERAL INTRODUCTION 1
1.1 Introduction 1
1.2 Thesis Organization 2

CHAPTER 2. LITERATURE REVIEW 5
2.1 Parasitic Nematodes 5
2.1.1 Soil-transmitted helminthiases 9
2.1.1.1 Ascariasis 9
2.1.2 Filariases 12
2.1.2.1 Onchocerciasis (River blindness) 12
2.1.2.2 Lymphatic filariasis (Elephantiasis) 18
2.2 Nematode Neuromuscular System 22
2.2.1 Nervous System 23
2.2.2 Muscular System 23
2.3 Nicotinic Acetylcholine Receptors (nAChRs) 24
2.3.1 *Caenorhabditis elegans* nAChRs 27
2.3.2 Parasitic nematode nAChRs 34
2.3.3 Vertebrate nAChRs 39
2.4 Medicinal plants 41
2.4.1 *Daniellia oliveri* 43
2.4.2 *Psorospermum febrifugum* 44
2.4.3 The drug development pipeline 44
2.5 Anthelmintics and anthelmintic resistance 47
2.5.1 Anthelmintics 47
2.5.1.1 Benzimidazoles (BZs) 48
2.5.1.2 Imidazothiazoles 49
2.5.1.3 Tetrahydropyrimidines 50
2.5.1.4 Macrocyclic lactones (MLs) 51
2.5.1.5 Amino-acetonitrile derivatives (AADs) 53
2.5.1.6 Spiroindoles 54
2.5.1.7 Cyclooctadepsipeptides 55
2.5.1.8 Tribendimidine 57
2.5.2 Anthelmintic resistance 59
2.6 *Xenopus laevis* oocytes heterologous expression system 62

CHAPTER 3. PHARMACOLOGICAL PROFILE OF *ASCARIS SUUM* ACR-16, A NEW HOMOMERIC NICOTINIC ACETYLCHOLINE RECEPTOR WIDELY DISTRIBUTED IN *ASCARIS* TISSUES 66
3.1 Summary 66
3.1.1 Background and Purpose 66
3.1.2 Experimental Approach 66
3.1.3 Key Results 67
3.1.4 Conclusions and Implications 67
3.2 Abbreviations 67
3.3 Table of Links 68
3.4 Introduction 68
3.5 Methods 70
3.5.1 Animals 70
3.5.2 Sequence analysis 70
3.5.3 *Asu*-ACR-16 receptor localization 71
3.5.4 cRNA preparation 72
3.5.5 Oocyte microinjection 73
3.5.6 Two-electrode voltage clamp electrophysiology (TEVC) in *Xenopus* Oocytes 73
3.5.7 Assessment of agonists and antagonists 74
3.5.8 Permeability of receptors to calcium 75
3.5.9 Data and statistical analysis 76
3.6 Materials 78
3.7 Results 78
3.7.1 Identification of *Asu*-ACR-16 sequence 78
3.7.2 *Asu*-ACR-16 sequence suggests pharmacological differences to host mammalian α7 nAChRs 79
3.7.3 Ubiquitous tissue and single-cell expression of ACR-16 in *Asu* 82
3.7.4 *ric-3* is required for functional expression of *Asu*-ACR-16 84
3.7.5 *Asu*-ACR-16 forms a nicotine-sensitive but levamisole-insensitive nAChR 86
3.7.6 *Asu*-ACR-16 desensitization 87
3.7.7 Nicotine as a potent agonist 89
3.7.8 Rank order antagonist potencies: *Asu*-ACR-16 is not sensitive to α-BTX 90
3.7.9 Non-competitive derquantel antagonism and mixed antagonism of dHβE 90
3.7.10 PAMS of human α7 nAChRs inhibit *Asu*-ACR-16 responses 92
3.7.11 Calcium permeability of *Asu*-ACR-16 94
3.8 Discussion 94
3.8.1 Comparison of pharmacology of *Asu*-ACR-16 with *Cel*-ACR-16 95
3.8.2 Comparison of pharmacology of *Asu*-ACR-16 with α7 nAChRs 95
3.8.3 Comparison of pharmacology of *Asu*-ACR-16 with levamisole receptors 95
3.8.4 Differences in α-BTX potency, allosteric modulation and Ca^{2+} permeability 97
3.8.5 Ubiquitous distribution of *Asu*-ACR-16 receptor and its function 98
3.8.6 Consideration of *Asu*-ACR-16 as a drug target 99

3.9 Acknowledgements 99
3.10 Author Contributions 100
3.11 Conflict of Interest 100
3.12 Declaration of Transparency and Scientific Rigour 100
3.13 Supporting Information 101

CHAPTER 4. FILARICIDAL ACTIVITIES OF *DANIELLIA OLIVERI* AND *PSOROSPERMUM FEBRIFUGUM* 105
4.1 Abstract 105
4.2 Author Summary 106
4.3 Introduction 107
4.4 Materials and Methods 111
4.4.1 Collection and identification of plants 111
4.4.2 Preparation of plants extracts 112
4.4.3 *Onchocerca ochengi* adult worm assay 113
4.4.4 *Onchocerca ochengi* microfilaria (mf) assay 116
4.4.5 *Brugia pahangi* adult worm assay 117
4.4.6 Bioassay-guided fractionation of plant extracts 118
4.4.7 Cytotoxicity on N27 cells using the MTS assay 120
4.4.8 Data analysis 121
4.4.9 Phytochemical screening 121
4.4.9.1 Test for saponins (Frothing test) 121
4.4.9.2 Test for flavonoids (Cyanidin test) 121
4.4.9.3 Test for steroids (Liebermann-Burchard test) 121
4.4.9.4 Test for tannins (Ferric chloride test) 122
4.4.9.5 Test for Alkaloids (Dragendorff's test) 122
4.4.9.6 Test for coumarins 122
4.4.9.7 Test for cardiac glycosides 122
4.5 Results 123
4.5.1 Activity of *D. oliveri* and *P. febrifugum* extracts on *O. ochengi* adult worms and mfs 123
4.5.2 Activity of extracts and chromatographic fractions of *D. oliveri* and *P. febrifugum* on adult *B. pahangi* 125
4.5.3 Cytotoxicity of active extracts 131
4.5.4 Phytochemical analysis of active extracts 133
4.6 Discussion 135
4.7 Acknowledgements 137
4.8 Author Contributions 138

CHAPTER 5. CURIOUSER AND CURIOUSER: THE MACROCYCLIC LACTONE, ABAMECTIN, IS ALSO A POTENT INHIBITOR OF PYRANTEL/ TRIBENDIMIDINE NICOTINIC ACETYLCHOLINE RECEPTORS OF GASTRO-INTESTINAL WORMS 139
5.1 Abstract 139
5.2 Introduction 140

5.3 Materials and Methods 143
5.3.1 Cloning of nAChR subunits from *O. dentatum* and ancillary factors from *Haemonchus contortus* 143
5.3.2 Expression of *Ode*-UNC-29:*Ode*-UNC-63:*Ode*-UNC-38 in *Xenopus laevis* oocytes 143
5.3.3 Two-microelectrode voltage-clamp (TEVC) electrophysiology 144
5.3.4 Drugs 144
5.3.5 Drug applications 145
5.3.6 Data analysis 145
5.4 Results 147
5.4.1 *Ode*-UNC-29:*Ode*-UNC-63:*Ode*-UNC-38 forms a pyrantel-sensitive nAChR 147
5.4.2 Effects of abamectin on *Ode*-UNC-29:*Ode*-UNC-63:*Ode*-UNC-38 147
5.4.3 Effects of derquantel and abamectin combination on *Ode*-UNC-29:*Ode*-UNC-63:*Ode*-UNC-38 152
5.5 Discussion 155
5.5.1 Abamectin as a non-competitive antagonist of *Ode*-UNC-29:*Ode*-UNC-63:*Ode*-UNC-38 155
5.5.2 Bi-phasic effects of abamectin on *Ode*-UNC-29:*Ode*-UNC-63:*Ode*-UNC-38 155
5.5.3 Derquantel and abamectin combination produces greater effects than either derquantel or abamectin used alone 156
5.6 Conclusion 157
5.7 Supporting Information 158
5.8 Acknowledgements 162
5.9 Funding 162
5.10 Author Contributions 162

CHAPTER 6. GENERAL DISCUSSION 163
Future Directions 164

REFERENCES 166

APPENDIX A. INVESTIGATION OF ACETYLCHOLINE RECEPTOR DIVERSITY IN A NEMATODE PARASITE LEADS TO CHARACTERIZATION OF TRIBENDIMIDINE- AND DERQUANTEL-SENSITIVE nAChRs 198

APPENDIX B. ANTHELMINTICS: THE BEST WAY TO PREDICT THE FUTURE IS TO CREATE IT 237

APPENDIX C. THE *ASCARIS SUUM* NICOTINIC RECEPTOR, ACR-16, AS A DRUG TARGET: FOUR NOVEL NEGATIVE ALLOSTERIC MODULATORS FROM VIRTUAL SCREENING 256

APPENDIX D. THE CHOLINOMIMETIC MORANTEL AS AN OPEN CHANNEL BLOCKER OF THE *ASCARIS SUUM* ACR-16 nAChR..... 295

APPENDIX E. LIST OF ALL CONFERENCE ABSTRACTS, AWARDS AND FUNDING..... 312

ACKNOWLEDGEMENTS

I lack words to express my gratitude to my supervisors: Distinguished Professor Richard J. Martin and Dr Alan P. Robertson, for accepting me into their lab and for educating me throughout my PhD program. Their self-less guidance, immeasurable support and encouragement made me the productive young scientist I am today. I will forever remain grateful to Dr Robertson for spending long hours on the bench with me just to make sure I fully understood the techniques used in my research; not forgetting to mention the times he allocated during weekends to work on my manuscripts and Schlumberger project. I am grateful to my program of study committee (POSC) members: Dr Michael J. Kimber, Dr Vellareddy Anantharam and Dr Douglas E. Jones, for agreeing to be on my POSC and for the academic guidance they provided me during my doctoral studies.

I would like to thank my lab colleagues, both past and present, especially Dr Samuel Buxton, Dr Sreekanth Puttachary, Dr Saurabh Verma, Dr Sudhanva Kashyap, Mark McHugh, Shivani Choudhary, Fudan Zheng and Dr Yoko Nagamori for the wonderful experience I had working with them. Special thanks to Dr Buxton for training me during my early days in the lab.

I would like to acknowledge our collaborators Professor Fidelis Cho-Ngwa and Dr Godfred A. Ayimele at the University of Buea, Cameroon for granting us access to their facilities and for providing insightful suggestions for the plant natural products project. I would like to thank all the members of Professor Cho-Ngwa's lab and the Organic Chemistry lab at the University of Buea, especially Dr Moses Samje, Smith Babiaka, Emmanuel Menang and Stanley Gamua for helping out with my research in Cameroon. I would also like to acknowledge the traditional healers and indigenes of Bambui, NW Cameroon for their

direction on the selection of the medicinal plants used in my research and for providing useful information on the traditional uses of these plants.

A special “Thank You” to Dr Jesse Goff, Dr Nicholas Koszewski, Cathy Martens and Carmen Reynolds for the help they gave me during my time in their lab. I would like to particularly thank Dr Koszewski for his recommendations and training on fractionating the plant extracts used in my research. I would like to thank Dr Bryan Bellaire for granting me access to his lab and for allowing me use the Worminator system in his lab. I would also like to thank Dr Vellareddy Anantharam and Adhithiya Charli for their help and training on cytotoxicity studies.

I would like to thank the Interdepartmental Toxicology program coordinator Linda Wild and the Department of Biomedical Sciences staff especially Kim Adams, Linda Erickson (retired), Amy Brucker, Rochelle Loonan and Emma Hashman for making my stay at Iowa State University a successful one at the departmental/administrative level.

I would like to thank the National Institutes for Health (NIH) and the Schlumberger Foundation for providing funding for my research. I would like to thank the Burroughs Wellcome Fund for providing me with a Collaborative Research Travel Award to visit Dr Judy Sakanari’s lab at the University of California San Francisco (UCSF) and also Christina Bulman and Chelsea Bidlow for assisting with the Worminator experiments at UCSF.

I would like to thank the University of Missouri-Columbia (UMC, Columbia, MO) and the NIAID/NIH Filariasis Research Reagent Resource Center (FR3) (Athens, GA) for their generous supply of adult *Brugia pahangi* used in my research. I would like to thank the members of the JBS Pork Plant at Marshalltown, Iowa, especially Rodney Howze for help collecting adult *Ascaris suum* for my research.

I would like to express my heartfelt gratitude to my American grandpa Mr Charles P. Andrews and grandma Mrs Elizabeth B. Eure for the love and support they gave me throughout my stay in Ames, Iowa. I would forever cherish my moments with grandpa and grandma and would never forget the lessons they taught me. I would like to thank my Heartland Baptist Church (HBC) family in Ames, Iowa for their prayers and love.

My deepest gratitude to my family and ALL my friends, relatives and well-wishers who during the course of my career provided any form of support to me. I am forever indebted to my parents, Mr James Tangwing Abongwa and Mrs Comfort Apongse Abongwa, for the enormous sacrifices they made in life to see that I succeed in my career pursuits as well as for their love, care, prayers, encouragement, and blessings. My special regards to my siblings: Delphine, Terence and Willibrod, who have always believed in me and have stood by me at ALL times whether good or bad.

ABSTRACT

Parasitic nematode infections remain a serious global public health threat to humans and animals. These infections cause debilitating conditions in humans and significant economic losses through infection of livestock and crop damage. Control of parasitic nematode diseases has continued to rely on use of anthelmintic drugs as there is presently no effective vaccine for the majority of these infections. Over the years, anthelmintic drug discovery has been very slow, and the majority of anthelmintic drugs used in human medicine today were initially developed for animal use as those affected live in the world's poorest nations that lack the financial means to afford conventional drugs. However, resistance to all the major anthelmintic drug classes has been reported in numerous veterinary parasite species and there are increasing concerns of resistance development in human parasite species. The emergence of widespread resistance therefore underscores the urgent need for the search of new targets, leads and strategies for anthelmintic drug discovery and development.

We have identified the nicotinic acetylcholine receptor (nAChR) subunit ACR-16 from *Ascaris suum* and showed that ACR-16 forms a functional homopentameric nAChR when expressed in *Xenopus* oocytes. *A. suum* is a gastrointestinal (GI) tract parasitic nematode of pigs that is very closely related to the human equivalent *A. lumbricoides*. ACR-16 is not activated by cholinergic anthelmintics and, although ACR-16 is most closely related to vertebrate α7 receptors based on amino acid sequence alignment, it has some marked pharmacological differences from vertebrate α7 receptors. As opposed to vertebrate α7 receptors, ACR-16 was insensitive to α-bungarotoxin and the effects of ivermectin, genistein and PNU120596 on ACR-16 were inhibitory rather than potentiating. The relative calcium

permeability ratio for ACR-16 was about 50x lower than that for vertebrate α7 receptors. We have showed using reverse transcription polymerase chain reaction (RT-PCR) that mRNA for ACR-16 is widely distributed throughout *Ascaris* tissues; suggesting ACR-16 may have functions other than neurotransmission. Our results showed, for the first time, the characterization of the pharmacology of ACR-16 from a parasitic nematode. Based on the pharmacology and expression pattern of ACR-16 in different tissues of the parasite, we suggest ACR-16 is an attractive new anthelmintic drug target with 'resistance-busting' properties that should be further exploited for therapeutic drug development.

Secondly, we have showed that the plants *Daniellia oliveri* and *Psorospermum febrifugum* have potential as sources of lead compounds for the development of the much-needed filaricidal drugs to treat onchocerciasis (river blindness) and lymphatic filariasis (elephantiasis). We prepared extracts of different polarities from *D. oliveri* and *P. febrifugum* and showed these extracts to be active against *Onchocerca ochengi* microfilariae and adults, and against adult *Brugia pahangi* based on visual motility scoring, MTT/formazan assay and the Worminator motility measurement system. Importantly, some extracts with *O. ochengi* microfilariae activity were also active on the adult worm. These extracts also showed activity against adult *B. pahangi*. We further fractionated the active extracts using Sep-Pak cartridges and High Performance Liquid Chromatography (HPLC) and showed some of these fractions retained activity against adult *B. pahangi*. We recommend that the active HPLC fractions be further purified to allow for the isolation of the bioactive compounds. This could significantly contribute to chemotherapeutic control of filarial infections currently hampered by the lack of macrofilaricides (adulticides).

Lastly, we have demonstrated that use of combination therapy over single drug therapy is a potentially useful tool for increasing efficacy, spectrum of action and reducing the likelihood of resistance development. We showed the combination of derquantel and abamectin to produce a greater inhibition of acetylcholine and pyrantel responses of expressed pyrantel/tribendimidine nAChRs from *Oesophagostomum dentatum* than derquantel or abamectin used alone. These nAChRs comprise of UNC-29, UNC-63 and UNC-38 subunits. Our results also showed abamectin acts on nAChRs, in addition to its known effects on glutamate-gated chloride channels (GluCls), implying abamectin has multiple targets. We further showed the action of abamectin on the expressed *O. dentatum* pyrantel/tribendimidine nAChRs to be bi-phasic, suggesting two allosteric sites of action: a high affinity negative allosteric modulation (NAM) site causing antagonism at lower concentrations (≤0.1 µM) and a lower affinity positive allosteric modulation (PAM) site causing a reduction in the antagonism at higher concentrations (≥0.3 µM).

CHAPTER 1. GENERAL INTRODUCTION

1.1 Introduction

Parasitic nematodes are a significant threat to both animals and humans, particularly in tropical and subtropical regions of the world. Parasitic nematodes also cause economic losses through infection of livestock and crop damage. In humans and animals, control of infections caused by parasitic nematodes relies mainly on the use of anthelmintic drugs, of which there are a limited number, and the majority of these act on ion channels. Anthelmintic drugs are grouped into different classes based on chemical structure and mode of action. The three major classes are the benzimidazoles (BZs), imidazothiazoles/tetrahydropyrimidines and macrocyclic lactones (MLs). The benzimidazoles (e.g thiabendazole, mebendazole, albendazole, flubendazole) target β-tubulin, an important protein in maintaining parasite cell structure. Imidazothiazoles/tetrahydropyrimidines (e.g levamisole, pyrantel, oxantel, morantel) act on nicotinic acetylcholine receptors (nAChRs), which are prototypical ligand-gated ion channels (LGICs) that mediate fast signal transmission at parasite neuromuscular and nerve-nerve junctions. Macrocyclic lactones (e.g ivermectin, abamectin, moxidectin) act on glutamate-gated chloride channels (GluCls). More recent anthelmintic drug classes include the amino-acetonitrile derivatives (AADs) (e.g monepantel), spiroindoles (e.g derquantel) and cyclooctadepsipeptides (e.g emodepside). Monepantel acts on the DEG-3-type nAChRs: ACR-20, ACR-23 and MPTL-1. Derquantel acts as an antagonist of several nAChR types. Emodepside acts on both SLO-1 potassium channels and latrophilin receptors. The recently introduced anthelmintic drug, tribendimidine, targets nAChRs just as imidazothiazoles/tetrahydopyrimidines, and is approved for human use in China. Anthelmintic drugs exhibit their effects by interfering with locomotion, feeding, egg laying

or growth. Regrettably, resistance has been reported for all three major anthelmintic drug classes, as well as the AAD monepantel, thus, underscoring the pressing need for strategies to slow down or overcome resistance. Therefore, these PhD studies seek to address three main strategies by which anthelmintic resistance can be overcome. The first aim was to characterize the pharmacology of a new nAChR drug target, ACR-16, from the pig parasite, *Ascaris suum*, a good laboratory model for the human parasite, *A. lumbricoides*. The second aim was to demonstrate that plant natural products may serve as potential sources for new anthelmintics by investigating the efficacy and cytotoxicity of extracts from traditional medicinal plants against *Onchocerca ochengi*, the best-known laboratory model for the human equivalent, *O. volvulus*, and against *Brugia pahangi*, a good model for *B. malayi*. The third aim was to investigate interactions between derquantel, abamectin and expressed nAChRs from *Oesophagostomum dentatum* to gain mechanistic insight into this recently developed combination therapy.

1.2 Thesis Organization

In this thesis, a general introduction is provided about parasitic nematodes and the target sites of anthelmintic drugs used to treat nematode infections. Ion channels are highlighted as targets for the majority of available anthelmintic drugs and an emphasis is placed on anthelmintic drug resistance and the need to overcome drug resistance. Three strategies are proposed as ways of overcoming drug resistance and these are: the characterization of new drug targets, the development of new drugs from plant natural products and the use of combination therapy. In chapter 2, I have reviewed the literature relating to parasitic nematodes particularly *Ascaris suum*, *Onchocerca volvulus* and *Brugia malayi*, nicotinic acetylcholine receptors (nAChRs) of parasitic nematodes, and the medicinal

plants, *Daniellia oliveri* and *Psorospermum febrifugum*. In chapters 3, 4 and 5, I present research work done by myself and collaborators that has been published (chapters 3 and 5) or in preparation for publication (chapter 4). Chapter 3 describes the cloning and pharmacological characterization of a new homomeric nicotinic acetylcholine receptor ACR-16 from *Ascaris suum* (*Asu*-ACR-16). ACR-16 may serve as a potential target for the development of new 'resistance-busting' anthelmintic drugs. I did all the work outlined in this paper, except *Asu-acr-16* cloning which was done by our collaborators at Institut National de la Recherche Agronomique (INRA-Nouzilly) in France and isolation of cytoplasm for single-cell PCR which was done in our lab. Chapter 4 shows the efficacy of extracts of *Daniellia oliveri* and *Psorospermum febrifugum* against *Onchocerca ochengi* and *Brugia pahangi*, bioassay-guided fractionation and cytotoxicity of active extracts of *D. oliveri* and *P. febrifugum*. All the work in this chapter was done by me, with significant input from our collaborators at the University of Buea, Cameroon, University of California San Francisco and Iowa State University. Chapter 5 describes the effects of the recently developed derquantel and abamectin combination on expressed pyrantel/tribendimidine nAChRs from *Oesophagostomum dentatum*. I did all the work presented in this paper, except the cloning of the receptor subunits which was done by a former graduate student in our lab. Chapter 6 is a general discussion and conclusions of my PhD research and suggestions for future work. Appendix A is a research paper on acetylcholine receptor diversity in *Oesophagostomum dentatum*. Appendix B is an invited review on advances in anthelmintic drug development. Appendix C is a research paper on modeling the *Ascaris suum* ACR-16 receptor. Appendix D is a research paper on the mode of action of the cholinomimetic

morantel on the *Ascaris suum* ACR-16 receptor. Lastly, Appendix E is a list of all conference abstracts, awards and funding obtained.

CHAPTER 2. LITERATURE REVIEW

2.1 Parasitic Nematodes

Parasites are organisms that live on or in another organism known as the host, and benefit at the expense of the host. Parasites are harmful to the host and may even cause death. Most generally, the host-parasite relationship is such that the host does not benefit from the relationship and stressors associated with harboring parasites can be deleterious. Parasites are classified as ectoparasites if the parasites live outside the body, and as endoparasites if they live inside the body. In animals, ectoparasites live on the skin and can cause itching and rashes, while endoparasites may live in the blood, muscles, liver, brain or digestive tract (Hopla *et al.*, 1994).

Nematodes (or roundworms) belong to the phylum Nematoda. There are over 25,000 known nematode species, of which more than 50% are parasitic (Zhang, 2013). These include the soil-transmitted helminths (STHs) and filarial worms. Parasitic nematode infections are a global public health problem. These infections include four of the seventeen diseases that are classified as "Neglected Tropical Diseases" (NTDs) by the World Health Organization (WHO). The seventeen NTDs are Buruli ulcer, Chagas disease, Dengue and Chikungunya, Dracunculiasis (guinea-worm disease), Echinococcosis, Foodborne trematodiases, Human African trypanosomiasis (sleeping sickness), Leishmaniasis, Leprosy (Hansen's disease), Lymphatic filariasis, Onchocerciasis (river blindness), Rabies, Schistosomiasis, Soil-transmitted helminthiases, Taeniasis/Cysticercosis, Trachoma and Yaws (Endemic treponematoses) (Johnston *et al.*, 2014). Of these seventeen NTDs, thirteen have been identified as core (Table 2.0), (Feasey *et al.*, 2010). Among the core NTDs are the

Table 2.0 The thirteen core NTDs. (Modified from Feasey *et al*., 2010, pp. 182-183)

Disease	Name of causative agent	Class of causative agent	Usual mechanism of acquisition	Site of infection with mature agent	Clinical features	Estimated number infected (millions)	Estimated DALYs lost (millions), 2002	Control strategy	Aim of control strategy
Ascariasis*	*A. lumbricoides*	Helminth	Ingestion of eggs	Small intestine	Abdominal distension, pain malabsorption, intestinal obstruction, impaired growth, reduced school performance	807–1221	1.8	Periodic mass deworming of children using benzimidazole antihelminthics	Prevention of morbidity in children living in endemic areas
Dracunculiasis	*D. medinensis*	Helminth	Ingestion of water containing copepods infected with larval stage	Subcutaneous tissues	Painful skin bulla that progresses to an ulcer, from which a worm protrudes	0.002	Not known	Provision of protected water sources, education, filtration of drinking water, case detection and containment, cyclopicides	Eradication
Hookworm infection*	*A. duodenale, N. americanus*	Helminth	Skin penetration by soil-dwelling infective (third-stage) larvae	Upper part of small intestine	Intestinal blood loss, iron deficiency, protein malnutrition, impaired growth, reduced school performance	576–740	0.06	Periodic mass deworming of children using benzimidazole antihelminthics	Prevention of morbidity in children living in endemic areas
Lymphatic filariasis*	*W. bancrofti, B. malayi, B. timori*	Helminth	Skin penetration by infective (third-stage) larvae at the site of the bite from the mosquito vector (*Anopheles, Aedes, Culex, Mansonia*, or *Ochlerotatus*), after escaping from the mosquito's proboscis	Lymphatic vessels	Hydrocoele, lymphoedema and elephantiasis	120	5.8	Annual mass drug administration of albendazole plus either diethylcarbamazine or (where co-endemic with onchocerciasis) ivermectin	Elimination as a public health problem by 2020
Onchocerciasis*	*O. volvulus*	Helminth	Injection of infective (third-stage) larvae in the saliva of a biting, parasitized female blackfly (*Simulium sp*.)	Subcutaneous tissues	Subcutaneous nodules, pruritus, skin atrophy, skin pigmentation, blindness	37	0.5	Annual mass drug administration of ivermectin	Elimination as a cause of blindness by 2020

Table 2.0 (Continued)

Disease	Name of causative agent	Class of causative agent	Usual mechanism of acquisition	Site of infection with mature agent	Clinical features	Estimated number infected (millions)	Estimated DALYs lost (millions), 2002	Control strategy	Aim of control strategy
Schistosomiasis*	*S. mansoni*, *S. haematobium*, *S. japonicum*, *S. intercalatum*, *S. mekongi*	Helminth	Penetration of skin by cercariae that have emerged from water-dwelling snail intermediate hosts	Perivesical venous plexus or mesenteric veins	Haematuria, bladder obstruction, renal failure, bladder cancer (*S. haematobium*); periportal fibrosis, portal hypertension, ascites and varices (mesenteric schistosomes).	200	1.7	Annual mass drug administration of praziquantel, improved access to safe water and sanitation, and health education	Prevention of morbidity in children living in endemic areas
Trichuriasis*	*Trichuris trichiuria*	Helminth	Ingestion of eggs	Large intestine, especially caecum	Colitis, chronic dysentery, rectal prolapsed, impaired growth, reduced school performance	604–795	1.0	Periodic mass deworming of children using benzimidazole antihelminthics	Prevention of morbidity in children living in endemic areas
Chagas disease	*T. cruzi*	Protozoon	Inoculation by host's fingers into conjunctival sac or site of bite following excretion of mature parasite in faeces of biting triatomine bug	Intracellularly in tissues throughout the body	Cardiomyopathy, cardiac dysrhythmia, mega-oesophagus, mega-colon	15	0.7	Vector control, insecticide-treated bed nets, dog collars, adequate housing	Varies by region
Human African trypanosomiasis	*T. brucei*	Protozoon	Injection by parasitized tsetse fly	Blood, lymph, cerebrospinal fluid	Fever, headache lymphadenopathy, neurological decline, daytime somnolence, coma, death	<0.1	1.5	Vector control, rapid diagnosis and prompt treatment	Not yet defined
Leishmaniasis	More than 20 species of *Leishmania*	Protozoon	Injection by parasitized sandfly	CL skin MCL: skin plus oropharnyx VL: disseminated disease	CL: skin ulcer MCL: skin ulcer plus oropharyngeal destruction VL: fevers, night sweats, weight loss, anaemia, immuno-suppression	12	2.1	Vector control, rapid diagnosis and prompt treatment	VL: elimination as a public health problem in Bangladesh, India and Nepal by 2015

Table 2.0 (Continued)

Disease	Name of causative agent	Class of causative agent	Usual mechanism of acquisition	Site of infection with mature agent	Clinical features	Estimated number infected (millions)	Estimated DALYs lost (millions), 2002	Control strategy	Aim of control strategy
Buruli ulcer	*M. ulcerans*	Bacterium	Unknown	Skin	Skin ulcer with an undermined edge	Unknown	Unknown	Rapid diagnosis and prompt treatment	Reduction in morbidity and socio-economic burden
Leprosy	*M. leprae*	Bacterium	Unknown	Skin and nerves	Skin changes, anaesthesia	0.4	0.2	Rapid diagnosis and prompt treatment with life-long follow-up	Microbiological cure, prevention of disability
Trachoma*	*C. trachomatis*	Bacterium	Mechanical transfer of elementary bodies by flies, fomites or fingers	Conjunctiva	Conjunctivitis, trachomatous scarring, trichiasis, corneal opacity, blindness	84	2.3	SAFE strategy: surgery for trichiasis, antibiotics (by MDA) to treat infection, face washing and environmenal improvement to reduce transmission	Elimination as a public health problem by 2020

*Diseases have both high prevalence and excellent prospects for control.

nematode infections: soil-transmitted helminthiases caused by intestinal parasitic worms and filariases (lymphatic filariaisis and onchocerciasis) caused by filarial worms. Over 3 billion people, primarily in developing countries with poor sanitation and lack of health education programs are infected with parasitic nematodes (Chan, 1997). Parasitic nematode infections do not only cause debilitating conditions in humans but also cause serious problems in livestock production worldwide. They cause significant economic losses and are a threat to food security (Fitzpatrick, 2013; Hotez *et al.*, 2009; Hotez & Kamath, 2009). As a result, affected communities are constantly trapped in a cycle of poverty and disease.

2.1.1 Soil-transmitted helminthiases

2.1.1.1 Ascariasis. Soil-transmitted helminthiases (STHs) are a group of NTDs caused by roundworms (*Ascaris lumbricoides*), hookworms (*Ancylostoma duodenale* and *Necator americanus*) and whipworms (*Trichuris trichuria*) (Bethony *et al.*, 2006). STHs are a public health concern in Africa, Latin America, Middle East and Asia (Figure 2.0) (Savioli & Albonico, 2004). Ascariasis is commonly seen in tropical and subtropical areas around the world where the infection has been strongly associated with poor hygiene, poor sanitation and use of human feces as fertilizers. Over 1 billion people worldwide are infected with *A. lumbricoides* (Crompton, 1988; de Silva *et al.*, 2003). The infection is most prevalent among school-aged children in rural areas (Fernandez *et al.*, 2002; Luong, 2003; Rayan *et al.*, 2010).

The life cycle of *Ascaris lumbricoides* requires only humans as the definitive host; there is no intermediate host (Figure 2.1). Adult female worms are larger (20 – 35 cm) than males (15 – 30 cm). The worms live in the lumen of the small intestine of infected persons. Eggs are passed in the feces and the infection is passed from one person to another by ingestion of soil that is contaminated with feces from infected persons. This can occur by

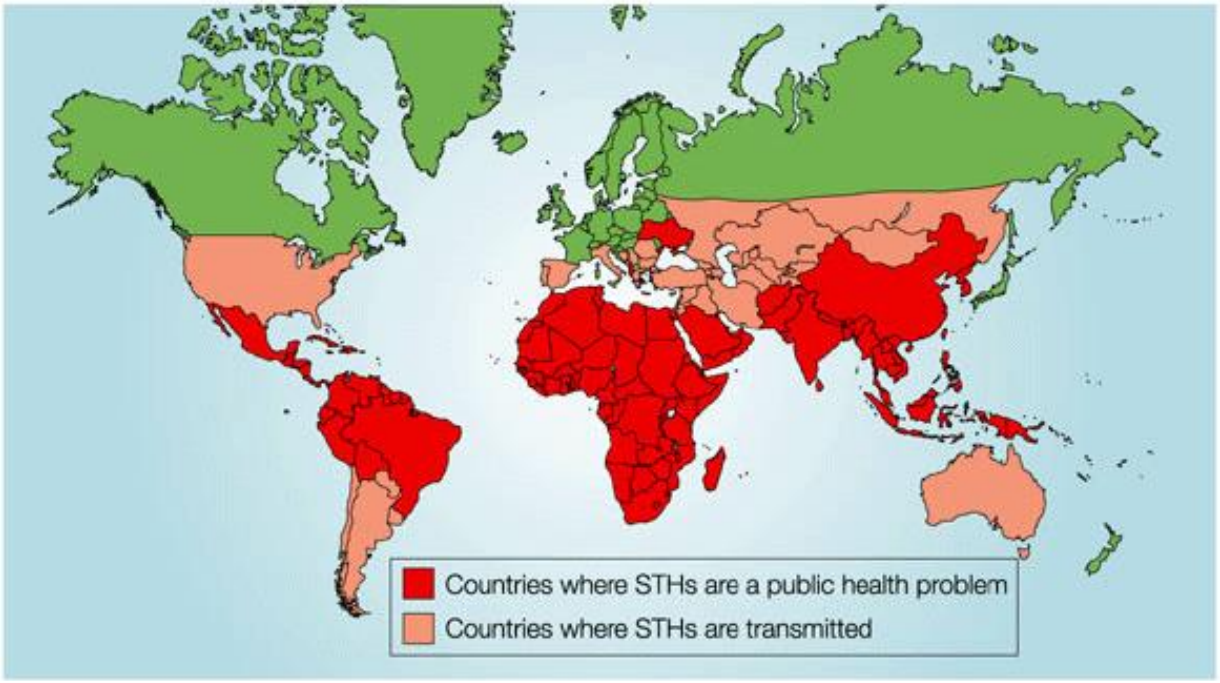

Source: Savioli & Albonico, 2004, p. 618.

Figure 2.0 Global distribution of soil-transmitted helminthiases (STHs). STHs are a major public health problem in Africa, Latin America, Middle East and Asia. Transmission of STHs also occurs in Australia and a few European countries, although not a major public health concern in these areas.

putting hands that have come in contact with contaminated soil in the mouth or by consuming improperly washed or peeled vegetables or fruits. An adult female produces up to 200,000 eggs per day which may be fertilized or unfertilized. Only fertilized eggs become infective while unfertilized eggs do not. Depending on environmental conditions, the fertilized eggs become infective after 18 days to several weeks after they embryonate. Moist, warm, shaded soil provides optimum conditions for this to occur. Once swallowed, the larvae hatch, invade the intestinal mucosa and are transported via the portal and systemic circulation to the lungs. While in the lungs, the larvae further mature in about 10 to 14 days and then

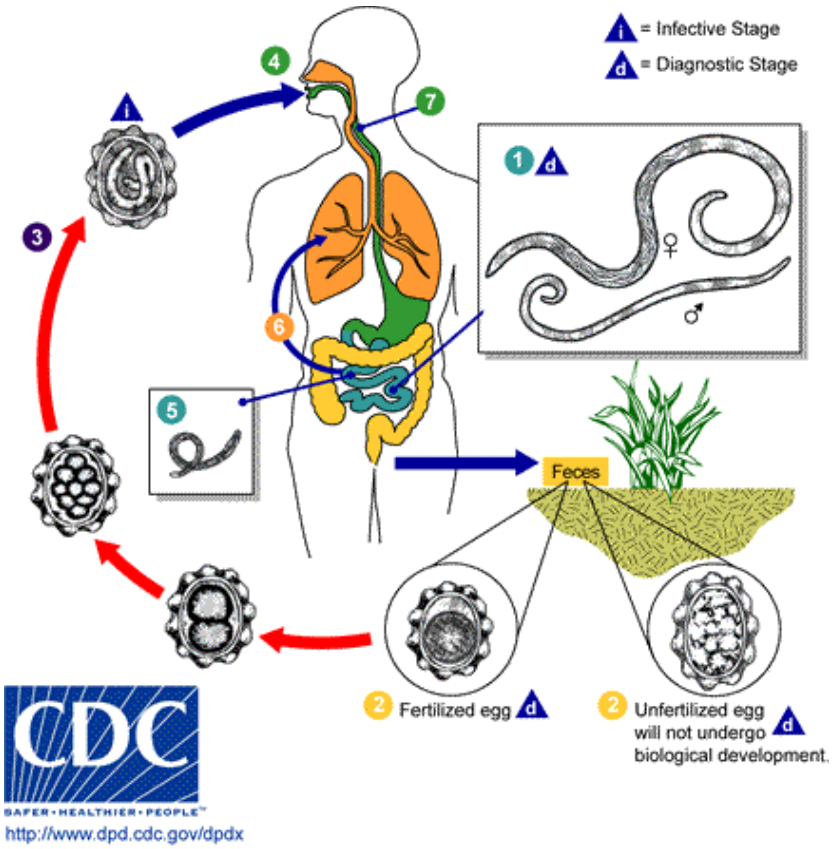

Source: Accessed on 03-19-17 at 11:45PM CST, from https://www.cdc.gov/parasites/images/ascariasis/ascariasis_lifecycle.gif

Figure 2.1 Life cycle of *Ascaris lumbricoides.*

penetrate the alveolar walls and ascend the bronchial tree to the throat and are swallowed. Once they reach the small intestine, they develop into adults which typically live for up to 1 – 2 years.

Infected persons are often asymptomatic. When symptoms occur, they range from light, such as abdominal discomfort to heavy, such as anemia, malnutrition, intestinal blockage and impaired physical and mental growth in children (Bethony *et al.*, 2006; Gyorkos *et al.*, 2011; Hughes *et al.*, 2004). Cough may occur as a result of migration of the worms through the (Hoenigl *et al.*, 2010). Irrespective of age, the prevalence of ascariasis is

higher among females than males (Elkins *et al.*, 1986; Elkins *et al.*, 1988; Haswell-Elkins *et al.*, 1989). *Ascaris* infection is diagnosed by microscopic examination of stool for the presence of eggs. A single dose of albendazole (400 mg) or mebendazole (500 mg) is effective in treating *Ascaris* infections (Albonico *et al.*, 1994; Norhayati *et al.*, 1997).

2.1.2 Filariases

2.1.2.1 Onchocerciasis (River blindness). *Onchocerca* is a genus of filarial nematodes of the order Spirurida, family Onchocercidea. Of the various *Onchocerca* species, only one, *O. volvulus* infects humans (Krueger *et al.*, 2007; Morales-Hojas *et al.*, 2006). *O. volvulus* is the causative agent of human onchocerciasis or river blindness, and is transmitted by the blackfly, *Simulium damnosum* (Nelson, 1970; Sharp, 1927). The disease is called river blindness because the blackfly vector breeds along fast flowing rivers (Winthrop *et al.*, 2011). Consequently, the disease is most prevalent around these rivers. These areas usually constitute fertile farmlands which are often abandoned for less fertile areas as an escape strategy from the bite of the blackfly and hence, transmission of onchocerciasis. Most of the endemic areas are often inhabited by peasant farmers, therefore, migration from fertile to infertile lands causes agricultural and economic losses (Bradley, 1976; Stingl, 1987). The scientific literature on onchocerciasis dates as far back as 1875 when O'Neill first detected *O. volvulus* microfilariae in the skin of patients with "craw-craw" in Ghana. In 1893, *O. volvulus* adult worms were described by Leuckart from subcutaneous nodules collected from patients in Ghana, and in the 1920s, Blacklock in Sierra Leone identified the blackfly *S. damnosum* as the disease vector. Hissette and Robles in the Congo and Guatemala respectively, associated blindness with onchocerciasis (Burnham, 1998; Cupp *et al.*, 2011; Nelson, 1991). Globally, onchocerciasis is endemic in 36 countries of sub-Saharan Africa,

the Yemen and Latin America, 30 of which are in Africa (Figure 2.2). An estimated 37 million people suffer from onchocerciasis, with 99% of infected persons living in Africa. Another 120 million people worldwide are at risk of contracting the disease, of which 90 million live in Africa (Basanez *et al.*, 2006; Gustavsen *et al.*, 2011). Onchocerciasis is the world's second leading infectious cause of blindness after trachoma (Thylefors *et al.*, 1995). About 1 million of infected persons have ocular onchocerciasis, with an estimated 500,000 having impaired vision and 270,000 blinded as a result of the infection (Boatin & Richards, 2006). In hyperendemic areas, infection rates can be as high as 100%, with about 50% of the population blinded as a result of onchocerciasis (Etya'ale, 2002; Taylor, 1990). Eye and skin lesions and severe itching produced by the microfilariae are the greatest burdens of onchocerciasis (Kale, 1998). Blindness and skin disease due to onchocerciasis have been associated with reduced life expectancy, poverty, decreased productivity, poor academic performance, higher rates of school dropout of children (predominantly females) of infected parents and social stigmatization, particularly among women (Benton, 1998; Brieger *et al.*, 1998; Malatt & Taylor, 1992; Vlassoff *et al.*, 2000).

Onchocerciasis is a chronic infection. Clinical manifestations develop years after infection. The most common early symptom of infection with onchocerciasis is pruritis which is as a result of localized host inflammatory responses to dead and dying microfilariae in the skin (Somorin, 1983; Udall, 2007). Other symptoms include disfiguring dermatitis or leopard skin, onchocercomata (subcutaneous nodules), lymphadenopathies and ocular lesions (Browne, 1960; Connor & Palmieri, 1985; Enk *et al.*, 2003; Okulicz *et al.*, 2004). Ocular lesions constitute the most serious of these clinical manifestations as they can progress to

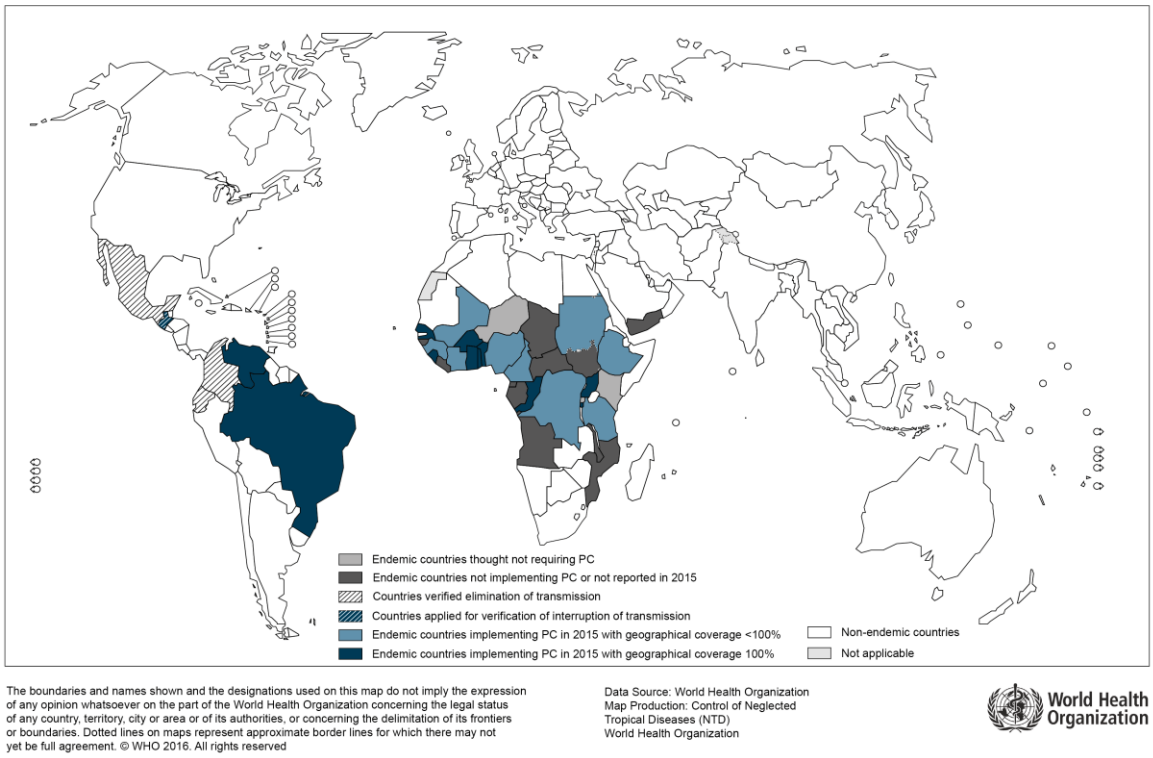

Source: Accessed on 02-22-17 at 12:00AM CST, from: http://www.who.int/entity/mediacentre/factsheets/Onchocerciasis_2015_310_px.png

Figure 2.2 Global distribution of onchocerciasis

blindness. It is thought that antigens of *Wolbachia* endobacteria which live in a symbiotic relationship with *O. volvulus* greatly contribute to the pathological reactions associated with onchocerciasis (Brattig, 2004; Saint Andre *et al.*, 2002). Presumptive diagnosis of onchocerciasis in endemic areas is therefore based on physical examination of these clinical manifestations. Nonetheless, it is important to differentiate clinical manifestations associated with onchocerciasis from those due to other skin infections such as scabies and contact dermatitis. For this reason, definitive methods ranging from use of microscopy to detect microfilariae through detection of *O. volvulus* specific antigens and antibodies to DNA

probes have been developed for diagnosis of onchocerciasis (Boatin *et al.*, 1998; Bradley & Unnasch, 1996; Harnett, 2002; Zimmerman *et al.*, 1994).

The life cycle of *O. volvulus* involves the blackfly and human stages (Figure 2.3). Adult female worms, during a blood meal, inject infective third stage (L3) larvae into the human host via the bite wound. Next, the L3 larvae develop into adults in subcutaneous nodules. Nodules typically contain on average 2 – 3 female worms and 1 – 2 adult male worms. Females are usually confined to nodules while males can migrate from nodule to nodule, perhaps in search of females (Schulz-Key & Karam, 1986). Adult female worms are generally larger, and measure 270 – 400 μm in diameter and 33 – 50 cm in length, compared to the adult male worms which measure 130 – 210 μm in diameter and 1.9 – 4.2 cm in length. Adult worms have a life span of up to 15 years. After mating, females produce hundreds of unsheathed microfilariae daily which are typically found in the skin and lymphatics of connective tissues, but sometimes in peripheral blood, urine, sputum and the eyes (Anderson *et al.*, 1975a; Anderson *et al.*, 1975b; Schulz-Key, 1990). Female worms are capable of producing microfilariae for up to 9 years. The microfilariae measure 5 – 9 μm in diameter and 220 – 360 μm in length and have a life span of up to 2 years. The blackfly during another blood meal from an infected person ingests microfilariae which migrate from the blackfly's gut to thoracic muscles where they moult into the first larval stage (L1). L1 larvae subsequently develop into L3 larvae which eventually migrate to the blackfly's head region and proboscis, ready to be injected into a human host during the next blood meal.

Control against onchocerciasis includes measures directed against the blackfly vector and the parasites by use of insecticides and chemotherapeutic agents respectively. Vector

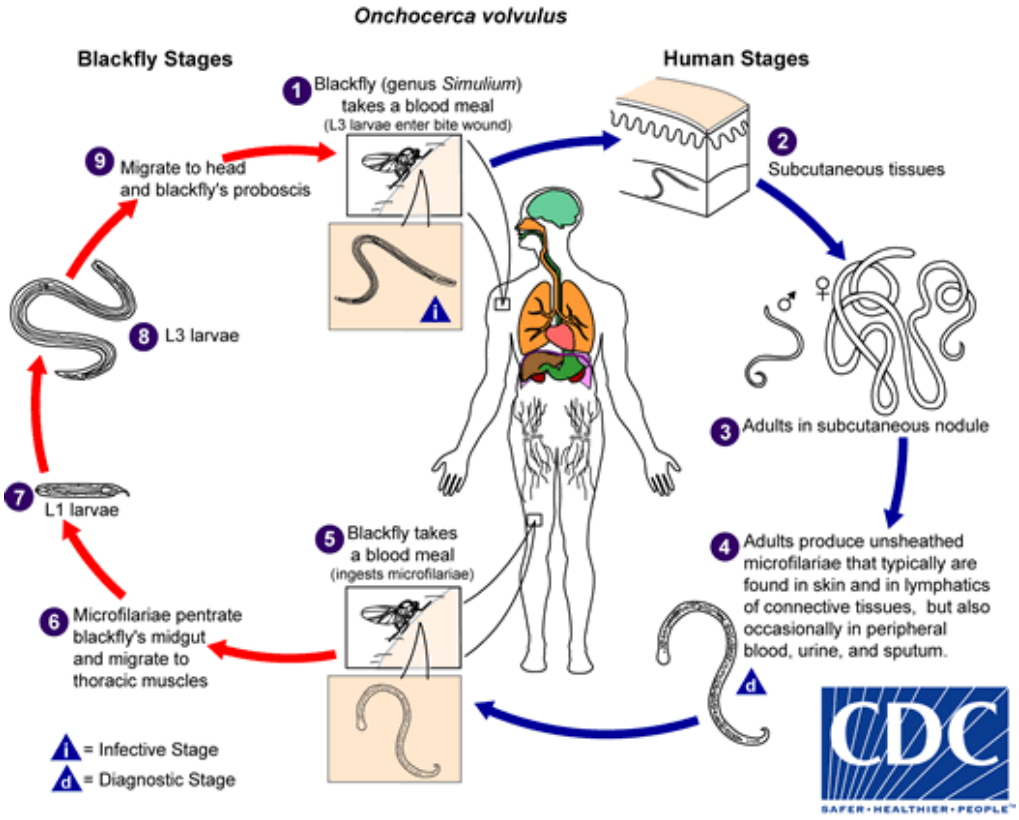

Source: Accessed on 02-21-17 at 08:38PM CST, from https://www.cdc.gov/dpdx/onchocerciasis/modules/o_volvulus_lifecycle.gif

Figure 2.3 Life cycle of *Onchocerca volvulus.*

control though successful to an extent, has some limitations; it is costly and also the thick canopies of the tropical forests prevent insecticides from reaching the breeding sites. Vector control is further limited by increasing resistance of the blackfly to insecticides (Davies, 1994). Therefore, chemotherapy remains the most efficient method of controlling onchocerciasis. Ivermectin, administered at a dose of 150 μg/kg, is the sole drug of choice for the control of onchocerciasis. Although ivermectin effectively kills microfilariae produced by adult worms (macrofilariae), it has little or no effects on the adults which may live for up to 15 years in human hosts (Duke, 1972). Hence, parasite control is hindered by

the lack of an effective adulticide (macrofilaricide) (Hopkins, 2005). There are also concerns about the development of resistance to ivermectin owing to its large scale repeated use (Osei-Atweneboana *et al.*, 2011; Richards *et al.*, 2001). Additionally, ivermectin can provoke severe life-threatening adverse reactions including encephalopathy, coma and death in patients heavily infected with the filarial parasite, *Loa loa* (eye worm) (Boussinesq *et al.*, 2003; Gardon *et al.*, 1997; Mackenzie *et al.*, 2007). These adverse reactions produced by the death of *L. loa* microfilariae greatly hinder use of ivermectin for treatment of onchocerciasis in areas of co-endemicity with loiasis. Studies have shown that targeting the endosymbiotic bacteria *Wolbachia* with the antibiotic, doxycycline for 4 to 6 weeks causes adult female worm sterility and a reduction in worm viability, development, embryogenesis and survival (Hoerauf *et al.*, 2002; Hoerauf *et al.*, 2008; Hoerauf *et al.*, 2009; Taylor *et al.*, 2000; Turner *et al.*, 2010). Treatment of onchocerciasis with doxycycline is also advantageous in patients co-infected with *L. loa* because of its lack of activity against *L. loa* microfilariae or adult worms (Wanji *et al.*, 2009). Although antibiotics have demonstrated activity against adult worms, the long treatment regimes required with antibiotic treatment present logistical problems for mass drug administration. Another limitation is contraindication of antibiotics in pregnant women and children under the age of 8 (Tamarozzi *et al.*, 2011). Ultimately, new drugs are needed for the effective control and elimination of onchocerciasis (Hotez, 2007).

Due to ethical constraints obtaining *O. volvulus* and difficulty maintaining *O. volvulus* under experimental conditions, other appropriate animal equivalents have been explored for studies on chemotherapy, host-parasite relationships and immunology of onchocerciasis. In this regard, the bovine *O. ochengi* has been identified as the closest relative to human *O. volvulus* (Makepeace & Tanya, 2016; Trees *et al.*, 1998). Both *O.*

ochengi and *O. volvulus* share the same *Simulium* vectors (Wahl *et al.*, 1998a). For this reason, a reduction in the vector biting rate for humans and hence a reduction in the transmission of human onchocerciasis has been observed in regions where there is a high bovine population and for which bovine and human onchocerciasis are endemic (Eisenbarth *et al.*, 2016; Wahl *et al.*, 1998b). *O. ochengi* and *O. volvulus* also demonstrate comparable drug sensitivities (Trees *et al.*, 2000). These similarities, along with the relative availability and low cost of obtaining *O. ochengi* make *O. ochengi* the best laboratory model for anti-*Onchocerca* drug screens and the study of host-parasite interplay in human onchocerciasis.

2.1.2.2 Lymphatic filariasis (Elephantiasis). Lymphatic filariasis (LF), commonly known as elephantiasis is a neglected tropical disease that is caused by filarial nematodes of the family Filariodidea. These include *Wuchereria bancrofti*, *Brugia malayi* and *Brugia timori*. *W. bancrofti* accounts for 90% of LF cases, while *B. malayi* and *B. timori* account for the remaining 10% (Palumbo, 2008). Bancroftian filariasis occurs in both urban and rural areas, while Brugian filariasis occurs mainly in rural areas. The parasites that cause LF are transmitted to humans by mosquitoes of the genera *Culex*, *Anopheles*, *Mansonia* and *Aedes*. *Culex* mosquitoes are found across urban and semi-urban areas, *Anopheles* are found mainly in rural areas, and *Aedes* are found mainly in endemic islands in the Pacific. Urban *W. bancrofti* is primarily transmitted by *Culex quinquefasciatus*, whereas *Anopheles* and *Aedes spp* mosquitoes are typical vectors of rural *W. bancrofti*. Brugian filariasis is mainly transmitted by *Mansonia*, *Anopheles* and *Aedes spp* mosquitoes (Mak, 1987). LF can lead to an altered lymphatic system and abnormal swelling of body parts, causing pain and severe disability, ranking as the second leading cause of permanent disability worldwide after mental illness (Noordin, 2007; Wynd *et al.*, 2007). Globally, over 120 million people are

infected with LF, with another 1.2 billion at risk and about 40 million disfigured and incapacitated as a result of the disease (Fenwick, 2012; Nutman, 2013). The majority of LF cases are seen in Africa (Figure 2.4).

The majority of infected persons are asymptomatic, but can show acute symptoms such as inflammation of the skin, lymph nodes and lymphatic vessels which often progress to chronic conditions like lymphedema (tissue swelling) or elephantiasis (tissue/skin thickening) of limbs and hydrocele (scrotal swelling) (Babu & Nutman, 2012; Shenoy, 2008).

Of these symptoms, elephantiasis is the most chronic and obvious, occurring in about 10% of LF cases. Chronic LF has serious mental, social and economic effects which include stigma and poor economic output, hence, poverty. The role of gender in social stigmatization due to chronic LF has been reported, with the burden falling more on women (Bandyopadhyay, 1996; Coreil *et al.*, 1998; Gyapong *et al.*, 1996). The conventional method

Source: Accessed on 03-20-17 at 04:15PM CST, from https://www.cdc.gov/parasites/images/lymphaticfilariasis/lf_geo_distrib.jpg

Figure 2.4 Global distribution of lymphatic filariasis indicated in red.

of diagnosing LF is microscopic detection of microfilariae in blood smears. Blood samples for microfilariae detection are usually collected at night because during the day, microfilariae hide in blood capillaries of internal organs. However, this conventional method has low sensitivity, leading to the development of more sensitive PCR-based methods, immunological and serological techniques (Melrose *et al.*, 2004; Weil & Ramzy, 2007). These methods also allow for blood samples to be collected from patients at anytime of the day.

The life cycle of parasites that cause LF is similar to that of *O. volvulus*, involving mosquito and human stages (Figure 2.5). Infected mosquitoes during a blood meal introduce L3 larvae into the body of a human host which migrate to the lymphatic vessels and develop into adult worms. Adult *B. malayi* females are larger (measuring 43 – 55 mm in length by 130 – 170 μm in width) than adult males (measuring 13 – 23 mm in length by 70 – 80 μm in width). Adult *W. bancrofti* are similar to adult *B. malayi* except both sexes are larger. Adult worms produce sheathed microfilariae (measuring 177 – 230 μm in length by 5 – 7 μm in width) which typically enter the bloodstream and are ready to be ingested by the mosquito during another blood meal. As with *O. volvulus*, once ingested by the arthropod vector, microfilariae shed their sheaths and migrate to mosquito's thoracic muscles via midgut where they moult into L1 larvae and subsequently develop into L3. L3 larvae then migrate to the mosquito's head and proboscis, ready to infect another human, thus continuing the transmission cycle.

Chemotherapy is the most cost-effective tool to control LF. This is achieved by mass treatment with a combination of albendazole (200 mg) with either ivermectin (150 – 200

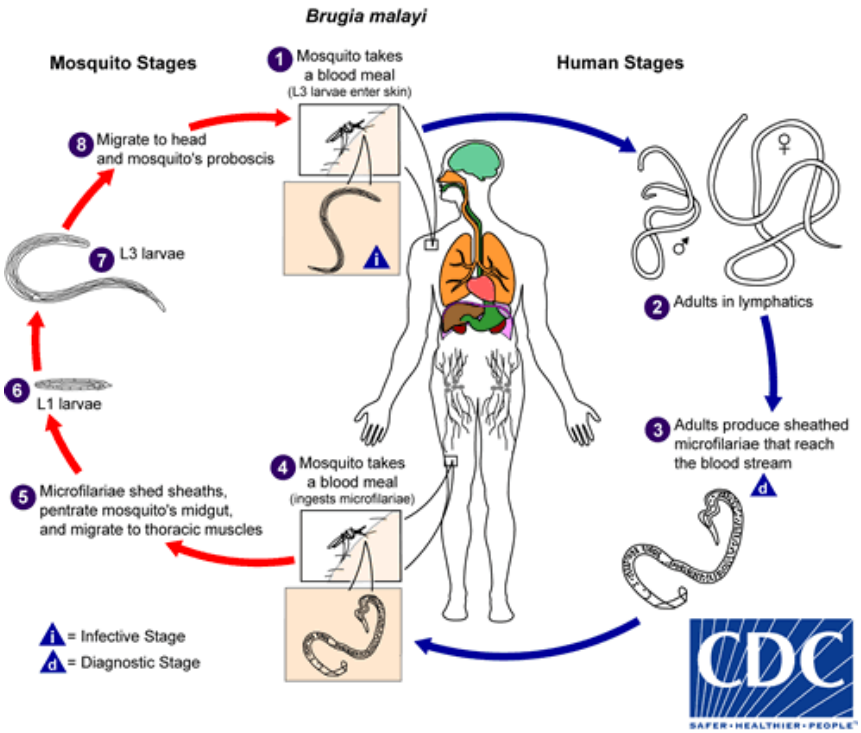

Source: Accessed on 03-05-17 at 02:08AM CST, from https://www.cdc.gov/parasites/images/lymphaticfilariasis/b_malayi_lifecycle.gif

Figure 2.5 Life cycle of *Brugia malayi*.

μg/kg) or diethylcarbamazine (DEC) (6 mg/kg) (Karam & Ottesen, 2000; Ottesen *et al.*, 1997). However, these drugs are only microfilaricidal, with limited activity against adult worms which can live for an average of 5 – 10 years and will continue to produce microfilariae. Clearly, new drugs effective against adult worms are needed. DEC is further contraindicated in onchocerciasis due to the possibility for the occurrence of severe treatment adverse reactions involving the skin and eye (Mazzotti reaction) (Awadzi & Gilles, 1992). Ideally, LF patients who are co-infected with onchocerciasis should be treated with the albendazole and ivermectin combination. Recently, the combination of DEC, albendazole and ivermectin was demonstrated to be more efficient than the DEC and albendazole

combination for the treatment of Bancroftian filariasis. Twelve patients who received a single dose of the DEC, albendazole and ivermectin combination tested negative for microfilariae at 12 and 24 months after treatment, suggesting adult worm death or sterility (Thomsen *et al.*, 2016). However, more studies are needed to ascertain the safety of this triple drug therapy, particularly in individuals who are co-infected with onchocerciasis and loiasis. Studies have also shown that targeting the *Wolbachia* endosymbiont with doxycycline (200 mg for 4 – 6 weeks) can result in adult worm sterility (Hoerauf *et al.*, 2003).

Due to the constraints in obtaining large numbers of *B. malayi* for drug screens, *B. pahangi* which naturally infects cats and wild animals is used. Cats respond to *B. pahangi* in a similar manner as humans respond to *B. malayi* and *W. bancrofti* (Denham & Fletcher, 1987). Likewise, *B. pahangi* is equally susceptible to drugs that act on *B. malayi*. Also, given the relatively high costs of maintaining cats, the gerbil-*B. pahangi* system is used as a suitable model for drug screens and host-parasite studies (Bulman *et al.*, 2015).

2.2 Nematode Neuromuscular System

Here we focus on the neuromuscular system of *Ascaris lumbricoides* var. *suum*. The neuromuscular system of *Ascaris spp* is the earliest and well-studied nematode neuromuscular system. The nematode neuromuscular system is unique in several ways. For instance, projections are sent from muscle cells to nerves as opposed to from nerves to muscle cells in vertebrates. Like other nematodes, *Ascaris spp* has a fixed number of cells and cell divisions. Other unique features are the small and constant number of neurons (*ca* 250) in the nervous system and the large cells which make up the musculature (del Castillo *et al.*, 1989).

2.2.1 Nervous System

The nervous system of *Ascaris* is made up of three components namely: (i) nerve ring and associated ganglia in the anterior region, (ii) major dorsal and ventral nerve cords and smaller subdorsal and subventral nerve cords, and (iii) a smaller set of ganglia in the posterior region. The motor nervous system (remaining region of the nervous system in a decapitated and tailless *Ascaris* that can still control movement) of *Ascaris* is composed of five repeating units or segments. Each unit or segment contains eleven motoneurons which based on morphology were classified into seven types with all their somata positioned in the ventral nerve cord (Stretton *et al.*, 1978). Three of the seven types namely; DI, DE2 and DE3 occur only once in each segment whereas the other four types namely; DE1, VI, V1 and V2 occur twice. Of these seven types, two (V1 and V2) are confined to the ventral nerve cord while the other five have processes in both dorsal and ventral nerve cords. The processes in dorsal and nerve cords of these motoneurons are linked by lateral processes known as commissures. Additionally, there are six non-segmental interneurons, three right-hand commissures and one left-hand commissure in each segment (Figure 2.6) (Martin, 1997; Martin *et al.*, 1991; Stretton *et al.*, 1978). The six non-segmental interneurons are located in the ventral nerve cord with their somata in the head or tail segments.

2.2.2 Muscular System

Transversely, the anterior portion of *Ascaris* body (from outside to inside, Figure 2.7A) shows the body to be composed of three concentric rings of cuticle, hypodermis and somatic muscle layer which surrounds the perienteric cavity containing the gut (Martin, 1997; Martin *et al.*, 1991). Two fields (dorsal and ventral) of mononucleated muscle cells (5 x 10^4 in number) which form the somatic muscle layer are separated by the two lateral lines

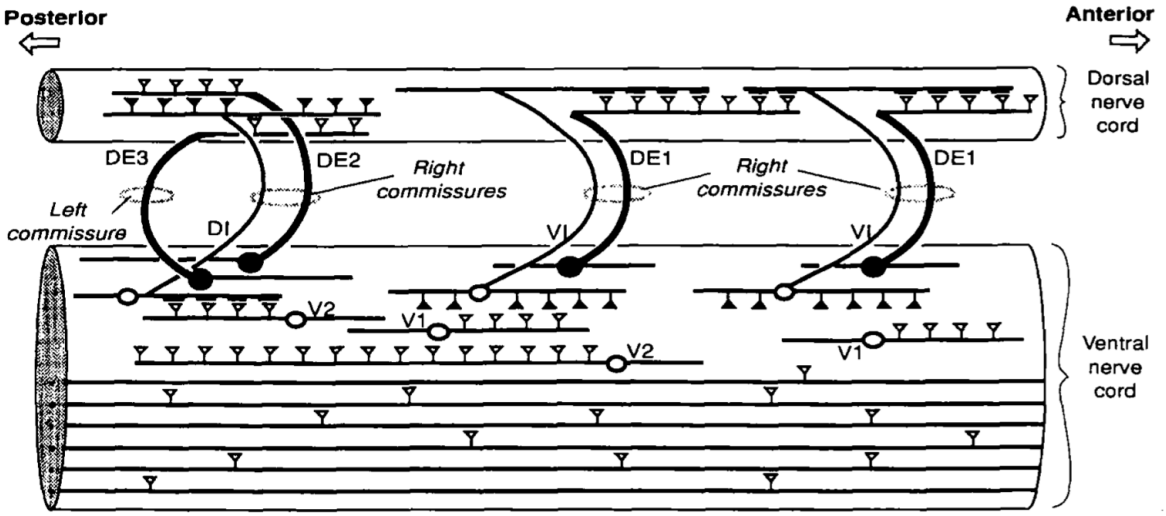

Source: Martin, 1997, p. 14.

Figure 2.6 Organization of *Ascaris suum* motor nervous system in one segment. Each segment contains eleven motoneurons and six non-segmental interneurons. The seven morphological types of motoneurons are indicated as DI: dorsal inhibitory, VI: ventral inhibitory, DE1: dorsal excitatory 1, DE2: dorsal excitatory 2, DE3: dorsal excitatory 3, V1 and V2: ventral excitatory.

(Stretton, 1976). Anchored to the hypodermis is the obliquely striated contractile substance known as the spindle or fibre which has an average length of *ca* 2 mm (del Castillo *et al*., 1989; Rosenbluth, 1965a). The muscle cell forms a large, balloon-like structure called the bag or belly around mid-point of the spindle. The muscle bag (Figure 2.7B) measures *ca* 200 – 250 μm in diameter and contains the single nucleus of the cell. Each muscle cell sends out processes called muscle arms which project from the base of the bag and transversely cross the muscle field to reach the syncytium over the nerve cord. Most muscle cells have more than one muscle arm, the mean number of arms is 2.7 (Stretton, 1976). Each arm branches from the nerve cord into thin terminal processes or fingers. The fingers of one arm form tight,

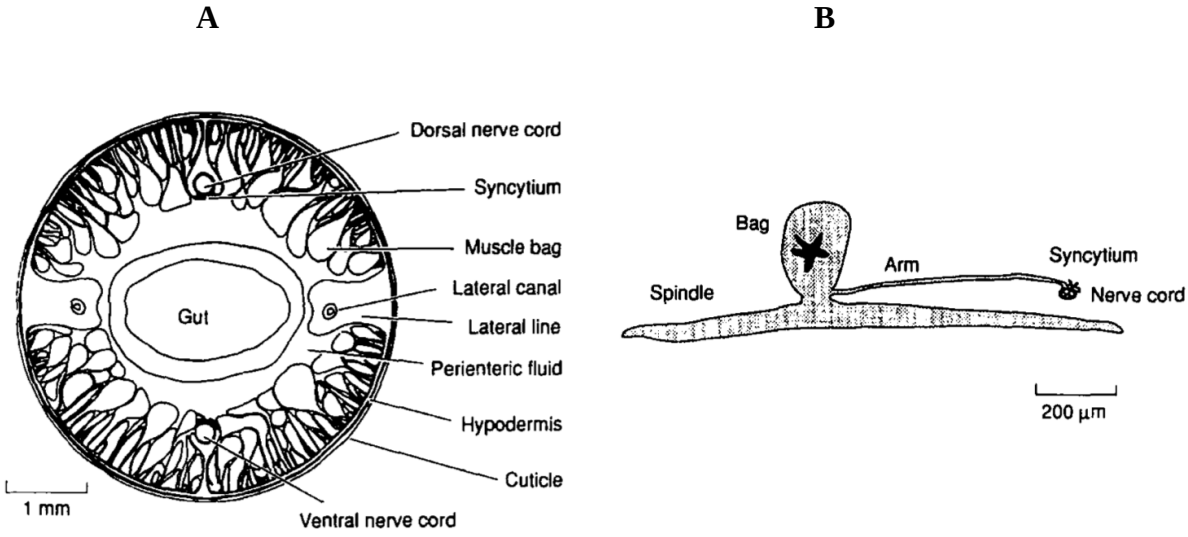

Source: Martin, 1997, p. 14.

Figure 2.7 Transverse section of anterior section of *Ascaris* body showing arrangement of the three concentric rings of cuticle, hypodermis, somatic muscle layer, perienteric fluid and gut (A) and *Ascaris* muscle cell showing the muscle bag, spindle, arm, syncytium and nerve cord (B).

interwined junctions with those of adjacent arms at the syncytium. The interwound fingers extend longitudinally apposed to the nerve cord and are responsible for electrical coupling of muscle cells (Debell *et al.*, 1963; Rosenbluth, 1965b).

2.3 Nicotinic Acetylcholine Receptors (nAChRs)

Nicotinic acetylcholine receptors (nAChRs) are prototypical Cys-loop ligand-gated ion channels that mediate fast synaptic transmission in the neuromuscular and nervous system of vertebrates and invertebrates. They are an important target for many anthelmintics (Brown *et al.*, 2006). Other members of the Cys-loop superfamily of ligand-gated ion channels (LGICs) include ionotropic receptors for 5-hydroxytryptamine (5-HT), γ-aminobutyric acid (GABA) and glycine (Connolly & Wafford, 2004). The electric ray

Torpedo californica nAChR is the most carefully studied nAChR (Changeux *et al.*, 1996). The structure of the nAChR of a related species (*Torpedo marmorata*) has also been resolved at 4.6Å and 4.0Å (Unwin, 2005). nAChRs are composed of five protein subunits arranged around a central pore that is permeable to cations in most cases (Changeux, 2012; Karlin, 2002). Each nAChR subunit consists of an N-terminal, extracellular domain that contains the cys-loop (two cysteine residues separated by 13 amimo acids), six loops (A – F) and four transmembrane domains (TM1 – TM4) (Figure 2.8). TM2 forms the lining of the ion pore. The subunits are differentiated as α and non-α, whereby α subunits contain two adjacent cysteine residues (linked by a disulfide bond) in loop C which are essential for acetylcholine binding, non-α subunits lack the adjacent cysteines. nAChRs are further differentiated on the basis of their subunit composition as homopentamers, in which all five subunits that make up the pentamer are identical, or as heteropentamers, where the subunits are non-identical and

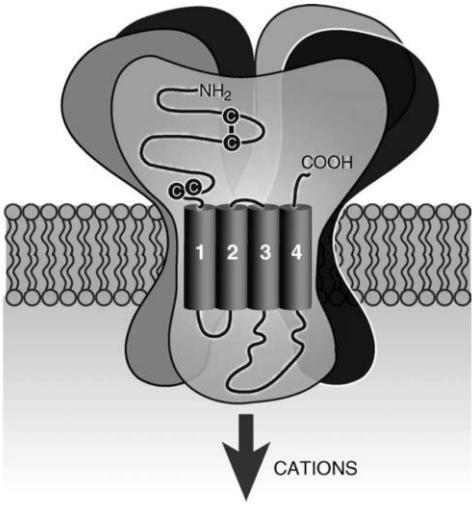

Source: Brown *et al.*, 2006, p. 619.

Figure 2.8 Structure of the nicotinic acetylcholine receptor. Each nAChR consists of five subunits arranged around a cationic channel pore. The cys loop, the vicinal cysteines characteristic if an α subunit and four transmembrane regions (TM1-4) are shown for one subunit

contain at least two α subunits (Bouzat, 2012; Taly *et al.*, 2009). The ligand binding domain of nAChRs has been carefully elucidated using the acetylcholine binding protein (AChBP) from *Lymnaea stagnalis* (Brejc *et al.*, 2001). AChBP though a structural and functional homolog of the N-terminal ligand binding domain of a nAChR subunit, lacks the domains required to form a transmembrane ion channel. AChBP forms a stable homopentamer comprising of 210 residues. It is most closely related to vertebrate nAChR α subunits. Acetylcholine binding involves both an α and an adjacent subunit which could be an α or non-α depending on nAChR pentamer composition. Loops A – F contribute to the ligand binding sites, loops A, B, C from the principal face of the α subunit and loops D, E, F from the complementary face of the adjacent subunit (Arias, 1997).

2.3.1 *Caenorhabditis elegans* nAChRs

C. elegans nAChRs are the most widely studied compared to parasitic nematode or vertebrate nAChRs. Hence, the free-living nematode, *C. elegans*, is a powerful tool for providing insights into the molecular basis of the pharmacology of nAChRs. There are at least 32 nAChR subunits in the model nematode *C. elegans*, 22 of which are α subunits. These subunits are divided into five groups, on the basis of sequence homology, with each group named after the first member to be identified in that group (Holden-Dye *et al.*, 2013). The five groups are DEG-3, ACR-16, ACR-8, UNC-38 and UNC-29 (Figure 2.9). Subunits which display significant homology to nAChRs but do not fall within the five core groups are designated ‘Orphan subunits’, many of whose function is unknown (Brown *et al.*, 2006).

Almost all the members of the DEG-3, ACR-16, ACR-8 and UNC-38 groups are α subunits while those in the UNC-29 group are non-α subunits (Table 2.1). Notably, some

members of the ACR-16 group closely resemble vertebrate homomeric neuronal α7 receptor subunits (Mongan *et al.*, 2002). Different nAChR subunit combinations make up different nAChR types and on this basis, four major nAChR types have been described namely, levamisole-sensitive, nicotine-sensitive, DEG-3/DES-2 and EAT-2 nAChRs. These nAChR types also show different expression patterns and play vital roles in a variety of physiological functions including feeding, motility, development and reproduction. Levamisole-sensitive and nicotine-sensitive receptors are expressed in body wall muscle (Richmond & Jorgensen, 1999). DEG-3/DES-2 receptors are also expressed in neurons (Treinin *et al.*, 1998). EAT-2 receptors are expressed in the pharynx, and require a small transmembrane protein, EAT-18, for pharyngeal pumping (McKay *et al.*, 2004). Still in *C. elegans* (and also parasitic nematodes), different stoichiometry of nAChR subunits produces further different nAChR subtypes (Figure 2.10).

Levamisole (levamisole-sensitive) receptors are the most widely explored group of receptors in both *C. elegans* and parasitic nematodes. The nAChR subunit genes *lev-1*, *unc-29* and *unc-38* have been identified as important for levamisole sensitivity. However, when these subunits were injected in *Xenopus laevis* oocytes, expression levels were generally low as revealed by the small current responses to the major excitatory neurotransmitter, acetylcholine, and the anthelmintic, levamisole (Fleming *et al.*, 1997). Fleming *et al.*, 1997, also showed mecamylamine and neosurugatoxin but not α-bungarotoxin to inhibit the levamisole current responses. Richmond and Jorgensen later showed from *in vivo* recordings from *C. elegans* body wall muscle cells, evidence for the presence of two nAChR types.

These included alevamisole-sensitive receptor, requiring both *unc-29* and *unc-38* subunit genes for its activity, and a second receptor type that was activated by both nicotine

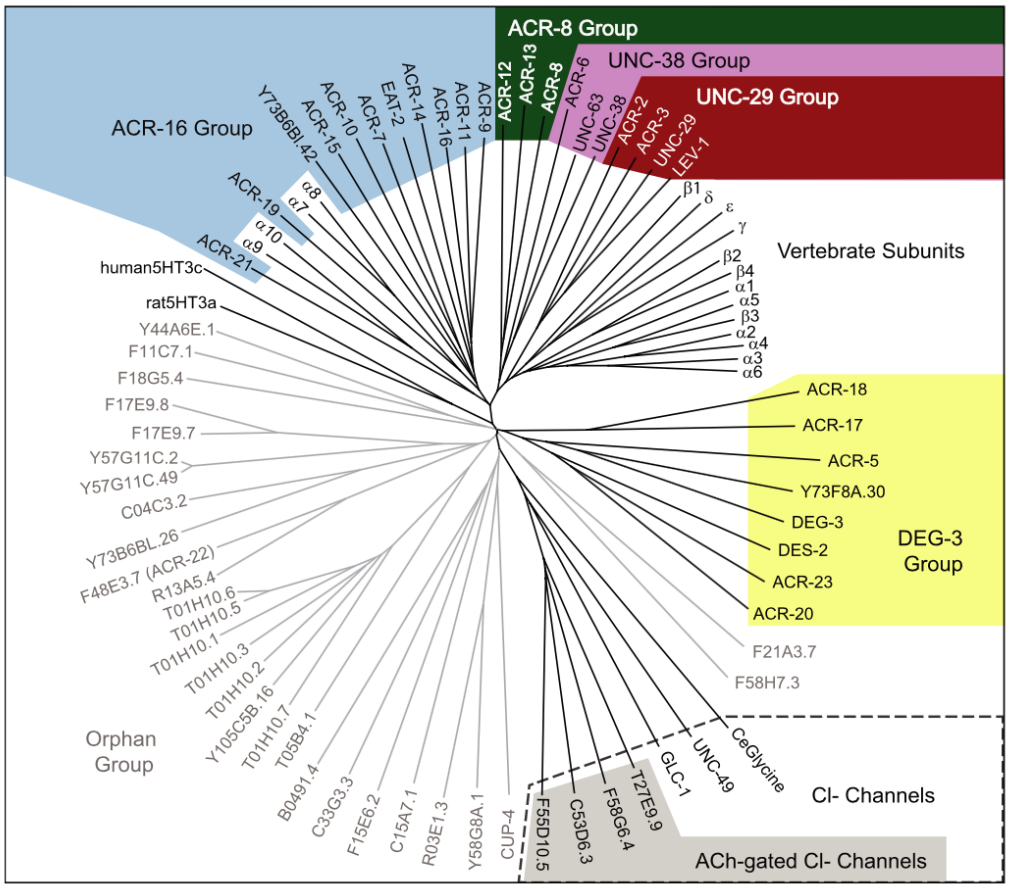

Source: Brown *et al.*, 2006, p. 620.

Figure 2.9 Tree showing the five core groups of nAChR subunits (indicated by the colored regions). Other groups such as the acetylcholine-gated chloride channels and the orphan group are also shown.

and acetylcholine. The receptor that was activated by both nicotine and acetylcholine was present in *unc-29* and *unc-38* mutants and showed rapid desensitization. Also, the levamisole response in wild-type *C. elegans* was completely blocked by d-tubocurarine whereas in *unc-29* mutants, the nicotine response was completely blocked by dihydro-β-erythroidine which caused only a slight block of the levamisole response. The acetylcholine response in wild-type *C. elegans* was only about 50% blocked by dihydro-β-erythroidine. While locomotion in

Table 2.1 Summary of the five core groups of nAChR subunits and their expression pattern in *C. elegans*. (Source: Holden-Dye *et al*., 2013, p. 607.)

Group	Subunit	Expression
DEG-3	ACR-17 α	?
	ACR-18 α	Body wall muscle and nervous system
	ACR-20 α7-like	Body wall muscle and nervous system
	ACR-22 non-α (lcg-11)	?
	ACR-23 α7-like	Body wall muscle and nervous system
	DES-2 α (ACR-4)	Body wall muscle (head) and nervous systems IL2, FLP, PVD, PVC, ALA, and AVG
	DEG 3 α	PVC,, sensory endings of IL2, ALM, and PLM
	ACR-24 α	Role in fast neurotransmission?
	ACR-5 α	Nervous system – head neurons, neurons along body, tail neurons
ACR-16	ACR-7 α7 like	Body wall muscle, pharyngeal muscle, tail neurons
	ACR-9 non-α	Neurons
	ACR-10 α7 like	Body wall muscle and nervous systems?
	ACR-11 α	Muscle
	ACR-14 non-α	DA, VB, AS, DB, DD, HSN, VC4&5, AIY, head and motoneurons, muscle, and intestine
	ACR-15 α	Muscle (head and body wall), AVA, AVB, DVA, RID, PVQ, SMB?, SMD, 15, RIM, SAA, SIA, and SIB, all ventral nerve cord motoneurons except DD
	ACR-16 α7 like	Body wall muscle & subset of neurons, AVA, RIB, RID, SIB, SMD, DM motoneuron head and tail neurons
	ACR-19 α	Neurons?
	ACR-21 α	Ventral nerve cord cholinergic neurons
	ACR-25 non-α?	?
	EAT-2 non-α	Pharyngeal muscel (pm4&5)
ACR-8	ACR-8 α	All body wall muscle, head & tail neurons, anal and vulval muscles, nerve ring, nerve cord, ventral nerve cord motoneurons
	ACR-12α	Ventral nerve cord neurons, head & tail nervous system
	LEV-8(ACR-13) α	Body wall (strongest in head regiou) and vulval muscles, head neurons, mechanosensory neurons, many ventral nerve cord motoneurons, socket cells
UNC-38	UNC-38 α	Body wall and vulval muscles, nervous system, colocalizes with TAX-6, ACR-8, ACR-12, and UNC-29; dorsal and ventral nerve cord
	UNC-63 α	Body wall & vulval muscle, ventral cord motoneurons, AS, DA, DB, VB, VD, DV, and VC, widespread in neurons
	ACR-6 α	Role in fast neurotransmission
UNC-29	ACR-2 non α	Forms functional channel with UNC-38, muscle & nervous system, ventral cord neurons, e.g., VA, VB, DA, DB (cholinergic motoneurons); PVQ, DVC, IL-1, RMD; tail neurons
	ACR-3 non-α	Body wall muscle and nervous systems, forms functional channels with UNC-38
	UNC-29 non-α	Body wall and head muscles, nervous system, ventral & dorsal cords, nerve ring
	LEV-1 (ACR-1) non-α	All body wall muscles, some ventral cord neurons

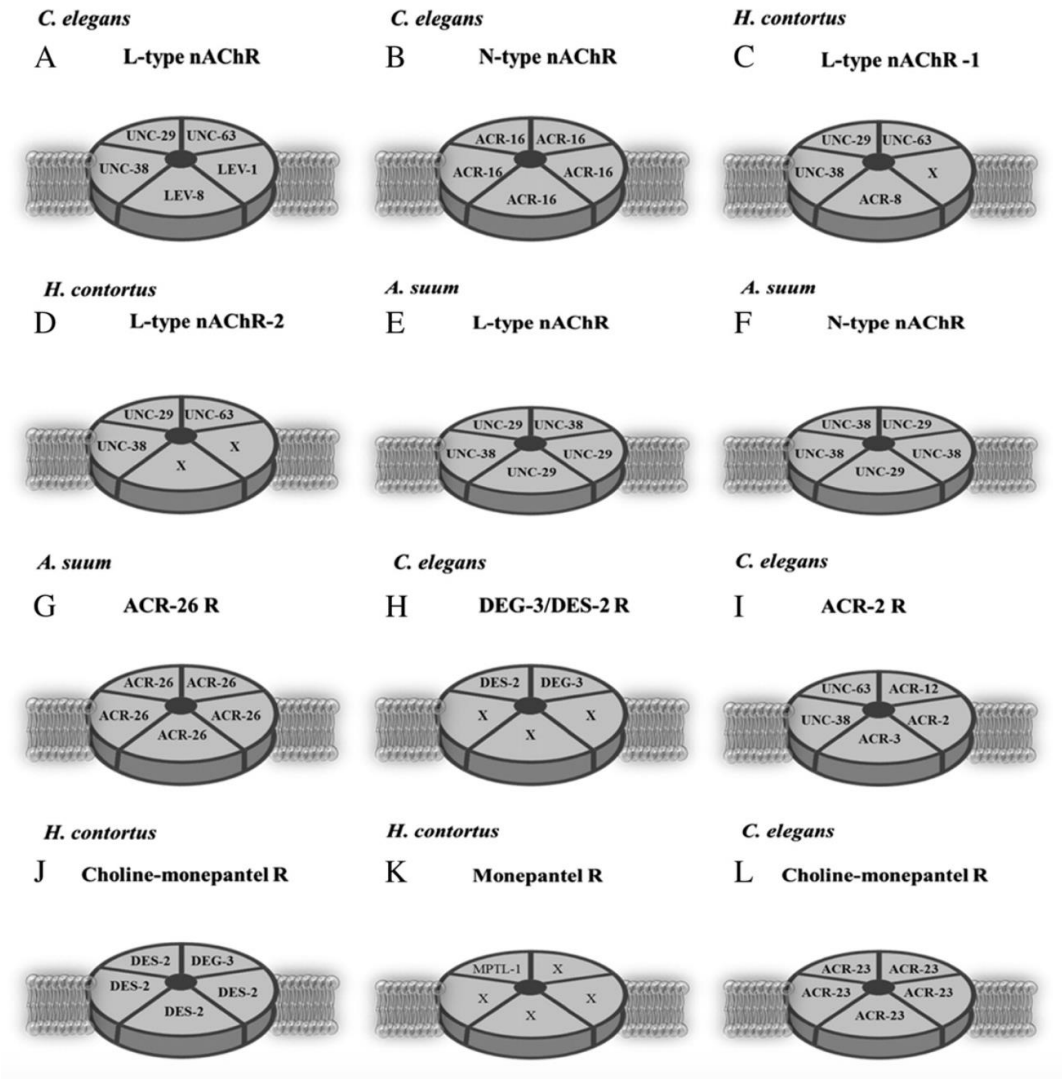

Source: From Holden-Dye *et al*., 2013, p. 608.

Figure 2.10 Proposed stoichiometry of nAChRs in *C. elegans* and parasitic nematodes, showing possible subunit combinations for the various nAChR types.

unc-29 and *unc-38* mutants wasimpaired, the response to acetylcholine was maintained, suggesting an equal contribution of the nicotine-sensitive, N-AChR and the levamisole-sensitive, L-AChR to the acetylcholine response (Richmond & Jorgensen, 1999). In addition to *lev-1*, *unc-29* and *unc-38*, the *C. elegans unc-63* subunit gene has been shown to confer levamisole sensitivity (Culetto *et al*., 2004). Subsequently, the L-AChR was described in *X.*

laevis oocyte expression studies to require five nAChR subunits, UNC-29, UNC-38, UNC-63, LEV-1 and LEV-8 (also known as ACR-13), LEV-1 and UNC-29 are non-α subunits while UNC-38, UNC-63 and LEV-8 are α subunits. All five subunits, in addition to three ancillary proteins (RIC-3, UNC-50 and UNC-74) were required for functional expression of the L-AChR (Boulin *et al.*, 2008). The ancillary proteins RIC-3, UNC-50 and UNC-74 are respectively involved in the maturation, trafficking and folding of the receptor (Eimer *et al.*, 2007; Halevi *et al.*, 2002; Haugstetter *et al.*, 2005). Boulin *et al*., 2008, also showed d-tubocurarine, methyllycaconitine and hexamethonium to be potent antagonists of the L-AChR, while α-bungarotoxin and dihydro-β-erythroidine had modest blocking effects, in agreement with observations by Richmond & Jorgensen (1999). Another subunit, ACR-8, has been identified in *C. elegans* body wall muscle but its role is uncertain as it neither contributes to levamisole-sensitive or insensitive nAChRs (Touroutine *et al.*, 2005).

Nicotine-sensitive nAChRs or N-AChRs are sensitive to nicotine but insensitive to levamisole. Unlike levamisole receptors which are composed of heteropentamers, N-AChRs are homopentamers. Five ACR-16 subunits make up a N-AChR in *C. elegans* (formerly called Ce21) which is closely related to vertebrate α7 receptors (Ballivet *et al.*, 1996; Raymond *et al.*, 2000). Also, N-AChRs require only RIC-3 for their functional expression in *X. laevis* oocytes. Ballivet *et al*. (1996), further demonstrated that levamisole not only failed to activate the *C. elegans* ACR-16 receptor but also antagonized acetylcholine responses. Additionally, dihydro-β-erythroidine acted as a potent antagonist of the *C. elegans* ACR-16 receptor, as opposed to very weak antagonism on L-AChRs. *C. elegans* ACR-16 is also strongly antagonized by d-tubocurarine but weakly antagonized by methyllycaconitine and

α-bungarotoxin. Ballivet *et al*. (1996), showed the *C. elegans* ACR-16 receptor to desensitize rapidly following application of acetylcholine or nicotine. Although nicotine was a more potent agonist of the *C. elegans* ACR-16 receptor than acetylcholine (EC_{50} 12.6 μM for nicotine versus 55.4 μM for acetylcholine), the maximum response for nicotine was lower than that for acetylcholine, suggesting nicotine is a partial agonist of the *C. elegans* ACR-16 receptor. Interestingly, *acr-16* mutants showed no obvious behaviorial phenotype but *unc-63:acr-16* or *unc-29:acr-16* double mutants showed more severe locomotory deficits than either *unc-63* or *unc-29* mutants (Li *et al.*, 2014; Touroutine *et al.*, 2005).

Members of the DEG-3 group of nAChRs are preferentially activated by the amino-acetonitrile derivative, monepantel, causing spastic paralysis of body wall and pharyngeal muscles. DEG-3-like nAChRs have been identified only in nematodes. The major subunit member is ACR-23 which is expressed mainly in *C. elegans* body wall muscles and in unidentified head and tail neurons (Rufener *et al.*, 2013). Rufener *et al*. (2013), also reconstituted functional receptors made up of *C. elegans* ACR-23 subunits in *Xenopus* oocytes and showed that these receptors responded to monepantel, in addition to choline, nicotine, and acetylcholine, in order of current response magnitude, with choline responses strongly potentiated by monepantel. Another subunit member of the DEG-3 group is ACR-20 which forms homomeric receptors just like ACR-23 (Baur *et al.*, 2015). According to Baur *et al.* (2015), low concentrations (<1 nM) of monepantel produced positive allosteric modulatory effects on the *C. elegans* ACR-20 receptor, while high concentrations (>0.1 μM) produced direct agonist effects on the receptor. Functional receptors comprising of *C. elegans* DEG-3 and DES-2 subunits have also been reconstituted in *X. laevis* oocytes where

the receptors were activated by choline and acetylcholine, with choline as the more potent agonist (Treinin *et al.*, 1998; Yassin *et al.*, 2001).

EAT-2 nAChRs are not a well-exploited target for anthelmintic drug development. These receptors are localized postsynaptically on pharyngeal muscle and require interaction with the protein EAT-18 for nicotinic transmission in *C. elegans* pharynx (McKay *et al.*, 2004). Hence, EAT-2 receptors are believed to play a role in pharyngeal pumping and therefore, feeding. At present, it is not known if EAT-2 is homomeric or requires other subunits to form the receptor.

2.3.2 Parasitic nematode nAChRs

Parasitic nematode nAChRs are therapeutic targets for many anthelmintics including levamisole, pyrantel, oxantel, bephenium and morantel. The nAChR from the pig parasitic nematode *Ascaris suum* (clade III) is the most extensively studied parasitic nematode nAChR. Initial patch clamp recordings from *Ascaris* muscles revealed the presence of at least two acetylcholine-activated channel types (Pennington & Martin, 1990). Single channel recordings from *Ascaris* muscle later showed low levamisole concentrations (1 – 10 μM) to cause channel opening and high levamisole concentrations (30 and 90 μM) to cause flickering channel block. The channel conductance was in the range of 18 – 50 pS (Robertson & Martin, 1993). Pyrantel and oxantel were also shown to act as agonists and open channel blockers of these channels (Dale & Martin, 1995; Robertson *et al.*, 1994). Muscle contraction studies using different agonists and antagonists revealed the existence of more than one nAChR type on *Ascaris* body wall muscle with different sensitivities to agonists and antagonists (Robertson *et al.*, 2002). Three nAChR types on *Ascaris* muscle having different channel conductances and mean open times have been characterized at the single channel

level using the patch clamp technique (Qian *et al.*, 2006). These nAChR types have been named after their preferred agonist and include the L-type preferentially activated by levamisole, the N-type preferentially activated by nicotine and the B-type preferentially activated by bephenium (Figure 2.11). The single channel conductance and mean open times are respectively, 24 pS and 0.6 ms for the N-type, 35 pS and 0.9 ms for the L-type, and 45 pS and 1.3 ms for the B-type. Unlike in *C. elegans* where the actions of levamisole and nicotine

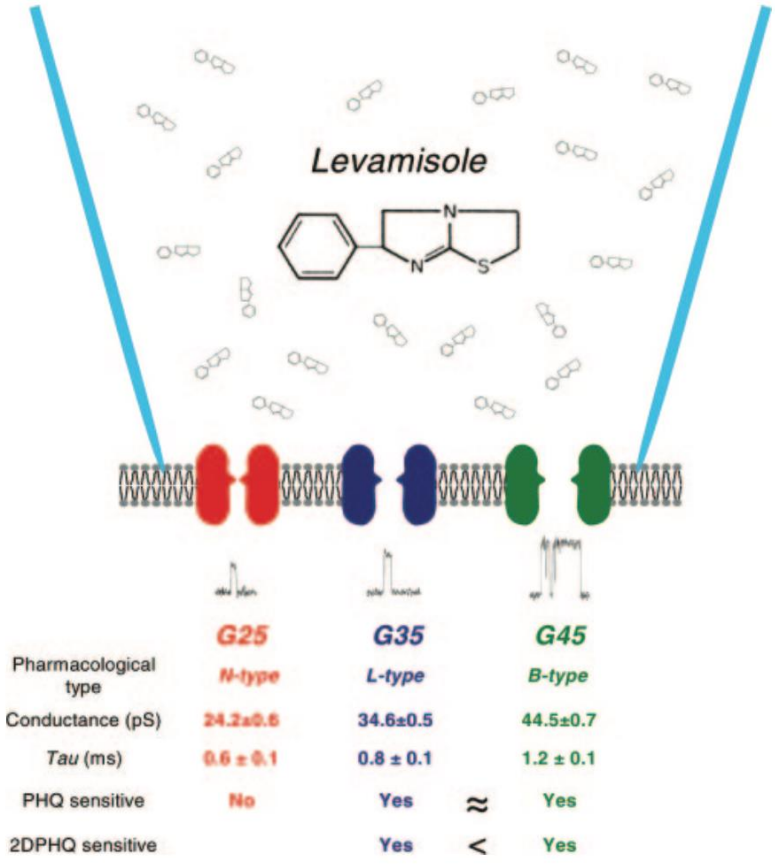

Source: Qian *et al*., 2006, p. E2115.

Figure 2.11 Summary diagram of nAChR subtypes on *Ascaris suum* somatic muscle cell membrane. The single channel as well as agonist and antagonist pharmacological properties of each subtype are indicated. N-subtype prefers nicotine, L-subtype prefers levamisole and B-subtype prefers bephenium. The subtypes show different sensitivities to the competitive antagonists paraherquamide (PHQ) and 2-desoxoparaherquamide (2DPHQ).

are selective (levamisole-sensitive currents are not activated by nicotine and vice versa), the differences in agonist action are subtler in *A. suum*. For instance, although levamisole preferentially activates L-type channels, it also opens N- and B-type channels to a lesser extent. Bephenium preferentially activates B-type channels but also opens some L-type but not N-type channels. Hence, nAChR types in *A. suum* are less distinct in terms of agonist pharmacology than those in *C. elegans*. At high concentrations, levamisole activates all three nAChR types in *A. suum*.

In addition to the 25 pS, 35 pS and 45 pS single channel conductances, a fourth levamisole-activated subtype with a conductance of 40 pS has been revealed in the strongylid nematode *Oesophagostomum dentatum* (clade V), suggesting the presence of four nAChR types in *O. dentatum* (Robertson *et al.*, 1999). Robertson *et al*. (1999), also showed loss of the G35 channel in levamisole-resistant (LEVR) parasites which was present in levamisole-sensitive (SENS) parasites (Figure 2.12). Therefore, just as in *A. suum*, the G35 channel is the L-type nAChR.

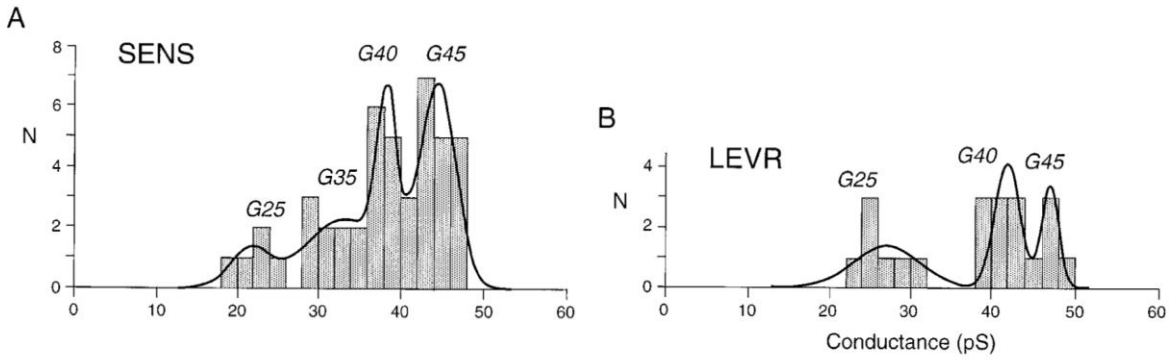

Source: Robertson *et al*., 1999, p. 757.

Figure 2.12 Frequency histograms of single channel conductances for SENS (A) and LEVR (B) parasites.

In *O. dentatum*, different nAChR subunit combinations expressed in *Xenopus* oocytes have revealed the presence of four distinguishable nAChR subtypes based on agonist sensitivities (Buxton *et al.*, 2014). These include the pyrantel (Pyr)-nAChR composed of UNC-29 and UNC-63 subunits, the pyrantel/tribendimidine (Pyr/Tbd)-nAChR composed of UNC-29, UNC-63 and UNC-38 subunits, the acetylcholine (ACh)-nAChR composed of UNC-29, UNC-63 and ACR-8 subunits, and the levamisole (Lev)-nAChR composed of UNC-29, UNC-63, UNC-38 and ACR-8 subunits (Figure 2.13). Note that the LEV-8 subunit has not been detected in any nematode parasite, however, a related subunit (ACR-8) can replace LEV-8 to reconstitute L-AChRs in the parasites. In accordance with *in vivo* studies, Buxton *et al*. (2014), showed the levamisole-nAChR comprising of UNC-29, UNC-63,

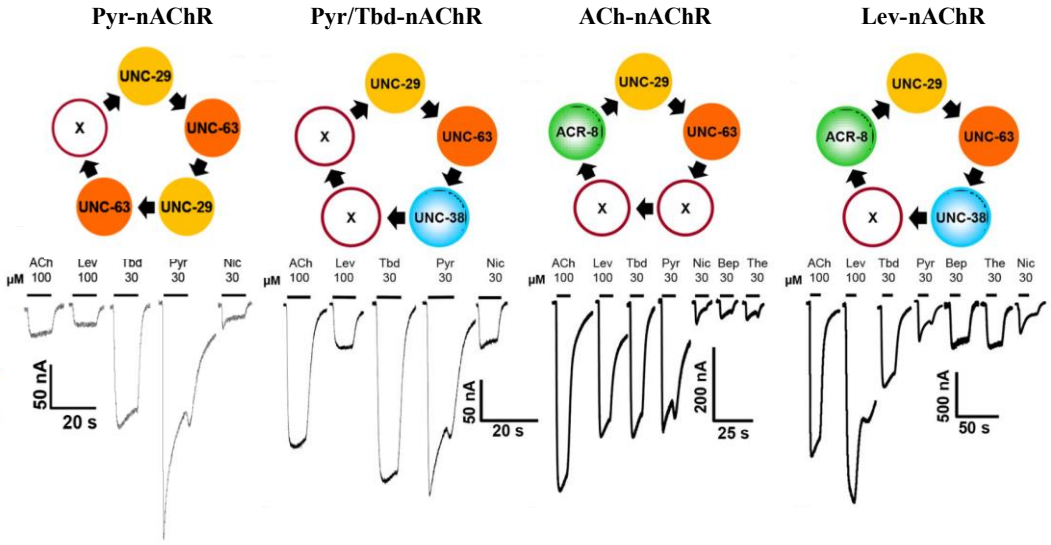

Source: Modified from Buxton *et al*., 2014, pp. 5 & 7.

Figure 2.13 Summary of the four *O. dentatum* nAChR subtypes based on different combinations of subunits reconstituted in *Xenopus laevis* oocytes. The pyrantel (Pyr)-nAChR is composed of UNC-29 and UNC-63 subunits, the pyrantel/tribendimidine (Pyr/Tbd)-nAChR is composed of UNC-29, UNC-63 and UNC-38 subunits, the acetylcholine (ACh)-nAChR is composed of UNC-29, UNC-63 and ACR-8 subunits, and the levamisole (Lev)-nAChR is composed of UNC-29, UNC-63, UNC-38 and ACR-8 subunits.

UNC-38 and ACR-8 subunits to have a single channel conductance of 35 pS. These authors also demonstrated that varying the subunit stoichiometry of the pyrantel-nAChR comprising of UNC-29 and UNC-63 subunits produced changes in its pharmacological properties. When the ratio of *unc-29:unc-63* injected cRNA was 1:5, the pyrantel and tribendimidine current responses were significantly increased, and when it was 5:1, the nicotine and levamisole current responses became significantly bigger than the acetylcholine response.

Two L-AChR subtypes have also been identified in *A. suum* by varying the stoichiometry using different ratios of UNC-38 and UNC-29 subunits (Williamson *et al.*, 2009). Oocytes injected with *unc-38* and *unc-29* cRNA at ratios of 5:1 and 1:5 produced robust current responses compared to those injected at ratios of 10:1 and 1:10 which produced very small current responses. Also, when the *unc-38:unc-29* ratio was 5:1, nicotine acted as a full agonist and levamisole acted as a partial agonist, whereas when the ratio was 1:5, levamisole was a full agonist and nicotine a partial agonist. Still with the 5:1 ratio, oocytes responded to oxantel but not pyrantel, while with the 1:5 ratio, oocytes responded to pyrantel but not oxantel.

Genes encoding UNC-38, UNC-29, UNC-63 and ACR-8 have been identified in *Hemonchus contortus*, which belongs to Clade V just as *O. dentatum* and *C. elegans*. Two types of L-AChRs namely Hco-L-AChR1 and Hco-L-AChR2 were identified in *H. contortus* by varying subunit combinations (Boulin *et al.*, 2011). The receptor Hco-L-AChR1 which is made up of all four subunits UNC-38, UNC-29, UNC-63 and ACR-8 was more sensitive to levamisole than acetylcholine and was weakly sensitive to pyrantel and nicotine. Omitting ACR-8 from the combination produced the Hco-L-AChR2 receptor which was more sensitive to pyrantel and acetylcholine than levamisole. Recently, four copies of the *unc-29*

L-AChR subunit gene (Hco-UNC-29.1, Hco-UNC-29.2, Hco-UNC-29.3 and Hco-UNC-29.4) were identified in *H. contortus*, and duplication of the *unc-29* L-AChR subunit gene was shown to be a common feature of the clade V parasitic nematodes (Duguet *et al.*, 2016). Substituting each of the four UNC-29 copies in the Hco-L-AChR1 receptor subunit composition produced three functional receptor types which differed from each other in terms of agonist and antagonist pharmacology. UNC-29.2 failed to reconstitute a functional receptor. L-AChR1.1 comprised of UNC-38, UNC-29.1, UNC-63 and ACR-8 subunits and was more responsive to levamisole than acetylcholine. Additionally, mecamylamine was a potent antagonist of L-AChR1.1. When the UNC-29.1 subunit was replaced with UNC-29.2 (L-AChR1.2), the oocytes did not produce any detectable current responses. When UNC-29.1 was replaced with UNC-29.3 (L-AChR1.3), the acetylcholine response was greater than the levamisole response and mecamylamine was a less potent antagonist. When UNC-29.1 was replaced with UNC-29.4 (L-AChR1.4), levamisole and acetylcholine responses were about equal and mecamylamine was more potent (Figure 2.14).

2.3.3 Vertebrate nAChRs

Vertebrate nAChRs contain five subunits namely α, β, γ, δ and ε and are important therapeutic targets for various neurodegenerative diseases including Alzheimer's disease, Parkinson's, disease and schizophrenia, as well targets to treat alcohol and nicotine dependence (Dineley *et al.*, 2015; Dwoskin *et al.*, 2009; Posadas *et al.*, 2013). A total of 17 nAChR subunits have been identified in vertebrates (Millar & Gotti, 2009). This number is less than the 32 subunits identified in *C. elegans*. Vertebrate nAChRs can be divided into two groups based on their primary site of expression as muscle and neuronal nAChRs. Muscle nAChRs are expressed at the neuromuscular junction and are composed of the subunits α1,

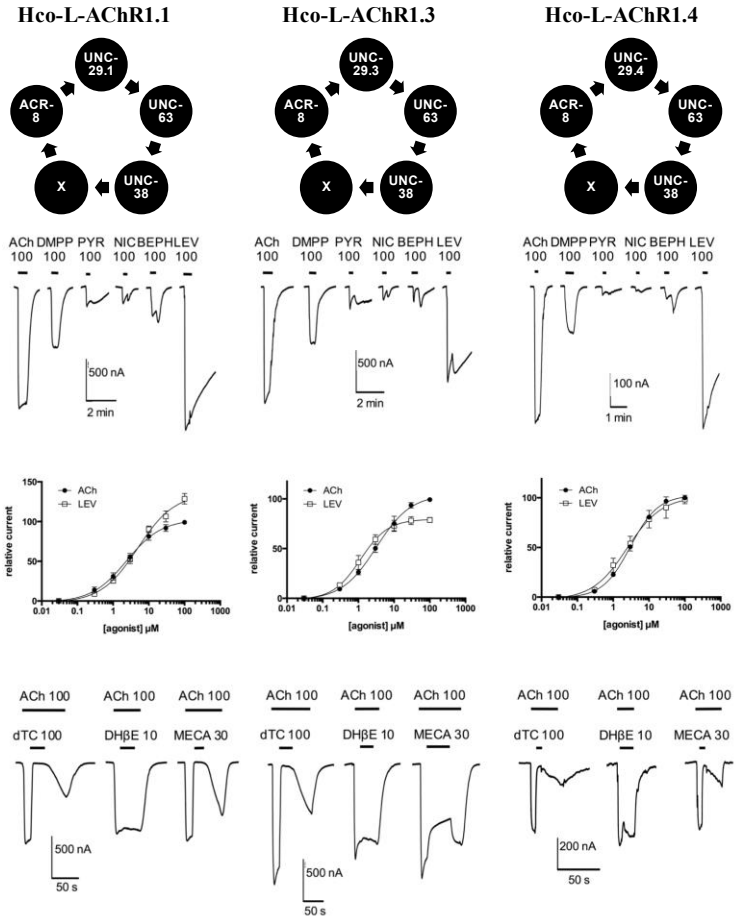

Figure 2.14 Pharmacological profile of *Hemonchus contortus* reconstituted receptors in *Xenopus* oocytes. *Hco-unc-29.1*, *Hco-unc-29.3* and *Hco-unc-29.4* were individually combined with *Hco-unc-63*, *Hco-unc-38* and *Hco-acr-8* and co-expressed with the three ancillaries *Hco-unc-3.1*, *Hco-unc-50* and *Hco-unc-74*. All responses were normalized to 100 µM acetylcholine to generate the acetylcholine and levamisole concentration-response curves. Modified from Duguet *et al*., 2016, pp. 12/26.

β1, δ, and either γ and ε. The five muscle nAChRs co-assemble into only two nAChR subtypes, embryonic and adult. Embryonic muscle nAChRs are composed of $(\alpha1)_2$, β1, γ and δ subunits whereas adult muscle nAChRs are composed of $(\alpha1)_2$, β1, δ and ε. Neuronal nAChRs are more diverse than muscle nAChRs and comprise of various homomeric or heteromeric combinations of twelve subunits: α2 – α10 and β2 – β4 (Kalamida *et al.*, 2007; Millar, 2003). Most vertebrate neuronal nAChRs are heteromeric, containing at least one α

and one β subunit (most commonly $(\alpha)_2(\beta)_3$). Only α7, α8 and α9 subunits reconstitute functional homomeric nAChRs in *Xenopus* oocytes (Couturier *et al.*, 1990; Elgoyhen *et al.*, 1994; Gerzanich *et al.*, 1994). Evidence for co-assembly and subunit diversity of vertebrate nAChRs has been revealed in the insect *Drosophila* and *C. elegans* models. In *Drosophila*, 10 nAChR subunits have been identified and 42 possible nAChR subunits have been predicted in *C. elegans* (Bargmann, 1998; Littleton & Ganetzky, 2000). Table 2.2 provides a summary of vertebrate nAChR subunit combinations from studies of native nAChRs and heterologous expression studies.

2.4 Medicinal plants

Broadly, medicinal plants are defined as plants which have similar therapeutic properties with conventional pharmaceutical drugs. Humans have used medicinal plants to cure or lessen disease symptoms since ancient times. Even today, a large proportion of the population in developing nations still rely on phytomedicine for primary health care and treatment of diseases in animals (Githiori *et al.*, 2005; Tagboto & Townson, 2001). Medicinal plants are frequently preferred because they are perceived to be well-tolerated and have fewer side effects compared to conventional pharmaceuticals (Petrovska, 2012). It is also important to remember that many drugs used in modern medicine today are modeled from medicinal plant products. Use of medicinal plants to treat anthelmintic infections in livestock and humans continues to be exploited as an alternative to pharmaceutical products (Githiori *et al.*, 2004). Remarkably, use of plants to treat worm infections in animals is no longer limited to developing nations. The developed world is experiencing a widespread reawakening in phytomedicine. This is driven in part by the limited availability of pharmaceutical anthelmintic drugs and the widespread occurrence of multidrug resistance

Table 2.2 Assembly and subunit diversity of vertebrate nicotinic acetylcholine receptors. (Modified from Millar, 2003, p. 871.)

Receptor subtype	Subunits	Subunit combinations
Muscle-type	$\alpha 1$, $\beta 1$, γ, δ, ε	$\alpha 1,\beta 1,\gamma,\delta$‡
		$\alpha 1,\beta 1,\varepsilon,\delta$‡
Neuronal (αBTX-insensitive)	$\alpha 2$–$\alpha 6$, $\beta 2$–$\beta 4$	$\alpha 2\beta 2$
		$\alpha 2\beta 4$
		$\alpha 3\beta 2$
		$\alpha 3\beta 4$
		$\alpha 4\beta 2$
		$\alpha 4\beta 4$
		$\alpha 6\beta 2$§
		$\alpha 6\beta 4$
		$\alpha 2\alpha 5\beta 2$
		$\alpha 3\alpha 5\beta 2$
		$\alpha 3\alpha 5\beta 4$
		$\alpha 3\alpha 6\beta 2$
		$\alpha 3\alpha 6\beta 4$
		$\alpha 3\beta 3\beta 4$
		$\alpha 4\alpha 5\beta 2$
		$\alpha 5\alpha 6\beta 2$
		$\alpha 6\beta 3\beta 4$
		$\alpha 3\alpha 5\beta 2\beta 4$
		$\alpha 3\alpha 6\beta 3\beta 4$
		$\alpha 4\alpha 5\alpha 6\beta 2$
		$\alpha 4\beta 2\beta 3\beta 4$
Neuronal (αBTX-sensitive)	$\alpha 7$, $\alpha 8$¶	$\alpha 7$
		$\alpha 8$
		$\alpha 7\beta 2$
		$\alpha 7\beta 3$
		$\alpha 7\alpha 8$
		$\alpha 5\alpha 7\beta 2$
		$\alpha 5\alpha 7\beta 4$
Sensory epithelia	$\alpha 9$, $\alpha 10$	$\alpha 9$
		$\alpha 9\alpha 10$

(Waller *et al.*, 2001). Although the bioactive compounds in medicinal plants have not been fully identified, scientific validation of the anthelmintic activity of several of these plant species have been reported (Al-Abd *et al.*, 2013; Githiori *et al.*, 2006). Interaction between additional healers and scientists as well as research aiming to identify the bioactive compounds in plants with anthelmintic activity should therefore be promoted as this could accelerate anthelmintic drug discovery and development.

2.4.1 *Daniellia oliveri*

Daniellia oliveri is a deciduous, medium-sized tree of the family Caesalpinaceae up to 25 – 35 m tall. The genus *Daniellia* comprises 10 species which are all confined to the forest areas of West and Central Africa. Only *D. oliveri* extends to Sudan and Uganda. *D. oliveri* flowers during the dry season from October to March and fruits from January to June. Various biological activities for *D. oliveri* have been reported. Cardiac glycosides present in the methanol extract of the bark showed non-competitive antagonism on muscarinic receptors on isolated rat bladder smooth muscle (Onwukaeme *et al.*, 1999a). Methanol extracts of the leaves and stem bark were showed to possess neuromuscular blocking properties on rat skeletal muscle (Onwukaeme *et al.*, 1999b). The smoke of the bark of *D. oliveri* is traditionally used to repel mosquitoes in Guinea Bissau, West Africa, and may significantly contribute to reducing prevalence of diseases transmitted by these mosquitoes (Palsson & Jaenson, 1999a; Palsson & Jaenson, 1999b). The leaves of *D. oliveri* are traditionally used to treat diarrhea in Northern Nigeria (Ahmadu *et al.*, 2007). Ahmadu *et al.* (2007), showed the n-butanol extract of *D. oliveri* leaves to protect against castor oil-induced diarrhea in mice. The anti-diarrheal effect of this extract was dose-dependent; 200 mg/kg of the extract provided 80% while 100 mg/kg and 50 mg/kg provided 60% protection against

diarrhea. Various aqueous and ethanol extracts of the leaves, bark and roots showed *in vitro* antibacterial activity against a range of pathogenic bacteria including *Staphylococcus aureus*. The ethanol extract of the leaves also showed significant antifungal activity against *Tricophyton rubrum* (Ahmadu *et al.*, 2004). Fodders supplemented with *D. oliveri* foliage improved performance of buckling goats fed threshed sorghum top basal diet (Isah *et al.*, 2015; Okunade *et al.*, 2016).

2.4.2 *Psorospermum febrifugum*

Psorospermum febrifugum (family Hypericaceae) is a flowering shrub or tree up to 4 m high that is widespread in tropical Africa but grows predominantly in the savanna from Guinea to West Cameroon. *P. febrifugum* as the name implies is known for its febrifugal action. The bark and roots are used to treat all sorts of skin infections including 'craw-craw' and other parasitic skin diseases. The bark is used in Bukoba Rural district in Tanzania for the traditional treatment of skin infections including body sores and Herpes zoster (Kisangau *et al.*, 2007). These authors showed the petroleum ether, dichloromethane and water extract of *P. febrifugum* bark to have antimicrobial activity against *Escherichia coli*. *P. febrifugum* is rich in antioxidants. Xanthones and emodines have been isolated from *P. febrifugum* and showed to possess antioxidant, anticancer, antiviral and antimicrobial potential (Permana *et al.*, 1994; Tsaffack *et al.*, 2009). The leaves, stem bark and root bark of *P. febrifugum* are used for traditional treatment of HIV/AIDS and its asscociated symptoms in some districts in Uganda (Lamorde *et al.*, 2010).

2.4.3 The drug development pipeline

The demand for new antiparasitic therapeutic agents to complement or replace existing ones is on the rise as resistance is likely to compromise every drug over time. Use of

existing drugs is also limited by their side effects, poor compliance and limited efficacy (Renslo & McKerrow, 2006). Therefore, a drug development pipeline is essential for securing the availability of new therapies should existing ones fail. The drug development pipeline represents the series of activities involved in the discovery and production of a new therapeutic product (Figure 2.15). For NTDs, this usually requires cross-sector partnerships with pharmaceutical companies, academic and nonprofit research institutions worldwide (Ramamoorthi *et al.*, 2014a; Ramamoorthi *et al.*, 2014b). Unfortunately, development of the drugs for NTDs is a low priority to pharmaceutical companies, causing the drug development pipeline for these diseases to dry up (Trouiller & Olliaro, 1998; Trouiller & Olliaro, 1999). Collaboration between nonprofit private and public research institutions in both developed and developing countries should therefore be promoted to significantly accelerate development of new drugs (McKerrow, 2005; Trouiller *et al.*, 2002). The very first step in pipeline is the identification and validation of targets. This is followed by high-throughput screening efforts for identification of hits. Hits are further screened to identify leads which show potentials for improvement via development of structure-activity relationships (Nwaka & Hudson, 2006). Lead compounds are screened for activity and toxicity, and those with pharmacological and toxicity profiles within acceptable limits are considered drug candidates and will undergo clinical trials (phases I, II and III) to ascertain their efficacy and safety in humans. Lastly, drug candidates that pass all 3 clinical trial phases are submitted to the Food and Drug Administration (FDA) for review and approval (Roses, 2008). Since it takes at least 15 years for a drug to go through the development pipeline to when it becomes available in the drug market, research leading to discovery of lead compounds must continue so that

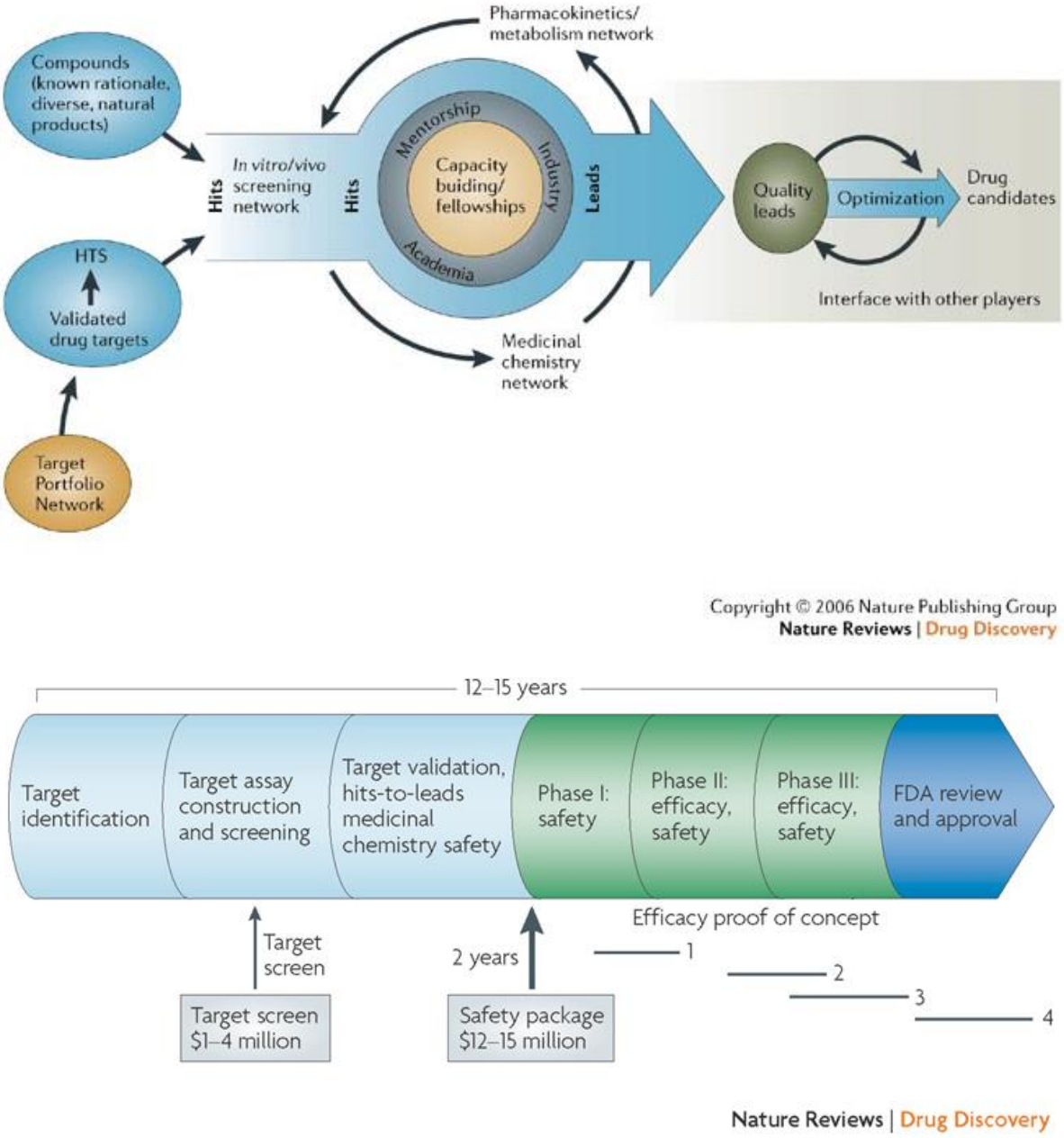

Source: Nwaka & Hudson, 2006, p. 944; Roses, 2008, p. 808.

Figure 2.15 Drug candidate and development pipeline. Top: Lead discovery strategy for tropical diseases. Bottom: Summary of steps involved in drug discovery and development.

compounds will always be available for further development should those in clinical trials or under review fail (Figure 2.15).

2.5 Anthelmintics and anthelmintic resistance

2.5.1 Anthelmintics

Anthelmintics are drugs that are used to treat infections caused by parasitic worms (helminths) (Holden-Dye & Walker, 2007). There are three major groups of helminths namely: nematodes (roundworms), trematodes (flukes) and cestodes (tapeworms) (Castro, 1996). These groups of helminths are divided into two phyla; nematodes (roundworms) and platyhelminths (trematodes and cestodes) (Hotez *et al.*, 2008; Wang *et al.*, 2008). Anthelmintics either kill worms or cause their expulsion from the body, without causing any significant damage to the host (Martin *et al.*, 1997). Although there is a high prevalence of parasitic worms, the progress of anthelmintic drug discovery and development by pharmaceutical companies has been slow over the years. One contributing factor is that the majority of those suffering from helminth infections live in developing nations who lack the resources to support a profitable drug market (Pink *et al.*, 2005). Development of new anthelmintics is limited by high costs and modest global markets for antiparasitic drugs and chemicals. The cost of development of a new drug is estimated at US $40 million for livestock use, and more than US $800 million for human use. The global market for antiparasitic drugs and chemicals are estimated at US $12 billion for plant pathogens, $11 billion for livestock and companion animals, and $0.5 for human health (DiMasi *et al.*, 2003; Evans & Chapple, 2002; Martin & Robertson, 2010; Morgan *et al.*, 2011). Many anthelmintic drugs used to treat humans were first developed and marketed as veterinary drugs (Crump & Omura, 2011; Geary, 2005; Omura, 2008). There are only a few classes of

anthelmintics including; benzimidazoles, imidazothiazoles, tetrahydopyrimidines, macrocyclic lactones, amino-acetonitrile derivatives, spiroindoles and cyclooctadepsipeptides.

2.5.1.1 Benzimidazoles (BZs). Thiabendazole was the first benzimidazole anthelmintic agent produced. Since the introduction of thiabendazole in 1961, a number of benzimidazoles with improved efficacy and extended spectrum of action have been developed (McKellar & Scott, 1990). These include mebendazole, albendazole and flubendazole (Figure 2.16). The initial mode of action of benzimidazoles was thought to be inhibition of various parasite metabolic enzymes including fumarate reductase and malate dehydrogenase (Prichard, 1970; Tejada *et al.*, 1987). However, it is now established that benzimidazoles selectively bind with high affinity to parasite β-tubulin and inhibit microtubule polymerization. This results in the destruction of cell structure and consequent death of the parasite (Lacey, 1990).

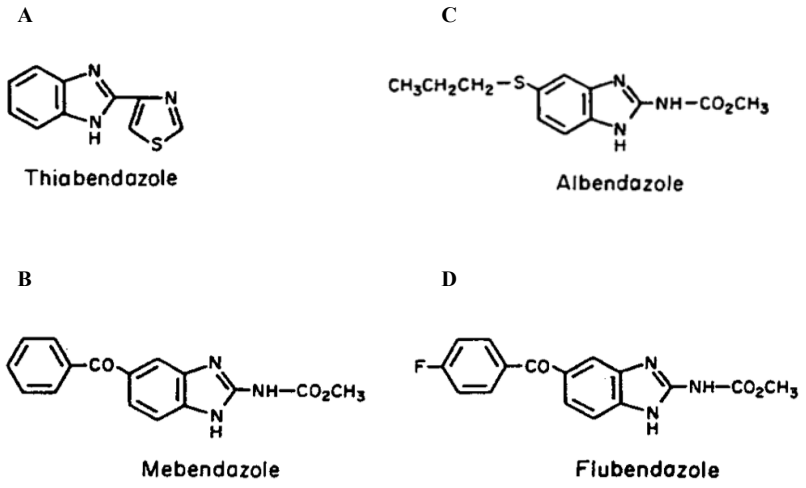

Source: McKellar & Scott, 1990, p. 227.

Figure 2.16 Chemical structures of thiabendazole (A), mebendazole (B), albendazole (C) and flubendazole (D).

2.5.1.2 Imidazothiazoles. Imidazothiazoles act as nicotinic acetylcholine receptor (nAChR) agonists. They bind to nAChRs on body wall muscles, causing spastic paralysis of the worm, and hence, its expulsion from the host (Aceves *et al.*, 1970). Tetramisole (Figure 2.17), an aminothiazol derivative, was the first member of this class of anthelmintics, and constitutes a racemic mixture of 50% L- or S- and D- or R-isomers (Raeymaekers *et al.*, 1966; Raeymaekers *et al.*, 1967; Thienpont *et al.*, 1966). The L-isomer was later demonstrated to be more potent than the racemic mixture or the the D-isomer (Thienpont *et al.*, 1969; Van den Bossche & Janssen, 1967). Consequently, the D-isomer was removed from the racemic mixture and this led to the development of the L-isomer as levamisole. The detailed mode of action of levamisole, the only existing drug in this class, has been carefully studied at the single-channel level in nematode body wall muscles (Qian *et al.*, 2006; Robertson *et al.*, 1999; Robertson & Martin, 1993). Robertson & Martin (1993), showed using the patch-clamp technique that at the single-channel level in *A. suum* muscles. Levamisole (1 – 90 μM concentrations) causes activation of cation-selective channels, in

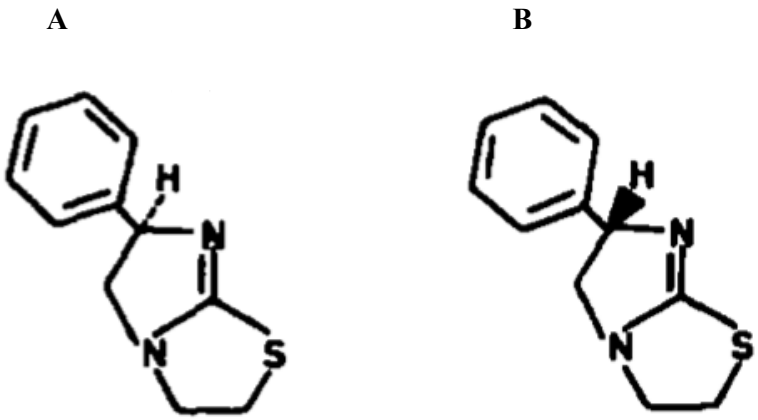

Source: Van den Bossche & Janssen, 1967, p. 1781.

Figure 2.17 Chemical structures of R (+)-tetramisole (A) and S (-)-tetramisole (levamisole) (B)

addition to voltage-sensitive open channel-block and desensitization. The mean open-times for single-channel currents activated by levamisole were 0.80 – 2.85 ms and the conductance levels were 19 – 46 pS, with a mean of 32.9 ± 1.23 pS. This corresponded to the levamisole-sensitive, L-subtype nAChR with a channel conductance of 35 pS, as revealed by Qian *et al.* (2006). Robertson *et al.* (1999) later revealed the presence of a similar nAChR subtype in levamisole-sensitive *O. dentatum* muscle patches which was absent in the levamisole-resistant muscle patches. In subsequent oocyte expression studies, the reconstituted *O. dentatum* L-subtype nAChR (UNC-29, UNC-38, UNC-63 and ACR-8) was preferentially sensitive to levamisole and also had a single channel conductance of ~35 pS (Buxton *et al.*, 2014). Levamisole not only causes spastic paralysis but it also stimulates egg-laying in wild-type *C. elegans* (Trent *et al.*, 1983).

2.5.1.3 Tetrahydropyrimidines. Tetrahydropyrimidines share a similar mode of action to imidazothiazoles and are commonly grouped together as nicotinic agonists (Aubry *et al.*, 1970; Martin, 1997). Examples of this anthelmintic drug class include pyrantel, oxantel and morantel (Figure 2.18). Pyrantel is an imidazothiazole-derived tetrahydropyrimidine that was discovered in 1966 as an anthelmintic agent with broad spectrum activity against roundworms and hookworms in domestic animals (Austin *et al.*, 1966; Howes & Lynch, 1967). Pyrantel however lacks activity against whipworms (McFarland & Howes, 1972). Studies on the mode of action of pyrantel at the single-channel level identified the L-subtype nAChR in *A. suum* as also preferentially activated by pyrantel (Martin *et al.*, 2005). Pyrantel, like levamisole, also causes open channel-block (Robertson *et al.*, 1994). Although not characterized at the single-channel level, the *O. dentatum* nAChR receptor subunits UNC-29, UNC-38 and UNC-63 reconstitute a pyrantel/tribendimidine- but not levamisole-sensitive

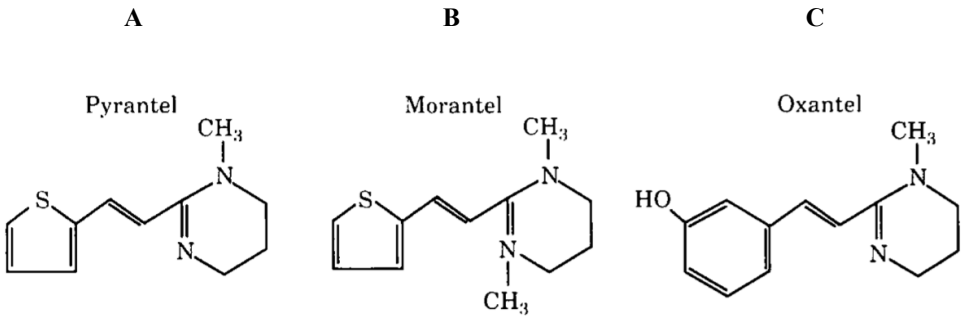

Source: Martin, 1997, p. 13.

Figure 2.18 Chemical structures of pyrantel (A), morantel (B) and oxantel (C).

nAChR subtype in *X. laevis* oocytes (Buxton *et al.*, 2014). The search for an agent with activity against whipworms led to the development of oxantel, an m-oxyphenol derivative of pyrantel (Howes 1972). Contrary to pyrantel, oxantel preferentially activates the N-subtype nAChRs in *A. suum* (Martin *et al.*, 2004). Oxantel, like levamisole and pyrantel, also causes open channel-block in *A. suum* (Dale & Martin, 1995). Morantel is a methyl ester analog of pyrantel which also targets the L-subtype nAChR in *A. suum* (Bamgbose *et al.*, 1973; Cornwell & Blore, 1970). At the single-channel level, morantel causes the activation and block of this receptor subtype (Evans & Martin, 1996). Recently, morantel was shown to act as an agonist of the nAChR subtype comprising ACR-26/ACR-27 subunits from *H. contortus* or *Parascaris equorum* expressed in *X. laevis* oocytes (Courtot *et al.*, 2015). In oocyte expression studies, morantel was seen to cause a non-competitive voltage-sensitive open channel block of the newly characterized *A. suum* ACR-16 receptor (Abongwa *et al.*, 2016a).

2.5.1.4 Macrocyclic lactones (MLs). Macrocyclic lactones (avermectins and milbemycins) are a group of chemical compounds derived from soil microorganisms of the genus *Streptomyces* (Burg *et al.*, 1979; Takiguchi *et al.*, 1980; Takiguchi *et al.*, 1983). MLs were introduced in the 1980s as antiparasitic agents with broad spectrum activity against

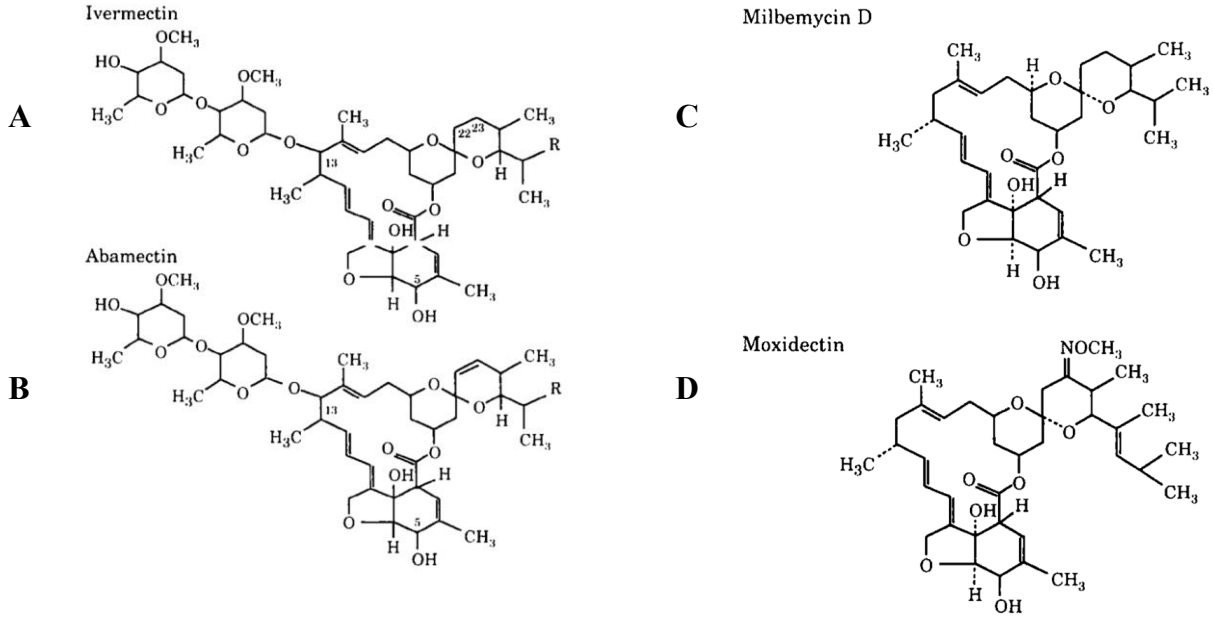

Source: Martin, 1997, p. 19.

Figure 2.19 Chemical structures of ivermectin (A), abamectin (B), milbemycin D (C) and moxidectin (D).

nematodes and arthropods (Davies & Green, 1986; McKellar & Benchaoui, 1996). Examples of commercially available avermectins are ivermectin, abamectin, doramectin and selamectin, while milbemycin oxime and moxidectin, are examples of commercially available milbemycins (Figure 2.19). MLs are selective agonists of glutamate-gated chloride channels (GluCls) which are present in neurons and pharyngeal muscles of nematodes and arthropods, but absent in humans. ML activation of GluCls inhibits movement and pharyngeal pumping (Cully *et al.*, 1994; Wolstenholme & Rogers, 2005). In addition to GluCl effects, the avermectins also act as antagonists of 4-aminobutyric acid (GABA) and nicotinic receptors expressed on somatic muscle cells of parasitic nematodes (Abongwa *et al.*, 2016b; Holden-Dye & Walker, 1990; Puttachary *et al.*, 2013). Ivermectin, the first member of the avermectins, although originally developed as a veterinary drug, was later

approved for use in humans for the control of onchocerciasis and lymphatic filariasis (Crump & Omura, 2011; Geary, 2005; Omura, 2008; Ottesen & Campbell, 1994). Also, ivermectin was shown to act as an irreversible agonist of recombinant human glycine receptors at higher concentrations >0.3 μM, but at lower concentrations (30 nM), it acted as a positive allosteric modulator (Shan *et al.*, 2001). Ivermectin showed a similar positive allosteric modulation effect on the vertebrate neuronal α7 nicotinic acetycholine receptor (Krause *et al.*, 1998).

2.5.1.5 Amino-acetonitrile derivatives (AADs). The AADs are a new class of synthetic anthelmintics with high broad spectrum activity against nematodes that are resistant to the benzimidazoles, imidazothiazoles and macrocyclic lactones (Ducray *et al.*, 2008; Kaminsky *et al.*, 2008a; Kaminsky *et al.*, 2008b). Monepantel, also known as AAD 1556, is the first member of this class to be developed for the control of a broad range of parasitic nematodes in sheep (Figure 2.20) (Kaminsky *et al.*, 2008b). Genetic screens of *C. elegans* identified ACR-23, which belongs to the nematode-specific DEG-3 subfamily of nAChRs, as the target of AADs (Kaminsky *et al.*, 2008a). Further studies on the mode of action of the AADs have led to the confirmation of ACR-23 as the principal target for monepantel in *C. elegans*, as well as the identification of other DEG-3-like nAChR target genes; *H. contortus monepantel-1* (*Hco-mptl-1*, formerly *Hc-acr-23*), *Hco-des-2*, *Hco-deg-3* and *C. elegans acr-20* (Baur *et al.*, 2015; Lecova *et al.*, 2014; Rufener *et al.*, 2013; Rufener *et al.*, 2009). Baur *et al.*, 2015, also demonstrated that at low concentrations (<1 nM), monepantel acts as a positive allosteric modulator of *H. contortus* MPTL-1 and *C. elegans* ACR-20 receptors, and at high concentrations (>0.1 μM), it acts as a direct agonist of these receptors. In a different study, monepantel by itself did not activate *H. contortus* DEG-3/DES-2 receptors expressed

in *X. laevis* oocytes, but did cause a potentiation in the receptors' current responses when co-applied with choline (Rufener *et al.*, 2010).

2.5.1.6 Spiroindoles. Derquantel (2-deoxy-paraherquamide or PNU-141962) is the first semi-synthetic member of this new class of anthelmintics (Figure 2.21) (Lee *et al.*, 2002). Derquantel which is also the first commercial member of the spiroindoles, was introduced in 2010 for use in combination with the macrocyclic lactone, abamectin, under the trade name STARTECT®, for the control of parasitic nematodes in sheep. Derquantel acts as an antagonist of nAChRs to cause flaccid paralysis which results in the expulsion of parasites from the host (Robertson *et al.*, 2002). The combination of derquantel and abamectin has an

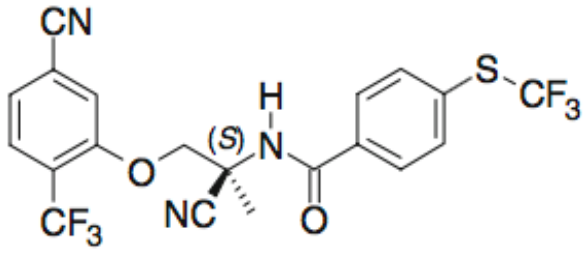

Source: Kaminsky *et al.*, 2008b, p. 935.

Figure 2.20 Chemical Structure of monepantel.

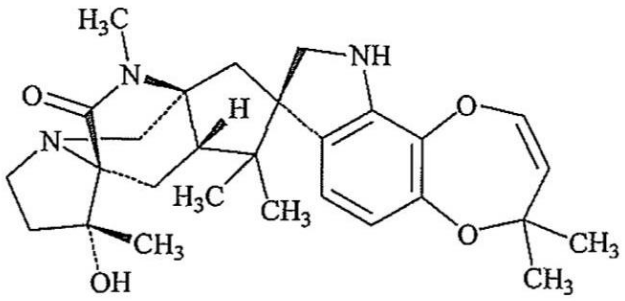

Source: Little et *et al.*, 2011, p. 182.

Figure 2.21 Chemical structure of derquantel.

excellent broad spectrum efficacy against several parasitic nematodes in sheep, including those resistant to benzimidazoles, levamisole and macrocyclic lactones (Geurden *et al.*, 2012; Little *et al.*, 2011). The efficacy of the derquantel and abamectin combination has also been shown in muscle contraction and electrophysiological studies on *A. suum* muscle flaps. Derquantel or abamectin alone inhibited responses to acetylcholine, and the inhibition was greater when a combination of derquantel and abamectin was used, producing a synergistic (greater than additive) effect (Puttachary *et al.*, 2013). Also, the derquantel and abamectin combination was shown to produce a greater inhibition of acetylcholine- or pyrantel-induced current responses from expressed pyrantel/tribendimidine *O. dentatum* receptors compared to derquantel or abamectin alone (Abongwa *et al.*, 2016b). The introduction of combination anthelmintics provides a useful tool to increase anthelmintic drug efficacy, overcome resistance to other anthelmintic classes and delay resistance development (Anderson *et al.*, 1988; Bartram *et al.*, 2012).

2.5.1.7 Cyclooctadepsipeptides. Cyclooctadepsipeptides were discovered in the early 1990s. In 1992, PF1022A, the parent compound, was isolated from the fungus, *Mycelia sterilia*, which grows on the leaves of the plant, *Camellia japonica* (Sasaki *et al.*, 1992). PF1022A is made up of four N-methyl-L-leucine, two D-lactate and two D-phenyllactate residues that are arranged as a cyclic octadepsipeptide with an alternating L-D-L configuration (Figure 2.22) (Harder *et al.*, 2003). Emodepside, formerly PF1022-221 and BAY 44-4400, is a semisynthetic derivative of PF1022A, produced by attaching a morpholine ring at the para position of the two D-phenyllactic acids (Harder *et al.*, 2005). This modification resulted in improved pharmacokinetic properties. The anthelmintic potential of PF1022A and emodepside has been reported in numerous *in vitro* and *in vivo*

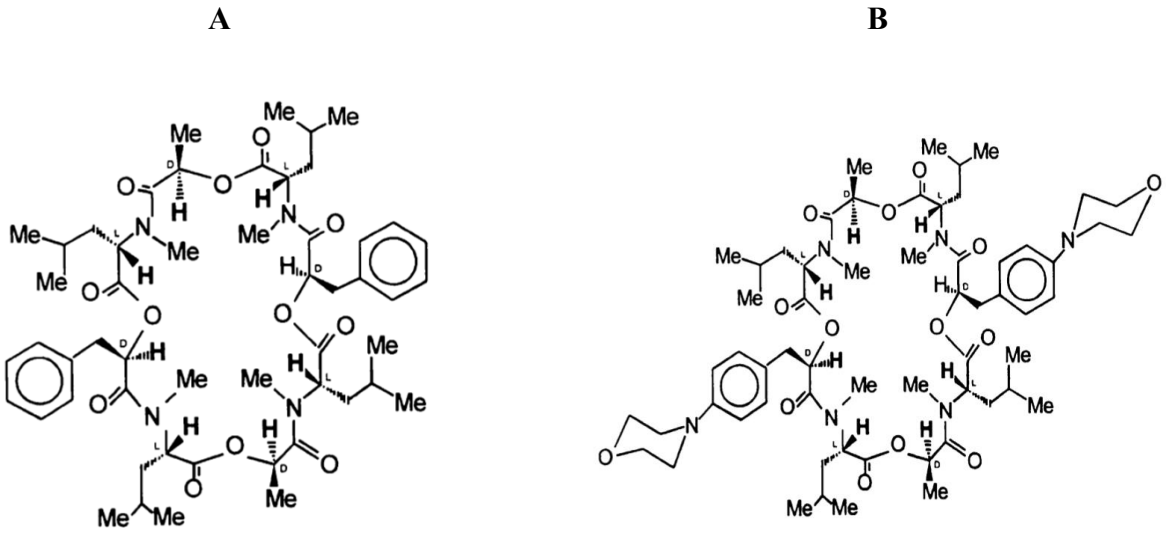

Source: Harder *et al.*, 2003, p. 320.

Figure 2.22 Chemical structure of PF1022A (A) and emodepside (B).

studies (Harder & von Samson-Himmelstjerna, 2001; Kulke *et al.*, 2013a; Kulke *et al.*, 2013b; Kulke *et al.*, 2014; Zahner *et al.*, 2001a; Zahner *et al.*, 2001b). Interestingly, PF1022A and emodepside have a broad spectrum of activity against several nematode species including those that are resistant to benzimidazoles, levamisole and ivermectin (von Samson-Himmelstjerna *et al.*, 2005). This indicated that the mode of action of the cyclooctadepsipeptides is different and that this class of anthelmintics possess 'resistance-busting' properties.

Studies on the mode of action suggest that emodepside targets the calcium-activated potassium channel (SLO-1), there is also evidence for the involvement of the latrophilin (LAT-1) receptor (Holden-Dye *et al.*, 2007; Krucken *et al.*, 2012; Martin *et al.*, 2012a). Mutagenesis screens in *C. elegans* revealed a lack of sensitivity of *slo-1* null mutants to emodepside's inhibitory effects on locomotion and feeding. Inhibition of locomotion was

achieved via the action of emodepside on SLO-1 expressed in body wall muscles or neurons, whereas inhibition of feeding was achieved via the action of emodepside on SLO-1 expressed in neurons but not muscle (Guest *et al.*, 2007). RNAi studies implicated a role for LAT-1 in mediating emodepside's inhibitory effect on pharyngeal pumping in the pharynx (Willson *et al.*, 2004). Guest et al. (2007) showed *C. elegans lat-1* null mutants had an estimated five-fold reduction in sensitivity to emodepside. These studies suggest that the inhibitory effect of emodepside on feeding is both SLO-1 and latrophilin-dependent. However, emodepside treatment inhibited locomotion in both wild type and *lat-1:lat-2* null *C. elegans*, implying that the inhibitory effect of emodepside on locomotion is latrophilin-independent (Guest *et al.*, 2007). The sensitivity of nematode SLO-1 channels to calcium is different from that of insects and humans (Crisford *et al.*, 2015).

2.5.1.8 Tribendimidine. Tribendimidine is a symmetrical diamidine derivative of amidantel (Figure 2.23). It was developed in the mid 1980s by the National Institute of Parasitic diseases in Shanghai, China, as a broad spectrum anthelmintic drug (Ren *et al.*, 1987). In 2004, tribendimidine was approved by the Chinese Food and Drug Administration for treatment of helminth infections in humans (Xiao *et al.*, 2005). It is the only new anthelmintic drug that has been approved for human use within the past 3 decades (Bergquist, 2016). Tribendimidine has been shown in laboratory and clinical studies to have a broad spectrum of activity against several nematode, trematode and cestode species (Keiser *et al.*, 2007; Kulke *et al.*, 2012; Steinmann *et al.*, 2008; Wu *et al.*, 2006; Xiao *et al.*, 2009; Xu *et al.*, 2014). The activity of tribendimidine against 20 helminth parasites has been documented (Xiao *et al.*, 2013). Earlier studies on the mode of action of tribendimidine in the nematode model *C. elegans* demonstrated that tribendimidine acts as an agonist of the L-

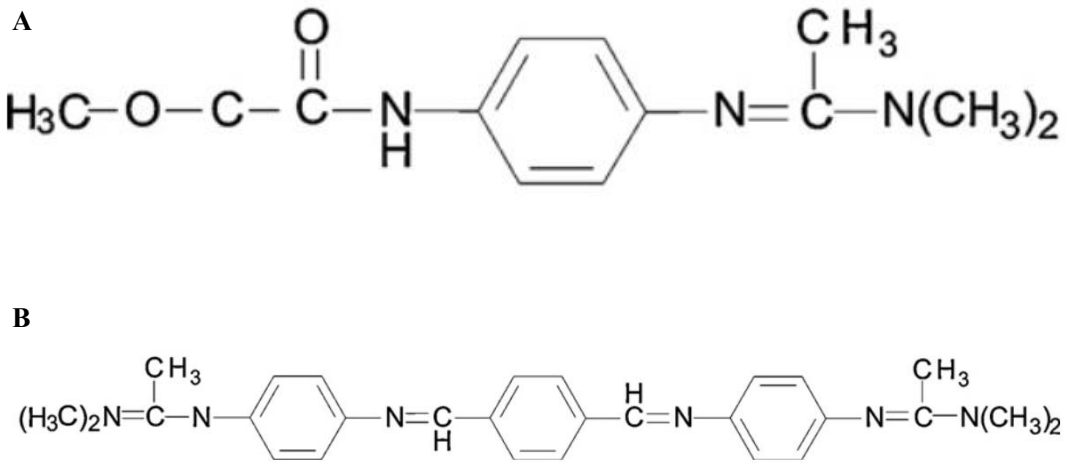

Source: Kulke *et al.*, 2012, p. 79.

Figure 2.23 Chemical structure of amidantel (A) and tribendimidine (B).

subtype nAChR in this species, similar to levamisole and pyrantel (Hu *et al.*, 2009). Parasitic nematodes however, show different nAChR subtype selectivity from *C. elegans*, and this varies across nematode species. Buxton *et al.* (2014), showed in oocyte expression studies that tribendimidine, just like pyrantel, is more selective for the reconstituted pyrantel/tribendimidine nAChR subtype comprising of UNC-29, UNC-38 and UNC-63 subunits from *O. dentatum* and had little effect on the levamisole-sensitive subtype. In *A. suum*, the action of tribendimidine is pharmacologically similar to that of bephenium rather than levamisole, leading to the conclusion that tribendimidine selectively acts on the bephenium-sensitive, B-nAChR subtype, not the L-subtype nAChR in *Ascaris* (Robertson *et al.*, 2015). Robertson *et al.* (2015), further showed tribendimidine to cause a more potent inhibition of migration of *O. dentatum* levamisole-resistant larvae (LEVR) than levamisole-sensitive larvae (SENS). Thus, confirming their hypothesis that unlike in *C. elegans*, tribendimidine does not act on the L-subtype nAChR in parasitic nematodes.

2.5.2 Anthelmintic resistance

In broad terms, anthelmintic resistance is referred to as the decline in the efficacy of an anthelmintic drug in a population of parasites that were once susceptible to the drug. The repeated and improper use of currently available anthelmintics has led to the development of resistance in numerous veterinary parasite species worldwide, with increasing concerns that this this may extend to human parasites (Coles *et al.*, 2006; Geerts & Gryseels, 2000; Geerts & Gryseels, 2001). Since anthelmintics within each drug class act in a similar manner, resistance to one anthelmintic in a given drug class is likely to be accompanied by resistance to other anthelmintics of that same class (side resistance). There is also the likelihood for the development of cross resistance from anthelmintics of one drug class to those of another, if the two drug classes share similar targets (Sangster, 1999). Hence, the widespread occurrence of resistance across the majority of anthelmintic drug classes (Tables 2.3 & 2.4). Sadly, the onset of anthelmintic resistance development can be rapid, thiabendazole resistance occurred 3 years after its introduction to the market (Conway, 1964).

Reports of resistance to anthelmintics in various parts of the world have been well-documented (Kaplan, 2004; Kaplan & Vidyashankar, 2012; Waller, 1997). In spite of the numerous reports of anthelmintic resistance, the mechanisms by which resistance occurs remain to be fully elucidated (Table 2.3). Resistance mechanisms include: (i) mutation or deletion of one or more amino acids in the target genes, (ii) reduction in the number of receptors, (iii) decreased affinity of receptors for drugs, and (iv) absence of bioactivating enzymes (Gilleard, 2006; Jabbar *et al.*, 2006; James *et al.*, 2009; Sangster & Gill, 1999; Wolstenholme *et al.*, 2004). Management practices can also delay or overcome

Table 2.3 Anthelmintic resistance and mechanisms of resistance to the major anthelmintic drug classes. (Modified from Kaplan, 2004, p. 478; Sangster & Gill, 1999, p. 141; & Wolstenholme *et al.*, 2004, p. 471.)

Anthelmintic class	**Host**	**Year of initial approval**	**Year of first published report of resistance**	**Potential mechanism of resistance**
Benzimidazoles				Mutations in β-tubulin; Phe200Try, Phe167Try or Glu198Ala.
Thiabendazole	Sheep	1961	1964	
	Horse	1962	1965	
Imidothiazoles-tetrahydropyrimidines				Changes in nicotinic acetylcholine receptors
Levamisole	Sheep	1970	1979	
Pyrantel	Horse	1974	1996	
Avermectin-milbemycins				Reduced sensitivity of GluCl/GABA receptors
Ivermectin	Sheep	1981	1988	
	Horse	1983	2002	
Moxidectin	Sheep	1991	1995	
	Horse	1995	2003	

anthelmintic resistance (Shalaby, 2013). Anthelmintic resistance can be delayed or overcome by: (i) identifying new drug targets with different pharmacological profiles from those of existing drugs, (ii) introducing new anthelmintics with different modes of action from those of existing anthelmintics, (iii) combination therapy, with members of the combination from different drug classes, (iv) rotating drugs with different modes of action between dosing seasons, and (v) keeping some parasites in untreated refugia (Coles, 2005; Leathwick *et al.*, 2009; Shalaby, 2013). A detailed understanding of the biochemical and genetic basis of

Table 2.4 Worldwide reports of anthelmintic resistance. (Modified from Jabbar *et al.*, 2006, pp. 2415-2416)

Species/genus of nematodes	Resistant to anthelmintic	Country
O. circumcincta	TBZ, LEV, Morantel	Australia
H. contortus	TBZ	Australia
H. contortus	BZ, Non-BZ, Organophosphorus Anthelmintics	Australia
Haemonchus, Trichostrongylus, Ostertagia spp.	FEN, LEV	Australia
T. colubriformis	OXF, LEV	Australia
Haemonchus, Trichostrongylus, Ostertagia, Nematodirus	TBZ, LEV	Australia
Trichostrongylus, Ostertagia spp.	TBZ, LEV, ALB, OXF, Morantel	Australia
H. contortus, Trichostrongylus, Ostertagia spp.	TBZ, LEV	Australia
Sheep nematodes	TBZ, LEV	Australia
H. contortus, T. colubriformis, O. circumcincta	OXL, LEV, Closantel, Morantel	Australia
H. contortus	BZ	Belgium
T. circumcincta	TBZ, IVM, LEV	Brazil
O. circumcincta	LEV	Denmark
Ostertagia, Trichostrongylus spp.	T5BZ, LEV, IVM	Denmark
Goat nematodes	BZ	France
H. contortus	BZ	France
H. contortus, Trichostrongylus, Ostertagia spp.	BZ, LEV	France
H. contortus	BZ	Germany
Gastrointestinal nematodes	TBZ, MBZ, FEN, ALB, OXF, IVM LEV, Febantel, Pyrantel Tartrate	Germany
Nematodes	BZ, LEV, Morantel	Greece
Nematodes	BZ	Ireland
H. contortus	BZ	India
H. contortus	BZ, LEV, IVM, Thiophanate, Morantel, Closantel	India
H. contortus	FEN, LEV, IVM, Closantel, Morantel	India
Gastrointestinal nematodes	ALB, LEV, IVM	India
H. contortus	FEN, LEV, IVM, Morantel	India
Sheep and goat nematodes	BZ	Italy
H. contortus Trichostrongylus spp.	BZ, FEN, LEV	Kenya
Gastrointestinal nematodes	BZ, LEV, IVM	Kenya
H. contortus	Thiophanate, Closantel, ALB, LEV, IVM	Kenya
H. contortus, Trichostrongylus, Oesophagostomum spp.	BZ, LEV, IVM, RAF	Kenya
Goat nematodes	TBZ	Malaysia
H. contortus, T, colubriformis	BZ, LEV, IVM, Closantel, Moxidectin	Malaysia
Trichostrongylus spp.	BZ	Netherlands
H. contortus, C. curticei, Ostertagia, Trichostrongylus spp.	OXF, IVM, LEV	Netherlands
H. contortus, O. circumcincta	BZ, LEV, IVM	Netherlands
Sheep nematodes	BZ, Non BZ	New Zealand
Cooperia oncophora	OXF	New Zealand
H. contortus, Trichostrongylus spp.	BZ, LEV, IVM	New Zealand
Sheep nematodes	BZ, LEV, IVM	New Zealand
Trichostrongyles	BZ	North West Cameroon
Sheep gastrointestinal nematodes	BZ, LEV	Pakistan
H. contortus	OXF	Pakistan
Sheep gastrointestinal nematodes	OXF, LEV	Pakistan

Table 2.4 (Continued)

Species/genus of nematodes	Resistant to anthelmintic	Country
Trichostrongylus spp.	BZ	Slovakia
Ostertagia, Trichostrongylus spp.	BZ, LEV, TMZ	Slovakia
H. contortus	IVM, BZ, CLOST, Rafoxanide	South Aftica
H. contortus, Ostertagia, Trichostrongylus spp	BZ, LEV, IVM, Closantel	Southern Latin America, Brazil
H. contortus Trichostrongylus, Oesophagostomum	BZ, LEV, IVM	South Latin America, Argentina
H. contortus Trichostrongylus, Oesophagostomum	BZ, LEV	Southern Latin America
H. contortus, Ostertagia spp.	BZ, LEV, IVM	Southern Latin America, Uruguay
T. circumcincta	Netobimin, BZ	Spain
H. contortus	TBZ	United Kingdom
O. circumcincta	TBZ	United Kingdom
H. contortus	FEN, IVM	United Kingdom
H. contortus, O. circumcincta		United Kingdom
H. contortus, O. circumcincta	BZ, IVM	United Kingdom
O. circumcincta	BZ	United Kingdom
Sheep nematodes	BZ	United Kingdom
Sheep and goat nematodes	BZ, LEV, IVM	United Kingdom
Sheep nematodes	BZ, LEV, IVM	United Kingdom
H. contortus	TBZ	United States of America
H. contortus, O. circumcinta	TBZ	United States of America
H. contortus	FEN, LEV, IVM, Pyrantel pamoate	United States of America
H. contortus	BZ, LEV, FEN, RAF	Zimbabwe

C. – Cooperia; H. – Haemonchus; O. – Ostertagia, T. – Trichostrongylus; T. – Teladorsagia; BZ – Benzimidazole; MBZ – Mebendazole; FEN – Fenbendazole; TBZ – Thiabendazole; ALB – Albendazole; OXF = Oxfendazole; Lev = Levamisole; IVM = Ivermectin; RAF = Rafoxanide; TMZ = Tetramizole; CLOST = Closantel.

anthelmintic action is, therefore, imperative as this will allow for the development of sensitive assays for early detection and, hence, more efficient management of anthelmintic resistance.

2.6 *Xenopus laevis* oocytes heterologous expression system

Oocytes of the South African clawed toad, *Xenopus laevis*, are an efficient and widely employed heterologous expression system for protein expression, including ion channels and membrane receptors (Broer, 2010; Buckingham *et al.*, 2006; Dascal, 1987; Sigel, 1990). The oocytes have 6 growth stages, namely, stages I – VI, which are distinguished based on size and level of pigmentation (Dumont, 1972). All 6 developmental stages of the oocytes are

contained in the ovaries of the adult female *Xenopus*. These oocytes, which are usually in thousands, can be surgically removed after blocking hormonal stimulation such that the oocytes are retained in the ovaries and do not pass into the oviduct (Bossi *et al.*, 2007; Theodoulou & Miller, 1995). Stages V and VI *Xenopus* oocytes are the largest and measure 1.0 – 1.2 and 1.2 – 1.3 mm in diameter respectively. Stages V and VI *Xenopus* oocytes are typically used as a system for expression and electrophysiological analysis of ion channels and membrane receptors, although the smaller stage IV oocytes are used for studying currents with very fast kinetics (Bianchi & Driscoll, 2006). The oocytes have two clearly distinct poles; the yellow vegetal pole, and the darker animal pole, surrounded by a vitelline membrane and a layer of follicle cells containing ion channels which are electrically coupled to the oocytes through gap junctions (Figure 2.24). Therefore, the oocytes must be defolliculated prior to conducting electrophysiological studies to prevent recording endogenous current responses. Additionally, for single channel studies where the patch clamp technique is used, the vitelline membrane must be removed prior to recordings. This is because interferes with the formation of high resistance gigaseal between the patch electrode and the oocyte membrane (Bianchi & Driscoll, 2006; Choe & Sackin, 1997). This gigaseal is crucial for improving signal-to-noise ratio during patch clamp recordings.

During oogenesis, *Xenopus* oocytes accumulate massive amounts of enzymes and organelles which after fertilization can be used for DNA transcription and RNA translation (Dumont, 1972). The introduction of *Xenopus* oocytes as an expression system can be traced as far back as 1971 when John B. Gurdon observed that mRNA injected into *Xenopus* oocytes were translated to the appropriate proteins after a period of incubation (Gurdon *et al.*, 1971). Nevertheless, it was only in 1982 that *Xenopus* oocytes came to the spotlight as a

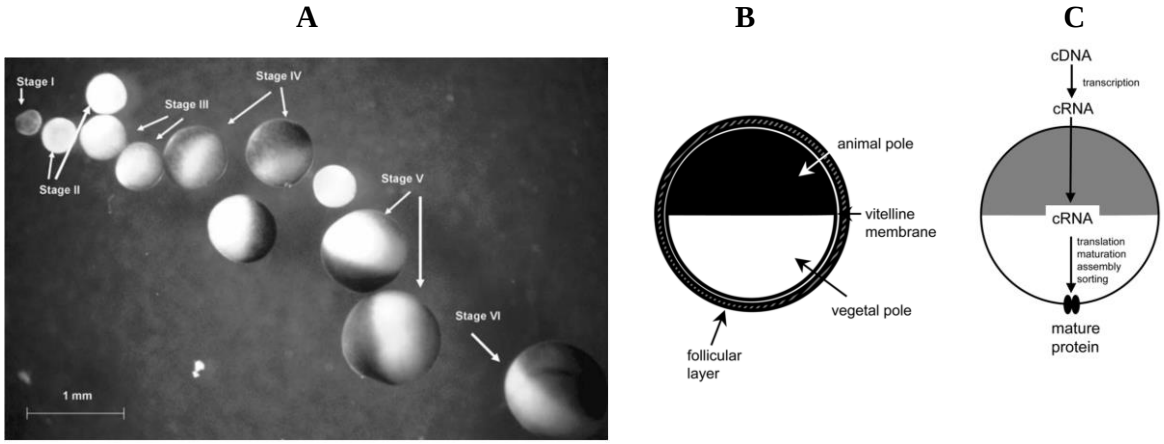

Source: Bossi *et al*., 2007, p. 124 and Bianchi & Driscoll, 2006, p. 3.

Figure 2.24 Structures of *Xenopus laevis* oocytes showing different stages of development (A), annotated anatomical features (B) and cartoon representation of protein expression (C).

system for the expression of membrane proteins such as nicotinic acetylcholine receptors (Barnard *et al.*, 1982; Miledi *et al.*, 1982). Subsequently, *Xenopus* oocytes have been greatly utilized for expression of nicotinic acetylcholine receptors, allowing for the characterization of these receptors using different electrophysiology techniques such as two-electrode voltage clamp and patch clamp (Papke & Smith-Maxwell, 2009; Wagner *et al.*, 2000). The two-electrode voltage clamp technique is usually employed for studying expressed nicotinic acetylcholine receptors as it is is more suitable for clamping large cells like *Xenopus* oocytes (Dascal, 2001; Guan *et al.*, 2013). RNA or DNA is injected into the oocyte cytoplasm or nucleus respectively, and the injected oocytes to allow for functional protein expression. Cytoplasmic injection of RNA is preferred over nuclear injection of DNA because of the technical difficulties associated with locating the nucleus (Miller & Zhou, 2000).

The ability of *Xenopus* oocytes to initiate protein synthesis, in addition to their abundance, large size and relative ease of manipulation make *Xenopus* oocytes a popular

heterologous expression system compared to *Escherichia coli*, yeast, or some eukaryotic cell lines (Lin-Moshier & Marchant, 2013; Markovich, 2008). For studies involving parasitic nematode ion channels, the *Xenopus* oocyte has two specific advantages; (i) electrophysiology requires a steady supply of viable parasites which is often problematic, and (ii) the *Xenopus* system allows expression of a single type (or subtype) of channels whereas *in vivo* recordings from nematode cells can be confounded by the presence of multiple channel types and subtypes.

There are also limitations of the *Xenopus* oocyte expression system which should be taken into consideration when interpreting results and these include: (i) oocytes are not the native cells the proteins are normally expressed in so results may be different from those obtained in native cells, (ii) seasonal variations in oocyte quality and alterations in protein expression ability, and (iii) oocytes are temperature sensitive; they can only survive at room temperature (18 – 22 ^{0}C) and will deteriorate at higher temperatures (Stuhmer, 1992).

CHAPTER 3. PHARMACOLOGICAL PROFILE OF *ASCARIS SUUM* ACR-16, A NEW HOMOMERIC NICOTINIC ACETYLCHOLINE RECEPTOR WIDELY DISTRIBUTED IN *ASCARIS* TISSUES

A paper published in the *British Journal of Pharmacology* (2016)[1]

Melanie Abongwa[2], Samuel K Buxton[2], Elise Courtot[3,4], Claude L Charvet[3,4], Cédric Neveu[3,4], Ciaran J McCoy[5], Saurabh Verma[2], Alan P Robertson[2], Richard J Martin[2*]

[1] Reprinted with permission of *Br J Pharmol* (2016), **173**: 2463–2477
[2] Department of Biomedical Sciences, College of Veterinary Medicine, Iowa State University, Ames, IA, USA
[3] INRA, UMR Infectiologie et Santé Publique, Nouzilly, France
[4] Université François Rabelais de Tours, UMR Infectiologie et Santé Publique, Tours, France
[5] School of Biological Sciences, Medical Biology Centre, Queen's University Belfast, Belfast, UK
[*] Corresponding author and Distinguished Professor, Department of Biomedical Sciences, Iowa State University

3.1 Summary

3.1.1 Background and Purpose

Control of nematode parasite infections relies largely on anthelmintic drugs, several of which act on nicotinic ACh receptors (nAChRs), and there are concerns about the development of resistance. There is an urgent need for development of new compounds to overcome resistance and novel anthelmintic drug targets. We describe the functional expression and pharmacological characterization of a homomeric nAChR, ACR-16, from a nematode parasite.

3.1.2 Experimental Approach

Using RT-PCR, molecular cloning and two-electrode voltage clamp electrophysiology, we localized *acr*-16 mRNA in *Ascaris suum* (*Asu*) and then cloned and

expressed *acr*-16 cRNA in *Xenopus* oocytes. Sensitivity of these receptors to cholinergic anthelmintics and a range of nicotinic agonists was tested.

3.1.3 Key Results

Amino acid sequence comparison with vertebrate nAChR subunits revealed ACR-16 to be most closely related to α7 receptors, but with some striking distinctions. *acr*-16 mRNA was recovered from *Asu* somatic muscle, pharynx, ovijector, head and intestine. In electrophysiological experiments, the existing cholinergic anthelmintic agonists (morantel, levamisole, methyridine, thenium, bephenium, tribendimidine and pyrantel) did not activate *Asu*-ACR-16 (except for a small response to oxantel). Other nAChR agonists: nicotine, ACh, cytisine, 3-bromocytisine and epibatidine, produced robust current responses which desensitized at a rate varying with the agonists. Unlike α7, *Asu*-ACR-16 was insensitive to α-bungarotoxin and did not respond to genistein or other α7 positive allosteric modulators. *Asu*-ACR-16 had lower calcium permeability than α7 receptors.

3.1.4 Conclusions and Implications

We suggest that ACR-16 has diverse tissue-dependent functions in nematode parasites and is a suitable drug target for development of novel anthelmintic compounds.

3.2 Abbreviations

α-BTX, α-bungarotoxin; BAPTA-AM, 1,2-bis(2-aminophenoxy)ethane-*N*,*N*,*N*′,*N*′-tetraacetic acid tetrakis (acetoxymethyl ester); blastP, protein–protein blast; DHβE, dihydro-β-erythroidine; DMPP, dimethyl-4-phenyllpiperazinium iodide; dTC, d-tubocurarine; GHK, Goldman Hodgkin Katz; MLA, methyllycaconitine; nAChR, nicotinic ACh receptor; PAM, positive allosteric modulator.

3.3 Table of Links

Table 3.0 Key protein targets and ligands.

TARGETS
Ligand–gated ion channels
Asu-ACR-16
ACR-16
Nicotinic ACh receptor α7 subunit

LIGANDS		
A844606	Dimethyl-4-phenylpiperazinium	Morantel
Acetylcholine	Epibatidine	Nicotine
Bephenium	Genistein	Oxantel
Betaine	Hexamethonium	Paraherquamide
Bromocytisine	Ivermectin	PNU120596
α-Bungarotoxin	Levamisole	Pyrantel
Choline	Lobeline	Thenium
Cytisine	Mecamylamine	Tribendimidine
Derquantel	Methyllycaconitine	d-Tubocurarine
Dihydro-β-erythroidine	Methyridine	

These Tables list key protein targets and ligands in this article which are hyperlinked to corresponding entries in http://www.guidetopharmacology.org, the common portal for data from the IUPHAR/BPS Guide to PHARMACOLOGY (Southan *et al.*, 2016) or the PubChem or Wormbase databases. Entries in the IUPHAR database are permanently archived in the Concise Guide to PHARMACOLOGY 2015/16 (Alexander *et al.*, 2015).

3.4 Introduction

Soil-transmitted helminths (gastrointestinal nematode parasites) cause significant global health problems in humans and animals. It is estimated that at least one-quarter of the world's human population (Brooker, 2010) and most animal species are infected with parasitic worms. Nematode parasite infections have a high morbidity and cause debilitating conditions such as weight loss, anaemia, compromised immunity, impaired learning ability and, in severe cases, death (Hotez *et al.*, 2007). No current vaccine against nematode parasite infections of humans is effective (Hewitson and Maizels, 2014), so control of these infections relies on chemotherapy. Regrettably, there are a limited number of classes of anthelmintics (Martin, 1997; Kaminsky *et al.*, 2008), which, with the repeated large scale use of the drugs, has led to the development of resistance in animals (Wolstenholme *et al.*, 2004), and concerns about the development of resistance in humans (Taman and Azab, 2014). The increasing resistance means that novel drug targets are required to overcome this resistance.

Nicotinic ACh receptors (nAChRs) of vertebrates and invertebrates serve a very wide range of functions. For example, in excitable cells, they are involved in neuronal and neuromuscular transmission and, in non-excitable cells, are involved in modulation, development of growth and differentiation (Wessler and Kirkpatrick, 2008). Nematode parasite nAChRs are pharmacologically different to their host nAChRs and are validated and exploited anthelmintic drug targets (Gopalakrishnan *et al.*, 2007). All nAChRs are five-subunit ligand-gated ion channels which open in the presence of ACh or choline, and are found on muscles, nerves, secretory cells and a wide range of non-excitable tissues in both vertebrates and invertebrates. The pharmacology of individual nAChRs depends on key amino acid sequences of each nAChR subunit of the pentamer and the composition of the subunits that form the receptor. The subunits that make up vertebrate nAChRs are derived from at least 17 genes (α1–α10, β1–β4, γ, δ, ϵ) (Karlin, 1993; Millar and Gotti, 2009) and from 29 genes in the free-living nematode, *Caenorhabditis elegans* (Jones *et al.*, 2007). The subunits of the pentameric receptor channel may be composed of five identical subunits (homomeric) or a mixture of different subunits (heteromeric) arranged around a central ion conducting pore (Chen, 2010).

The older, cholinergic anthelmintics, levamisole and pyrantel, and the more recently introduced anthelmintics, tribendimidine and derquantel, activate heterogeneous pentameric nAChRs composed of a mixture of UNC-29, UNC-38, ACR-8 or UNC-63 subunits (Buxton *et al.*, 2014). The more recently introduced cholinergic anthelmintic, monepantel, activates nAChRs composed of a mixture of DEG-3-like subunits, including ACR-23, ACR-20 and MPTL-1 (Baur *et al.*, 2015). Resistance to some of these anthelmintics has been observed in animal parasites (McMahon *et al.*, 2013; Scott *et al.*, 2013), and although the mechanism(s)

of field resistance have not been well characterized, there is evidence that the resistance can involve altered subunit sequence or subunit truncation (Fauvin *et al.*, 2010; Neveu *et al.*, 2010).

Here, we have cloned and expressed, in *Xenopus* oocytes, *acr*-16 cRNA from *Ascaris suum*, a clade III nematode parasite, which is very similar to the significant human parasite, *A. lumbricoides*. This receptor was expressed as a homomeric receptor in *Xenopus* oocytes, and transcripts are found in muscle, intestine, reproductive tract and other tissues of the *Ascaris* body, suggesting diverse physiological functions in addition to neuromuscular transmission. Knowing that ACR-16 is a nicotine-sensitive nAChR and that nicotine has in the past been used as the drug of choice for treatment of *Ascaridia galli* infections (Kerr and Cavett, 1952), a selective drug targeted against ACR-16 could affect motility, digestion and reproduction of parasites and be an effective anthelmintic.

3.5 Methods

3.5.1 Animals

No vertebrate animals were used directly in the study. Adult female *A. suum* worms were collected from Marshalltown Pork Plant, Marshalltown, IA, USA. Defolliculated *Xenopus laevis* oocytes were obtained from Ecocyte Bioscience (Austin, TX, USA).

3.5.2 Sequence analysis

For convenience, the sources of the AChR subunits are indicated, in this article, by three letter prefixes. Thus, *Ace, Asu, Cel, Hco, Llo, Nam, Sra, Tca and Xle*, refer to *Ancylostoma ceylanicum*, *Ascaris suum*, *Caenorhabditis elegans*, *Haemonchus contortus*, *Loa loa*, *Necator americanus*, *Strongyloides ratti*, *Toxocara canis* and *Xenopus laevis* respectively.

Database searches around the sequence of *Asu*-ACR-16 were performed with the blast Network Service (NCBI), using the protein–protein blast (blastP) algorithm (Altschul *et al.*, 1997). Signal peptide predictions were carried out using the SignalP 4.0 server (Bendtsen *et al.*, 2004), and membrane-spanning regions were predicted using TMpred (Hofmann and Stoffel, 1993). Distance trees were generated on the full-length deduced amino acid sequences aligned with the MUSCLE programme (Edgar, 2004). The alignment was analysed using the SEAVIEW suite (Gouy *et al.*, 2010) with the neighbour-joining method and bootstrapped with 1000 replicates. The resulting tree was visualized and edited using FigTree 1.4 (http://tree.bio.ed.ac.uk/software/figtree/).

3.5.3 *Asu*-ACR-16 receptor localization

Total RNA was extracted with TRIzol (Invitrogen™, Carlsbad, CA, USA) from different body tissues of five dissected adult female *Asu* worms. The tissues were the gut, ovijector, head, single muscle cells (RNA extracted via micropipette), bulk somatic muscle, single muscle cells of the pharynx (RNA extracted via micropipette) and bulk muscle cells of the pharynx. Specific primers were designed for PCR for *acr*-16 (forward primer GACTTGCAACCAGGCAAAGG; reverse primer ACGGGTCGTTATGCCCATTT) and *gapdh* (positive control) (forward primer CTGCTGGACCAATGAAGGGT; reverse primer CACTCCACTCACAGCCACTT) using the online Primer-blast tool. With these primer sets, the expected product size for *acr*-16 was 468 and 411 bp for *gapdh*. The presence or absence of *acr*-16 in the RNA samples was detected using RT-PCR and single-cell RT-PCR (QIAGEN OneStep RT-PCR Kit; Valencia, CA, USA) at an annealing temperature of 55°C and for 45 PCR cycles. The PCR products from both RT-PCR and single-cell RT-PCR were run on a 1% agarose gel, at the end of which the gel was viewed and captured on a UVP

BioSpectrum Multi Spectral Imaging System (UVP LLC, Upland, CA, USA). Representative bands were sequenced to confirm the identity of *acr*-16.

3.5.4 cRNA preparation

Total RNA samples were extracted with TRIzol (Invitrogen™) from a 1 cm muscle flap and dissected whole pharynx of *Asu*. RT-PCR was used to synthesize first-strand cDNA from muscle and pharynx total RNA with both oligo (dT) RACER primer and Random Hexamer, and superscript III reverse transcriptase (Invitrogen). To amplify the full-length coding sequence of *Asu-ACR*-16, specific primer pairs were designed on the putative 5′- and 3′-UTRs mRNA sequence deduced from *Asu* whole genome shotgun contig N°AEUI02000378 (*Asu*-acr-16-F0 ATCACGCATTACGGTTGATG, *Asu*-acr-16-F1 TTGATGTAGTGGCGTCGTGT, *Asu*-acr-16-R0 ATTAGCGTCCCAAGTGGTTG, *Asu*-acr-16-R1 GCATTGATGTTCCCTCACCT) for a first round of PCRs. We used a classical nested PCR approach with F0/R0, F0/R1, F1/R0 and F1/R1 respectively to perform four separate PCR reactions for the first round to increase the chance of amplification success. These four PCR products were subsequently used as templates for a second round of four separate PCR reactions using the following specific primers containing *Hind*III and *Apa*I restriction enzyme sites (*Asu*-acr-16-F-Hind3AAAAAGCTTATGAGCGTGCAGCGGGCATT, *Asu*-acr-16-R-*Apa*I TTTGGGCCCTAGAGTGCTGATGATGTGCTA) to facilitate directional cloning into the PTB-207 expression vector. PCR products were then digested with *Hind*III and *Apa*I restriction enzymes, purified using the NucleoSpin® Gel and PCR Clean-up kit (Macherey-Nagel Inc. Bethlehem, PA, USA), cloned into PTB-207 as previously described (Boulin *et al.*, 2011) and sequenced. A positive clone was selected and linearized with NheI for

subsequent *in vitro* transcription with the mMessage mMachine T7 transcription kit (Ambion). The cRNA was precipitated with lithium chloride, resuspended in RNAse-free water, aliquoted and stored at −80°C.

3.5.5 Oocyte microinjection

The *Xenopus* oocytes were kept at 19°C for ~3 h prior to injections in incubation solution (100 mM NaCl, 2 mM KCl, 1.8 mM $CaCl_2.2H_20$, 1 mM $MgCl_2.6H_20$, 5 mM HEPES, 2.5 mM Na pyruvate, 100 $U \cdot mL^{-1}$ penicillin and 100 $\mu g \cdot mL^{-1}$ streptomycin, pH 7.5). Depending on the cRNA mix, 10–25 ng of *acr*-16 cRNA either alone or in combination with 2.5–15 ng of each ancillary (*ric*-3, *unc*-50 and *unc*-74), in a total volume of 50 nL in RNAse-free water, was injected into the animal pole of the oocytes using a nanoject II microinjector (Drummond Scientific, Broomall, PA, USA). The injected oocytes were transferred into 96-well culture plates containing 200 μL incubation solution per well; each well contained one oocyte. Oocytes were incubated at 19°C for 2–7 days to allow for receptor expression; incubation solution was changed daily. Oocytes with membrane potentials less than −15 mV were excluded from recording. Oocyte recordings that failed (shown by a change in the holding current following wash) before the complete series of drug applications were excluded from the analysis.

3.5.6 Two-electrode voltage clamp electrophysiology (TEVC) in *Xenopus* oocytes

Two-electrode voltage clamp electrophysiology was used to record currents produced by activation of the expressed *Asu*-ACR-16 receptor (Buxton *et al.*, 2014). Four hours prior to recording, 100 μM BAPTA-AM (final concentration), a cell-permeant calcium chelator, was added to the oocyte incubation solution to prevent activation of endogenous calcium-activated chloride channels during recordings. Recordings from non-injected oocytes served

as control experiments. Recordings were made using an Axoclamp 2B amplifier (Warner Instruments, Hamden, CT, USA) with the oocytes voltage clamped at −60 mV and data acquired on a computer with Clampex 9.2 (Molecular Devices, Sunnyvale, CA, USA). The microelectrodes used to impale the oocytes were pulled using a Flaming/Brown horizontal electrode puller (Model P-97; Sutter Instruments, Novato, CA, USA) set to pull micropipettes that when filled with 3 M KCl had a resistance of 20–30 MΩ. The micropipettes tips were carefully broken with a piece of tissue paper in order to achieve a resistance of 2–5 MΩ in recording solution (100 mM NaCl, 2.5 mM KCl, 1 mM $CaCl_2.2H_2O$ and 5 mM HEPES, pH 7.3). The low resistance pipettes allowed large currents to be passed to maintain adequate voltage clamp.

3.5.7 Assessment of agonists and antagonists

Except where indicated, agonists were used at a final concentration of 100 μM, while the antagonists were used at a final concentration of 10 μM for rank order potency experiments and 1 μM for the dose–response experiments. Effects of the positive allosteric modulators (PAMs): ivermectin (10 μM), genistein (3 μM) and PNU120596 (3 μM), were tested. Control responses were obtained first with agonists applied for 10 s. Responses were again observed after the antagonists or PAMs were applied for 2 min and observed in the continued presence of antagonist or PAM. In the case of the antagonist rank order potency experiments, a control application of 100 μM ACh was first applied for 10 s, immediately followed by a test 10 s application of antagonist in the continued presence of 100 μM ACh and then a final 10 s application of 100 μM ACh. Note that, with this approach, the potency for each antagonist is likely to be slightly underestimated due to the short time of drug

application. In order to minimize desensitization effects, at least 2 min was allowed for drug wash off between applications.

Dose–response studies were conducted in ascending order of concentrations and were not presented randomly. This approach minimizes desensitization by high concentrations of agonist. The application of the sequence of agonists for determining the potency series was random and not predetermined.

Blinding was not used because it was necessary to allow the appropriate technique and study methods to be used to test if the drug was a potential agonist, potential antagonist or potential PAM. In all our recordings, we applied an initial 100 μM ACh control, and all other responses were normalized to this control 100 μM ACh current. The normalized ACh current (100%) was not used for statistical analysis. Log dose–response plots are used for display and determination of the EC_{50}, *nH* and maximum response.

3.5.8 Permeability of receptors to calcium

Calcium permeability experiments were conducted by increasing the external Ca^{2+} concentration from 1 to 10 mM in the recording solution without changing the concentration of other cations. Oocytes were challenged with 30 μM ACh in the recording solution, with the membrane of the oocytes held at different potentials between −60 and +30 mV. The Goldman Hodgkin Katz (GHK) constant field equation was used to calculate the permeability ratio, P_{Ca}/P_{Na}. Because the oocytes were BAPTA-treated prior to recording, the assumptions made in calculating the permeability ratio of the expressed *Asu*-ACR-16 receptor were that the internal [Ca^{2+}] is negligible and permeability of Na and K, P_{Na} and P_K is equal. Ionic activity coefficients used for the calculations were 0.56 for Ca^{2+} and 0.72 for

Na^+ and K^+. The GHK equation (with ionic activity inserted) used in calculating the P_{Ca}/P_{Na} was:

$$E_{rev} = RT/F \ \ln\{(P_{Na}{*}0.72[Na]_o + P_K{*}0.72[K]_o + 4P'{*}0.56[Ca]_o) /P_{Na}{*}0.72[Na]_i + P_K{*}0.72[K]_i\},$$

where E_{rev} is the reversal potential (potential at which current changes direction), R is the universal gas constant (8.314 $J{\cdot}K^{-1}{\cdot}mol^{-1}$), T is room temperature in Kelvin (298 K), F is Faraday's constant (96 485 $C{\cdot}mol^{-1}$) and $P' = P_{Ca}/P_{Na}\{1/(1 + e^{FErev/RT})\}$.

3.5.9 Data and statistical analysis

The data and statistical analysis comply with the recommendations on experimental design and analysis in pharmacology (Curtis *et al*., 2015). The acquired data from electrophysiological recordings were analysed with Clampfit 9.2 (Molecular Devices, Sunnyvale, CA, USA) and GraphPad Prism 5.0 (Graphpad Software Inc., La Jolla, CA, USA). In all recordings, the peak currents in response to applied drugs were measured, and except where otherwise indicated, peak current values obtained were normalized to 100 µM ACh and expressed as mean ± SEM. Dose–response relationships were analysed by fitting log dose–response data points with the Hill equation as previously described (Boulin *et al*., 2008), while desensitization kinetics in response to the potent agonists were fitted using a single exponential decay fit:

$$f(t) = \sum_{i=1}^{n} A_i e^{-t/\tau i} + C$$

where n is the number of components, A the amplitude, t the time, τ the time constant and C the constant y-offset for each i component.

The group sizes varied with the type of experiment performed, as described below. To optimize our expression and recording conditions, we injected 10 ng of *Asu*-acr-16 alone and with 1.8 ng each of the ancillary factors, *ric*-3, *unc*-50 and *unc*-74 from *A.suum*, *H. contortus* and *X.laevis* (n = 21 for *Asu-acr*-16 alone; n = 15 for *Asu-acr*-16 + *Hco-ric*-3, *Hco-unc*-50 and *Hco-unc*-74; n = 15 for *Asu-acr*-16 + *Asu-ric*-3, *Asu-unc*-50 and *Asu-unc*-74; n = 17 for *Asu-acr*-16 + *Hco-ric*-3; n = 20 for *Asu-acr*-16 + *Xle-ric*-3; and n = 23 for *Asu-acr*-16 + *Asu-ric*-3). We found that *Asu-unc*-50 and *Asu-unc*-74 were not required for expression and that *Asu-acr*-16 + *Asu-ric*-3 produced the large robust currents (290.6 ± 63.7, n = 23). We also tested different amounts of *Asu-acr*-16 and *Asu-ric*-3 (n = 6 for 25 ng *Asu-acr*-16 + 5 ng *Asu-ric*-3, n = 6 for 10 ng *Asu-acr*-16 + 5 ng *Asu-ric*-3, n = 6 for 10 ng *Asu-acr*-16 + 10 ng *Asu-ric*-3 and n = 6 for 15 ng *Asu-acr*-16 + 15 ng *Asu-ric*-3) and observed that the size of the currents depended on the amount of *Asu-acr*-16 and *Asu-ric*-3 injected.

Thereafter, we injected 25 ng *Asu-acr*-16 + 5 ng *Asu-ric*-3 (which produced the biggest currents) for all subsequent experiments. For nAChR agonists and cholinergic anthelmintics, we tested larger numbers of oocytes (n = 21 for nicotine, n = 21 for cytisine, n = 15 for 3-bromocytisine, n = 15 for epibatidine, n = 21 for DMPP, n = 36 for oxantel, n = 15 for choline, n = 15 for betaine, n = 15 for lobeline, n = 15 for A844606, n = 21 for morantel, n = 21 for levamisole, n = 15 for methyridine, n = 15 for thenium, n = 15 for bephenium, n = 15 for tribendimidine and n = 15 for pyrantel) to measure and examine variability of responses between oocytes. Once we had confirmed the reproducible nature of the responses (the mean and standard errors for each of the nAChR agonist and cholinergic anthelmintics shown in Figure 3.3), we reduced our n number to 6 for all other experiments, except the antagonist experiment where the n number was 5.

Data were analysed statistically as follows. All completed drug application sequences on the oocytes were used for analysis without exclusion. If the recording became unstable, indicated by a change in the baseline holding current, all of that recording was rejected for analysis. Statistical analyses were performed on groups of values using ANOVA to determine if the group means are similar and if there was variance inhomogeneity (Bartlett's test). *Post hoc* tests (Tukey's multiple comparison test for Figures 3.2B, 3.3 and 3.6A; Dunnett's test to compare with control, for Figure 3.4) were used to determine significance of differences between groups. We analysed the effects of PAMs on *Asu*-ACR-16 using two-way ANOVA. We defined $P < 0.05$ as showing statistical significance.

3.6 Materials

The drugs used in this study, with the exception of paraherquamide, tribendimidine and derquantel were purchased from Sigma-Aldrich (St Louis, MO, USA), Tocris Bioscience (Ellisville, MO, USA) or Calbiochem (San Diego, CA, USA). The drugs were solubilized in recording solution, DMSO or ethanol. Paraherquamide and derquantel were gifts from Zoetis (Kalamazoo, MI, USA) and tribendimidine was a gift of Prof Shu Hua Xiao (National Institute of Parasitic Diseases, China).

3.7 Results

3.7.1 Identification of *Asu*-ACR-16 sequence

We used the *Cel*-ACR-16 sequence (Supporting Information Figure S3.0) as a query in a blastP search in protein databases from nematodes which allowed the identification of a potential complete coding sequence of an ACR-16 homologue in the pig parasite *Asu* (ERG81952.1). RT-PCR experiments using primers designed using this predicted sequence

led to the amplification of a full coding sequence (Figure 3.0A), which was submitted to GenBank under the accession number KP756901.

When we used the *Asu-acr*-16 transcript sequence as a query, a blastP search resulted in the identification of highly conserved (complete or partial) homologous sequences from other parasitic nematode species belonging to Clade III (*T. canis* and *L. loa*), Clade IV (*S. ratti*) and Clade V (*H. contortus, A. ceylanicum* and *Necator americanus*) (Figure 3.0B and Supporting Information S3.1). The distance tree presented in Figure 3.0B indicates the orthologous relationship of the ACR-16 sequences from parasitic nematodes with the *Cel*-ACR-16 sequence and also shows the orthologous relationship to the other nAChR subunits of *C elegans*. The predicted complete sequences corresponding to ACR-16 orthologues in parasitic nematodes from Clade III and V were further analysed in a structural alignment. All amino acid sequences were found to share typical features of nAChR subunits including a predicted signal peptide, four transmembrane domains, a Cys-loop motif and a cysteine doublet in the potential agonist site defining them as α-subunits. Of note is that, despite their phylogenetic separation, ACR-16 sequences from Clade III and Clade V species were found to be highly conserved (i.e. 80% identities between *Asu*-ACR-16 and *Hco*-ACR-16), suggesting that their pharmacology may also be similar.

3.7.2 *Asu*-ACR-16 sequence suggests pharmacological differences to host mammalian α7 nAChRs

Alignment of the *Asu*-ACR-16 amino acid sequence with that of human-α7 nAChRs using the Clustal Omega online alignment tool (Sievers *et al.*, 2011) showed *Asu*-ACR-16 and human-α7 receptors share 44.90% identity in their amino acid sequences. Figure 3.0A shows the amino acid sequence alignment of *Asu*-ACR-16, which is compared with that of

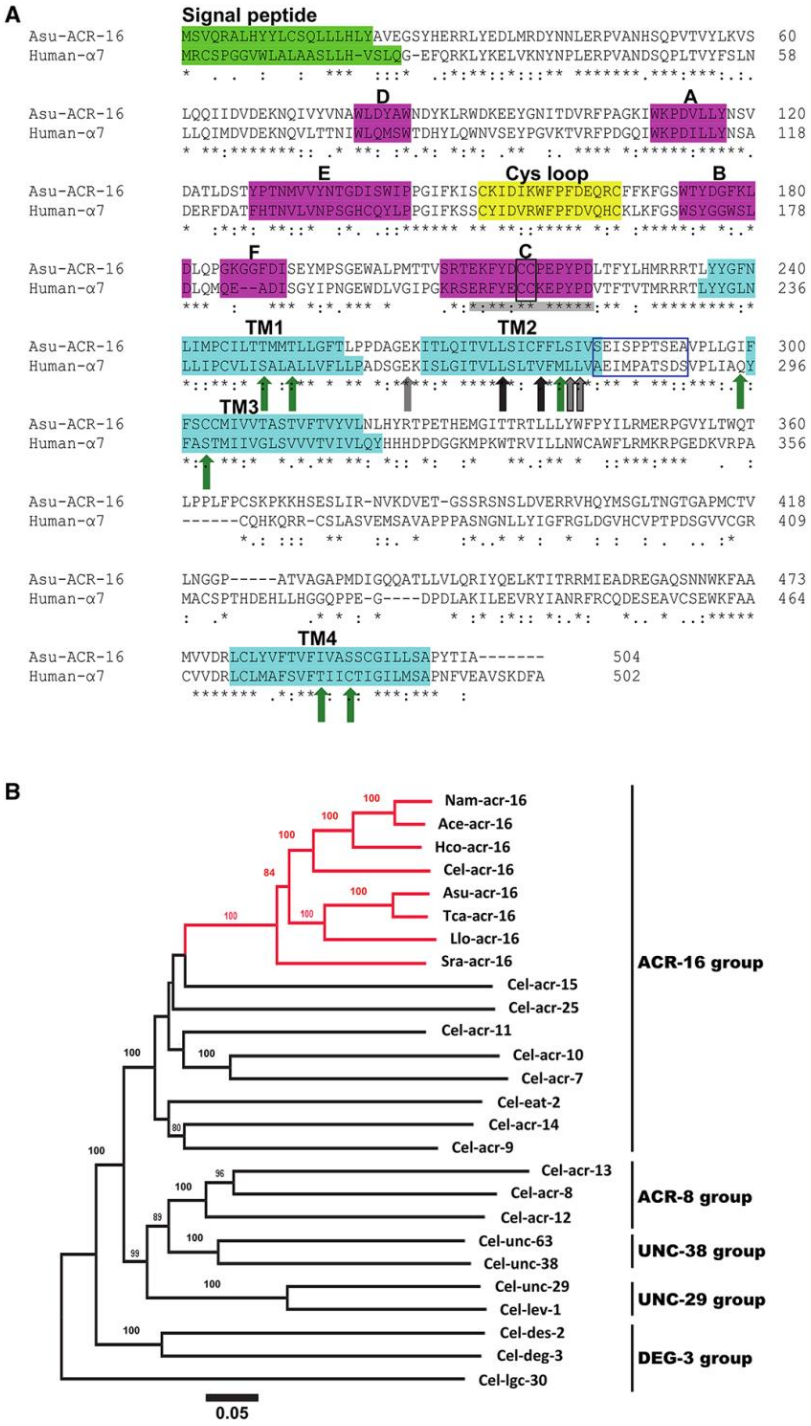

Figure 3.0 (A) Amino acid sequence alignment of *Asu*-ACR-16 and human-α7 nAChR subunits. The signal peptide (bright green box), ACh-binding loops A–F (pink boxes), cys-loop (yellow box) and transmembrane regions TM1–TM4 (turquoise boxes) are indicated. The vicinal cysteines (black-edged box) that characterize an α-subunit are present in the C-binding loop. The blue-edged box between TM2 and TM3 represents the region where PNU120596 acts on α7 nAChRs. Green arrows are residues important for positive allosteric modulation of α7 receptors by ivermectin. Grey (and grey outline) arrows are residues important for permeability of α7 receptors to Ca^{2+}. Black (and black outline) arrows are residues affecting α7 receptor desensitization. Residues in C-binding loop of α7 nAChRs that bind α-BTX are highlighted in grey. (B) Distance tree showing relationships of ACR-16 homologues in parasitic nematode species with AChR subunit sequences from *C. elegans*. A neighbour joining tree was generated with deduced amino acid sequence from AChR subunits representative from the ACR-16, ACR-8, UNC-38, UNC-29 and DEG-3 group as defined by Mongan *et al.*, ([1]). Three letter prefixes in AChR subunit names: *Ace*, *Asu*, *Cel*, *Hco*, *Llo*, *Nam*, *Sra* and *Tca*, refer to *A. ceylanicum*, *A. suum*, *C. elegans*, *H. contortus*, *L. loa*, *N. americanus*, *S. ratti* and *T. canis* respectively. ACR-16 orthologues are highlighted in red. Numbers at each branch indicate percentage bootstrap values (>80%) corresponding to 1000 replicates. The scale bar represents substitutions per site. The *Cel*-*lgc*-30 subunit sequence was used as an outgroup**.**

human-α7 receptors (Raymond *et al.*, 2000; Touroutine *et al.*, 2005). *Asu*-ACR-16 has the characteristic vicinal cysteine residues (Y-x-C-C) found in the C-loop of most nAChR α-subunits; these C-C residues play an essential role in ACh binding (Kao *et al.*, 1984). Significantly, the Y-x-C-C residues of the C-loop of *Asu*-ACR-16 (Supporting Information S3.2) differ from the C-loop of the levamisole receptor α-subunits, *Cel*-UNC-38 and *Cel*-ACR-13, which have a Y-x-x-C-C motif (Mongan *et al.*, 1998); this C-loop difference encouraged our view that the *Asu*-ACR-16 nAChR would differ in its pharmacology from that of the levamisole receptors.

We were further encouraged to investigate the pharmacology of *Asu*-ACR-16 because of other significant differences in amino acid residues which are known to affect activation, desensitization and modulation in α7 nAChRs. For example, Figure 3.0A shows four amino acids (black and black outline arrows in the TM2 region known as L247, V251, L254 and

L255 when mature peptide numbering of α7 subunits is used) that change the desensitization of α7 receptors (Revah *et al.*, 1991; Bertrand *et al.*, 1992; Corringer *et al.*, 1999b). Note that only the first of these (L247) is conserved in *Asu*-ACR-16. Consequently, we chose to investigate the rate of desensitization of *Asu*-ACR-16. Other amino acid differences between the α7 and the levamisole α-receptor subunits, which we describe subsequently, suggest that the *Asu*-ACR-16 receptor pharmacology will be different.

3.7.3 Ubiquitous tissue and single-cell expression of ACR-16 in *Asu*

We examined the distribution of *Asu*-ACR-16 in dissected adult female *Asu* tissues using RT-PCR. We found reproducible and clear evidence of expression of *Asu*-ACR-16 message in strips of intestine (Figure 3.1A; g, gut), sections of the reproductive tract (Figure 3.1A; o, oviduct, uterus), whole dissected pharynx (Figure 3.1A; p), body muscle strips (Figure 3.1A; m) and head (Figure 3.1A; h) region. We observed similar expression patterns of *Asu*-ACR-16 message in the gut, oviduct, whole pharynx, body muscle strip and head from four other adult female *Asu*. The expression of *Asu*-ACR-16 in tissues other than nerves and body muscle tissue, like the non-excitable tissues of the intestine and reproductive tract (uterus), was not anticipated. But it was reproducible and may be part of an ACh-mediated paracrine system (Proskocil *et al.*, 2004; Bschleipfer *et al.*, 2007) rather than part of a neurotransmitter process. The *Asu*-ACR-16 ACh receptor may serve multiple roles in reproduction, digestion, etc., as well as neuromuscular transmission in the parasite.

Single-cell RT-PCR was conducted to further investigate the localization of *Asu*-ACR-16 in the pharyngeal and somatic muscle cells of *A. suum*. We used intracellular micropipettes to collect cytoplasm from individual somatic and pharyngeal muscle cells for PCR analysis. We recovered *Asu*-ACR-16 message from single body muscle cells but not

from pharyngeal muscle cells (Figure 3.1B). The presence of *Asu*-ACR-16 positive bands in the whole pharynx and absence in single-cell RT-PCR samples suggests that *Asu*-ACR-16 is present in the neurons of the circum-pharyngeal nerve ring but not present on pharyngeal muscle cells. In contrast to the pharyngeal muscle cells, we observed that *Asu*-ACR-16 expression is widespread in somatic muscle as well as other tissues of the *Ascaris* body, implying tissue-related functions in addition to a neuromuscular function.

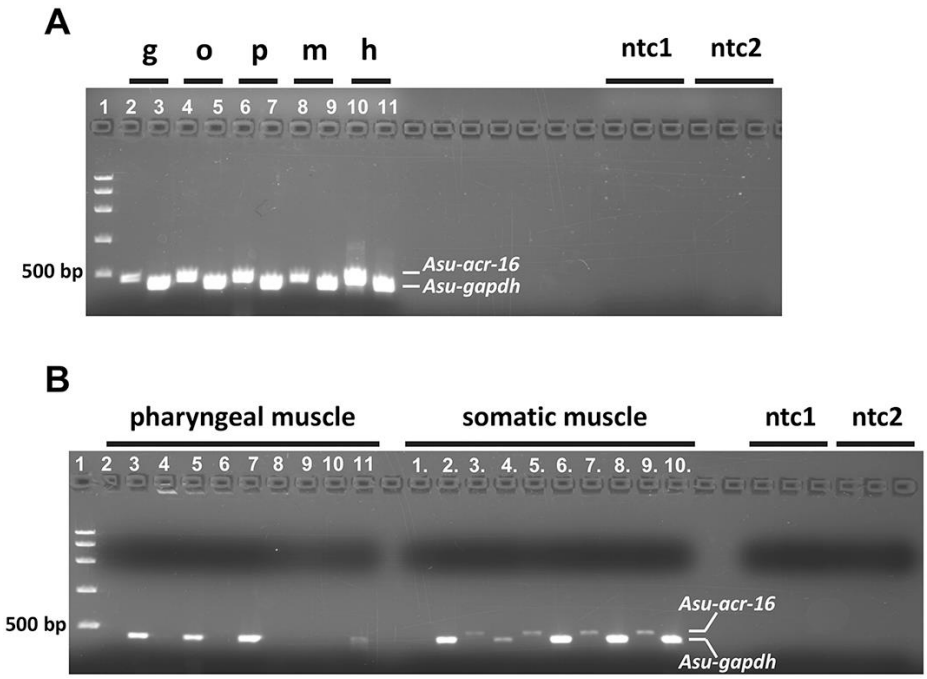

Figure 3.1 Localization of *Asu*-ACR-16 in different body tissues of the *A. suum* worm using RT-PCR and single-cell RT-PCR (n = 5). **(**A) RT-PCR analysis of *Asu-acr*-16 (lanes 2, 4, 6, 8, 10) and *gapdh* control (lanes 3, 5, 8, 9, 11) in gut (g), oviduct (o), pharynx (p), somatic muscle strip (m) and head region (h). The PCR products size for *acr*-16 and *gapdh* is 468 and 411 bp respectively. (B) Single-cell RT-PCR of *Asu*-ACR-16 in pharyngeal muscle (2, 4, 6, 8, 10) and in somatic muscle (1., 3., 5., 7., 9.). RT-PCR of *gapdh* control in pharyngeal muscle (3, 5, 7, 9, 11) and in somatic muscle (2., 4., 6., 8., 10.). 1, FastRuler High Range DNA ladder; ntc1, no-template controls for *acr*-16; ntc2, no-template controls for *gapdh*.

3.7.4 *ric-3* is required for functional expression of *Asu*-ACR-16

After we cloned *Asu*-ACR-16, we examined ancillary protein requirements for its expression in *Xenopus* oocytes. Figure 3.2 shows the effects of co-injecting the cRNA for the ancillary proteins: *ric*-3, *unc*-50 and *unc*-74 from *A.suum*; *ric*-3, *unc*-50 and *unc*-74 from *H.contortus*; and *ric*-3 from *X. laevis.* We measured oocyte responses to 100 μM ACh. Figure 3.2A shows representative traces of inward currents induced by the different combinations of ancillary proteins and *Asu-acr*-16. Figure 3.2B is a bar chart of the mean ± SEM of the 100 μM ACh responses. Oocytes injected with *Asu-acr*-16 cRNA alone did not respond to 100 μM ACh (n = 21). The largest currents (I_{max} = 290.6 ± 63.7 nA, n = 23) were seen in oocytes where just *ric*-3 from *A. suum* was co-injected with *Asu-acr*-16: these oocytes had larger current responses to 100 μM ACh than oocytes in which all three of the ancillaries (*ric*-3, *unc*-50 and *unc*-74 from either *H. contortus* or *A. suum*) were injected with *Asu-acr*-16. The currents were also larger than when just *Hco-ric*-3 was co-injected with *Asu-acr*-16, suggesting that there is a species-selective interaction between *Asu*-ACR-16 and *Asu*-RIC-3. Interestingly, *Xle-ric*-3 produced mean currents that lay between those produced by *Ascaris and Haemonchus ric*-3. We concluded that the robust expression of *Asu*-ACR-16 in *Xenopus* oocytes requires *ric*-3, but not *unc*-50 and *unc*-74.

We also varied the amount of cRNA of *Asu-acr*-16 (10–25 ng) and cRNA of *Asu-ric*-3 (5–15 ng) injected to test the effects on expression. Supporting Information S3A, B shows representative current traces and bar charts of mean ± SEM of the current responses. The largest response (1062 ± 94.1 nA, n = 6) was obtained from oocytes injected with 25 ng *Asu-acr*-16 and 5 ng *Asu-ric*-3. We observed that the responses were dependent on the amounts of *Asu-acr*-16 and *Asc-ric*-3 injected and that increased *ric*-3 did not overcome the effects of

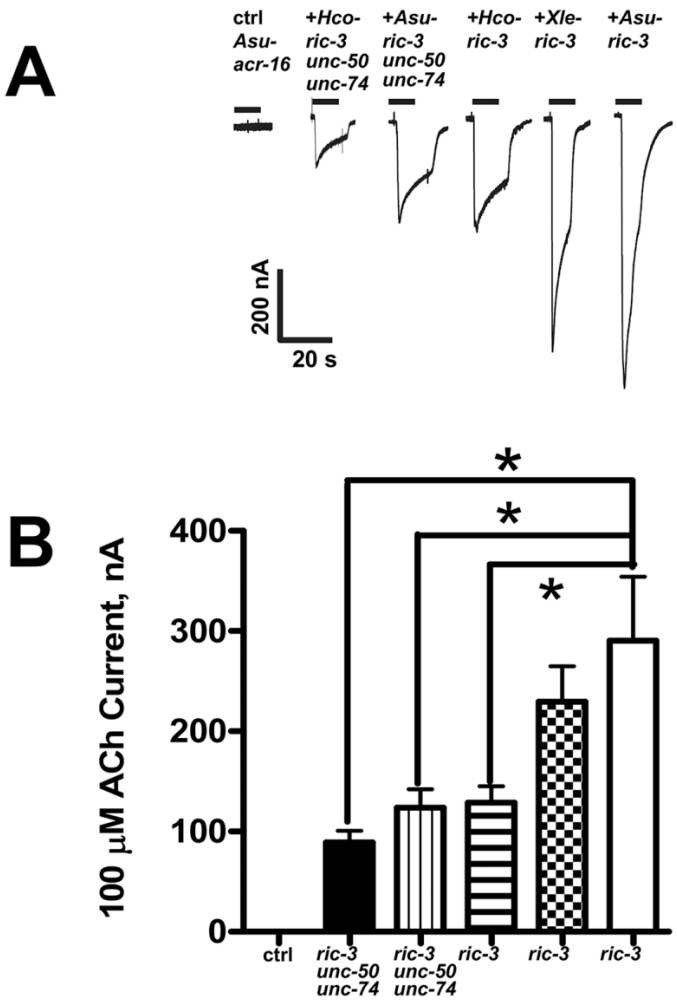

Figure 3.2 Effects of the ancillary proteins, RIC-3, UNC-50 and UNC-74, from different nematode species, on *Asu*-ACR-16 expression. (A) Sample traces represented as inward currents produced in response to 100 μM ACh. (B) Bar chart (mean ± SEM) showing (left to right) current (in nA) generated in response to 100 μM ACh produced. Control (ctrl): *Asu-acr*-16 alone (n = 21). Black bar: *Asu-acr*-16 plus *Hco-ric*-3, *unc*-50 and *unc*-74 (n = 15). Vertical line fill: *Asu-acr*-16 plus *Asu ric*-3, *unc*-50 and *unc*-74 (n = 15). Horizontal line fill: *Asu-acr*-16 plus *Hco-ric*-3 (n = 17). Checkered fill: *Asu-acr*-16 plus *Xle-ric*-3 (n = 20). No fill: *Asu-acr*-16 plus *Asu-ric*-3 (n = 23). *Asu-acr*-16 on its own did not respond to ACh, and the largest current size was obtained when *Asu-acr*-16 was co-injected with *Asu-ric*-3. * $P < 0.05$; significantly different as indicated; Tukey's multiple comparison tests.

3.7.5 *Asu*-ACR-16 forms a nicotine-sensitive but levamisole-insensitive nAChR

reduced *acr*-16. All subsequent recordings were carried out on oocytes in which 25 ng *Asu*-*acr*-16 was co-injected with 5 ng *Asu*-*ric*-3.

3.7.5 *Asu*-ACR-16 forms a nicotine-sensitive but levamisole-insensitive nAChR

Figure 3.3 shows the rank order potency series for a selection of nine nicotinic agonists and eight cholinergic anthelmintic agonists tested on the expressed *Asu*-ACR-16 nAChR. The nicotinic and anthelmintic agonists were tested at 100 μM, except for

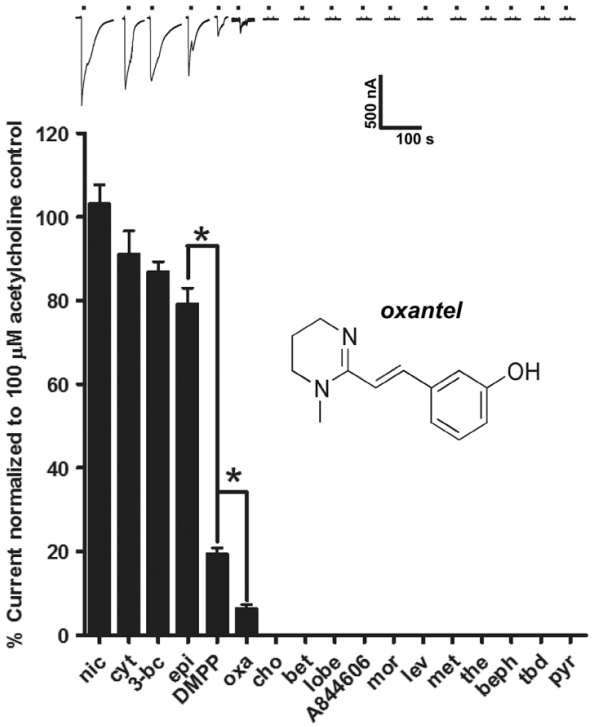

Figure 3.3 Effects of nAChR agonists and anthelmintics on *Asu*-ACR-16. Sample traces and bar chart (mean ± SEM) showing rank order potency series for nAChR agonists: nicotine (nic), cytisine (cyt), 3-bromocytisine (3-bc), epibatidine (epi), DMPP, choline (cho), betaine (bet), lobeline (lobe) and A844606; and cholinergic anthelmintics: oxantel (oxa), morantel (mor), levamisole (lev), methyridine (met), thenium (the), bephenium (beph), tribendimidine (tbd) and pyrantel (pyr); on *Asu*-ACR-16. Overall, the rank order potency series for agonists and anthelmintics on *Asu*-ACR-16 when normalized to the control 100 μM ACh current was as follows: 100 μM nic (n = 21) ~ 100 μM cyt (n = 21) ~ 100 μM 3-bc (n = 15) ~ 100 μM epi (n = 15) > 100 μM DMPP (n = 21) > 100 μM oxa (n = 36) >>> 100 μM cho (n = 15) = 100 μM bet (n = 15) = 100 μM lobe (n = 15) = 100 μM A844606 (n = 15) = mor (n = 21) = 100 μM lev (n = 21) = 100 μM met (n = 15) = 100 μM the (n = 15) = 100 μM beph (n = 15) = 30 μM tbd (n = 15) = 100 μM pyr (n = 15). * P < 0.05; significantly different as indicated; Tukey's multiple comparison tests.

tribendimidine, which was tested at a concentration of 30 μM due to its limited solubility. Representative traces of inward currents induced by each nicotinic or anthelmintic agonist are shown along with their mean ± SEM normalized values as bar charts. Nicotine, cytisine, 3-bromocytisine and epibatidine were the most potent (>80% of the control ACh current), whereas DMPP was least potent (<20% of the control ACh current). Choline, betaine, lobeline and A844606 were not active on the *Asu*-ACR-16 nAChR. With the exception of oxantel, which showed a very weak agonist effect (<10% of the control ACh current), the *Asu*-ACR-16 nAChR was not activated by any of the other anthelmintic drugs tested (morantel, levamisole, methyridine, thenium, bephenium, tribendimidine and pyrantel). The rank order potency series for agonists and anthelmintics on *Asu*-ACR-16 when normalized to the internal standard control 100 μM ACh current was as follows: *nicotine ~ cytisine* ~ 3-*bromocytisine ~ epibatidine > DMPP > oxantel >> > choline = betaine = lobeline = A*844606 = *morantel = levamisole = methyridine = thenium = bephenium = tribendimidine = pyrantel.* Nicotine was among the most potent agonists, while none of the cholinomimetic anthelmintics produced any effect, except for the small effect of oxantel. This agonist potency series shows that this nAChR is distinct from the levamisole receptors of nematodes.

3.7.6 *Asu*-ACR-16 desensitization

Desensitization was a feature of the *Asu*-ACR-16 receptor responses and was characterized by the peak and waning current responses observed during maintained (for 10 s) agonist applications. We observed receptor desensitization with all potent agonists. The time constants for desensitization observed with different agonists are shown in Figure 3.4: the mean time constants for desensitization rates ranged between 6.2 and 12.6 s, with the

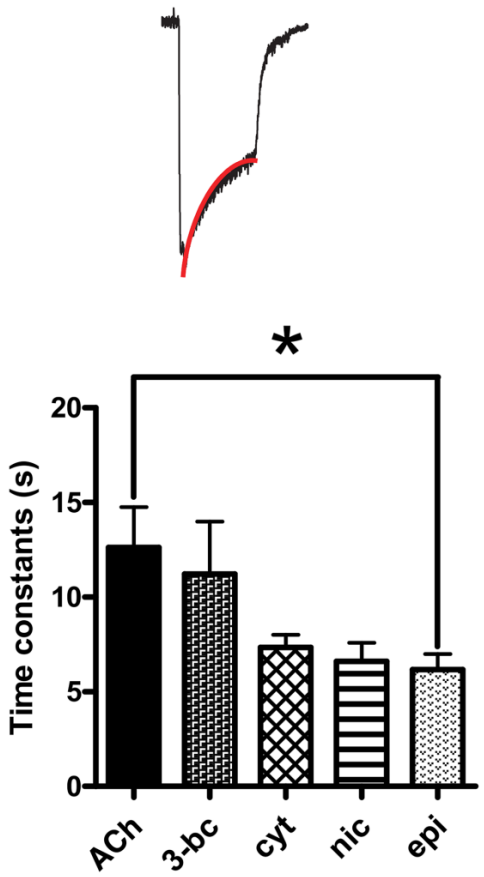

Figure 3.4 *Asu*-ACR-16 desensitization rate constant fit. Bar chart (mean ± SEM) showing *Asu*-ACR-16 desensitization in response to ACh, 3-bromocytisine (3-bc), cytisine (cyt), nicotine (nic) and epibatidine (epi). The rank order for *Asu*-ACR-16 time constants of desensitization was as follows: 100 μM ACh (12.6 ± 2.1 s, $n = 6$) ~ 100 μM 3-bc (11.2 ± 2.8 s, $n = 6$) ~ 100 μM cyt (7.3 ± 0.7 s, $n = 6$) ~ 100 μM nic (6.6 ± 1.0 s, $n = 4$) ~ 100 μM epi (6.2 ± 0.8 s, $n = 6$). *Insert*: Sample trace with red line signifying desensitization fit. * $P < 0.05$; significantly different as indicated; Tukey's multiple comparison tests.

time constant for desensitization depending on the agonist and significantly higher for ACh than for epibatidine. However, these time constants were markedly longer than the vertebrate α7 receptor, which has desensitization time constants in the 230–1300 ms range (McCormack *et al.*, 2010): the slower desensitization rates may be explained in part by the absence of the amino acids: V251, L254 and L255 in *Asu*-ACR-16.

3.7.7 Nicotine as a potent agonist

Figure 3.5 shows representative recordings and concentration–response relationships of inward currents induced by the application of different concentrations of ACh (Figure 3.5A), top trace, and nicotine (Figure 3.5A), lower trace. The first application of an agonist for each new recording was always 100 μM ACh, which was used as the internal standard for normalization. The EC_{50} for nicotine (4.5 ± 0.2 μM, n = 6) was statistically significantly smaller than that for ACh (EC_{50} of 5.9 ± 0.1 μM, n = 6), which, on this basis, nicotine is more potent than ACh. Interestingly, there was no significant difference between the maximum response for nicotine (I_{max} of 82.5 ± 3.4%, n = 6) and that for ACh (I_{max} of 82.7 ± 2.4%, n = 6). There was also no significant difference between the Hill slopes, n_H, for

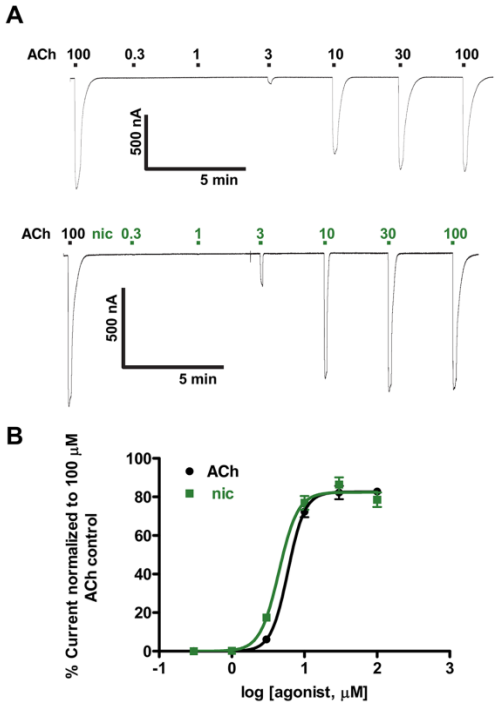

Figure 3.5 Nicotine (nic) and ACh concentration–response relationships for *Asu*-ACR-16 in the absence of antagonists. (A) Sample traces for ACh (top trace) and nicotine (lower trace) dose–response relationships for *Asu*-ACR-16. (B) ACh and nic dose–response curves for *Asu*-ACR-16. EC_{50} values (mean ± SEM, μM) were 5.9 ± 0.1 for ACh, Hill slope (n_H) = 3.9 ± 0.3, n = 6, and 4.5 ± 0.2 for nic, n_H = 3.4 ± 0.2, n = 6.

both nicotine and ACh. However, both the nicotine and ACh concentration–response curves were very steep, with Hill slopes, N_H, of 3.4 ± 0.2, n = 6, for nicotine and 3.9 ± 0.3, n = 6, for ACh, showing strong cooperativity consistent with homomeric receptors containing multiple ligand binding sites.

3.7.8 Rank order antagonist potencies: *Asu*-ACR-16 is not sensitive to α-BTX

We tested 10 μM concentrations of eight nAChR antagonists of mammalian or nematode receptors on the expressed *Asu*-ACR-16 nAChR. The antagonists were α-bungarotoxin (α-BTX), dihydro-β-erythroidine (DHβE), d-tubocurarine (dTC), hexamethonium, mecamylamine, methyllycaconitine (MLA), derquantel, and paraherquamide. The mean % inhibition of the control 100 μM ACh current response wasused to determine the rank order potency of the antagonists. α-BTX, an α7 receptor selective antagonist, had little effect on the *Asu*-ACR-16 receptor and was the least potent (inhibition, 5.5 ± 0.8% n = 6) antagonist in the rank order series. In this respect, the *Asu*-ACR-16 receptor was unlike the mammalian α7 nAChR. Mecamylamine, MLA and dTC were the most potent. The rank order of potency (Figure 3.6A) was

mecamylamine = MLA = dTC > paraherquamide ~ derquantel ~ hexamethonium ~ DHβE > α-BTX.

3.7.9 Non-competitive derquantel antagonism and mixed antagonism of dHβE

We tested the effects of the nAChR antagonists, derquantel and DHβE on ACh (Figure 3.6B1). The concentration–response plots (Figure 3.6B2) show that derquantel acts as a non-competitive antagonist, with 1 μM derquantel producing a statistically significant reduction in the maximum response, but no significant change in the EC_{50}. I_{max} and EC_{50} values were respectively 82.7 ± 2.4% and 5.9 ± 0.1 μM, n = 6, for ACh and 63.8 ± 2.8% and

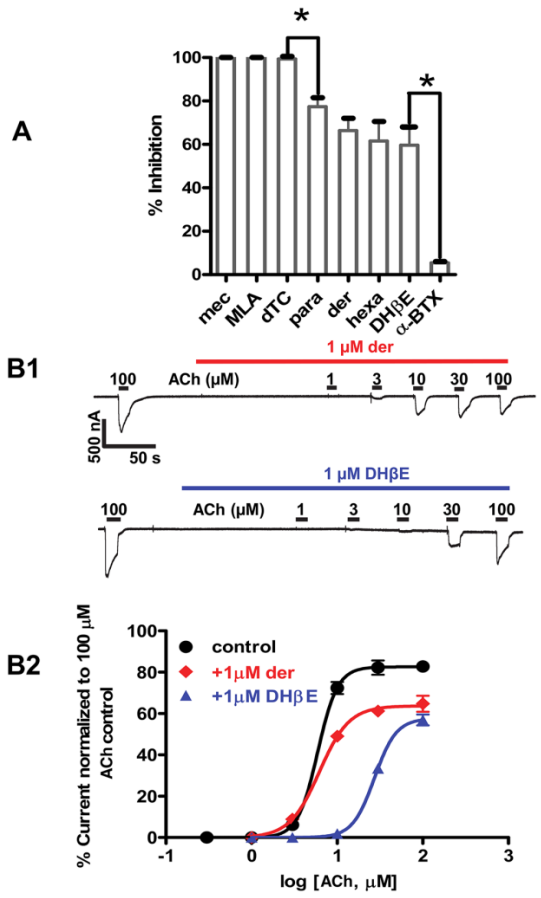

Figure 3.6 (A) Effects of selected nAChR antagonists on *Asu*-ACR-16-mediated ACh responses. Bar chart showing effects of selected nAChR antagonists on *Asu*-ACR-16. Results were expressed as mean (± SEM) % inhibition of currents elicited by 100 μM ACh, $n = 6$, for all antagonists. dTC, mecamylamine (mec) and MLA completely blocked *Asu*-ACR-16-mediated ACh responses, while paraherquamide (para), derquantel (der), hexamethonium (hexa) and DHβE only produced a partial block of *Asu*-ACR-16-mediated ACh responses and α-BTX produced an almost insignificant block of *Asu*-ACR-16-mediated ACh responses. Rank order potency series for the nAChR antagonists each tested at a concentration of 10 μM was as follows: mecamylamine ($n = 6$) = MLA ($n = 6$) ≈ dTC ($n = 6$) > paraherquamide ($n = 6$) ~ derquantel ($n = 6$) ~ hexamethonium (hexa) ($n = 6$) ~ DHβE ($n = 6$) > α-BTX ($n = 6$). * $P < 0.05$; significantly different as indicated; Tukey's multiple comparison tests. We used ANOVA and Bartlett's test for variance inhomogeneity and found no significant difference and Tukey's multiple comparison tests. (B) Dose–response relationships for *Asu*-ACR-16 in the presence of antagonists. (B1) Sample traces for ACh concentration–response relationships for *Asu*-ACR-16 in the presence of 1 μM derquantel and 1 μM DHβE. (B2) ACh concentration–response plots for *Asu*-ACR-16 in the presence of 1 μM derquantel and 1 μM DHβE. Derquantel caused a reduction in the maximum response, but no change in EC_{50}, whereas DHβE caused both a reduction in the maximum response and a right shift in the EC_{50}.

6.2 ± 0.5 μM, n = 6, for derquantel. DHβE produced mixed competitive and non-competitive antagonism (Figure 3.6B2) characterized by a significant right shift in the EC_{50} and a statistically significant reduction of the maximum response. EC_{50} and I_{max} values were respectively 5.9 ± 0.1 μM and 82.7 ± 2.4%, n = 6, for ACh and 29.0 ± 1.0 μM and 58.0 ± 3.1%, n = 6, for DHβE. These observations suggest that antagonists of this receptor act at more than one site that may include the agonist-binding site and/or a different allosteric site.

3.7.10 PAMS of human α7 nAChRs inhibit *Asu*-ACR-16 responses

Ion channel receptor opening may be increased (agonists) or decreased (competitive antagonists) by drugs binding to the ligand binding site, or the opening can be increased by PAMs or decreased by negative allosteric modulators binding to a site other than the ligand binding site (allosteric sites). Ivermectin and genistein are α7 receptor type 1 PAMs (Sattelle *et al.*, 2009), which increase the response to a fixed concentration of an agonist by increasing the amplitude of the current response; PNU120596 is an α7 receptor type 2 PAM (Kalappa and Uteshev, 2013) whose action is characterized by both an increased amplitude of response and the reduction of desensitization of the current response to a fixed concentration of agonist.

We were interested to see if ivermectin, genistein and PNU120596 were PAMs of the *Asu*-ACR-16. We tested the effects of ivermectin (10 μM), genistein (3 μM) and PNU120596 (3 μM) separately on responses to 10, 30 and 100 μM ACh (Supporting Information S3.3). We did not observe potentiation in any experiment, but we saw modest reductions in the amplitudes of the responses. Figure 3.7 shows bar charts of the mean ± SEM [n = 6 (ivermectin), n = 6 (genistein), n = 6 (PNU120596)] currents of the control and test responses

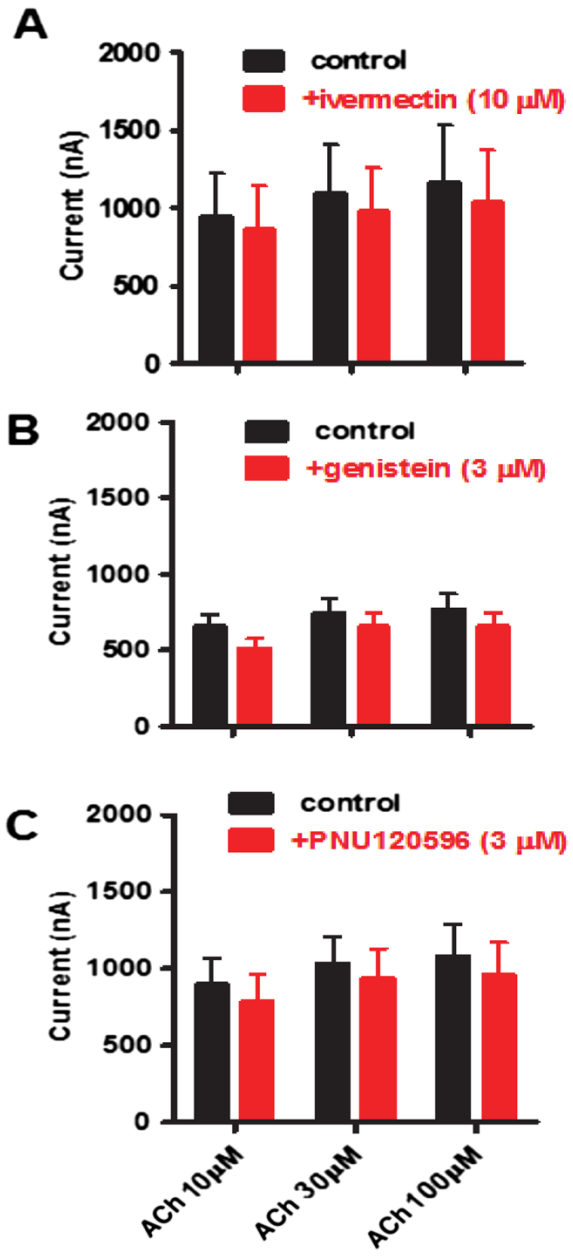

Figure 3.7 Effects of PAMs of human-α7 on *Asu*-ACR-16-mediated ACh responses. Bar charts showing blocking actions of human-α7 PAMs; (A) 10 µM ivermectin (n = 6), (B) 3 µM genistein (n = 6) and (C) 3 µM PNU120596 (n = 6), on the responses of *Asu*-ACR-16 to ACh. The type 1 PAMs, ivermectin and genistein, as well as the type 2 PAM, PNU120596, caused a reduction in *Asu*-ACR-16 responses to 10, 30 and 100 µM ACh, with the reduction being more pronounced at 10 than at 30 or 100 µM ACh.

3.7.11 Calcium permeability of *Asu*-ACR-16

in the presence of the allosteric modulator. Two-way ANOVA showed that ivermectin, genistein and PNU120596 had a statistically significant inhibitory effect on *Asu*-ACR-16 ACh responses. This inhibitory effect of ivermectin, genistein and PNU120596 was opposite to the stimulatory effect on mammalian α7 receptors (Sattelle *et al.*, 2009).

3.7.11 Calcium permeability of *Asu*-ACR-16

The calcium permeability of nAChRs varies and relates to the channel pore region formed by the TM2 domain of the subunit (Corringer *et al.*, 1999a; Tapia *et al.*, 2007). We tested the calcium permeability of the *Asu*-ACR-16 receptor by determining the shift in the reversal potential of the current–voltage (I–V) plot following a change in the concentration of Ca^{2+} in the extracellular solution (Supporting Information S3.4). Increasing the concentration of Ca^{2+} from 1 to 10 mM produced an inward rectification of the current through the *Asu*-ACR-16 receptor and a small positive shift of the I–V plot of 2.4 ± 2.1 mV (n = 6). A shift of 2.4 mV indicates relative calcium permeability (P_{Ca}/P_{Na}) of 0.4 when calculated from the GHK equation. The α7 receptor is much more permeable to calcium than the *Asu*-ACR-16 receptor. The P_{Ca}/P_{Na} reported for α7 nAChRs is 20, calculated from a 29 ± 3 mV shift under similar conditions (Séquéla *et al.*, 1993), which was significantly (two-tailed t-test) bigger than the 2.4 mV shift observed for *Asu-ACR*-16.

3.8 Discussion

This study reports for the first time the reconstitution in the *Xenopus* oocyte expression system of a fully functional homomeric nAChR, ACR-16, from a parasitic nematode. This finding is of significant importance in anthelmintic drug discovery in that it provides an efficient platform for screening anthelmintic compounds.

3.8.1 Comparison of pharmacology of *Asu*-ACR-16 with *Cel*-ACR-16

Previous work on the functional reconstitution in *Xenopus* oocytes and pharmacological characterization of ACR-16 has focused on the model nematode, *C. elegans* (Ballivet *et al.*, 1996). In agreement with Ballivet *et al.* (1996), *Asu*-ACR-16 was more sensitive to nicotine than ACh, but insensitive to levamisole and pyrantel. However, the Hill slopes for nicotine (n_H = 3.4 ± 0.2, n = 6) and ACh (n_H = 3.9 ± 0.3, n = 6) concentration–response curves for *Asu*-ACR-16 were slightly steeper than those reported for *Cel*-ACR-16 (n_H = 2.2 for nicotine and n_H = 2.1 for ACh). In any case, the Hill slopes for both *Asu*-ACR-16 and *Cel*-ACR-16 reveal strong cooperativity associated with homomeric receptors. The steeper Hill slopes for *Asu*-ACR-16 may account for its higher sensitivity (as shown by EC_{50} values) to nicotine and ACh when compared with those for *Cel*-ACR-16 (*Asu*-ACR-16's EC_{50} values were 4.5 ± 0.2 μM, n = 6, for nicotine and 5.9 ± 0.1 μM, n = 6, for ACh. On the other hand, for *Cel*-ACR-16, EC_{50} values were 12.6 μM for nicotine and 55.4 μM for ACh. Despite the high degree of sequence identity (74.75% identity) between *Asu*-ACR-16 and *Cel*-ACR-16 (Ce21), there exist significant differences in terms of the antagonist pharmacology of these two receptors. In accordance with Ballivet *et al.* (1996), *Asu*-ACR-16 was nearly insensitive to α-BTX, but highly sensitive to dTC. In contrast, *Asu*-ACR-16 was highly sensitive to MLA, but moderately sensitive to hexamethonium and DHβE.

3.8.2 Comparison of pharmacology of *Asu*-ACR-16 with α7 nAChRs

Alignment of *Asu*-ACR-16 with human α7 nAChRs shows similarities but important differences in amino acid residues, suggesting differences in their pharmacologies. We findsimilarities in agonist sensitivity to ACh, nicotine and epibatidine of *Asu*-ACR-16 and α7 receptors (Raymond *et al.*, 2000; Li *et al.*, 2011). However, *Asu*-ACR-16 was insensitive to

the α7-selective agonist, A844606. *Asu*-ACR-16 was highly sensitive to MLA just like α7 (Briggs *et al.*, 1995), but in contrast to the sensitivity of α7 receptors to α-BTX (Zhao *et al.*, 2003), we observed *Asu*-ACR-16 to be quite insensitive to α-BTX. The PAMs of α7 (ivermectin, genistein and PNU120596) were inhibitory on *Asu*-ACR-16. Lastly, we found that the relative calcium permeability ratio of *Asu*-ACR-16 was about 50× smaller than that of the α7 receptor (Séquéla *et al.*, 1993). The pharmacology of *Asu*-ACR-16 receptors is thus different to that of α7 nAChRs, indicating that the *Asu*-ACR-16 receptor has potential as a drug target site.

3.8.3 Comparison of pharmacology of *Asu*-ACR-16 with levamisole receptors

Asu-ACR-16 is different from the classical cholinergic levamisole receptor. The levamisole receptor subtypes are composed of different mixtures of heterologous subunits (UNC-29, UNC-38, ACR-8, LEV-1, ACR-13 and UNC-63) (Martin *et al.*, 2012b), whereas *Asu*-ACR-16 consists of only one subunit (ACR-16). Unlike the levamisole receptors, which are sensitive to levamisole but insensitive to nicotine, *Asu*-ACR-16 is sensitive to nicotine but insensitive to levamisole. All three ancillary proteins, RIC-3, UNC-50 and UNC-74, are required for robust expression of levamisole-sensitive receptors (Boulin *et al.*, 2008), while ACR-16 requires only RIC-3 for optimal expression in *Xenopus* oocytes (Sattelle *et al.*, 2009; Bennett *et al.*, 2012).

Another important difference between *Asu*-ACR-16 and the levamisole receptor can be seen in their antagonist pharmacologies. The levamisole receptor was only slightly inhibited by the nAChR antagonist, DHβE (Richmond and Jorgensen, 1999), whereas *Asu*-ACR-16 was strongly inhibited by DHβE. MLA and hexamethonium are also less potent on levamisole receptors. Because the pharmacology of ACR-16 is different from the levamisole

receptors, a selective anthelmintic directed at ACR-16 may have the appropriate properties to bypass resistance.

3.8.4 Differences in α-BTX potency, allosteric modulation and Ca^{2+} permeability

Site-directed mutagenesis of nAChR subunits has been exploited as one of the tools in understanding the pharmacological differences between nAChR types. In a bid to provide reasons for the differences between the pharmacology of α7 receptors and *Asu*-ACR-16, we reviewed and compared the amino acids known to affect receptor pharmacology. In α7 for instance, the amino acids critical for α-BTX binding are ERFYECCKEPYPD in the C-loop (Balass *et al.*, 1997). The corresponding residues in *Asu*-ACR-16 are E**K**FY**D**CC**P**EPYPD: the RK, ED and KP substitutions may explain why α-BTX is not as potent as an antagonist of the *Asu*-ACR-16 receptor.

There are seven residues in α7 nAChRs important for positive allosteric modulation by ivermectin (Figure 3.0A, dark green arrows). Remarkably, none of these amino acids are conserved in *Asu*-ACR-16, which may explain why a positive allosteric effect of ivermectin for *Asu*-ACR-16 was not detected. Mutations in four of these residues (A225D, Q272, T456Y and C459) caused a significant reduction in the potency of ivermectin as a PAM, while mutations in the other three (S222M, M253L and S276V) caused ivermectin to act as an antagonist (Collins and Millar, 2010). *Asu*-ACR-16 contains the M253L substitution consistent with the observed inhibitory effect of ivermectin. Furthermore, we found that PNU120596 was not an allosteric modulator of *Asu*-ACR-16, in contrast to its action at α7 receptors. The amino acid residues between TM2 and TM3 in α7 responsible for PNU120596 positive allosteric modulation (AEIMPATSDS) (Bertrand *et al.*, 2008) are replaced with **S**EI**S**P**P**TS**EA** in *Asu*-ACR-16 (blue-edged box, Figure 3.0A). These differences may

account for the lack of positive allosteric modulation by PNU120596 in *Asu*-ACR-16. The amino acid differences in allosteric modulatory sites may allow for the design of selective drugs targeted at *Asu*-ACR-16.

Three residues, E237, L254 and L255, play key roles in the Ca^{2+} permeability of α7 nAChRs (grey and grey outline arrows, Figure 3.0A). In these receptors, mutations E237A, L254R/T and L255R/T/G cause a reduction in Ca^{2+} permeability (Bertrand *et al.*, 1993). When compared with *Asu*-ACR-16, only one (E237) of these three residues is conserved. Amino acid differences at one or more positions may account for the reduction in the Ca^{2+} permeability of the *Asu*-ACR-16 compared with the α7 receptor.

3.8.5 Ubiquitous distribution of *Asu*-ACR-16 receptor and its function

ACR-16 has been identified as one of the proteins required for the excitatory current at the neuromuscular junction of *C. elegans* (Richmond and Jorgensen, 1999; Francis *et al.*, 2005). In fact, *acr*-16 null mutants show nearly normal motor behaviour. Severe locomotion deficits were, however, seen with *acr*-16:*unc*-63 or *acr*-16:*unc*-29 double mutants (Touroutine *et al.*, 2005; Li *et al.*, 2014), showing that, in combination with other subunits, its function was essential.

The ubiquitous distribution of the *Asu*-ACR-16 message in tissues like the intestine and reproductive tract suggests that this receptor has functions which are not limited to regulation of fast neuromuscular transmission. The presence of *Asu*-ACR-16 in non-excitable tissues suggests that *Asu*-ACR-16 also has slower paracrine/autocrine and homeostatic or differentiation functions associated with digestion and reproduction (Kawashima and Fujii, 2008). A paracrine and endocrine intestinal function for ACh is also supported by the presence of an organized distribution of acetylcholinesterase just beneath and adjacent to the

intestinal epithelium (Lee, 1996). The wide tissue distribution of *Asu*-ACR-16 message suggests that a selective agonist may have advantages as an anthelmintic.

3.8.6 Consideration of *Asu*-ACR-16 as a drug target

Our findings show the *Asu*-ACR-16 receptor is pharmacologically different from previously characterized nAChRs and may serve as a potential target for therapeutic drug discovery. Given that *Asu*-ACR-16 shares some similarities with the mammalian α7 nAChR in terms of agonist pharmacology, it seems more likely that a drug directed at allosteric modulation sites may be more selective because the actions of α7 PAMs on the *Asu*-ACR-16 receptor were clearly different from those observed on the mammalian α7 receptor. This is particularly of interest because in recent years, PAMs have received considerable attention as nAChR-targeted therapeutic agents (Williams *et al.*, 2011). The α7 nAChR has been more exploited in this regard because of its implication in cognitive disorders such as Alzheimer's disease and schizophrenia, and drugs targeting α7 PAM sites have been suggested to have therapeutic potential for these disorders (Bertrand and Gopalakrishnan, 2007). Therefore, targeting the corresponding sites in *Asu*-ACR-16 may give rise to potential therapeutics which will not affect the mammalian host. It may therefore be possible to identify a suitable novel cholinergic anthelmintic which is ‘resistance busting’ if it were to activate a vital cholinergic receptor that was composed of different novel nAChR subunits.

3.9 Acknowledgements

We would like to express our gratitude to Debra J Woods, Zoetis Animal Health, Kalamazoo, MI, USA, for the generous supply of derquantel. We would also like to thank Professor Shu Hua Xiao, National Institute of Parasitic Diseases, Shanghai, Peoples' Republic of China, for the gift of tribendimidine. Research funding was by The Hatch Act,

State of Iowa; NIH grant R01 AI047194 National Institute of Allergy and Infectious Diseases to R.J.M.; NIH grant R21AI092185 National Institute of Allergy and Infectious Diseases to A.P.R.; and the Schlumberger "Faculty for the Future" programme to M.A. and A.P.R. The funding agencies had no role in the design, execution or publication of this study. The content is solely the responsibility of the authors and does not necessarily represent the official views of the National Institute of Allergy and Infectious Diseases.

3.10 Author Contributions

M.A. conceived and designed the research study, performed the research, analysed the data, contributed reagents/materials/analysis tools and wrote the paper. S.K.B. performed the research. E.C. performed the research, analysed the data and contributed reagents/materials/analysis tools. C.L.C. wrote the paper. C.N. analysed the data, contributed reagents/materials/analysis tools and wrote the paper. C.J.M. performed the research. S.V. performed the research. A.P.R. conceived and designed the research study, analysed the data, contributed reagents/materials/analysis tools and wrote the paper. R.J.M. conceived and designed the research study, analysed the data, contributed reagents/materials/analysis tools and wrote the paper.

3.11 Conflict of interest

The authors declare no conflicts of interest.

3.12 Declaration of transparency and scientific rigour

This Declaration acknowledges that this paper adheres to the principles for transparent reporting and scientific rigour of preclinical research recommended by funding agencies, publishers and other organisations engaged with supporting research.

3.13 Supporting Information

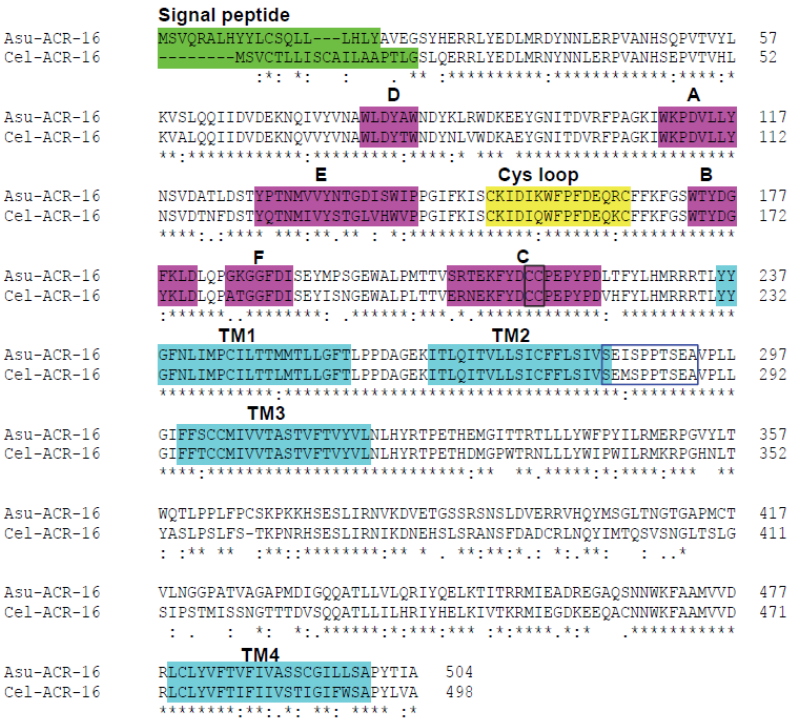

Supporting Figure S3.0 Amino acid sequence alignment of *Asu*-ACR-16 and *Cel*-ACR-16 nAChR subunits. The signal peptide (bright green box), ACh-binding loops A‑F (pink boxes), cys-loop (yellow box) and transmembrane regions TM1‑TM4 (turquoise boxes) are indicated. The vicinal cysteines (blackedged box) that characterize an α-subunit are present in the C-binding loop. The blue-edged box between TM2 and TM3 represents the region where PNU120596 acts on α7.

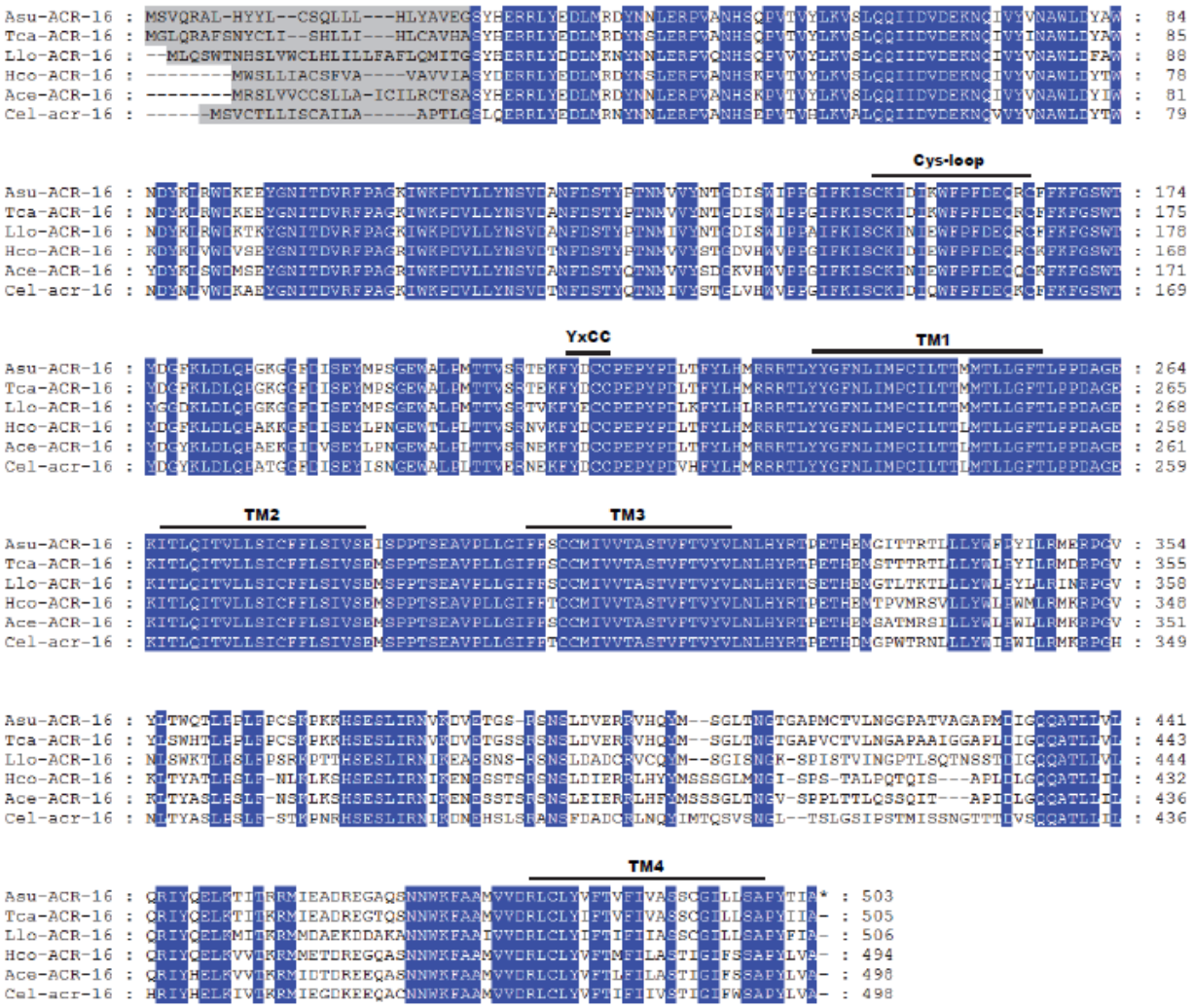

Supporting Figure S3.1 Alignment of ACR-16 sequences from *Asu*, *Toxocara canis*, *Loa loa*, *Hco*, *Ancylostoma ceylanicum* and *C. elegans*. Predicted signal peptide sequences are shaded in grey. Amino acids conserved between the different ACR-16 sequences are highlighted in blue. The Cys-loop, the four transmembrane regions (TM1-TM4) and the primary agonist binding site are noted above the sequence.

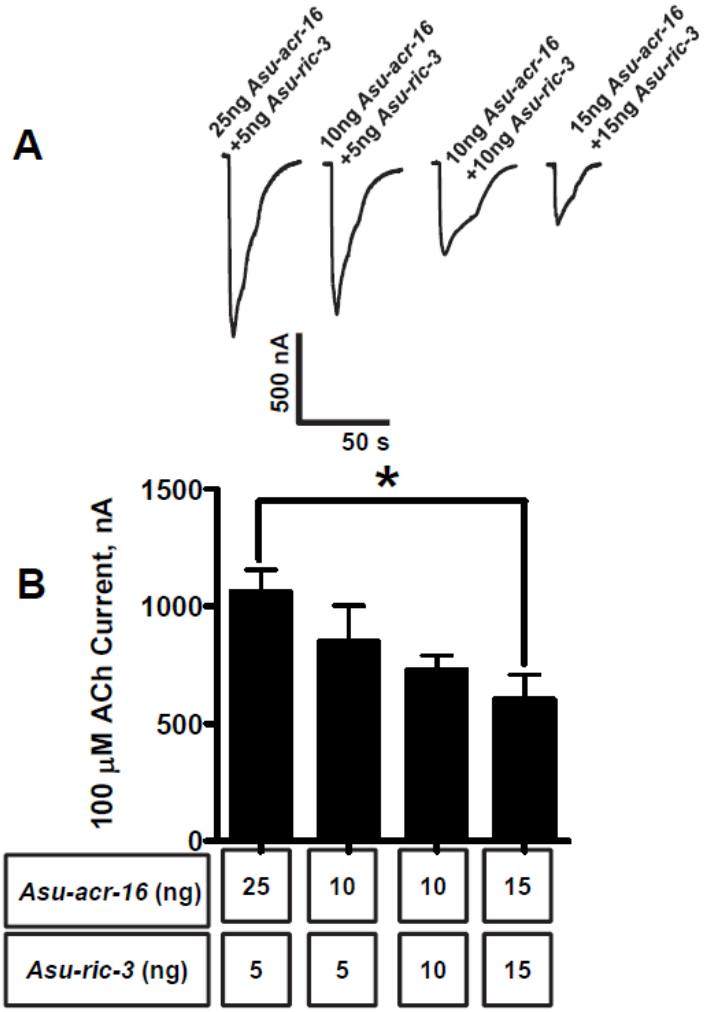

Supporting Figure S3.2 Effects of varied amounts of *Asu-acr*-16 and *Asu-ric*-3 on *Asu*-ACR-16 expression. (A) Sample traces represented as inward currents produced in response to 100 µM ACh. (B) Bar chart (mean ± SEM) showing current sizes produced by 25 ng *Asu-acr*-16 and 5 ng *Asu-ric*-3 (1062 ± 94.1, n = 6), 10 ng *Asu-acr*-16 and 5 ng *Asu-ric*-3 (848.8 ± 155.4, n = 6), 10 ng *Asu-acr*-16 and 10 ng *Asu-ric*-3 (727.3 ± 63.1, n = 6); 15 ng *Asu-acr*-16 and 15 ng *Asu-ric*-3 (602.8 ± 106.8, n = 6) in response to 100 µM ACh. * $P < 0.05$, Tukey's multiple comparison tests.

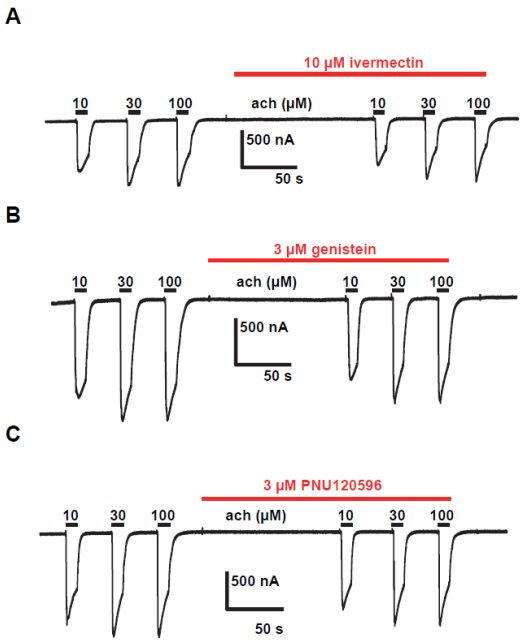

Supporting Figure S3.3 Sample traces showing the effects of PAMs of α7; (A) 10 µM ivermectin, (B) 3 µM genistein and (C) 3 µM PNU120596, on *Asu*-ACR-16-mediated ACh responses.

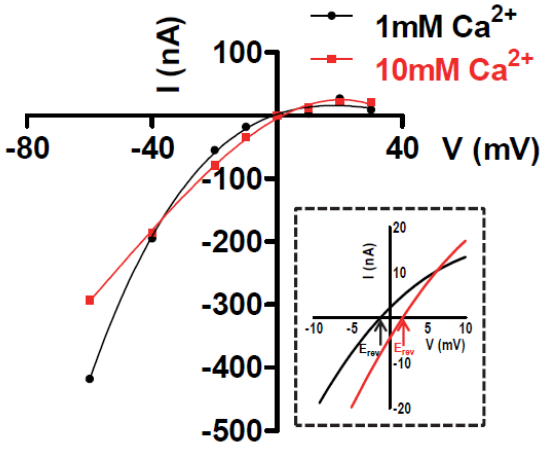

Supporting Figure S3.4 Calcium permeability of *Asu*-ACR-16 with 30 µM ACh currents: representative I-V plot for oocytes expressing *Asu*-ACR-16, showing current change with voltage in 1 mM (black line) and 10 mM (red line) Ca^{2+} recording solutions. I-V relationship was plotted using a cubic polynomial equation and interpolated to measure the E_{rev}. The mean ± SEM for the positive shift of the I-V plot for six observations was 2.4 ± 2.1mV, and this corresponded to a relative calcium permeability ratio of 0.4. Insert: magnified view of the I-V fitted line from -10 to 10 mV, showing the E_{rev} in 1 and 10 mM Ca^{2+}.

CHAPTER 4. FILARICIDAL ACTIVITIES OF *DANIELLIA OLIVERI* AND *PSOROSPERMUM FEBRIFUGUM*

Manuscript in preparation for submission to *PLoS Neglected Tropical Diseases* (2017)

Melanie Abongwa[1], Fidelis Cho-Ngwa[2], Godfred A. Ayimele[3], Moses Samje[2], Smith B. Babiaka[3], Christina Bulman[4], Judy Sakanari[4], Nicholas Koszewski[1], Saurabh Verma[1], Richard J. Martin[1], Alan P. Robertson[1*]

[1] Department of Biomedical Sciences, College of Veterinary Medicine, Iowa State University, Ames, Iowa, United States of America
[2] Department of Biochemistry and Molecular Biology, Faculty of Science, University of Buea, Buea, South West Region, Cameroon
[3] Department of Chemistry, Faculty of Science, University of Buea, Buea, South West Region, Cameroon
[4] Center for Discovery and Innovation in Parasitic Diseases, University of California San Francisco, San Francisco, California, United States of America
[*] Corresponding author and Associate Professor, Department of Biomedical Sciences, Iowa State University

4.1 Abstract

Currently approved drugs for treatment of onchocerciasis and lymphatic filariasis; ivermectin, diethylcarbamazine (DEC) and albendazole, are only effective against the microfilariae (mfs), with little or no effect on adult worms (macrofilariae). Effective control is therefore hindered by the lack of macrofilaricides, leaving the adult worms, which may live for over 15 years to continue to produce mfs and exacerbate the disease symptoms. Additionally, the repeated use of ivermectin, DEC and albendazole has generated concerns of resistance development. Clearly, there is the need for the development of new drugs that will be effective against the adult worms, while more effective microfilaricidal compounds are also desirable. To contribute to the search for new antifilarial drugs, we screened extracts and chromatographic fractions of the plants; *Daniellia oliveri and Psorospermum febrifugum* for activity against *O. ochengi* mfs and against both adult *O. ochengi* and *B. pahangi*. We found

crude extracts of *D. oliveri* to be effective in killing adult *O. ochengi* and *B. pahangi* based on the MTT/formazan assay and the Worminator system. Additionally, some extracts of *D. oliveri* and *P. febrifugum* were also active on *O. ochengi* microfilariae based on motility reduction. Results from our three assay systems identified *D. oliveri* hexane bark (DO_{BHEX}), dichloromethane stem bark (DO_{BDCM}) and dichloromethane leaf (DO_{LDCM}) as active in all three assay systems. The activity and lack of cytotoxicity for these extracts encouraged us to select them for bioassay-guided fractionation. Importantly, DO_{BHEX} IC_{50} for adult *O. ochengi* was about 12x smaller than that for the mfs, which is desirable in cases of co-endemicity with *Loa loa* due to severe adverse reactions associated with *L. loa* mf death. Furthermore, *B. pahangi* activity was retained in some of the Sep-Pak and HPLC fractions, although our results also suggest the possibility of compounds acting in synergy which may be present in 2 or more HPLC fractions. We conclude therefore that *D. oliveri* has potential as a natural plant source for the discovery and development of suitable macrofilaricides and that there is some validity in its traditional use.

4.2 Author Summary

Human onchocerciasis and lymphatic filariasis are classified by the WHO as "Neglected Tropical Diseases" (NTDs), and have the highest disease burdens of the filarial infections, affecting over 150 million people worldwide and placing a billion people at risk. Current control of these infections is limited to the use of antifilarial drugs which are only microfilaricidal. Effective control is therefore hindered by the lack of adulticides (macrofilarides), the adult worms can live for over 15 years in humans continuing to exacerbate symptoms of the disease and reproduce. Clearly, macrofilarides are needed, while more efficacious and safer microfilaricides are also desirable. In this study, we used the

MTT/formazan assay and the Worminator system to screen plant extracts and chromatographic fractions for activity against *O. ochengi* microfilariae and adults, the best-known laboratory model for *O. volvulus*, and against adult *Brugia pahangi* as a model for human lymphatic filariasis-causing species.

4.3 Introduction

Subcutaneous filariasis, otherwise known as onchocerciasis or river blindness, and lymphatic filariasis (LF), commonly known as elephantiasis, are debilitating diseases of the poor. They are among the diseases currently classified by the World Health Organization as "Neglected Tropical Diseases" (NTDs) (Hotez *et al.*, 2007). Onchocerciasis is caused by the filarial nematode, *Onchocerca volvulus*, and transmitted by the bite of the blackfly, *Simulium damnosum* (Winthrop *et al.*, 2011). Approximately 37 million people globally suffer from onchocerciasis, the majority of which are in Africa where >100 million people are at high risk of infection (Gustavsen *et al.*, 2011). Onchocerciasis is the world's second leading infectious cause of blindness, after trachoma. In Africa, hyper endemic villages can have significantly higher infection rates, where >10% of an entire village may be blind (Boatin & Richards, 2006). Additionally, onchocerciasis presents a spectrum of other debilitating pathologies which include grave and unbearable itching, disfiguring dermatitis, and depigmentation (Enk, 2006). LF is caused by the filarial nematode parasites Brugia *malayi*, *B. timori*, and *Wuchereria bancrofti*, and is transmitted by a variety of mosquitoes (*Anopheles spp, Culex spp, Aedes spp, Mansonia spp*) depending on the geographical area (de Souza *et al.*, 2012). Disease manifestations include painful and profound disfigurement of the skin (particularly of the lower portion of the body), lymphedema, elephantiasis and scrotal swelling which may eventually lead to permanent disability. LF is the second leading

cause of chronic disability worldwide, after mental illness. Over 1.2 billion people are threatened by LF, with ≥120 million people infected, and ~40 million people disfigured or incapacitated by the disease (Ottesen *et al.*, 1997). Hence, individuals infected with either onchocerciasis and/or LF not only suffer physical disability, but also suffer mental, social and economic losses, resulting in depression, stigma and poverty (Hotez *et al.*, 2006; Weiss, 2008).

Current control of onchocerciasis and LF relies on mass drug administration of ivermectin, DEC and albendazole (Gyapong *et al.*, 2005; Liang *et al.*, 2008; Richard-Lenoble *et al.*, 2003). However, these drugs are only effective against the juvenile worms (microfilariae) or larval stage of the parasites, with limited activity against the adults. This leaves the adult worms to continue to produce microfilariae and exacerbate the disease symptoms. Effective control of onchocerciasis and LF is therefore hindered by the lack of adulticides (macrofilaricides). There also exist other factors such as poor compliance, and poor safety, which limit the use of these drugs. Despite ≥15 years of mass treatment with ivermectin, in some parts of Africa (e.g North and West Regions of Cameroon) transmission of onchocerciasis has still not been interrupted (Katabarwa *et al.*, 2013; Katabarwa *et al.*, 2011). Additionally, the emergence of ivermectin resistance in parasites of veterinary importance has generated concern that resistance will eventually extend to *O. volvulus* (Felippelli *et al.*, 2014; Lustigman & McCarter, 2007). Current treatment also poses life-threatening side effects in onchocerciasis and LF patients who are co-infected with *Loa loa*. Co-infection with high levels of *L. loa* microfilariae present can cause serious adverse reactions including encephalopathy (brain damage), kidney failure, and even death (Awadzi, 2003; Boussinesq & Gardon, 1997; Boussinesq *et al.*, 2003; Gardon *et al.*, 1997). These

adverse reactions are attributed to the sudden killing of the very large microfilariae population. DEC is further contraindicated in onchocerciasis patients due to the likelihood of severe reactions involving the skin and eye (Molyneux *et al.*, 2003). Therefore, there is a pressing need for new and safer filaricidal compounds for more effective control or eradication of onchocerciasis and LF.

Historically, plants have been important sources of therapeutic compounds (Farnsworth, 1990; Farnsworth *et al.*, 1985). For instance, *Papaver somniferum* (the opium poppy) is the source of morphine (Vallejo *et al.*, 2011); *Cinchona officinalis* is the source for the antimalarial medication, quinine; artemisinin which is also used for treatment of malaria was isolated from *Artemisia annua* (sweet wormwood) (Willcox, 2009); and *Digitalis lanata* (foxglove) is the source for digoxin used in treatment of congestive heart failure (Hollman, 1996). Plants as traditional medicine have been identified to play an important role in the remedy of diseases (Martkoplishvili & Kvavadze, 2015). About 70-80% of the population in developing countries rely on traditional medicine for their health needs (Wachtel-Galor & Benzie, 2011). Nevertheless, use of traditional medicine has evolved over the years and is no longer limited to developing countries. Interest in natural therapy has greatly increased in developed countries like the United States, with an increased interest in some forms of traditional medicine like herbal, dietary or nutritional supplements (Harrison *et al.*, 2004; Qato *et al.*, 2008). Literature on the antifilarial activities of plant extracts and chromatographic fractions of medicinal plants implies plant natural products may serve as sources of lead compounds for the development of new and safe filaricides (Cho-Ngwa *et al.*, 2010; Ndjonka *et al.*, 2011; Samje *et al.*, 2014).

Daniellia oliveri (DO) and *Psorospermum febrifugum* (PF) are among the plants commonly used for the traditional treatment of onchocerciasis and LF in Bambui, North West Cameroon. Bambui is a village located in the highlands of the North West Region of Cameroon where the vegetation is predominantly of the forest savannah type. This area has many fast-flowing streams, providing a good breeding site for blackfly and mosquito species and thus transmission of arthropod-borne infections including onchocerciasis and LF.

D. oliveri (family Caesalpiniaceae) is a deciduous, medium-sized flowery tree that can reach up to 25 – 35 m tall. The plant predominantly grows in the forest areas of West and Central Africa. The genus *Daniellia* comprises of 10 species, with only *D. oliveri* extending to Sudan and Uganda. *D. oliveri*, locally known as 'kahi' in Bambui, NW Cameroon is traditionally used for the treatment of all worm infections including onchocerciasis and lymphatic filariasis and is also used for treating stomach upset. It is administered as a decoction of the stem bark, prepared by boiling and drinking one cup twice daily.

P. febrifugum (family Hypericaceae) is a flowering shrub or tree that can reach 4 m tall. The plant is generally widespread in tropical Africa, predominantly in the savanna from Guinea to West Cameroon. *P. febrifugum* is locally known as 'sawayki' in Bambui, NW Cameroon where it is traditionally used to treat onchocerciasis and rashes of any sort. It is prepared and administered just like *D. oliveri* except that the decoction is also bathed with and the oily supernatant applied as body lotion.

Treatment of onchocerciasis and LF is greatly hampered by the lack of macrofilaricides, new and safer microfilaricides to replace or complement currently available filaricidal drugs are needed. Despite the claimed efficacy of *D. oliveri* and *P. febrifugum* in the traditional treatment of onchocerciasis and LF, no scientific evidence for this claim has

been demonstrated. The overall aim of our study was to screen extracts and chromatographic fractions of *D. oliveri* and *P. febrifugum* for activity against adult *Onchorcerca sp* and *Brugia sp* as a way of contributing to the search for suitable macrofilaricides. We also screened plant extracts for microfilaricidal activity. For this study, we used *O. ochengi* as a model for the human equivalent, *O. volvulus* for screening for *Onchocerca* activity. *B. pahangi* was used for screening for LF activity because it is a suitable laboratory model organism for *B. malayi* (Bulman *et al.*, 2015).

4.4 Materials and Methods

4.4.1 Collection and identification of plants

Plants were collected from Bambui in Tubah Sub-Division, North West Cameroon based on ethnopharmacological information (Figure 4.0A: *Daniellia oliveri*; Figure 4.0B: *Psorospermum febrifugum*). Voucher specimens of all plants harvested were prepared and taken to the National Herbarium, Yaounde, Cameroon for expert identification. The plants and parts used for this study and other valuable information can be seen in Table 4.0.

Figure 4.0 Pictures of *Daniellia oliveri* (A) and *Psorospermum febrifugum* (B).

Table 4.0 Classification and traditional uses of plants screened.

Family	Scientific Name	Common Name	Traditional uses	Preparation and administration	Plant parts used	Code adopted
Caesalpiniaceae	*Daniellia oliveri*	Kahi	Treatment of all worm infections including river blindness, lymphatic filariasis, as well as stomach upset	Bark boiled and decoction drunk one cup x2/day	Leaves **(L)** and stem bark **(B)**	**DO**
Hypericaceae	*Psorospermum febrifugum*	Sawayki	Treatment of onchocerciasis and rashes of any sort	Bark boiled and decoction drunk one cup x2/day. Decoction also bathed with. Oily supernatant applied as body lotion	Leaves **(L)** and stem bark **(B)**	**PF**

4.4.2 Preparation of plants extracts

The plant parts collected were air-dried in Bambui to eliminate moisture before transporting them to the University of Buea. They were further dried in an oven (40 ^{o}C) for 2 days, and ground to fine powder using an electric blender or a grinding mill. The resultant powders were weighed and put in labeled receptacles. Powders were then sequentially macerated with HPLC grade hexane (HEX), dichloromethane (DCM) and methanol (MeOH), with the plant material always fully submerged in solvent. For each solvent, the slurry was allowed to stand closed at room temperature for 48 hours to prevent the solvent from evaporating and then filtered using Whatmann No. 1 filter paper. Extracts were concentrated under reduced pressure on a rotary evaporator (BUCHI Rotavapor R-200, Switzerland). The concentrated extracts were transferred into labeled vials and residual solvent evaporated at

ambient temperature. Once all residual solvent had evaporated, the resultant crude extracts were weighed, and their respective percentage (%) yield determined as shown in Table 4.1. The % yield for each plant extract was calculated using the formula:

$$\%\ yield = (Weight\ of\ crude\ extract \div Dry\ weight\ of\ plant\ part) \times 100$$

The vials were then sealed and stored at –20 ^{o}C or –80 ^{o}C.

Table 4.1 Percent (%) yield of plant extracts.

Plant	Dry weight (Wt) of plant part (g)	Hexane (HEX)		Dichloromethane (DCM)		Methanol (MeOH)	
		Wt (g)	% yield	Wt (g)	% yield	Wt (g)	% yield
Daniella oliveri	750.0 (leaves)	17	2.3	12	1.6	16.8	2.2
	500.0 (stem bark)	4.6	0.9	4.3	0.9	52.3	10.5
Psorospermum febrifugum	600.0 (leaves)	3.0	0.5	10.9	1.8	51.4	8.6
	300.0 (stem bark)	21.7	7.2	48.1	16.0	120.2	40.1

4.4.3 *Onchocerca ochengi* adult worm assay

Viable *O. ochengi* adult worm masses were extracted from cattle skin as previously described (Cho-Ngwa *et al.*, 2010). Fresh pieces of umbilical cattle skin containing palpable nodules were obtained from the slaughterhouse in Douala, Cameroon and immediately transported to the laboratory. The skin was thoroughly washed 2x with soap and distilled water, drained and transferred to a sterile laminar flow hood where it was entirely covered

with 70% ethanol and allowed to evaporate completely (Figure 4.1: *Left*). Adult worm masses, which are generally pale orange-yellow in appearance, were extracted from the nodules by careful dissection with a sterile blade (Figure 4.1: *Right*). Individual worm masses were immediately submerged in sterile 24-well culture plates containing 1 ml of complete culture medium (CCM) [RPMI-1640 supplemented with 25 mM HEPES, 2.0 g/L sodium bicarbonate, 20 mM L-glutamine, 10% new born calf serum (SIGMA, USA), 200 units/ml penicillin, 200 µg/ml streptomycin and 2.5 µg/ml amphotericin B (Sigma, USA)], pH 7.4] per well. Worm masses were incubated at 37 ^{o}C, 5% CO_2 supplemented humidified air (HERACell 150, Haraeus, Germany) overnight. Viability of the extracted adult worms was ascertained by microscopic examination using an inverted microscope (Euromex, Holland). Dead and damaged worms were discarded, and only viable worms were retained for our assays.

For the *O. ochengi* adult worm assay, a stock solution of 25 mg/ml of the plant extracts was prepared by dissolving 25 mg of the plant extract in 1 ml of ≥99.9% dimethyl sulfoxide (DMSO). The extracts were tested in triplicate at an initial single concentration of 500 µg/ml by adding 40 µl of extract stock in 1 ml of CCM to each well of a 24-well plate

Figure 4.1 *Onchocerca ochengi* nodular masses. *Left*: Inner surface of infected cattle skin revealing nodules. *Right*: Extracted nodular worm masses.

already containing one worm in 1 ml CCM. Extracts that showed no activity at this concentration were not investigated further. 1% DMSO (the highest concentration of used in our assays) served as the negative control, while 10 µM auranofin served as positive control. Macrofilariae cultures were incubated at 37 ^{o}C, 5% CO_2 in humidified air for 5 days (120 hours), without any change of CCM. After incubation, adult worm viability was assessed using the MTT/formazan assay (Comley *et al.*, 1989). Each nodular worm mass was placed in a well of a 48-well plate containing 500 µl of 0.5 mg/ml MTT (Sigma-Aldrich) in incomplete culture medium (CCM without serum). The plates were then incubated in the dark at 37 ^{o}C for 30 mins, after which individual worms were blotted on tissue paper and transferred to a clean white sheet of paper (Figure 4.2). % inhibition of purple color formazan formation relative to the negative control was then visually estimated. Mean % inhibition of purple color formazan formation relative to the negative control worm masses correlates with

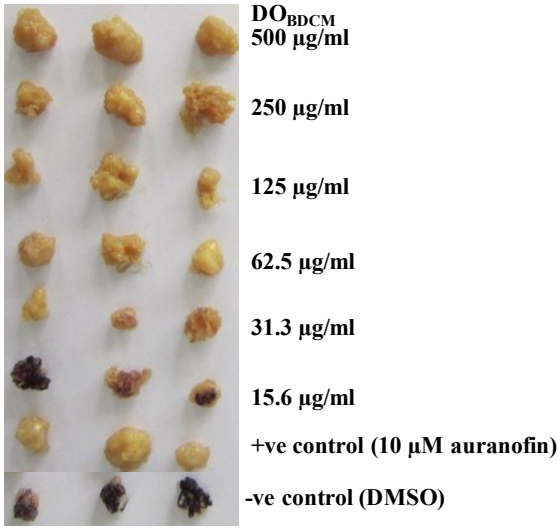

Figure 4.2 Illustration of the MTT/formazan assay for an active extract (*Daniellia oliveri* dichloromethane stem bark extract, DO_{BDCM}). Each extract concentration was tested in triplicate. DO_{BDCM} caused a 100% inhibition of purple formazan formation (which correlates with worm death) from 500 µg/ml down to 31.3 µg/ml.

worm death. Extracts that showed 100% inhibition of formazan were considered active and further tested at 6 concentrations from 500 µg/ml to 15.6 µg/ml to determine their IC_{50} values.

4.4.4 *Onchocerca ochengi* microfilaria (mf) assay

Extraction of *O. ochengi* mfs followed the method of Cho-Ngwa *et al*. (2010) with slight modification. Infected cattle skin was obtained, cleaned and sterilized as described in section 4.4.3. Using autoclaved thumbtacks, the skin was tightly attached to a wooden board whose surface had been covered with 70% ethanol with the outer surface of the skin was facing up (Figure 4.3: *Left*). The outer surface was shaved with a sterile blade, and then rinsed twice with distilled water. Excess moisture from the skin was removed with a clean dry cloth. The entire skin was covered with 70% ethanol and then evaporated in a laminar flow hood. Skin snips approximately 0.5 – 1 mm apart were obtained. Individual skin snips were submerged in 20 ml of CCM and incubated at room temperature for 2 hours to allow for emergence of mfs. Emerged mfs were concentrated by centrifugation at 400 xg for 10 minutes. The supernatant was discarded and the pelleted mfs were resuspended in fresh CCM, and the highly motile mfs quantified with the aid of an inverted microscope (Euromex, Holland) (Figure 4.3: *Right*). Mfs were distributed into 96-well culture plate to obtain an average of 10-15 mfs per well (final volume 100 µl).

Fully confluent monkey kidney epithelial cells (LLC-MK2) obtained from American Type Culture Collection (ATCC, Virginia, USA) served as a feeder layer for the mf assays. The cultures were maintained under the same conditions as described for the adult worm assay. Extracts were tested in duplicate at 8 different serially diluted concentrations from 250

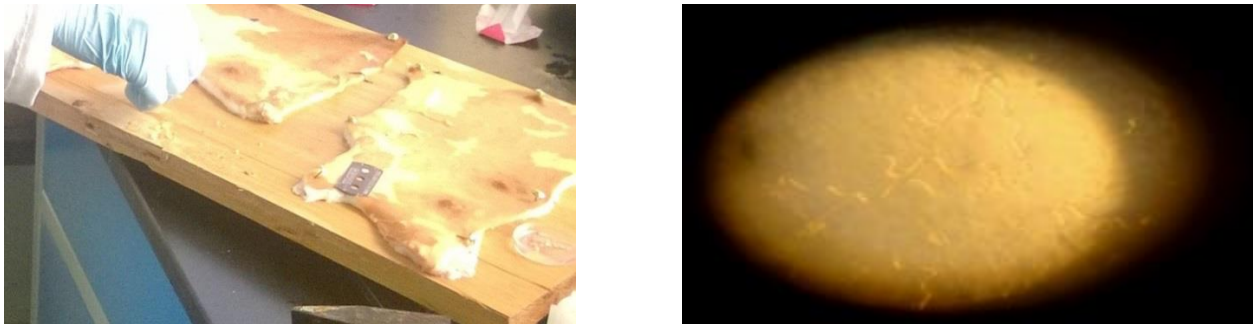

Figure 4.3 *Onchocerca ochengi* microfilariae. *Left*: Outer surface of infected cattle skin for extraction of skin snips. *Right*: Extracted microfilariae observed under the microscope.

µg/ml to 1.95 µg/ml. 100 µl of 2x the concentration of each serial dilution was added to corresponding wells of plates already containing 100 µl of mfs to give a total volume of 200 µl, and a final 1x concentration. 1% DMSO was used as negative control while 10 µg/ml ivermectin served as positive control. Mf viability was assessed by microscopic examination for mean motility scoring (relative to the positive control) every 24 hours post addition of drug for 120 hours. The scale used for motility scoring ranged from 0 – 100% (100% for complete inhibition, 75% for only head or tail moving, 50% for entire worm moving sluggishly, 25% for little change in motility, 0% for no inhibition). 10 µg/ml ivermectin produced 100% inhibition of mf motility by day 5. An extract was considered active if it produced 100% inhibition of mf motility ≤250 µg/ml. The serial dilutions also allowed for the determination of the IC_{50} values of the active extracts.

4.4.5 *Brugia pahangi* adult worm assay

The *B. pahangi* assays were carried out using the Worminator motility tracking system described by Marcellino *et al*. (2012). Adult female *B. pahangi* were shipped from University of Missouri-Columbia (UMC, Columbia, MO) or the NIAID/NIH Filariasis Research Reagent Resource Center (FR3) (Athens, GA) in 24-well plates or 50 ml falcon

tubes containing media (RPMI-1640 with 25 mM HEPES, 2.0 g/L $NaHCO_3$, 5% heat inactivated FBS, and 1X Antibiotic/Antimycotic solution), with 1 worm per well or 80 worms per falcon tube. Individual worms were carefully transferred into fresh 24-well plates containing 500 µl/well fresh media. Worms were observed under an inverted microscope to ascertain viability. Damaged or sluggish worms were discarded, and only highly motile worms were retained for assays. A stock extract or chromatographic fraction concentration of 30 mg/ml in DMSO was prepared and tested in quadruplicate at an initial working concentration of 300 µg/ml. The negative control wells had 1% DMSO and positive control wells had 10 µM auranofin. Worms were cultured in a 5% CO_2 incubator at 37 ^oC for 72 hours (3 days) post drug addition.

The Worminator was used to record videos of each worm plate for approximately 60 seconds, and mean motility units (MMUs) (number of pixels displayed per second) determined for each worm (Marcellino *et al.*, 2012). Videos were recorded at time 0, 4, 24, 48 & 72 hours post drug exposure. % inhibition of motility was calculated by dividing MMUs of test worms by the average MMUs of the controls, multiplying the value by 100, and subtracting from 100. Extracts which showed ≥95% inhibition of motility or chromatographic fractions which showed ≥75% inhibition of motility were considered active and further screened under the same conditions at 6 concentrations (300, 100, 30, 10, 3 and 1 µg/ml) to determine IC_{50} values.

4.4.6 Bioassay-guided fractionation of plant extracts

Bioassay-guided fractionation was done on the most active plant extracts based on IC_{50} values using Sep-Pak cartridges (Waters corporation, MA, USA), followed by semi-preparative High Performance Liquid Chromatography (HPLC).

Sep-Pak Silica Plus cartridges were used for non-polar (hexane) extracts. Elution was achieved with a step gradient of hexane and isopropanol mixture (100:0, 100:0, 90:10, 50:50, 10:90), and a final elution with 100% chloroform ($CHCl_3$) or dichloromethane (DCM). For dichloromethane extracts whose polarity is midway that of hexane and methanol, we carried out an additional fractionation using Sep-Pak C-18 Plus cartridges. Here, elution was achieved with a step gradient of methanol and water mixture (20:80, 20:80, 40:60, 80:20, 100:0) For both cartridges, the ratio of extracts to solvent system was always 2:1, which was achieved by re-suspending 10 mg of extract in 5 ml of the appropriate solvent system. The resulting Sep-Pak fractions generated were separately concentrated using in-house air at a maximum temperature of 40 ^{o}C.

Active Sep-Pak fractions were selected for further fractionation using a Hewlett Packard 1050 Series HPLC System coupled with a Hewlett Packard/Agilent 1050 Diode Array Detector (DAD)/Multiple Wavelength UV Detector (MWD) and silica (straight phase) semi-preparative column (SUPELCOSIL LC-SI SEMI-PREP, 25 cm x 10 mm, 5 µm; Catalog No. 58365). Elution was performed with a 100 – 0% gradient of 99.6% hexane in 0.4% isopropanol (solvent A) and a 0 – 100% gradient of 50% hexane in 50% isopropanol (solvent B) during 30 mins, with an additional 5 mins collection of the eluent, at a flow rate of 4 ml/min to produce 7 subfractions (F1 – F7), collected over 5 min intervals. Detection was accomplished in a Hewlett Packard 1050 Series HPLC System coupled with a Hewlett Packard/Agilent 1050 Diode Array Detector (DAD)/Multiple Wavelength UV Detector (MWD) at 220, 264 and 320 nm.

4.4.7 Cytotoxicity on N27 cells using the MTS assay

Cytotoxicity of active extracts on N27 cells, an immortalized rat mesencephalic neuronal cell line was assessed using the MTS [3-(4,5-dimethylthiazol-2-yl)-5-(3-carboxymethoxyphenyl)-2-(4-sulfophenyl)-2H-tetrazolium, inner salt] assay (Cory *et al.*, 1991). The MTS assay is a colorimetric method for assessing the viability of cells in proliferation or cytotoxicity assays, and is based on the ability of the mitochondria of viable cells to biologically reduce the pale-yellow MTS compound to a purple formazan product. The resulting formazan product formed is quantified by colorimetry, and the quantity of formazan formed is directly proportional to the amount of viable cells in culture.

For our cytotoxicity studies, N27 cells were seeded in 96-well culture plates 5,000 cells/100 µl of RPMI growth media (RPMI-1640 medium containing 10% fetal bovine serum, 2 mM L-glutamine, 50 units penicillin, and 50 µgml streptomycin). Treatment with active extracts followed once the cells had achieved 40 – 50% confluence. All treatments were performed in sextuplicate. 30 µM H_2O_2 served as positive control, while the negative control had cells and growth media containing 1% DMSO. After plating, cells were incubated at 37 ^oC, 5% CO_2 in humidified air (Forma Scientific CO_2 water jacketed incubator) for 24 hours. At the end of the incubation, 10 µl of MTS reagent (CellTiter 96® Aqueous One Solution Reagent, Promega G3580) was added to each well and mixed. The plates were then covered with aluminium foil and incubated at 37 ^oC, 5% CO_2 in humidified air (Forma Scientific CO_2 water jacketed incubator) for 90 mins. The plates were then read at 490 nm and 670 nm using a SpectraMax $M2^e$ reader (Molecular Devices, USA). Cell viability was assessed as ($Abs_{490\text{-}670nm}$) for the extracts and H_2O_2 treated cells relative to the

untreated controls. SI values were then calculated by mean IC_{50} N27 cell/mean IC_{50} parasite. Extracts with SI values >1 are more selective for parasites than N27 cells.

4.4.8 Data analysis

Results obtained for biological activity and cytotoxicity assays were analyzed using GraphPad Prism 5.0 or 6.0 software (Molecular Devices, USA), and expressed as mean ± S.E.M. Statistical analysis for the cytotoxicity assay was done using unpaired student t-test. A *p*-value < 0.05 was considered significant.

4.4.9 Phytochemical screening

Concentrated crude extract residues were used to detect the presence of the secondary plant metabolites; alkaloids, steroids, flavonoids, saponins, tannins, coumarins and cardiac glycosides using standard methods with some modifications (Schiff, 1980).

4.4.9.1 Test for saponins (Frothing test). Briefly, saponins were tested by dissolving 0.5 g of the crude extract in a test tube containing 3 ml of distilled hot water, followed by vigorous shaking for 1 minute. The observation of persistent foaming indicated the presence of saponins.

4.4.9.2 Test for flavonoids (Cyanidin test). 0.5 g of crude extract was dissolved in ~3 ml methanol plus 2 ml of concentrated hydrochloric acid. ~0.1 g of magnesium turnings was then added to the mixture. A brick red coloration with effervescence indicated the presence of flavonoids.

4.4.9.3 Test for steroids (Liebermann-Burchard test). 0.5 g of crude extract was dissolved in 5 ml dichloromethane, then 0.5 ml of acetic anhydride was added, followed by three drops of concentrated sulphuric acid. Observation of a blue-green coloration indicated the presence of steroids.

4.4.9.4 Test for tannins (Ferric chloride test). 0.5 g of crude extract was dissolved in a boiling tube containing 20 ml distilled water and boiled for an hour. 3 – 4 drops of ferric chloride were added and allowed to stand for ~15 minutes. A blue-black coloration indicated a positive test for tannins.

4.4.9.5 Test for Alkaloids (Dragendorff's test). The sample (~0.5 g) was dissolved in about 3 ml of dichloromethane and then spotted on a thin layer chromatographic plate which was developed in 20% hexane in ethylacetate. The presence of alkaloids in the developed chromatogram was detected by spraying with freshly prepared Dragendorff's reagent in a fume chamber. A positive reaction on the chromatogram was indicated by an orange or darker colored spot against a yellow background, confirming the presence of alkaloids.

4.4.9.6 Test for coumarins. To 2 ml of the crude extract was added 1 ml of ammonium hydroxide. One drop was spotted on filter paper and observed under a UV lamp for the presence of blue or green fluorescence, indicating the presence of coumarins.

4.4.9.7 Test for cardiac glycosides. Approximately 1 ml of aqueous extract of the plants was added to 2 ml of glacial acetic acid plus one drop of ferric chloride. 1 ml of concentrated sulfuric acid was then added. The appearance of violet and brownish rings below the interface, followed by the formation of a greenish ring in the acetic acid layer confirmed the presence of cardiac glycosides.

4.5 Results

4.5.1 Activity of *D. oliveri* and *P. febrifugum* extracts on *O. ochengi* adult worms and mfs

A total of 12 extracts were generated from the leaves and stem bark of the 2 plants (6 extracts per plant) using solvents of different polarities (hexane, dichloromethane and methanol). A summary of the activity of the plant extracts is provided in Table 4.2.

Table 4.2 IC_{50} values (mean ± S.E.M) of extracts with macro- and/or microfilaricidal activity against *O. ochengi.*

Extracts	*Onchocerca ochengi*	
	IC_{50} mf (µg/ml)	**IC_{50} adult worm (µg/ml)**
DO_{LHEX}	Inactive	Inactive
DO_{LDCM}	16.2 ± 0.0, n = 2	43.3 ± 9.2, n = 3
DO_{LMeOH}	Inactive	Inactive
DO_{BHEX}	185.2 ± 0.0, n = 2	13.9 ± 1.7, n = 3
DO_{BDCM}	9.7 ± 0.0, n = 2	22.5 ± 0.0, n = 3
DO_{BMeOH}	Inactive	Inactive
PF_{LHEX}	Inactive	Inactive
PF_{LDCM}	132.4 ± 0.0, n = 2	Inactive
PF_{LMeOH}	8.8 ± 0.0, n = 2	Inactive
PF_{BHEX}	4.0 ± 0.0, n = 2	Inactive
PF_{BDCM}	7.2 ± 0.0, n = 2	Inactive
PF_{BMeOH}	6.6 ± 0.0, n = 2	Inactive

Of the 12 extracts screened, 3 were active against adult *O. ochengi* (Figure 4.4). These were the hexane extract of the stem bark, and the dichloromethane extracts of the leaves and stem bark of *D. oliveri* (DO_{BHEX}, DO_{LDCM} and DO_{BDCM}). Of these 3, DO_{BHEX} recorded the lowest IC_{50} of 13.9 ± 1.7 µg/ml (n = 3) for *O. ochengi* macrofilaricidal activity. Remarkably, DO_{BHEX} also recorded the lowest IC_{100} of 31.3 µg/ml (n = 3).

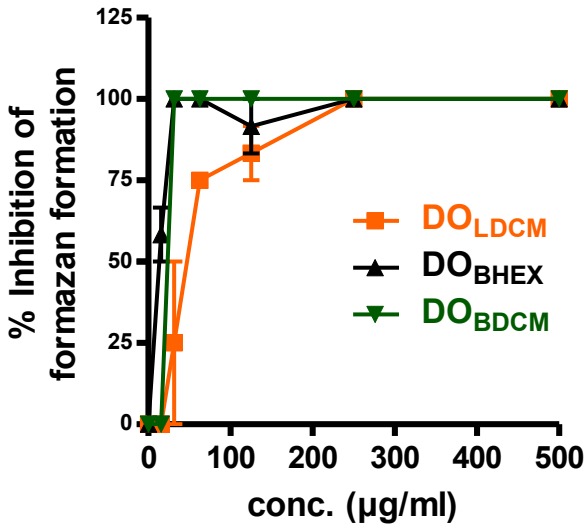

Figure 4.4 Dose-dependent inhibition of formazan formation (decrease in worm viability) after 120 hours of incubation with extracts of *Daniellia oliveri*. Results are plotted as mean ± S.E.M. The order of potency was DO_{BHEX} (IC_{50} 13.9 ± 1.7 µg/ml, n = 3) > DO_{BDCM} (IC_{50} 22.5 ± 0.0 µg/ml, n = 3) > DO_{LDCM} (IC_{50} 43.3 ± 9.2 µg/ml, n = 3).

For the *O. ochengi* mf assay, 8 of the 12 extracts screened showed a dose-dependent microfilaricidal activity (Figure 4.5). These were DO_{BHEX}, DO_{LDCM}, DO_{BDCM}, dichloromethane leaf extract of *P. febrifugum* (PF_{LDCM}), methanol leaf extract of *P. febrifugum* (PF_{LMeOH}), hexane stem bark extract of *P. febrifugum* (PF_{BHEX}), dichlomethane stem bark extract of *P. febrifugum* (PF_{BDCM}), and methanol stem back extract of *P. febrifugum* (PF_{BMeOH}). The effects of these extracts were also time-dependent. Note, of the

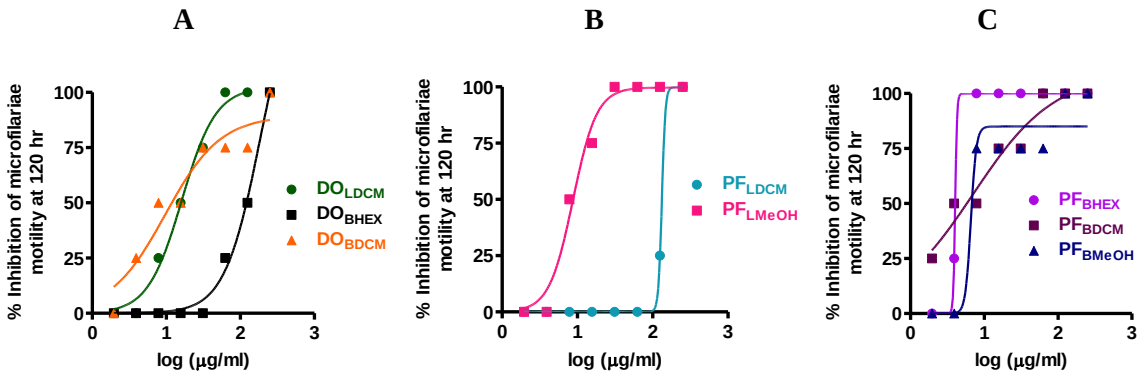

Figure 4.5 Dose-dependent inhibition of microfilariae motility after 120 hours of incubation with extracts of *Daniellia oliveri* (A) and *Psorospermum febrifugum* (B & C). Results are plotted as mean ± S.E.M (n = 2). Note that the *D. oliveri* microfilaricidal extracts (DO_{BHEX}, DO_{LDCM}, DO_{BDCM}) were also active against adult worms.

extracts that showed both *O. ochengi* adult worm and mf activity (DO_{BHEX}, DO_{LDCM} and DO_{BDCM}), DO_{BHEX} was more active on adult *O. ochengi* (IC_{50} 13.9 ± 1.7 µg/ml, n = 3) compared to the mfs (IC_{50} 185.2 ± 0.0 µg/ml, n = 2). PF_{BHEX} recorded the lowest IC_{50} of 4.0 ± 0.0 µg/ml (n = 2) for *O. ochengi* microfilaricidal activity, and the lowest IC_{100} of 7.8 µg/ml. PF_{LMeOH} had an IC_{50} and IC_{100} of respectively 8.8 ± 0.0 µg/ml and 31.3 µg/ml (n = 2) for *O. ochengi* microfilaricidal activity.

4.5.2 Activity of extracts and chromatographic fractions of *D. oliveri* and *P. febrifugum* on adult *B. pahangi*

Adult *B. pahangi* were more sensitive to the extracts than *O. ochengi*. Of the 12 extracts initially screened for activity against adult *B. pahangi* at 300 µg/ml, 11 (DO_{LHEX}, DO_{LDCM}, DO_{LMeOH}, DO_{BHEX}, DO_{BDCM}, DO_{BMeOH}, PF_{LHEX}, PF_{LDCM}, PF_{BHEX}, PF_{BDCM} and PF_{BMeOH}) were active, while only PF_{LMeOH} was inactive (Figure 4.6). The effects were also time-dependent, with DO_{LDCM} and DO_{BDCM} causing close to 100% inhibition of motility after only 4 and 24 hours of incubation.

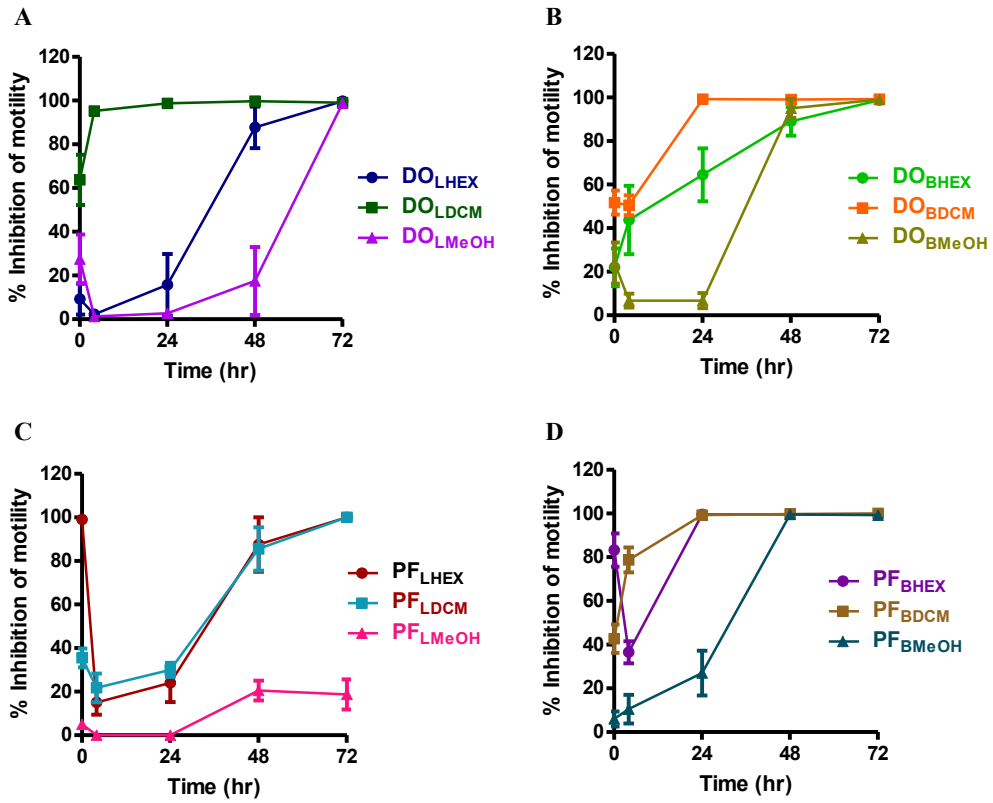

Figure 4.6 Time-dependent inhibition of adult *Brugia pahangi motility* following incubation with extracts of *Daniellia oliveri* and *Psorospermum febrifugum*. Results are plotted as mean ± S.E.M (n = 4). All 12 extracts tested (except PF_{LMeOH}) caused a 100% inhibition of motility after 72 hours of incubation. Remarkably, DO_{LDCM} and DO_{BDCM} caused close to 100% inhibition of motility after only 4 and 24 hours of incubation.

Of these 11 active extracts, 3 (DO_{BHEX}, DO_{LDCM} and DO_{BDCM}) were selected for further screening for IC_{50} determination as they were also active on both adult *O. ochengi* and mfs (Figure 4.7). DO_{LDCM} and DO_{BDCM} were equally potent on adult *B. pahangi* with IC_{50} values of 6.1 ± and 6.3 ± µg/ml respectively (n = 4). These IC_{50} values were lower than the 59.0 ± 1.2 µg/ml (n = 4) recorded for DO_{BHEX} (Table 4.3).

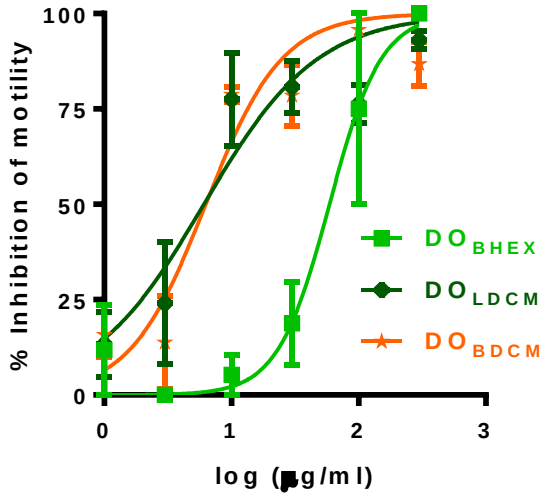

Figure 4.7 Dose-dependent inhibition of adult *Brugia pahangi* motility after 72 hours of incubation with extracts of *Daniellia oliveri*. Results are plotted as mean ± S.E.M (n = 4). The order of potency was DO_{LDCM} (IC_{50} 6.1 ± 1.3 µg/ml, n = 4) ~ DO_{BDCM} (IC_{50} 6.3 ± 1.2 µg/ml, n = 4) > DO_{BHEX} were (IC_{50} 59.0 ± 1.2 µg/ml, n = 4).

Table 4.3 IC_{50} values (mean ± S.E.M) for all active extracts.

Extracts	*Onchocerca ochengi*		*Brugia pahangi*
	IC_{50} mf (µg/ml)	IC_{50} adult worm (µg/ml)	IC_{50} adult worm (µg/ml)
DO_{LHEX}	Inactive	Inactive	< 300
DO_{LDCM}	16.2 ± 0.0, n = 2	43.3 ± 9.2, n = 3	6.1 ± 1.3, n = 4
DO_{LMeOH}	Inactive	Inactive	< 300
DO_{BHEX}	185.2 ± 0.0, n = 2	13.9 ± 1.7, n = 3	59.0 ± 1.2, n = 4
DO_{BDCM}	9.7 ± 0.0, n = 2	22.5 ± 0.0, n = 3	6.3 ± 1.2, n = 4
DO_{BMeOH}	Inactive	Inactive	< 300
PF_{LHEX}	Inactive	Inactive	< 300
PF_{LDCM}	132.4 ± 0.0, n = 2	Inactive	< 300
PF_{LMeOH}	8.8 ± 0.0, n = 2	Inactive	Inactive
PF_{BHEX}	4.0 ± 0.0, n = 2	Inactive	< 300
PF_{BDCM}	7.2 ± 0.0, n = 2	Inactive	< 300
PF_{BMeOH}	6.6 ± 0.0, n = 2	Inactive	< 300

Following IC_{50} determination, DO_{BHEX}, DO_{LDCM} and DO_{BDCM} were subjected to solid-phase extraction using Sep-Pak Plus cartridges. 18 Sep-Pak fractions were generated from DO_{BHEX}, DO_{LDCM} and DO_{BDCM} (6 fractions per extract), and tested for adult *B. pahangi* activity in quadruplicate at 300 µg/ml for 72 hours (Figure 4.8).

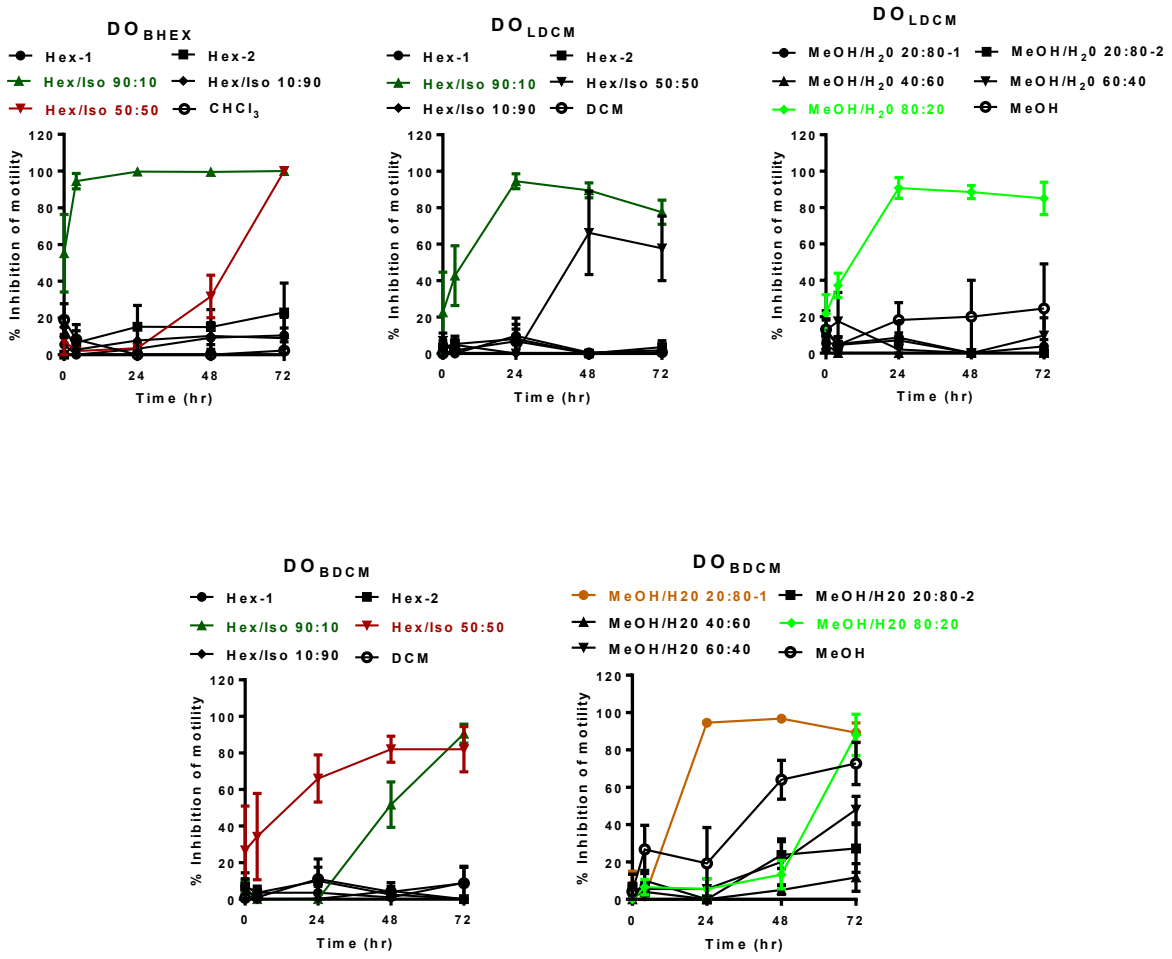

Figure 4.8 Time-dependent inhibition of adult *Brugia pahangi* motility following treatment with *Daniellia oliveri* Sep-Pak fractions. Results are plotted as mean ± S.E.M (n = 4). Active fractions from Sep-Pak Silica Plus cartridges are colored green and red, green for Hex/Iso 90:10 and red for Hex/Iso 50:50 fractions. Active fractions from Sep-Pak C-18 Plus cartridges are colored light green ($MeOH/H_20$ 80:20) and brown ($MeOH/H_20$ 20:80-1).

Sep-Pak fractions that showed activity after 72 hours of incubation were selected for IC_{50} determination (Figure 4.9). These were DO_{BHEX} eluted with 90% hexane in 10% isopropanol (DO_{BHEX} Hex/Iso 90:10), DO_{BHEX} eluted with 50% hexane in 50% isopropanol (DO_{BHEX} Hex/Iso 50:50), DO_{LDCM} eluted with 90% hexane in 10% isopropanol (DO_{LDCM} Hex/Iso 90:10) and DO_{LDCM} eluted with 80% methanol in 20% water (DO_{LDCM} MeOH/H_2O 80:20). Of the 2 active DO_{BHEX} Sep-Pak fractions (DO_{BHEX} Hex/Iso 90:10 and DO_{BHEX} Hex/Iso 50:50, Figure 4.9A), DO_{BHEX} Hex/Iso 90:10 was selected for HPLC because based on IC_{50}, it was more potent (IC_{50} 27.3 ± 1.2 µg/ml, n = 4) than DO_{BHEX} Hex/Iso 50:50 (IC_{50} 122.2 ± 1.3 µg/ml, n = 4). Likewise, DO_{LDCM} Hex/Iso 90:10 was selected for HPLC as it was more potent (IC_{50} 15.2 ± 1.3 µg/ml, n = 4) than DO_{LDCM} MeOH/H_2O 80:20 (IC_{50} 33.3 ± 1.3 µg/ml, n = 4), Figure 4.9B.

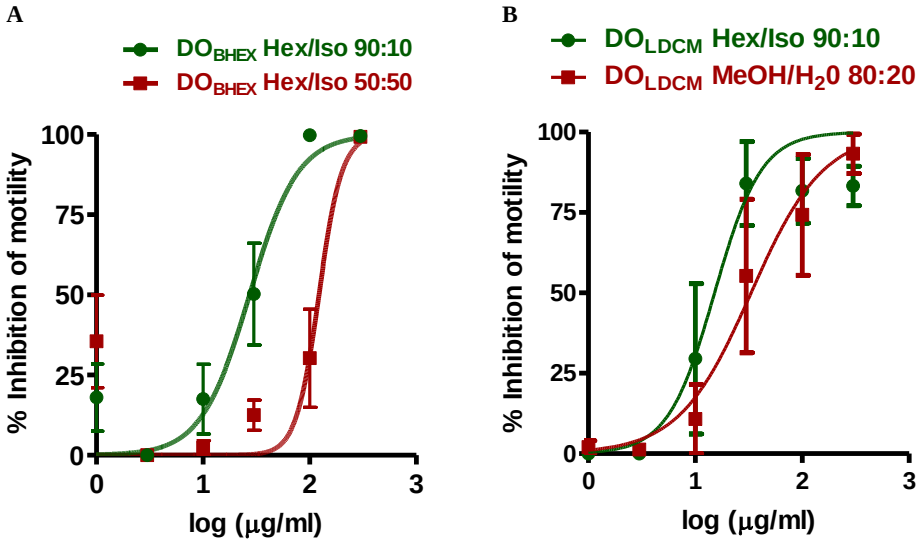

Figure 4.9 Dose-dependent inhibition of adult *B. pahangi* motility after 120 hrs of incubation with Sep-Pak fractions from *D. oliveri* stem bark hexane extract (A) and leaf dichloromethane extract (B). Results are plotted as mean ± S.E.M (n = 4). DO_{BHEX} Hex/Iso 90:10 (IC_{50} 27.3 ± 1.2 µg/ml, n = 4) was more potent than DO_{BHEX} Hex/Iso 50:50 (IC_{50} 122.2 ± 1.3 µg/ml, n = 4). DO_{LDCM} Hex/Iso 90:10 (IC_{50} 15.2 ± 1.3 µg/ml, n = 4) was more potent than DO_{LDCM} MeOH/H_2O 80:20 (IC_{50} 33.3 ± 1.3 µg/ml, n = 4).

Seven HPLC subfractions (F1 – F7) from each of the selected Sep-Pak fractions were generated and again tested for adult *B. pahangi* activity at 300 µg/ml (Figures 4.10). Only active fractions were selected for IC_{50} determination and further purification. These were DO_{BHEX} Hex/Iso 90:10 F4 (IC_{50} 50.7 ± 1.0 µg/ml, n = 4) and DO_{LDCM} Hex/Iso 90:10 F3 (IC_{50} 141.5 ± 1.1 µg/ml, n = 4) (Figures 4.11A & 4.11B).

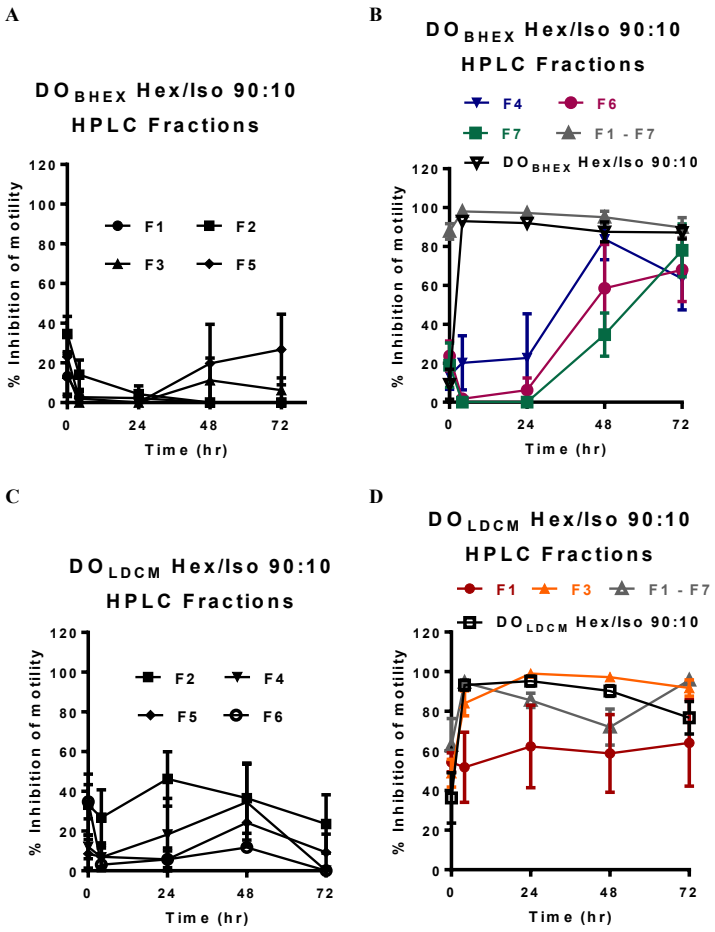

Figure 4.10 Time-dependent inhibition of adult *Brugia pahangi* motility following treatment with HPLC fractions from the hexane stem bark Sep-Pak fraction eluted with 90% hexane in 10% isopropanol (DO_{BHEX} Hex/Iso 90:10) (A & B) and the dichloromethane leaf Sep-Pak fraction eluted with 90% hexane in 10% isopropanol (DO_{LDCM} Hex/Iso 90:10) (C & D). Results are plotted as mean ± S.E.M (n = 4). Active HPLC fractions were: F4, F6 & F7 from the Sep-Pak fraction DO_{BHEX} Hex/Iso 90:10, and F3 from Sep-Pak fraction DO_{LDCM} Hex/Iso 90:10.

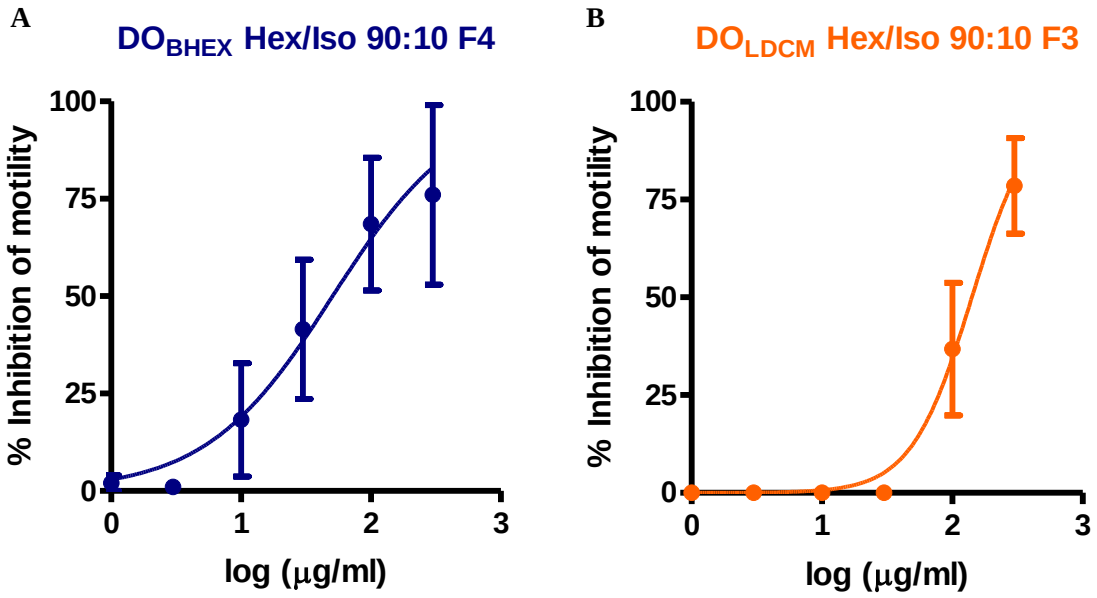

Figure 4.11 Dose-dependent inhibition of adult *Brugia pahangi* motility after 72 hours of incubation with HPLC fractions; F4 from the hexane stem bark Sep-Pak fraction eluted with 90% hexane in 10% isopropanol (A) and F3 from the dichloromethane leaf Sep-Pak fraction eluted with 90% hexane in 10% isopropanol (B). Results are plotted as mean ± S.E.M (n = 4). DO_{BHEX} Hex/Iso 90:10 F4 (IC_{50} 50.7 ± 1.0 µg/ml, n = 4) was more potent than DO_{LDCM} Hex/Iso 90:10 F3 (IC_{50} 141.5 ± 1.1 µg/ml, n = 4).

4.5.3 Cytotoxicity of active extracts

N27 cytotoxicity was established for the active extracts using the MTS assay. The N27 IC_{50} values were compared to the IC_{50} values for the parasites to determine the Selectivity Index (SI). Of all 12 active extracts evaluated at an initial single high concentration of 250 µg/ml for toxicity to N27 cells, DO_{BHEX} and PF_{BDCM} showed no cytotoxicity when compared to the untreated controls (Figure 4.12A). On the other hand, all the other extracts tested showed a significant reduction ($p < 0.001$) in cell viability compared to the untreated control. These extracts were further tested at 8 serially diluted concentrations from 500 to 3.91 µg/ml to determine their IC_{50} values (Figures 4.12B–D).

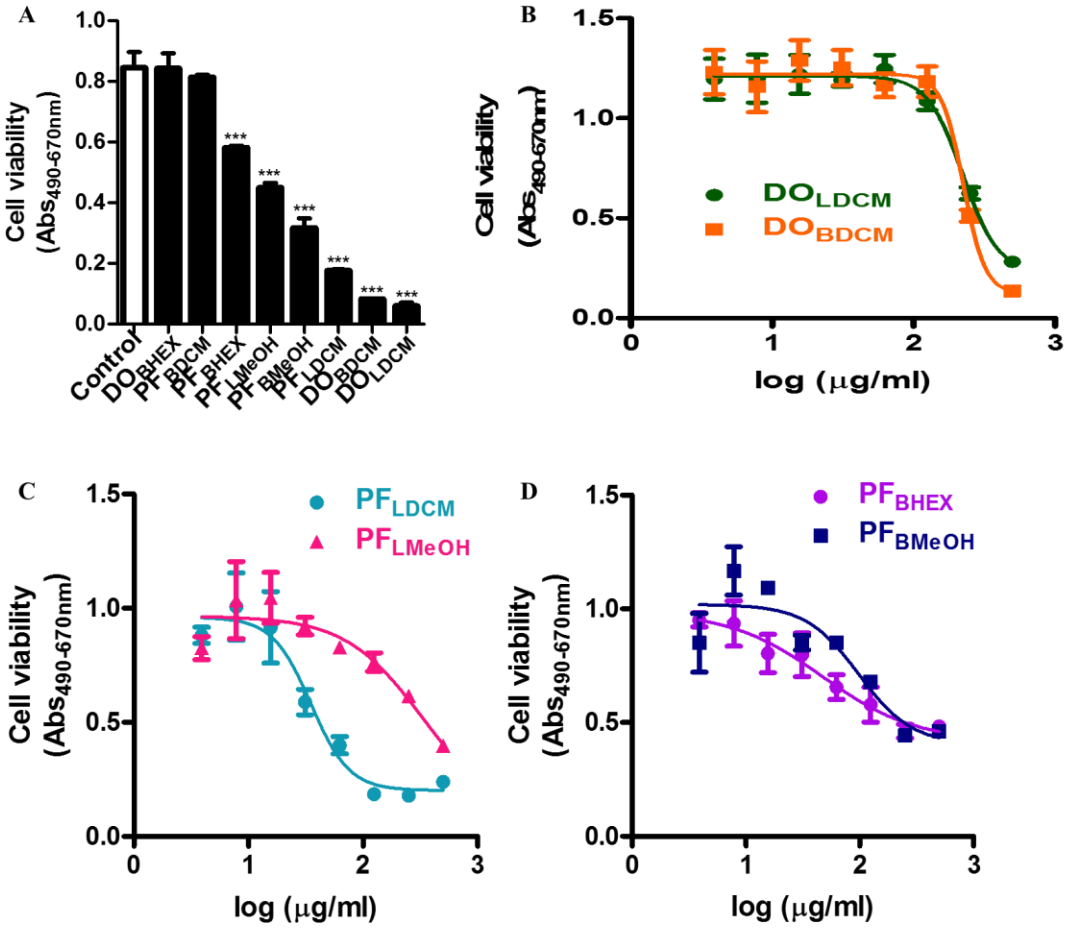

Figure 4.12 Effects of extracts of *Daniellia oliveri* and *Psorospermum febrifugum* on N27 cell viability after 24 hours of incubation with 250 µg/ml (n = 6) (A) and 500 down to 3.91 µg/ml (B – D) of the extracts. Results are plotted as mean ± S.E.M. Mean IC_{50} ranged from 35 to >250 µg/ml (n = 4). ***p < 0.001 (unpaired student t-test).

IC_{50} (mean ± S.E.M) values for the extracts on N27 cells are shown in Table 4.4. Comparing the IC_{50} values for N27 cells with that for parasites revealed only PF_{LDCM} to be more toxic to N27 cells than to parasites (Table 4.5). All other extracts were more selective for parasites than for N27 cells with an SI of >1. The higher the SI value, the more toxic the extract is to parasites than cells. Therefore, the higher the SI value, the better or 'safer' the extract and the more potentially useful for therapeutic drug development.

Table 4.4 IC_{50} (mean ± S.E.M) for extracts of *Daniellia oliveri* and *Psorospermum febrifugum* on N27 cells.

Extract	IC_{50} (Mean ± S.E.M, µg/ml)
DO_{LDCM}	222.8 ± 1.1, n = 4
DO_{BDCM}	224.6 ± 1.1, n = 4
PF_{LDCM}	35.1 ± 1.2, n = 4
PF_{LMeOH}	331.1 ± 6.9, n = 4
PF_{BHEX}	47.0 ± 1.8, n = 4
PF_{BMeOH}	98.2 ± 1.4, n = 4

4.5.4 Phytochemical analysis of active extracts

The active extracts were screened for the presence of phytochemicals as described in the Materials and Methods section. The presence (+) and absence (-) of the different phytochemicals screened are shown in Table 4.6. In general, steroids and saponins were found to be present in all active extracts, while cuomarins were absent. The 3 promising extracts (DO_{BHEX}, DO_{LDCM} and DO_{BDCM}) with activity against both *O. ochengi* and *B. pahangi* tested positive for one or more of the following phytochemicals: alkaloids, flavonoids and cardiac glycosides, but negative for tannins.

Table 4.5 Selectivity index (SI) values (Mean IC_{50} cell/Mean IC_{50} parasite) for extracts of *Daniellia oliveri* and *Psorospermum febrifugum.*

Extracts	Mean IC_{50} N27 cells (µg/ml)	*Onchocerca ochengi*				*Brugia pahangi*	
		Mf		Adult		Adult	
		Mean IC_{50} (µg/ml)	SI	Mean IC_{50} (µg/ml)	SI	Mean IC_{50} (µg/ml)	SI
DO_{LHEX}	tbd	Inactive	/	Inactive	tbd	89.8	/
DO_{LDCM}	222.8	16.2	13.8	43.3	5.1	6.1	36.5
DO_{LMeOH}	tbd	Inactive	/	Inactive	/	81.9	/
DO_{BHEX}	> 250	185.2	> 1.3	13.9	> 18.0	59.0	> 4.2
DO_{BDCM}	224.6	9.7	23.2	22.5	10.0	6.3	35.7
DO_{BMeOH}	/	Inactive	/	Inactive	/	44.0	/
PF_{LHEX}	/	Inactive	/	Inactive	/	153.7	/
PF_{LDCM}	35.1	132.4	0.3	Inactive	/	< 300	/
PF_{LMeOH}	331.1	8.8	37.6	Inactive	/	Inactive	/
PF_{BHEX}	47.0	4	11.8	Inactive	/	< 300	/
PF_{BDCM}	> 250	7.2	> 34.7	Inactive	/	< 300	/
PF_{BMeOH}	98.2	6.6	14.9	Inactive	/	< 300	/

Table 4.6 Phytochemical analysis of all active extracts.

Class of compound	*Daniellia oliveri* extracts			*Psorospermum febrifugum* extracts				
	DO_{LDCM}	DO_{BHEX}	DO_{BDCM}	PF_{LDCM}	PF_{LMeOH}	PF_{BHEX}	PF_{BDCM}	PF_{BMeOH}
Alkaloids	-	+	-	+	+	+	+	+
Steroids	+	+	+	+	+	+	+	+
Flavonoids	+	-	+	+	+	+	+	+
Saponins	+	+	+	+	+	+	+	+
Tannins	-	-	-	+	+	-	-	+
Cuomarins	-	-	-	-	-	-	-	-
Cardiac glycosides	+	-	+	-	+	+	-	-

Key: (+) = present, (-) = absent

4.6 Discussion

Onchocerciasis and LF are two major NTDs whose control is hindered by the lack of suitable drugs that will kill adult worms. The aim of this project was to screen medicinal plants for activity against the parasites that cause onchocerciasis and LF in a bid to identify new compounds that could serve as leads for macrofilaricidal drug development. Based on ethnopharmacological information, *D. oliveri* and *P. febrifugum* are plants commonly used by the traditional healers of Bambui, NW Cameroon to treat onchocerciasis and LF. However, there is no documented scientific evidence to support the claimed efficacy of *D. oliveri* and *P. febrifugum* in treating onchocerciasis and LF. Our study is the first report of scientific evidence for *in vitro* filaricidal activity of *D. oliveri* and *P. febrifufum*. Of 12 crude extracts prepared from *D. oliveri* and *P. febrifufum* using solvents of different polarities

(hexane, dichloromethane and methanol), all 12 extracts showed a time- and dose-dependent activity against *O. ochengi* mfs, adult *O. ochengi* or adult *B. pahangi*. Interestingly, 3 (DO_{BHEX}, DO_{LDCM} and DO_{BDCM}) of the 12 extracts were active against all life cycle stages of *O. ochengi* and *B. pahangi* used in this study. Thus, DO_{BHEX}, DO_{LDCM} and DO_{BDCM} have potential as sources of lead compounds for broad spectrum filaricidal activity. The low IC_{50} values (6 – 185 µg/ml) recorded by DO_{BHEX}, DO_{LDCM} and DO_{BDCM} and their lack of cytotoxicity encouraged us to select these extracts for further purification (Table 4.5).

Sep-Pak fractions of DO_{BHEX}, DO_{LDCM} and DO_{BDCM} which showed activity against *B. pahangi* were further fractionated using semi-preparative HPLC. Seven HPLC fractions collected at different time points were generated for each active Sep-Pak fraction. These fractions were tested for activity against *B. pahangi* and IC_{50}'s determined from dose-response curves. After analysis of the HPLC fractions, we propose that DO_{BHEX} Hex/Iso 90:10 F4 (IC_{50} 50.7 ± 1.0 µg/ml, n = 4) and DO_{LDCM} Hex/Iso 90:10 F3 (IC_{50} 141.5 ± 1.1 µg/ml, n = 4) are further purified to identify the active compounds.

The potency of extracts varied during the course of the fractionation process. For example, crude extract DO_{BHEX} recorded an IC_{50} adult *B. pahangi* of 59.0 ± 1.2 µg/ml, the most potent resulting Sep-Pak fraction was DO_{BHEX} Hex/Iso 90:10 IC_{50} 27.3 ± 1.2 µg/ml, while HPLC fraction DO_{BHEX} Hex/Iso 90:10 F4 IC_{50} 50.7 ± 1.0 µg/ml was the most potent. However, when we combined all seven HPLC fractions of extract DO_{BHEX} Hex/Iso 90:10, the activity was similar to that of the parent Sep-Pak fraction (Figure 4.10B). This led us to conclude that active compounds are present in two or more HPLC fractions acting additively or in synergy.

Our results show that the HPLC fractions DO_{BHEX} Hex/Iso 90:10 F4 and DO_{LDCM} Hex/Iso 90:10 F3 have potential as sources of macrofilaricides. Additionally, we recommend that various combinations of the HPLC fractions be tested as this may yield combinations with enhanced activity. Knowing that phytochemicals have a wide range of pharmacological activities, the phytochemicals present in our promising extracts which we report in Table 4.6 suggest that the bioactive compounds in the extracts may be from these groups of plant chemicals (alkaloids, steroids, flavonoids, saponins and cardiac glycosides). The presence of one or more of these phytochemicals have been reported in the following plants with demonstrated activity against *O. ochengi*: *Margaritaria discoidea*, *Homalium africanum*, *Craterispermum laurinum*, *Morinda lucida*, *Tragia benthami*, *Piper umbellatum* and *Annona senegalensis* (Cho-Ngwa *et al.*, 2010; Cho-Ngwa *et al.*, 2016; Ndjonka *et al.*, 2011). Also, the anthelmintic activity for some of these phytochemicals like alkaloids, flavonoids and saponins has been published elsewhere (Ayers *et al.*, 2007; Wang *et al.*, 2010a; Wang *et al.*, 2010b). Overall, our results justify the traditional use of *D. oliveri*. However, more studies focusing on identifying the active compounds are necessary, as well as determining their mode of action.

4.7 Acknowledgements

We would like to express our gratitude to the indigenes and traditional healers of Bambui, North West Cameroon for providing us with valuable information on the medicinal plants used in this study.

This work was funded by Schlumberger Foundation Faculty for the Future Grant to MA & APR; NIH R01 AI047194–12 to RJM; and R21AI092185–01 to APR. We would like to acknowledge the Burroughs Wellcome Fund Collaborative Research Travel Award to MA.

We are grateful to the Biotechnology Unit members of the University of Buea Department of Biochemistry and Molecular Biology; Organic Chemistry Lab members of the University of Buea Department of Chemistry; team members of the UC San Francisco Small Molecule Discovery Center; Dr Goff lab members at ISU; Adhithiya Charli and Dr Vellareddy Anantharam of ISU.

4.8 Author Contributions

Conceived and designed the experiments: MA, FCN, GAA, RJM & APR. Performed the experiments: MA, MS, SBB, CB, NK, SV. Analyzed the data: MA, NK, RJM & APR. Contributed reagents/materials/analysis tools: MA, FCN, GAA, JS, RJM & APR. Wrote the manuscript: MA, RJM & APR.

CHAPTER 5. CURIOUSER AND CURIOUSER: THE MACROCYCLIC LACTONE, ABAMECTIN, IS ALSO A POTENT INHIBITOR OF PYRANTEL/TRIBENDIMIDINE NICOTINIC ACETYLCHOLINE RECEPTORS OF GASTRO-INTESTINAL WORMS

A paper published in *PLoS One* (2016)[1]

Melanie Abongwa[2], Samuel K. Buxton[2], Alan P. Robertson[2], Richard J. Martin[2*]

[1] Reprinted with permission of *PLoS One* (2016), **11**(1): e0146854
[2] Department of Biomedical Sciences, College of Veterinary Medicine, Iowa State University, Ames, Iowa, United States of America
[*] Corresponding author and Distinguished Professor, Department Biomedical Sciences, Iowa State University

5.1 Abstract

Nematode parasites may be controlled with drugs, but their regular application has given rise to concerns about the development of resistance. Drug combinations may be more effective than single drugs and delay the onset of resistance. A combination of the nicotinic antagonist, derquantel, and the macrocyclic lactone, abamectin, has been found to have synergistic anthelmintic effects against gastro-intestinal nematode parasites. We have observed in previous contraction and electrophysiological experiments that derquantel is a potent selective antagonist of nematode parasite muscle nicotinic receptors; and that abamectin is an inhibitor of the same nicotinic receptors. To explore these inhibitory effects further, we expressed muscle nicotinic receptors of the nodular worm, *Oesophagostomum dentatum* (Ode-UNC-29:Ode-UNC-63:Ode-UNC-38), in *Xenopus* oocytes under voltage-clamp and tested effects of abamectin on pyrantel and acetylcholine responses. The receptors were antagonized by 0.03 μM abamectin in a non-competitive manner (reduced R_{max}, no

change in EC_{50}). This antagonism increased when abamectin was increased to 0.1 μM. However, when we increased the concentration of abamectin further to 0.3 μM, 1 μM or 10 μM, we found that the antagonism decreased and was less than with 0.1 μM abamectin. The bi-phasic effects of abamectin suggest that abamectin acts at two allosteric sites: c We also tested the effects of 0.1 μM derquantel alone and in combination with 0.3 μM abamectin. We found that derquantel on these receptors, like abamectin, acted as a non-competitive antagonist, and that the combination of derquantel and abamectin produced greater inhibition. These observations confirm the antagonistic effects of abamectin on nematode nicotinic receptors in addition to GluCl effects, and illustrate more complex effects of macrocyclic lactones that may be exploited in combinations with other anthelmintics.

5.2 Introduction

Gastro-intestinal nematode parasite infections of both humans and animals are a global public health problem. These infections cause livestock production losses, morbidity, and if left uncontrolled, may result in death (Pullan *et al.*, 2014). In the absence of effective sanitation and vaccines, control of nematode parasite infections is achieved by the use of anthelmintic drugs, many of which act on ligand-gated ion channels (LGICs) (Beech & Neveu, 2015; Greenberg, 2014; Wolstenholme, 2011). The nicotinic acetylcholine receptor (nAChR) is a prototypic pentameric LGIC. Different subunit combinations or different stoichiometry of the same nAChR subunits can give rise to multiple receptor subtypes with different pharmacological properties (Buxton *et al.*, 2014; Williamson *et al.*, 2009). There are a limited number of anthelmintics which are currently approved for use (Wolstenholme, 2011). Those that act on nAChRs include: imidazothiazoles (levamisole) (Martin & Robertson, 2007), tetrahydropyrimidine derivatives (pyrantel, oxantel, morantel) (Rayes *et*

al., 2001), spiroindoles (derquantel) (Lee *et al.*, 2002), and tribendimidine (Robertson *et al.*, 2015). The macrocyclic lactones (ivermectin, abamectin, moxidectin) act on glutamate-gated chloride channels (GluCls) (Wolstenholme & Rogers, 2005); the benzimidazoles (albendazole, mebendazole) act on β-tubulin (Lacey, 1990); and piperazine acts on GABA receptors (Martin, 1997). Other more recent drugs include the amino-acetonitrile derivatives (monepantel) which act on LGICs receptors comprised of DEG-3/DES-2 nAChR subunits (Rufener *et al.*, 2010); and the cyclooctadepsipeptide (emodepside) whose mode of action is understood to be on SLO-1 potassium channels (Guest *et al.*, 2007; Martin *et al.*, 2012a) and latrophilin receptors (Saeger *et al.*, 2001).

The increased use of anthelmintics has led to the development of resistance in both animal and human nematode parasites (Wolstenholme & Martin, 2014). Resistance to anthelmintics presents a serious drawback in the control of nematode parasite infections and is an increasing medical concern (Kotze *et al.*, 2014). Combination therapy involving anthelmintic drugs of different classes is an important approach that may slow the development of anthelmintic drug resistance. The simultaneous development of resistance to two drugs is less likely than the development of resistance to one drug alone; hence combinations are predicted to slow the development of resistance (Leathwick, 2012). Startect® (derquantel and abamectin combination, Figure 5.0) is a more recently introduced anthelmintic combination that is marketed for use in sheep, but it has been shown to have effects on nematode parasites of other host species such as *Ascaris suum* of pigs (Puttachary *et al.*, 2013). In this study, we investigated the effects of derquantel alone, abamectin alone, and a combination of derquantel and abamectin on a nAChR subtype from the nematode parasite *Oesophagostomum dentatum*. This subtype is comprised of *Ode*-UNC-29:*Ode*-UNC-

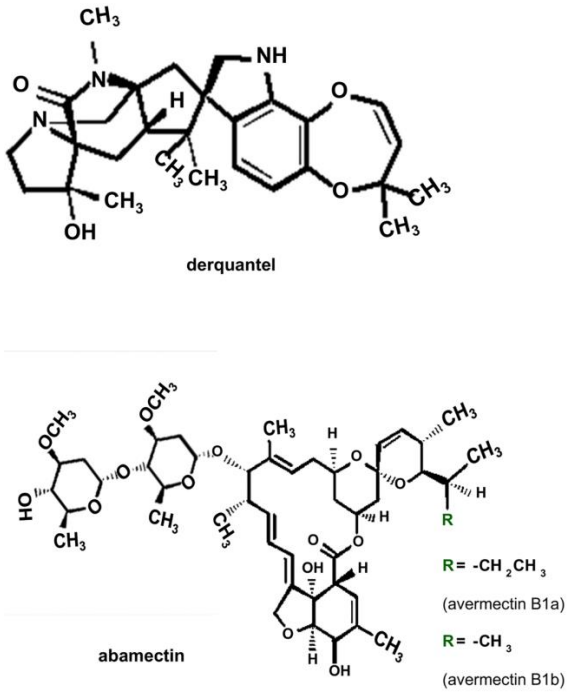

Figure 5.0 Structures of derquantel and abamectin. **A**: Structure of derquantel. **B**: Structure of abamectin. Abamectin is a mixture of avermectin B1a and avermectin B1b. Avermectin B1a differs from avermectin B1b by a functional group at the 'R' position, and makes up more than 80% of abamectin, while avermectin B1b makes up less than 20% of abamectin.

63:*Ode*-UNC-38 (29-63-38) nAChR subunits. Other pharmacologically characterized nAChR subtypes of *O. dentatum* are *Ode*-UNC-29:*Ode*-UNC-63 (pyrantel-sensitive nAChR), *Ode*-UNC-29:*Ode*-UNC-63:*Ode*-ACR-8 (acetylcholine-sensitive nAChR), and *Ode*-UNC-29:*Ode*-UNC-63:*Ode*-UNC-38:*Ode*-ACR-8 (levamisole-sensitive nAChR) (Buxton *et al.*, 2014). We chose *O. dentatum* parasite for further investigation because the worm is easily maintained and passaged, and it is a Clade V nematode, just like the model free-living nematode, *Caenorhabditis elegans* (Blaxter *et al.*, 1998). *O. dentatum* is a common nodule worm in pigs, very similar to other *Oesophagostomum* species which infect humans, most notably in northern Togo and Ghana (Polderman *et al.*, 1991). The *O. dentatum* nAChR subtype, *Ode*-UNC-29:*Ode*-UNC-63:*Ode*-UNC-38 used in this study is

preferentially activated by pyrantel and tribendimidine, and it is antagonized in a non-competitive manner by derquantel (Buxton *et al.*, 2014). We show here that abamectin is a potent antagonist of these nAChRs, and that a combination of derquantel and abamectin has greater effects than derquantel or abamectin used alone. These additive effects support the continued use of the derquantel and abamectin combination for the control of nematode parasites.

5.3 Materials and Methods

Experiments described in this study have been conducted according to US national and international welfare guidelines. The Office for Responsible Research at Iowa State University, IACUC Log #3-2-5134-s specifically approved this study and granted permission for the culture of the *Oesophagostomum* parasites. There was no animal suffering or surgery required.

5.3.1 Cloning of nAChR subunits from *O. dentatum* and ancillary factors from *Haemonchus contortus*

O. dentatum nAChR subunits and *H. contortus* ancillary factors used in this research study have been previously cloned and reported (Buxton *et al.*, 2014).

5.3.2 Expression of *Ode*-UNC-29:*Ode*-UNC-63:*Ode*-UNC-38 in *Xenopus laevis* oocytes

Defolliculated *X. laevis* oocytes were purchased from Ecocyte Bioscience (Austin, TX, USA). Oocyte microinjection was done using a Drummond nanoject II microinjector (Drummond Scientific, PA, and USA). 1.8 ng of each subunit cRNA (*Ode-unc-29, Ode-unc-63* and *Ode-unc-38*) and ancillary factor cRNA (*Hco-ric-3, Hco-unc-50* and *Hco-unc-74*) in a total volume of 36 nL in RNAse-free water were microinjected into the animal pole of the

oocytes. Once micro-injected, the oocytes were transferred to a sterile 96-well culture plate (one oocyte/well) containing 200 µL incubation solution (100 mM NaCl, 2 mM KCl, 1.8 mM $CaCl_2.2H_20$, 1 mM $MgCl_2.6H_20$, and 5 mM HEPES, 2.5 mM Na pyruvate, 100 U/mL penicillin and 100 µg/mL streptomycin, pH 7.5) in each well. The oocytes were incubated at 19°C for 2–5 days, with a daily change of incubation solution.

5.3.3 Two-microelectrode voltage-clamp (TEVC) electrophysiology

We followed methods we have described in detail before (Buxton *et al.*, 2014). Briefly, 100 µM BAPTA-AM was added to the oocytes in incubation media approximately 3 hours prior to electrophysiological recordings from the oocytes. TEVC recordings were carried out by impaling the oocytes with two microelectrodes; a voltage sensing electrode, Vm, and a current injecting electrode, Im, were used to inject the current required to hold the membrane at the set voltage. The microelectrodes were pulled with a Flaming/Brown horizontal electrode puller (Model P-97, Sutter Instruments), filled with 3 M potassium chloride and the microelectrode tips carefully broken with a piece of tissue paper to achieve a low resistance of 2–5 MΩ in recording solution (100 mM NaCl, 2.5 mM KCl, 1 mM $CaCl_2.2H_2O$ and 5 mM HEPES, pH 7.3). Current/voltage signals were amplified by an AxoClamp 2B amplifier (Molecular Devices, CA, USA). The amplified signals were converted from analog to digital format by a Digidata 1322A digitizer (Molecular Devices, CA, USA) and finally acquired on a desktop computer with the Clampex 9.2 data acquisition software (Molecular Devices, CA, USA).

5.3.4 Drugs

Acetylcholine (ach) and pyrantel (pyr) were purchased from Sigma-Aldrich (St Louis, MO, USA), while derquantel (der) and abamectin (aba) were gifts from Zoetis (Kalamazoo,

MI). Acetylcholine and pyrantel were dissolved in recording solution. Derquantel and abamectin were dissolved in DMSO and added to recording solution at a final concentration of ≤ 0.01% DMSO.

5.3.5 Drug applications

Acetylcholine which is a natural agonist of many nAChRs served for normalization and as a control in our experiments. Each agonist concentration was applied for 10 s, with sufficient time allowed for wash off between drug applications. For every oocyte recording, 100 μM acetylcholine was applied initially and this current response was measured, subsequent responses were measured and normalized to this acetylcholine current. To generate control agonist concentration-response plots, acetylcholine was applied at different concentrations between 0.1–100 μM or pyrantel was applied at different concentrations between 0.03–10 μM. Higher concentrations of pyrantel were not tested because pyrantel acts as an open channel blocker at high concentrations (Robertson *et al.*, 1994). For the antagonist experiments, a control 100 μM acetylcholine was also first applied for 10s, and then followed by a 2 min or 10 min challenge with the antagonist (derquantel and/or abamectin), and a final application of the agonist (pyrantel) in the continued presence of the antagonist.

5.3.6 Data analysis

We used Clampfit 9.2 (Molecular Devices, CA, and USA) to measure peak current responses and normalized them to the first 100 μM acetylcholine responses. GraphPad Prism 5.0 software (GraphPad Software Inc., USA) was used to analyze the data, and results were expressed as mean ± S.E.M. Concentration-response data points were fitted with the Hill equation as previously described: where R_{max} is the maximum response % relative to the

control 100 μM ach response; the EC_{50} is the concentration producing the half-maximum response and n_H is the slope factor or Hill coefficient (Boulin *et al.*, 2008). We used the unpaired two-tailed Student's t-test to test for statistical significance and a p value < 0.05 was considered significant.

The Bliss additive effect dose-response relationship for pyrantel current responses was calculated as previously described (Greco *et al.*, 1996) to predict the linear additive effects of derquantel and abamectin on the *Ode*-UNC-29:*Ode*-UNC-63:*Ode*-UNC-38 nAChR. To do so, we determined: the normalized mean current responses to each control pyrantel concentration (*CR[pyr]*); the mean current responses to each concentration of pyrantel in the presence of derquantel (derquantel effect) and; the mean current responses to each concentration of pyrantel in the presence of abamectin (abamectin effect). We then used the fractional inhibition (mean reduction in response/*CR[pyr]*) produced by derquantel alone, *Fd*, and abamectin alone, *Fa*, at each pyrantel concentration to determine the additive effect. We used *Fa(1-Fd)* to denote the fractional inhibition produced by abamectin when derquantel is already present, and *Fd+Fa(1-Fd)* to denote the fractional inhibition produced by the combination of derquantel and abamectin. Lastly, the normalized additive response was calculated as:

$$CR[pyr] - CR[pyr]\{Fd + Fa(1 - Fd)\}$$

The difference between the observed and calculated additive effects for the combination of derquantel and abamectin were tested for statistical significance using the paired two-tailed Student's t-test, taking p < 0.05 as significant.

5.4 Results

5.4.1 *Ode*-UNC-29:*Ode*-UNC-63:*Ode*-UNC-38 forms a pyrantel-sensitive nAChR

Representative traces (inward currents from oocytes expressing *Ode*-UNC-29:*Ode*-UNC-63:*Ode*-UNC-38) produced in response to different concentrations of acetylcholine and pyrantel are shown in Figure 5.1A and Figure 5.1B respectively. Figure 5.1C shows acetylcholine and pyrantel concentration-response relationships for *Ode*-UNC-29:*Ode*-UNC-63:*Ode*-UNC-38. The EC_{50} and maximum response (R_{max}) values for acetylcholine were 13.0 ± 1.6 μM and 114.3 ± 4.3%, n = 4. The EC_{50} and R_{max} values for pyrantel were 0.4 ± 0.0 μM and 135.5 ± 7.9%, n = 6 (S5.0 Table). Our results showed the EC_{50} for pyrantel to be significantly smaller ($p < 0.001$) than the EC_{50} for acetylcholine, but showed no significant difference ($p > 0.05$) in R_{max} between acetylcholine and pyrantel. Based on these EC_{50} values, pyrantel is 32.5 times more potent than acetylcholine on the *Ode*-UNC-29:*Ode*-UNC-63:*Ode*-UNC-38 nAChR. Also there was a slightly steeper Hill slope (*nH*) for pyrantel than acetylcholine (*nH* = 1.2 ± 0.1, n = 6 for pyrantel; *nH* = 1.0 ± 0.1, n = 4 for acetylcholine; $p < 0.05$). We used pyrantel rather than acetylcholine for most subsequent experiments because of its potency and because it is a more selective agonist than acetylcholine for this nAChR subtype (Buxton *et al.*, 2014).

5.4.2 Effects of abamectin on *Ode*-UNC-29:*Ode*-UNC-63:*Ode*-UNC-38

We investigated pyrantel concentration-response relationships on *Ode*-UNC-29:*Ode*-UNC-63:*Ode*-UNC-38 in the presence of 0.03 μM and 0.1 μM abamectin. A representative trace is shown in Figure 5.2A. The concentration-response plots, Figure 5.2B, show abamectin to be an antagonist of *Ode*-UNC-29:*Ode*-UNC-63:*Ode*-UNC-38. The EC_{50} and R_{max} values were: 0.4 ± 0.0 μM and 135.5 ± 7.9%, n = 6 for pyrantel in the absence of

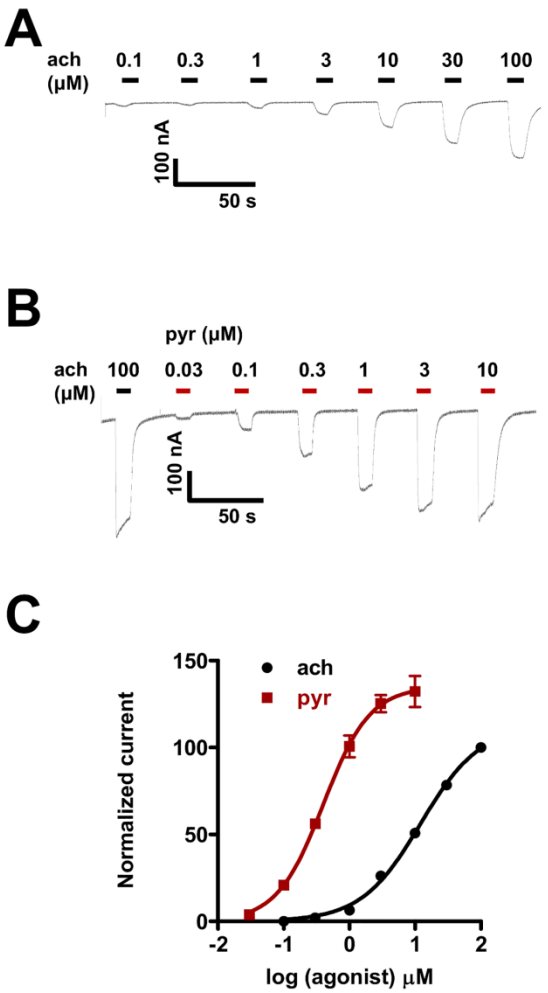

Figure 5.1 Acetylcholine and pyrantel concentration-response relationships for the *Ode*-UNC-29:*Ode*-UNC-63:*Ode*-UNC-38 receptor. **A**: Representative trace (inward currents, holding potential -60mV, from oocytes expressing *Ode*-UNC-29:*Ode*-UNC-63:*Ode*-UNC-38) following 10 seconds applications of different acetylcholine concentrations, from 0.1 μM to 100 μM. **B**: Representative trace (inward currents, holding potential -60mV, from oocytes expressing *Ode*-UNC-29:*Ode*-UNC-63:*Ode*-UNC-38) of the 10 seconds application of different pyrantel concentrations, from 0.03 μM to 10 μM. An initial 10 seconds application of 100 μM acetylcholine served as the control. **C**: Concentration-response plots for acetylcholine (n = 4, black) and pyrantel (n = 6, red). Results were normalized to 100 μM acetylcholine current responses and expressed as mean ± S.E.M.

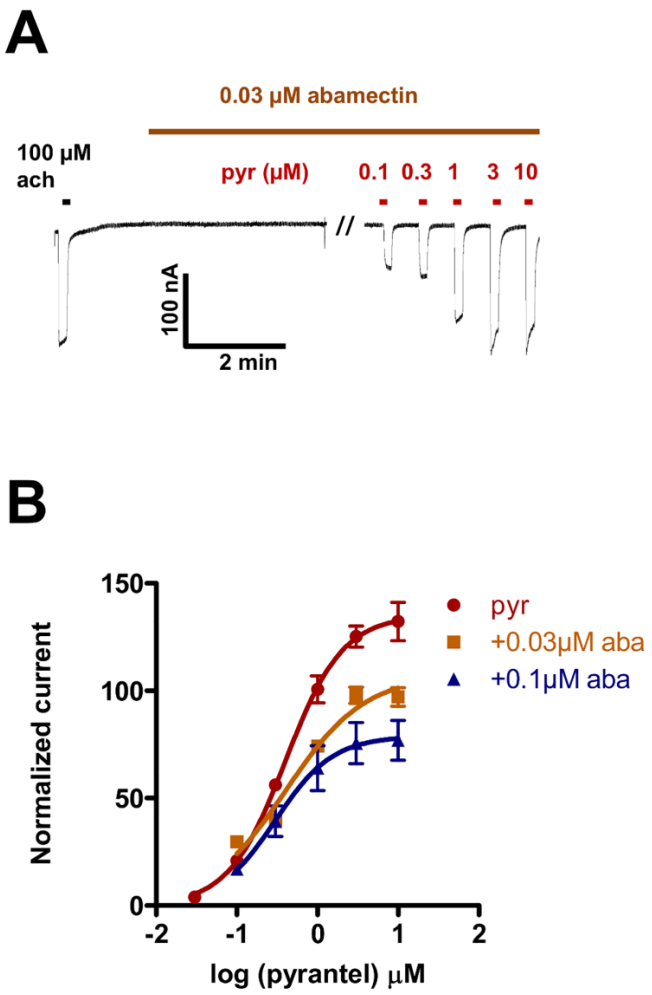

Figure 5.2 Pyrantel concentration-response relationships in the presence of 0.03 µM and 0.1 µM abamectin. **A**: Representative trace (inward currents, holding potential -60mV, from oocytes expressing *Ode*-UNC-29:*Ode*-UNC-63:*Ode*-UNC-38) of the 10 seconds application of the control 100 µM acetylcholine, followed by a 10 minutes application of abamectin (0.03 µM) and finally, a 10 seconds application of different pyrantel concentrations in the continued presence of abamectin. **B**: Concentration-response plots for pyrantel in the absence (n = 6, red) and presence of 0.03 µM abamectin (n = 5, orange) and 0.1 µM abamectin (n = 6, dark blue). Results were normalized to 100 µM acetylcholine current responses and expressed as mean ± S.E.M. Notice 0.03 µM abamectin caused an inhibition of current responses to pyrantel, and this inhibition was greater with 0.1 µM abamectin.

abamectin; 0.4 ± 0.0 μM and 107.3 ± 4.7%, n = 5 for pyrantel in the presence of 0.03 μM abamectin; and 0.3 ± 0.0 μM and 80.6 ± 8.4%, n = 6 for pyrantel in the presence of 0.1 μM abamectin. There was no significant difference ($p > 0.05$) in the EC_{50s} between pyrantel in the absence and presence of 0.03 μM or 0.1 μM abamectin. But, there was a significant difference ($p < 0.05$) in R_{max} for pyrantel in the absence and presence of 0.03 μM abamectin, and this difference was greater ($p < 0.001$) in the presence of 0.1 μM abamectin. Hence, abamectin did not cause a significant change in EC_{50}, but did cause a significant reduction in R_{max}, showing that abamectin acts as a non-competitive antagonist of the *Ode*-UNC-29:*Ode*-UNC-63:*Ode*-UNC-38 nAChR.

When we increased the concentration of abamectin from 0.1 μM to 0.3 μM, Figure 5.3A, we noticed that the EC_{50} for pyrantel in the presence of 0.3 μM abamectin remained unchanged: 0.3 ± 0.1 μM, n = 5 ($p > 0.05$). Although not statistically significant ($p > 0.05$), the mean value for the R_{max} for pyrantel in the presence of 0.1 μM abamectin (80.6 ± 8.4, n = 6) appeared smaller than R_{max} in the presence of 0.3 μM abamectin (98.4 ± 6.5, n = 5). This suggested that the inhibitory effects of lower concentrations of abamectin can be greater than those of higher concentrations. This reversed inhibitory effect was tested and confirmed when we increased the concentration of abamectin from 0.3 μM to 1 μM and 10 μM. While the EC_{50} values did not change (0.3 ± 0.1 μM, n = 6 in the presence of 1 μM abamectin, and 0.4 ± 0.1 μM, n = 5 in the presence of 10 μM abamectin), the R_{max} values increased to 108.0 ± 3.5%, n = 6 in the presence of 1 μM abamectin, and 106.0 ± 9.4%, n = 5 in the presence of 10 μM abamectin. We point out that the effects of abamectin were reversible on washing, although the current responses did not return to control responses even after a 10 mins wash.

S5.1 Table summarizes the EC_{50}, R_{max}, n_H and n numbers for these experiments.

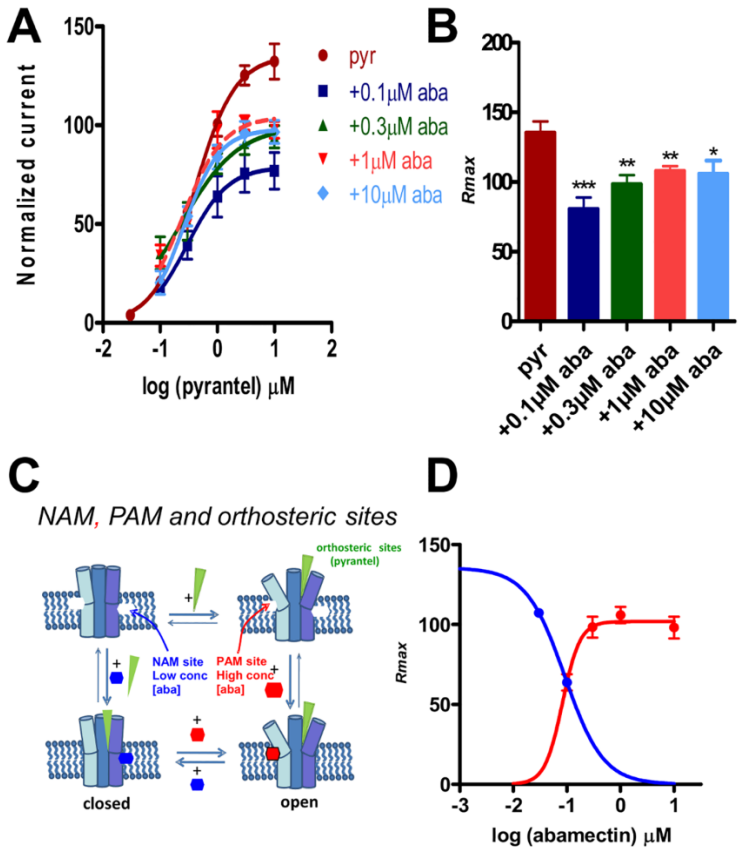

Figure 5.3. Effects of increasing concentrations of abamectin (above 0.1 µM) on the pyrantel concentration-response plots. **A**: Concentration-response plots for pyrantel in the absence (n = 6, red) and presence of 0.1 µM abamectin (n = 6, dark blue); 0.3 µM abamectin (n = 5, dark green); 1 µM abamectin (n = 6, pink); 10 µM abamectin (n = 5, light blue). Results were normalized to 100 µM acetylcholine current responses and expressed as mean ± S.E.M. Increasing the concentration of abamectin from 0.1 µM to 0.3, 1 and 10 µM rather caused a reduction in the inhibition instead of a potentiation. **B**: Bar chart showing the mean ± S.E.M of the maximum current responses (R_{max}) for pyrantel and the different abamectin concentrations. R_{max} for 0.1 µM abamectin (n = 6, dark blue), 0.3 µM abamectin (n = 5, dark green), 1 µM abamectin (n = 6, pink) and 10 µM abamectin (n = 5, light blue) were significantly lower than R_{max} for pyrantel alone (n = 6, red). * $p < 0.05$, ** $p < 0.01$ and *** $p < 0.001$, unpaired two-tailed student t-test. **C**: Model of ligand sites of action. Pyrantel binds to the orthosteric sites opening the channel. Low concentrations of abamectin (0.03 and 0.1 µM) bind to a negative allosteric site (NAM) in the lipid phase of the channel, inhibiting opening. Higher concentrations of abamectin (0.3, 1 and 10 µM) bind to a positive allosteric site (PAM) increasing opening. **D**: Abamectin R_{max} inhibition (blue curve) and inhibition reduction (red curve) dose response plots. The data points for inhibition used data from 0.03 µM and 0.1 µM abamectin from Figure 5.2. The data points for inhibition reduction used data from Figure 5.3B.

Interestingly, when the EC_{50s} for pyrantel alone are compared with that for pyrantel in the presence of 0.1 μM, 0.3 μM, 1 μM or 10 μM abamectin, there were no significant differences in the EC_{50} values. In contrast however, the R_{max} values for pyrantel in the presence of 0.1 μM, 0.3 μM, 1 μM and 10 μM abamectin were significantly less than the R_{max} for pyrantel alone, Figure 5.3B. We emphasize again that the R_{max} for pyrantel in the presence of abamectin concentrations ≥0.3 μM were greater than the R_{max} for pyrantel in the presence of 0.1 μM abamectin, with the difference being statistically significant ($p < 0.05$) for 1 μM. These observations show that abamectin has a bi-phasic effect, suggesting two allosteric sites of action: a high affinity site causing antagonism, and a lower affinity site causing a reduction in the antagonism, Figures 5.3C and 5.3D.

5.4.3 Effects of derquantel and abamectin combination on *Ode*-UNC-29:*Ode*-UNC-63:*Ode*-UNC-38

For this set of experiments, we tested the combination of 0.3 μM abamectin and 0.1 μM derquantel. We selected 0.3 μM abamectin because it is the reported concentration in *H. contortus* following the administration of abamectin at its therapeutic dose of 0.2 μM at 12 hours (Lloberas *et al.*, 2013). 0.1 μM derquantel was selected because the reported concentration is 13 μM at 12 hours in the intestine (Jin, 2010) with an uncertain but lower concentration being present within the worm. Figures 5.4A and 5.4B show representative traces for *Ode*-UNC-29:*Ode*-UNC-63:*Ode*-UNC-38 responses to pyrantel in the presence of 0.3 μM abamectin alone, and the 0.1 μM derquantel plus 0.3 μM abamectin combination respectively. Concentration-response plots for pyrantel in the absence and presence of 0.1 μM derquantel alone, 0.3 μM abamectin alone, and the 0.1 μM derquantel and 0.3 μM abamectin combination are shown in Figure 5.4C. The calculated additive effect of the

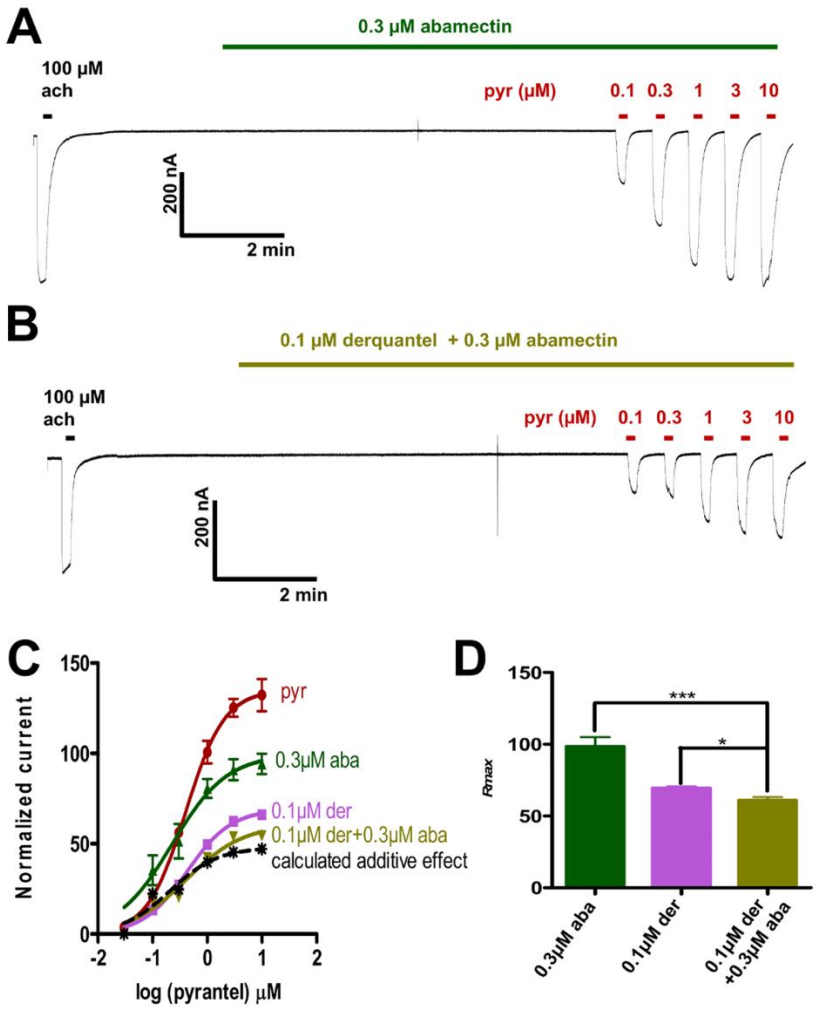

Figure 5.4 Effects of 0.1 µM derquantel alone, 0.3 µM abamectin alone, and derquantel and abamectin combination (0.1 µM derquantel + 0.3 µM abamectin) on the pyrantel concentration-response plots. **A**: Representative trace (inward currents from oocytes expressing *Ode*-UNC-29:*Ode*-UNC-63:*Ode*-UNC-38) of the 10 seconds application of the control 100 µM acetylcholine, followed by a 10 minutes application of 0.3 µM abamectin and finally, a 10 seconds application of different pyrantel concentrations in the continued presence of abamectin. **B**: Representative trace (inward currents from oocytes expressing *Ode*-UNC-29:*Ode*-UNC-63:*Ode*-UNC-38) of the 10 seconds application of the control 100 µM acetylcholine, followed by a 10 minutes application of derquantel and abamectin combination and finally, a 10 seconds application of different pyrantel concentrations in the continued presence of the derquantel and abamectin combination. **C**: Concentration-response plots for pyrantel in the absence (n = 6, red) and presence of 0.1 µM derquantel (n = 4, light purple); 0.3 µM abamectin (n = 5, dark green); 0.1 µM derquantel + 0.3 µM abamectin combination (n = 6, olive green). Results were normalized to 100 µM acetylcholine current responses and expressed as mean ± S.E.M. Inhibition with 0.1 µM derquantel + 0.3 µM abamectin combination was greater than that with 0.1 µM derquantel alone and 0.3 µM abamectin alone. The calculated additive effect for the combination of derquantel and

abamectin (broken black) was not statistically different ($p > 0.05$, paired two-tailed student t-test) from the observed additive effect for the combination of derquantel and abamectin (olive green). **D**: Bar chart showing the mean ± S.E.M of the maximum current responses (R_{max}) for 0.1 μM derquantel (n = 4, light purple); 0.3 μM abamectin (n = 5, dark green); 0.1 μM derquantel + 0.3 μM abamectin combination (n = 6, olive green). R_{max} for the combination of 0.1 μM derquantel + 0.3 μM abamectin was significantly smaller than R_{max} for 0.1 μM derquantel alone and for 0.3 μM abamectin alone. * $p < 0.05$ and *** $p < 0.001$, unpaired two-tailed student t-test.

combination of derquantel and abamectin is also shown in Figure 5.4C. The observed effect was not greater than the calculated additive effect ($p > 0.05$) so this combination does not show synergism. S5.2 Table shows the EC_{50} and R_{max} values for these experiments. There was no significant difference ($p > 0.05$) between EC_{50} values for pyrantel in the absence and presence of derquantel alone, abamectin alone or the derquantel and abamectin combination. However, as before the R_{max} values for pyrantel in the presence of 0.1 μM derquantel alone, 0.3 μM abamectin alone, and 0.1 μM derquantel and 0.3 μM abamectin combination were significantly smaller ($p < 0.001$) than the R_{max} for pyrantel in the absence of derquantel and/or abamectin. Thus both derquantel and abamectin show non-competitive antagonism on the *Ode*-UNC-29:*Ode*-UNC-63:*Ode*-UNC-38 receptor. Figure 5.4D also shows that R_{max} values for pyrantel in the presence of 0.1 μM derquantel alone and 0.3 μM abamectin alone were significantly greater ($p < 0.05$ and $p < 0.001$) than R_{max} in the presence of 0.1 μM derquantel and 0.3 μM abamectin combination. Thus the combination of abamectin and derquantel together increases the antagonism but their combination was not significantly greater than the calculated additive effect.

We used pyrantel as the preferred agonist to study the effects of abamectin and derquantel on the *Ode*-UNC-29:*Ode*-UNC-63:*Ode*-UNC-38 receptor because it is more selective than acetylcholine for this receptor (Buxton *et al.*, 2014). However, we also tested

the effects of abamectin and derquantel with acetylcholine as the agonist instead of pyrantel. We found, as with pyrantel, that a lower concentration of 0.1 μM abamectin was a more potent non-competitive acetylcholine antagonist than 0.3 μM or 1 μM abamectin, S5.0 Figure. We also found that 0.3 μM derquantel acts as a non-competitive antagonist of acetylcholine and that the combination of derquantel and abamectin shows additive inhibitory effects without demonstrating synergism, S5.1 Figure.

5.5 Discussion

5.5.1 Abamectin as a non-competitive antagonist of *Ode*-UNC-29:*Ode*-UNC-63:*Ode*-UNC-38

Abamectin, a mixture of avermectins B1a and B1b (Figure 5.0), belongs to the macrocyclic lactone class of anthelmintics which have been shown to act on GluCls (Wolstenholme & Rogers, 2005). In addition to the effect of abamectin on GluCls, Puttachary et al (Puttachary *et al.*, 2013) showed, using muscle contraction and current-clamp electrophysiological techniques, that abamectin acts as a non-competitive antagonist of *Ascaris suum* (Clade III nematode) somatic muscle nAChRs. In this paper we were interested to see if abamectin had similar effects on the expressed *O. dentatum* (Clade V nematode) receptor, *Ode*-UNC-29:*Ode*-UNC-63:*Ode*-UNC-38. Interestingly, we found that abamectin was also a potent non-competitive antagonist of this receptor (Figure 5.2B).

5.5.2 Bi-phasic effects of abamectin on *Ode*-UNC-29:*Ode*-UNC-63:*Ode*-UNC-38

The inverse dose-dependent bi-phasic effects of abamectin on *Ode*-UNC-29:*Ode*-UNC-63:*Ode*-UNC-38 suggest that abamectin has two allosteric sites of action on this receptor: one, a higher affinity negative allosteric modulator (NAM) site causing antagonism; and the other, with lower affinity, a positive allosteric modulator (PAM) site, causing a

reduction in the antagonism (Figure 5.3D). The NAM and PAM sites of action of abamectin on the receptors may be in the outer lipid phase of the membrane (Martin & Kusel, 1992) between the TM1 transmembrane domain of one receptor subunit and the TM3 domain of the adjacent receptor subunit (Hibbs & Gouaux, 2011). Since the receptor channel is composed of heterogeneous subunits, binding between one pair of subunits may stabilize closing (negative allosteric modulator) while binding between another pair of subunits may stabilize opening (positive allosteric modulator).

5.5.3 Derquantel and abamectin combination produces greater effects than either derquantel or abamectin used alone

The effects of a combination of derquantel and abamectin on a mixture of *in situ A. suum* somatic nAChR subtypes have been described by Puttachary at al (Puttachary *et al.*, 2013): when derquantel was used alone, *A. suum* somatic nAChRs were antagonized in a competitive manner (right-shift in EC_{50}, but no change in *Rmax*); when abamectin was used alone, *A. suum* somatic nAChRs were antagonized in a non-competitive manner (reduction in *Rmax*, but no change in EC_{50}); when derquantel and abamectin were used in combination, abamectin potentiated the antagonism of derquantel. In our experiments with *Ode*-UNC-29:*Ode*-UNC-63:*Ode*-UNC-38, derquantel showed non-competitive (Figure 5.4C) rather than competitive antagonism. With the combination of derquantel and abamectin together, the R_{max} was significantly smaller than for derquantel alone and abamectin alone (Figure 5.4D). Additionally, the effects of the combination were greater than those of 0.1 μM derquantel at pyrantel concentrations ≥ 0.3 μM suggesting that the use of abamectin and derquantel in combination is likely to be more effective than either one of the two drugs administered alone.

5.6 Conclusion

Our observations reveal that abamectin, in addition to its recognized effects on GluCl channels also has effects on an UNC-29: UNC-63: UNC-38 subtype of nematode nAChR and that the antagonism is non-competitive with a bi-phasic inverse dose-dependent effect characteristic of two sites of action. The higher affinity site, a negative allosteric site, produces more closing of the nAChR in contrast to the other lower affinity site, a positive allosteric site that produces more opening. The significant observation is that lower concentrations of abamectin produced greater inhibition of the nAChR than higher concentrations. The combination of derquantel and abamectin as Startect^{R} can produce inhibition of nematode worm movement and feeding. Derquantel and abamectin inhibits the nAChRs; and in addition, abamectin inhibits movement and feeding by activating GluCls. The double action of the combination of derquantel and abamectin has the potential to slow resistance development in nematode parasites by acting at a number of different sites of action. The emergence of resistance in numerous nematode parasite species makes the control of helminth infections with the currently available anthelmintics more difficult but the recent introduction and careful use of appropriate anthelmintic combinations may be used to reduce the rate of development of anthelmintic resistance. It should also be noted that effects of abamectin does not involve a simple mode of action and that there are effects on more than one LGIC in addition to the GluCls.

5.7 Supporting Information

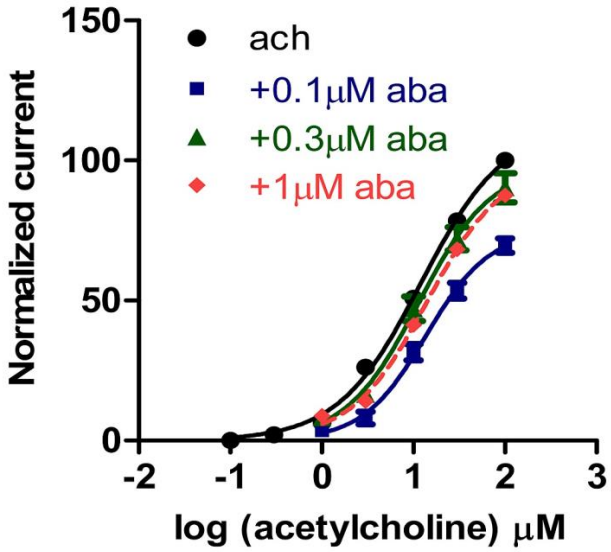

S5.0 Figure Concentration-response plots for acetylcholine in the absence (n = 4, black) and presence of 0.1 μM abamectin (n = 4, dark blue), 0.3 μM abamectin (n = 4, dark green) and 1 μM abamectin (n = 3, pink). Results were normalized to 100 μM acetylcholine current responses and expressed as mean ± S.E.M. The standard errors are smaller than the symbols and some are not visible. Notice 0.1 μM abamectin caused an inhibition of current responses to acetylcholine, and this inhibition was reduced with 0.3 and 1 μM abamectin.

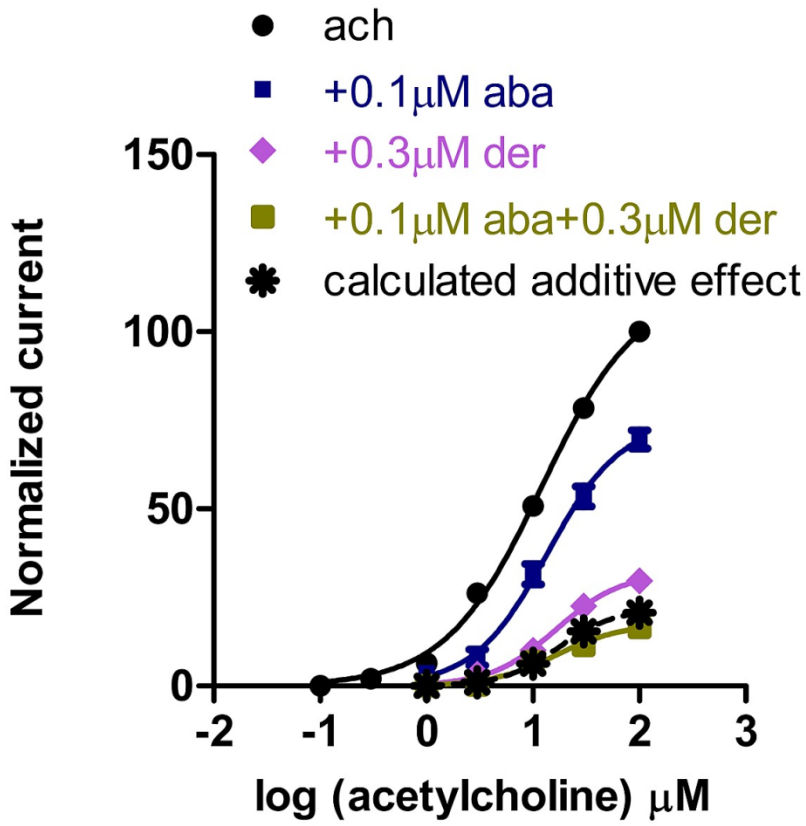

S5.1 Figure. Concentration-response plots for acetylcholine in the absence (n = 4, black) and presence of 0.3 μM derquantel (n = 4, light purple); 0.1 μM abamectin (n = 4, dark blue); 0.3 μM derquantel + 0.1 μM abamectin combination (n = 4, olive green). Results were normalized to 100 μM acetylcholine current responses and were expressed as mean ± S.E.M. The standard errors are smaller than the symbols and some are not visible. Inhibition with 0.3 μM derquantel + 0.1 μM abamectin combination was greater than that with 0.3 μM derquantel alone and 0.1 μM abamectin alone. The calculated additive effect (*) is also plotted.

S5.0 Table. EC_{50}, R_{max}, n_H and n numbers for acetylcholine and pyrantel on *Ode*-UNC-29:*Ode*-UNC-63:*Ode*-UNC-38.

Drug	EC_{50} **(mean ± S.E.M, µM)**	R_{max} **(mean ± S.E.M, % 100 µM acetylcholine response)**	n_H	**n**
Acetylcholine	13.0 ± 1.6	114.3 ± 4.3	1.0 ± 0.1	4
Pyrantel	0.4 ± 0.0	135.5 ± 7.9	1.2 ± 0.1	6

S5.1 Table. EC_{50}, R_{max}, n_H and n numbers for pyrantel in the absence and presence of abamectin on *Ode*-UNC-29:*Ode*-UNC-63:*Ode*-UNC-38.

Drug	EC_{50} **(mean ± S.E.M, µM)**	R_{max} **(mean ± S.E.M, % 100 µM acetylcholine response)**	n_H	**n**
Pyrantel	0.4 ± 0.0	135.5 ± 7.9	1.2 ± 0.1	6
Pyrantel + 0.03 µM abamectin	0.4 ± 0.0	107.3 ± 4.7	0.9 ± 0.1	5
Pyrantel + 0.1 µM abamectin	0.3 ± 0.0	80.6 ± 8.4	1.2 ± 0.2	6
Pyrantel + 0.3 µM abamectin	0.3 ± 0.1	98.4 ± 6.5	1.0 ± 0.1	5
Pyrantel + 1 µM abamectin	0.3 ± 0.1	108.0 ± 3.5	1.2 ± 0.1	6
Pyrantel + 10 µM abamectin	0.4 ± 0.1	106.0 ± 9.4	1.5 ± 0.4	5

S5.2 Table. EC_{50}, R_{max}, n_H and n numbers for pyrantel in the absence and presence of derquantel, abamectin, and a combination of derquantel and abamectin on *Ode*-UNC-29:*Ode*-UNC-63:*Ode*-UNC-38.

Drug	**EC_{50} (mean ± S.E.M, µM)**	**R_{max} (mean ± S.E.M, % 100 µM acetylcholine response)**	**n_H**	**n**
Pyrantel	0.4 ± 0.0	135.5 ± 7.9	1.2 ± 0.1	6
Pyrantel + 0.1 µM derquantel	0.4 ± 0.0	69.4 ± 1.1	1.1 ± 0.1	4
Pyrantel + 0.3 µM abamectin	0.3 ± 0.1	98.4 ± 6.5	1.0 ± 0.1	5
Pyrantel + 0.1 µM derquantel + 0.3 µM abamectin	0.3 ± 0.1	60.9 ± 2.3	0.9 ± 01	6

S5.3 Table. EC_{50}, R_{max}, n_H and n numbers for acetylcholine in the absence and presence of 0.1 µM, 0.3 µM and 10 µM abamectin on *Ode*-UNC-29:*Ode*-UNC-63:*Ode*-UNC-38.

Drug	**EC_{50} (mean ± S.E.M, µM)**	**R_{max} (mean ± S.E.M, % 100 µM acetylcholine response)**	**n_H**	**n**
Acetylcholine	13.0 ± 1.6	114.3 ± 4.3	1.0 ± 0.1	4
Acetylcholine + 0.1 µM abamectin	14.0 ± 1.1	75.1 ± 2.0	1.3 ± 0.1	4
Acetylcholine + 0.3 µM abamectin	11.6 ± 1.0	98.5 ± 4.7	1.1 ± 0.0	4
Acetylcholine + 1 µM abamectin	14.4 ± 1.0	99.6 ± 1.6	1.1 ± 0.1	3

S5.4 Table. EC_{50}, R_{max}, n_H and n numbers for acetylcholine in the absence and presence of derquantel, abamectin, and a combination of derquantel and abamectin on *Ode*-UNC-29:*Ode*-UNC-63:*Ode*-UNC-38.

Drug	**EC_{50} (mean ± S.E.M, µM)**	**R_{max} (mean ± S.E.M, % 100 µM acetylcholine response)**	**n_H**	**n**
Acetylcholine	13.0 ± 1.6	114.3 ± 4.3	1.0 ± 0.1	4
Acetylcholine + 0.3 µM derquantel	16.6 ± 1.1	32.1 ± 1.9	1.4 ± 0.1	4
Acetylcholine + 0.1 µM abamectin	14.0 ± 1.1	75.1 ± 2.0	1.3 ± 0.1	4
Acetylcholine + 0.3 µM derquantel + 0.1 µM abamectin	15.8 ± 1.6	17.2 ± 1.6	1.5 ± 0.2	4

5.8 Acknowledgements

We will like to thank Debra Woods of Zoetis (Kalamazoo, MI) for providing us with derquantel and abamectin.

5.9 Funding

Research reported in this publication was supported by the National Institute of Allergy and Infectious Diseases of the National Institutes of Health under Award Number R01AI047194 to RJM, R21AI092185-01A1 to APR and the Schlumberger Foundation to MA. The content is solely the responsibility of the authors and does not necessarily represent the official views of the National Institutes of Health.

5.10 Author Contributions

Conceived and designed the experiments: MA APR RJM. Performed the experiments: MA SKB. Analyzed the data: MA APR RJM. Contributed reagents/materials/analysis tools: MA SKB APR RJM. Wrote the paper: MA APR RJM.

CHAPTER 6. GENERAL DISCUSSION

Many of the currently available anthelmintics used to control parasitic nematode infections act on nematode ion channels. However, there are a limited number of these anthelmintics and their repeated use has led to increasing worldwide reports of anthelmintic resistance development. Thus, the increased need for the development of alternative strategies to slow down or overcome the resistance problem. This PhD research has addressed three strategies by which resistance can be slowed or overcome. These include: (i) the identification of a new drug target ACR-16, (ii) identifying new therapeutic compounds from plant natural sources, and (iii) understanding interactions of drugs used in combination therapy.

ACR-16 is an α7-like nAChR that forms homomeric receptors in nematodes. Earlier studies have focused on the cloning and expression of ACR-16 from the free-living model nematode, *C. elegans*. We have showed for the first time the cloning and expression of ACR-16 from a parasitic nematode, *A. suum*. We have demonstrated that although *A. suum* ACR-16 shares a high degree of similarity with *C. elegans* ACR-16, these two receptors have significant differences in antagonist pharmacology. We have shown that *A. suum* ACR-16 is different from the carefully studied levamisole receptors. *A. suum* ACR-16 is insensitive to levamisole (and other cholinomimetic anthelmimntics) but very sensitive to nicotine. Based on these differences with levamisole receptors, developing drugs that target *A. suum* ACR-16 may circumvent resistance. Importantly, *A. suum* ACR-16 though closely related to vertebrate α7 receptors showed striking differences in sensitivity to α-BTX, allosteric modulation and calcium permeability which could be related to differences in key amino acid residues known to affect α7 receptor pharmacology. Therefore, targeting sites in *A. suum*

ACR-16 that are distinct from vertebrate α7 receptors are unlikely to affect the vertebrate host.

We have demonstrated that plant natural products have potential as sources of lead compounds for the development of macrofilaricidal drugs. We have showed that there is some validity for the traditional uses of *D. oliveri* and *P. febrifugum* in the treatment of filarial infections and that extracts from the medicinal plants *D. oliveri* and *P. febrifugum* are useful to medical practice. Our work focused on *D. oliveri* because extracts of this plant showed good activity against adult *O. ochengi* and *B. pahangi*, in addition to activity against *O. ochengi* microfilariae. This is interesting because a desirable anthelmintic drug is one that has a broad spectrum of action against various parasite species. Therefore, our study has shed more light on the discovery of novel therapeutic drugs from traditionally used plants. We have also demonstrated that *D. oliveri* has potential as a natural source for isolating macrofilaricidal compounds that would contribute to more effective control or elimination of filarial infections.

Finally, we have identified at least one mechanism in which a combination therapy is more effective than single drug approach. We showed that abamectin not only acts on GluCls but also has potent effects on pyrantel/tribendimidine nAChRs in *O. dentatum*. The inhibitory effect of abamectin on nAChRs increases the inhibition caused by derquantel (the other component of the combination therapy).

Future Directions

We would recommend more experiments be done in order to further validate ACR-16 as a potential drug target for anthelmintic development. First, we would recommend the expression of ACR-16 in a mammalian cell line which will provide a platform for high

throughput screening. Once this is done, various compounds known to be specific for the closely related human α7 receptors should be tested on ACR-16. Doing so will confirm our observations in electrophysiology studies that ACR-16's pharmacology is different from that of human α7, thus, confirming ACR-16 is a potential anthelmintic drug target. Since we have demonstrated that ACR-16, unlike levamisole receptors desensitizes quickly, we would not recommend the use of specific agonists as anthelmintic compounds. An agonist effect would not produce long term inhibition of ACR-16 mediated behaviors. Additionally, the observation that *acr-16* null *C. elegans* have a close to wild-type phenotype implies that antagonists are also unlikely to be effective. We propose that research should focus on the discovery of positive allosteric modulators of ACR-16 as the most attractive potential drugs.

For the filaricidal plant extracts, we intend to pursue the following: (i) active HPLC fractions will be further purified to allow for isolation of the compounds that are responsible for biological activity, (ii) structure-activity relationship studies will be exploited to increase the potency of the identified compounds if necessary, (iii) the mode of action of lead compounds will be determined, (iv) various combinations of bioactive compounds will be tested for synergistic effects as potential combination therapies, and (v) the efficacy and safety of identified compounds will be evaluated in both *in vitro* and *in vivo* systems.

REFERENCES

Abongwa M, Baber KE, Martin RJ, & Robertson AP (2016a). The cholinomimetic morantel as an open channel blocker of the Ascaris suum ACR-16 nAChR. Invert Neurosci 16: 10.

Abongwa M, Buxton SK, Robertson AP, & Martin RJ (2016b). Curiouser and Curiouser: The Macrocyclic Lactone, Abamectin, Is also a Potent Inhibitor of Pyrantel/Tribendimidine Nicotinic Acetylcholine Receptors of Gastro-Intestinal Worms. PLoS One 11: e0146854.

Aceves J, Erlij D, & Martinez-Maranon R (1970). The mechanism of the paralysing action of tetramisole on Ascaris somatic muscle. Br J Pharmacol 38: 602-607.

Ahmadu A, Haruna AK, Garba M, Ehinmidu JO, & Sarker SD (2004). Phytochemical and antimicrobial activities of the Daniellia oliveri leaves. Fitoterapia 75: 729-732.

Ahmadu AA, Zezi AU, & Yaro AH (2007). Anti-diarrheal activity of the leaf extracts of Daniellia oliveri Hutch and Dalz (Fabaceae) and Ficus sycomorus Miq (Moraceae). Afr J Tradit Complement Altern Med 4: 524-528.

Al-Abd NM, Nor ZM, Al-Adhroey AH, Suhaimi A, & Sivanandam S (2013). Recent advances on the use of biochemical extracts as filaricidal agents. Evid Based Complement Alternat Med 2013: 986573.

Albonico M, Smith PG, Hall A, Chwaya HM, Alawi KS, & Savioli L (1994). A randomized controlled trial comparing mebendazole and albendazole against Ascaris, Trichuris and hookworm infections. Trans R Soc Trop Med Hyg 88: 585-589.

Alexander SPH, Peters JA, Kelly E, Marrion N, Benson HE, Faccenda E, *et al.* (2015). The Concise Guide to PHARMACOLOGY 2015/16: Ligand-gated ion channels. Br J Pharmacol 172: 5870-5903.

Altschul SF, Madden TL, Schaffer AA, Zhang J, Zhang Z, Miller W, *et al.* (1997). Gapped BLAST and PSI-BLAST: a new generation of protein database search programs. Nucleic Acids Res 25: 3389-3402.

Anderson N, Martin PJ, & Jarrett RG (1988). Mixtures of anthelmintics: a strategy against resistance. Aust Vet J 65: 62-64.

Anderson RI, Fazen LE, & Buck AA (1975a). Onchocerciasis in Guatemala. II. Microfilariae in urine, blood, and sputum after diethylcarbamazine. Am J Trop Med Hyg 24: 58-61.

Anderson RI, Thomas DB, MacRae AA, & Buck AA (1975b). Onchocerciasis: prevalence of microfilaruria and other manifestations in village of Cameroon. Am J Trop Med Hyg 24: 66-70.

Arias HR (1997). Topology of ligand binding sites on the nicotinic acetylcholine receptor. Brain Res Brain Res Rev 25: 133-191.

Aubry ML, Cowell P, Davey MJ, & Shevde S (1970). Aspects of the pharmacology of a new anthelmintic: pyrantel. Br J Pharmacol 38: 332-344.

Austin WC, Courtney W, Danilewicz JC, Morgan DH, Conover LH, Howes HL, Jr., *et al.* (1966). Pyrantel tartrate, a new anthelmintic effective against infections of domestic animals. Nature 212: 1273-1274.

Awadzi K (2003). Clinical picture and outcome of Serious Adverse Events in the treatment of Onchocerciasis. Filaria J 2 Suppl 1: S6.

Awadzi K, & Gilles HM (1992). Diethylcarbamazine in the treatment of patients with onchocerciasis. Br J Clin Pharmacol 34: 281-288.

Ayers S, Zink DL, Mohn K, Powell JS, Brown CM, Murphy T, *et al.* (2007). Anthelmintic activity of aporphine alkaloids from Cissampelos capensis. Planta Med 73: 296-297.

Babu S, & Nutman TB (2012). Immunopathogenesis of lymphatic filarial disease. Semin Immunopathol 34: 847-861.

Balass M, Katchalski-Katzir E, & Fuchs S (1997). The alpha-bungarotoxin binding site on the nicotinic acetylcholine receptor: analysis using a phage-epitope library. Proc Natl Acad Sci U S A 94: 6054-6058.

Ballivet M, Alliod C, Bertrand S, & Bertrand D (1996). Nicotinic acetylcholine receptors in the nematode Caenorhabditis elegans. J Mol Biol 258: 261-269.

Bamgbose SO, Marquis VO, & Salako LA (1973). Some pharmacological effects of the nematocide, morantel. Br J Pharmacol 47: 117-123.

Bandyopadhyay L (1996). Lymphatic filariasis and the women of India. Soc Sci Med 42: 1401-1410.

Bargmann CI (1998). Neurobiology of the Caenorhabditis elegans genome. Science 282: 2028-2033.

Barnard EA, Miledi R, & Sumikawa K (1982). Translation of exogenous messenger RNA coding for nicotinic acetylcholine receptors produces functional receptors in Xenopus oocytes. Proc R Soc Lond B Biol Sci 215: 241-246.

Bartram DJ, Leathwick DM, Taylor MA, Geurden T, & Maeder SJ (2012). The role of combination anthelmintic formulations in the sustainable control of sheep nematodes. Vet Parasitol 186: 151-158.

Basanez MG, Pion SD, Churcher TS, Breitling LP, Little MP, & Boussinesq M (2006). River blindness: a success story under threat? PLoS Med 3: e371.

Baur R, Beech R, Sigel E, & Rufener L (2015). Monepantel irreversibly binds to and opens Haemonchus contortus MPTL-1 and Caenorhabditis elegans ACR-20 receptors. Mol Pharmacol 87: 96-102.

Beech RN, & Neveu C (2015). The evolution of pentameric ligand-gated ion-channels and the changing family of anthelmintic drug targets. Parasitology 142: 303-317.

Bendtsen JD, Nielsen H, von Heijne G, & Brunak S (2004). Improved prediction of signal peptides: SignalP 3.0. J Mol Biol 340: 783-795.

Bennett HM, Lees K, Harper KM, Jones AK, Sattelle DB, Wonnacott S, *et al.* (2012). Xenopus laevis RIC-3 enhances the functional expression of the C. elegans homomeric nicotinic receptor, ACR-16, in Xenopus oocytes. J Neurochem 123: 911-918.

Benton B (1998). Economic impact of onchocerciasis control through the African Programme for Onchocerciasis Control: an overview. Ann Trop Med Parasitol 92 Suppl 1: S33-39.

Bergquist R (2016). Tribendimidine: great expectations. Lancet Infect Dis 16: 1089-1091.

Bertrand D, Bertrand S, Cassar S, Gubbins E, Li J, & Gopalakrishnan M (2008). Positive allosteric modulation of the alpha7 nicotinic acetylcholine receptor: ligand interactions with distinct binding sites and evidence for a prominent role of the M2–M3 segment. Mol Pharmacol 74: 1407-1416.

Bertrand D, Devillers-Thiery A, Revah F, Galzi JL, Hussy N, Mulle C, *et al.* (1992). Unconventional pharmacology of a neuronal nicotinic receptor mutated in the channel domain. Proc Natl Acad Sci U S A 89: 1261-1265.

Bertrand D, Galzi JL, Devillers-Thiery A, Bertrand S, & Changeux JP (1993). Mutations at two distinct sites within the channel domain M2 alter calcium permeability of neuronal alpha 7 nicotinic receptor. Proc Natl Acad Sci U S A 90: 6971-6975.

Bertrand D, & Gopalakrishnan M (2007). Allosteric modulation of nicotinic acetylcholine receptors. Biochem Pharmacol 74: 115-1163.

Bethony J, Brooker S, Albonico M, Geiger SM, Loukas A, Diemert D, *et al.* (2006). Soil-transmitted helminth infections: ascariasis, trichuriasis, and hookworm. Lancet 367: 1521-1532.

Bianchi L, & Driscoll M (2006). Heterologous expression of C. elegans ion channels in Xenopus oocytes. WormBook: 1-16.

Blaxter ML, De Ley P, Garey JR, Liu LX, Scheldeman P, Vierstraete A, *et al.* (1998). A molecular evolutionary framework for the phylum Nematoda. Nature 392: 71-75.

Boatin BA, & Richards FO, Jr. (2006). Control of onchocerciasis. Adv Parasitol 61: 349-394.

Boatin BA, Toe L, Alley ES, Dembele N, Weiss N, & Dadzie KY (1998). Diagnostics in onchocerciasis: future challenges. Ann Trop Med Parasitol 92 Suppl 1: S41-45.

Bossi E, Fabbrini MS, & Ceriotti A (2007). Exogenous protein expression in Xenopus oocytes: basic procedures. Methods Mol Biol 375: 107-131.

Boulin T, Fauvin A, Charvet CL, Cortet J, Cabaret J, Bessereau JL, *et al.* (2011). Functional reconstitution of Haemonchus contortus acetylcholine receptors in Xenopus oocytes provides mechanistic insights into levamisole resistance. Br J Pharmacol 164: 1421-1432.

Boulin T, Gielen M, Richmond JE, Williams DC, Paoletti P, & Bessereau JL (2008). Eight genes are required for functional reconstitution of the Caenorhabditis elegans levamisole-sensitive acetylcholine receptor. Proc Natl Acad Sci U S A 105: 18590-18595.

Boussinesq M, & Gardon J (1997). Prevalences of Loa loa microfilaraemia throughout the area endemic for the infection. Ann Trop Med Parasitol 91: 573-589.

Boussinesq M, Gardon J, Gardon-Wendel N, & Chippaux JP (2003). Clinical picture, epidemiology and outcome of Loa-associated serious adverse events related to mass ivermectin treatment of onchocerciasis in Cameroon. Filaria J 2 Suppl 1: S4.

Bouzat C (2012). New insights into the structural bases of activation of Cys-loop receptors. J Physiol Paris 106: 23-33.

Bradley AK (1976). Effects of onchoceriasis on settlement in the Middle Hawal Valley, Nigeria. Trans R Soc Trop Med Hyg 70: 225-229.

Bradley JE, & Unnasch TR (1996). Molecular approaches to the diagnosis of onchocerciasis. Adv Parasitol 37: 57-106.

Brattig NW (2004). Pathogenesis and host responses in human onchocerciasis: impact of Onchocerca filariae and Wolbachia endobacteria. Microbes Infect 6: 113-128.

Brejc K, van Dijk WJ, Klaassen RV, Schuurmans M, van Der Oost J, Smit AB, *et al.* (2001). Crystal structure of an ACh-binding protein reveals the ligand-binding domain of nicotinic receptors. Nature 411: 269-276.

Brieger WR, Oshiname FO, & Ososanya OO (1998). Stigma associated with onchocercal skin disease among those affected near the Ofiki and Oyan Rivers in western Nigeria. Soc Sci Med 47: 841-852.

Briggs CA, McKenna DG, & Piattoni-Kaplan M (1995). Human alpha 7 nicotinic acetylcholine receptor responses to novel ligands. Neuropharmacology 34: 583-590.

Broer S (2010). Xenopus laevis Oocytes. Methods Mol Biol 637: 295-310.

Brooker S (2010). Estimating the global distribution and disease burden of intestinal nematode infections: adding up the numbers – a review. Int J Parasitol 40: 113-1144.

Brown LA, Jones AK, Buckingham SD, Mee CJ, & Sattelle DB (2006). Contributions from Caenorhabditis elegans functional genetics to antiparasitic drug target identification and validation: nicotinic acetylcholine receptors, a case study. Int J Parasitol 36: 617-624.

Browne SG (1960). The role of Onchocerca volvulus in lymphadenopathy and associated conditions. Cent Afr J Med 6: 302-306.

Bschleipfer T, Schukowski K, Weidner W, Grando SA, Schwantes U, Kummer W, *et al.* (2007). Expression and distribution of cholinergic receptors in the human urothelium. Life Sci 80: 2303–2307.

Buckingham SD, Pym L, & Sattelle DB (2006). Oocytes as an expression system for studying receptor/channel targets of drugs and pesticides. Methods Mol Biol 322: 331-345.

Bulman CA, Bidlow CM, Lustigman S, Cho-Ngwa F, Williams D, Rascon AA, Jr., *et al.* (2015). Repurposing auranofin as a lead candidate for treatment of lymphatic filariasis and onchocerciasis. PLoS Negl Trop Dis 9: e0003534.

Burg RW, Miller BM, Baker EE, Birnbaum J, Currie SA, Hartman R, *et al.* (1979). Avermectins, new family of potent anthelmintic agents: producing organism and fermentation. Antimicrob Agents Chemother 15: 361-367.

Burnham G (1998). Onchocerciasis. Lancet 351: 1341-1346.

Buxton SK, Charvet CL, Neveu C, Cabaret J, Cortet J, Peineau N, *et al.* (2014). Investigation of acetylcholine receptor diversity in a nematode parasite leads to characterization of tribendimidine- and derquantel-sensitive nAChRs. PLoS Pathog 10: e1003870.

Castro GA (1996). Helminths: Structure, Classification, Growth, and Development. In Medical Microbiology. ed Baron S.: Galveston (TX).

Chan MS (1997). The global burden of intestinal nematode infections--fifty years on. Parasitol Today 13: 438-443.

Changeux JP (2012). The nicotinic acetylcholine receptor: the founding father of the pentameric ligand-gated ion channel superfamily. J Biol Chem 287: 40207-40215.

Changeux JP, Bessis A, Bourgeois JP, Corringer PJ, Devillers-Thiery A, Eisele JL, *et al.* (1996). Nicotinic receptors and brain plasticity. Cold Spring Harb Symp Quant Biol 61: 343-362.

Chen L (2010). In pursuit of the high-resolution structure of nicotinic acetylcholine receptors. J Physiol 588: 557–564.

Choe H, & Sackin H (1997). Improved preparation of Xenopus oocytes for patch-clamp recording. Pflugers Arch 433: 648-652.

Cho-Ngwa F, Abongwa M, Ngemenya MN, & Nyongbela KD (2010). Selective activity of extracts of Margaritaria discoidea and Homalium africanum on Onchocerca ochengi. BMC Complement Altern Med 10: 62.

Cho-Ngwa F, Monya E, Azantsa BK, Manfo FP, Babiaka SB, Mbah JA, *et al.* (2016). Filaricidal activities on Onchocerca ochengi and Loa loa, toxicity and phytochemical screening of extracts of Tragia benthami and Piper umbellatum. BMC Complement Altern Med 16: 326.

Coles GC (2005). Anthelmintic resistance--looking to the future: a UK perspective. Res Vet Sci 78: 99-108.

Coles GC, Jackson F, Pomroy WE, Prichard RK, von Samson-Himmelstjerna G, Silvestre A, *et al.* (2006). The detection of anthelmintic resistance in nematodes of veterinary importance. Vet Parasitol 136: 167-185.

Collins T, & Millar NS (2010). Nicotinic acetylcholine receptor transmembrane mutations convert ivermectin from a positive to a negative allosteric modulator. Mol Pharmacol 78: 198-204.

Comley JC, Townson S, Rees MJ, & Dobinson A (1989). The further application of MTT-formazan colorimetry to studies on filarial worm viability. Trop Med Parasitol 40: 311-316.

Connolly CN, & Wafford KA (2004). The Cys-loop superfamily of ligand-gated ion channels: the impact of receptor structure on function. Biochem Soc Trans 32: 529-534.

Connor DH, & Palmieri JR (1985). Blackfly bites, onchocerciasis and leopard skin. Trans R Soc Trop Med Hyg 79: 415-417.

Conway DP (1964). Variance in the Effectiveness of Thiabendazole against Haemonchus Contortus in Sheep. Am J Vet Res 25: 844-846.

Coreil J, Mayard G, Louis-Charles J, & Addiss D (1998). Filarial elephantiasis among Haitian women: social context and behavioural factors in treatment. Trop Med Int Health 3: 467-473.

Cornwell RL, & Blore MA (1970). Anthelmintic activity of pyrantel and morantel against adult and larval stages of Nippostrongylus brasiliensis and Nematospiroides dubius. Ann Trop Med Parasitol 64: 525-531.

Corringer PJ, Bertrand S, Galzi JL, Devillers-Thiery A, Changeux JP, & Bertrand D (1999a). Molecular basis of the charge selectivity of nicotinic acetylcholine receptor and related ligand-gated ion channels. Novartis Found Symp 225: 215-224. discussion 224-230

Corringer PJ, Bertrand S, Galzi JL, Devillers-Thiery A, Changeux JP, Bertrand D (1999b). Mutational analysis of the charge selectivity filter of the alpha7 nicotinic acetylcholine receptor. Neuron 22: 831-843.

Cory AH, Owen TC, Barltrop JA, & Cory JG (1991). Use of an aqueous soluble tetrazolium/formazan assay for cell growth assays in culture. Cancer Commun 3: 207-212.

Courtot E, Charvet CL, Beech RN, Harmache A, Wolstenholme AJ, Holden-Dye L, *et al.* (2015). Functional Characterization of a Novel Class of Morantel-Sensitive Acetylcholine Receptors in Nematodes. PLoS Pathog 11: e1005267.

Couturier S, Bertrand D, Matter JM, Hernandez MC, Bertrand S, Millar N, *et al.* (1990). A neuronal nicotinic acetylcholine receptor subunit (alpha 7) is developmentally regulated and forms a homo-oligomeric channel blocked by alpha-BTX. Neuron 5: 847-856.

Crisford A, Ebbinghaus-Kintscher U, Schoenhense E, Harder A, Raming K, O'Kelly I, *et al.* (2015). The Cyclooctadepsipeptide Anthelmintic Emodepside Differentially Modulates Nematode, Insect and Human Calcium-Activated Potassium (SLO) Channel Alpha Subunits. PLoS Negl Trop Dis 9: e0004062.

Crompton DW (1988). The prevalence of Ascariasis. Parasitol Today 4: 162-169.

Crump A, & Omura S (2011). Ivermectin, 'wonder drug' from Japan: the human use perspective. Proc Jpn Acad Ser B Phys Biol Sci 87: 13-28.

Culetto E, Baylis HA, Richmond JE, Jones AK, Fleming JT, Squire MD, *et al.* (2004). The Caenorhabditis elegans unc-63 gene encodes a levamisole-sensitive nicotinic acetylcholine receptor alpha subunit. J Biol Chem 279: 42476-42483.

Cully DF, Vassilatis DK, Liu KK, Paress PS, Van der Ploeg LH, Schaeffer JM, *et al.* (1994). Cloning of an avermectin-sensitive glutamate-gated chloride channel from Caenorhabditis elegans. Nature 371: 707-711.

Cupp EW, Sauerbrey M, & Richards F (2011). Elimination of human onchocerciasis: history of progress and current feasibility using ivermectin (Mectizan((R))) monotherapy. Acta Trop 120 Suppl 1: S100-108.

Curtis MJ, Bond RA, Spina D, Ahluwalia A, Alexander SP, Giembycz MA, *et al*. (2015). Experimental design and analysis and their reporting: new guidance for publication in BJP. Br J Pharmacol 172: 3461-3471.

Dale VM, & Martin RJ (1995). Oxantel-activated single channel currents in the muscle membrane of Ascaris suum. Parasitology 110 (Pt 4): 437-448.

Dascal N (1987). The use of Xenopus oocytes for the study of ion channels. CRC Crit Rev Biochem 22: 317-387.

Dascal N (2001). Voltage clamp recordings from Xenopus oocytes. Curr Protoc Neurosci Chapter 6: Unit 6 12.

Davies HG, & Green RH (1986). Avermectins and milbemycins. Nat Prod Rep 3: 87-121.

Davies JB (1994). Sixty years of onchocerciasis vector control: a chronological summary with comments on eradication, reinvasion, and insecticide resistance. Annu Rev Entomol 39: 23-45.

de Silva NR, Brooker S, Hotez PJ, Montresor A, Engels D, & Savioli L (2003). Soil-transmitted helminth infections: updating the global picture. Trends Parasitol 19: 547-551.

de Souza DK, Koudou B, Kelly-Hope LA, Wilson MD, Bockarie MJ, & Boakye DA (2012). Diversity and transmission competence in lymphatic filariasis vectors in West Africa, and the implications for accelerated elimination of Anopheles-transmitted filariasis. Parasit Vectors 5: 259.

Debell JT, Delcastillo J, & Sanchez V (1963). Electrophysiology of the Somatic Muscle Cells of Ascaris Lumbricoides. J Cell Comp Physiol 62: 159-177.

del Castillo J, Rivera A, Solorzano S, & Serrato J (1989). Some aspects of the neuromuscular system of Ascaris. Q J Exp Physiol 74: 1071-1087.

Denham DA, & Fletcher C (1987). The cat infected with Brugia pahangi as a model of human filariasis. Ciba Found Symp 127: 225-235.

DiMasi JA, Hansen RW, & Grabowski HG (2003). The price of innovation: new estimates of drug development costs. J Health Econ 22: 151-185.

Dineley KT, Pandya AA, & Yakel JL (2015). Nicotinic ACh receptors as therapeutic targets in CNS disorders. Trends Pharmacol Sci 36: 96-108.

Ducray P, Gauvry N, Pautrat F, Goebel T, Fruechtel J, Desaules Y, *et al.* (2008). Discovery of amino-acetonitrile derivatives, a new class of synthetic anthelmintic compounds. Bioorg Med Chem Lett 18: 2935-2938.

Duguet TB, Charvet CL, Forrester SG, Wever CM, Dent JA, Neveu C, *et al.* (2016). Recent Duplication and Functional Divergence in Parasitic Nematode Levamisole-Sensitive Acetylcholine Receptors. PLoS Negl Trop Dis 10: e0004826.

Duke BO (1972). Onchocerciasis. Br Med Bull 28: 66-71.

Dumont JN (1972). Oogenesis in Xenopus laevis (Daudin). I. Stages of oocyte development in laboratory maintained animals. J Morphol 136: 153-179.

Dwoskin LP, Smith AM, Wooters TE, Zhang Z, Crooks PA, & Bardo MT (2009). Nicotinic receptor-based therapeutics and candidates for smoking cessation. Biochem Pharmacol 78: 732-743.

Edgar RC (2004). MUSCLE: a multiple sequence alignment method with reduced time and space complexity. BMC Bioinformatics 5: 113.

Eimer S, Gottschalk A, Hengartner M, Horvitz HR, Richmond J, Schafer WR, *et al.* (2007). Regulation of nicotinic receptor trafficking by the transmembrane Golgi protein UNC-50. EMBO J 26: 4313-4323.

Eisenbarth A, Achukwi MD, & Renz A (2016). Ongoing Transmission of Onchocerca volvulus after 25 Years of Annual Ivermectin Mass Treatments in the Vina du Nord River Valley, in North Cameroon. PLoS Negl Trop Dis 10: e0004392.

Elgoyhen AB, Johnson DS, Boulter J, Vetter DE, & Heinemann S (1994). Alpha 9: an acetylcholine receptor with novel pharmacological properties expressed in rat cochlear hair cells. Cell 79: 705-715.

Elkins DB, Haswell-Elkins M, & Anderson RM (1986). The epidemiology and control of intestinal helminths in the Pulicat Lake region of Southern India. I. Study design and pre- and post-treatment observations on Ascaris lumbricoides infection. Trans R Soc Trop Med Hyg 80: 774-792.

Elkins DB, Haswell-Elkins M, & Anderson RM (1988). The importance of host age and sex to patterns of reinfection with Ascaris lumbricoides following mass anthelmintic treatment in a South Indian fishing community. Parasitology 96 (Pt 1): 171-184.

Enk CD (2006). Onchocerciasis--river blindness. Clin Dermatol 24: 176-180.

Enk CD, Gardlo K, Ruzicka T, & BenEzra D (2003). [Onchocerciasis]. Hautarzt 54: 513-517.

Etya'ale D (2002). Eliminating onchocerciasis as a public health problem: the beginning of the end. Br J Ophthalmol 86: 844-846.

Evans AM, & Martin RJ (1996). Activation and cooperative multi-ion block of single nicotinic-acetylcholine channel currents of Ascaris muscle by the tetrahydropyrimidine anthelmintic, morantel. Br J Pharmacol 118: 1127-1140.

Evans T, & Chapple N (2002). The animal health market. Nat Rev Drug Discov 1: 937-938.

Farnsworth NR (1990). The role of ethnopharmacology in drug development. Ciba Found Symp 154: 2-11; discussion 11-21.

Farnsworth NR, Akerele O, Bingel AS, Soejarto DD, & Guo Z (1985). Medicinal plants in therapy. Bull World Health Organ 63: 965-981.

Fauvin A, Charvet C, Issouf M, Cortet J, Cabaret J, & Neveu C (2010). cDNA–AFLP analysis in levamisole-resistant Haemonchus contortus reveals alternative splicing in a nicotinic acetylcholine receptor subunit. Mol Biochem Parasitol 170: 105-107.

Feasey N, Wansbrough-Jones M, Mabey DC, & Solomon AW (2010). Neglected tropical diseases. Br Med Bull 93: 179-200.

Felippelli G, Lopes WD, Cruz BC, Teixeira WF, Maciel WG, Favero FC, *et al.* (2014). Nematode resistance to ivermectin (630 and 700mug/kg) in cattle from the Southeast and South of Brazil. Parasitol Int 63: 835-840.

Fenwick A (2012). The global burden of neglected tropical diseases. Public Health 126: 233-236.

Fernandez MC, Verghese S, Bhuvaneswari R, Elizabeth SJ, Mathew T, Anitha A, *et al.* (2002). A comparative study of the intestinal parasites prevalent among children living in rural and urban settings in and around Chennai. J Commun Dis 34: 35-39.

Fitzpatrick JL (2013). Global food security: the impact of veterinary parasites and parasitologists. Vet Parasitol 195: 233-248.

Fleming JT, Squire MD, Barnes TM, Tornoe C, Matsuda K, Ahnn J, *et al.* (1997). Caenorhabditis elegans levamisole resistance genes lev-1, unc-29, and unc-38 encode functional nicotinic acetylcholine receptor subunits. J Neurosci 17: 5843-5857.

Francis MM, Evans SP, Jensen M, Madsen DM, Mancuso J, Norman KR, *et al.* (2005). The Ror receptor tyrosine kinase CAM-1 is required for ACR-16-mediated synaptic transmission at the C. elegans neuromuscular junction. Neuron 46: 581-594.

Gardon J, Gardon-Wendel N, Demanga N, Kamgno J, Chippaux JP, & Boussinesq M (1997). Serious reactions after mass treatment of onchocerciasis with ivermectin in an area endemic for Loa loa infection. Lancet 350: 18-22.

Geary TG (2005). Ivermectin 20 years on: maturation of a wonder drug. Trends Parasitol 21: 530-532.

Geerts S, & Gryseels B (2000). Drug resistance in human helminths: current situation and lessons from livestock. Clin Microbiol Rev 13: 207-222.

Geerts S, & Gryseels B (2001). Anthelmintic resistance in human helminths: a review. Trop Med Int Health 6: 915-921.

Gerzanich V, Anand R, & Lindstrom J (1994). Homomers of alpha 8 and alpha 7 subunits of nicotinic receptors exhibit similar channel but contrasting binding site properties. Mol Pharmacol 45: 212-220.

Geurden T, Hodge A, Noe L, Winstanley D, Bartley DJ, Taylor M, *et al.* (2012). The efficacy of a combined oral formulation of derquantel-abamectin against anthelmintic resistant gastro-intestinal nematodes of sheep in the UK. Vet Parasitol 189: 308-316.

Gilleard JS (2006). Understanding anthelmintic resistance: the need for genomics and genetics. Int J Parasitol 36: 1227-1239.

Githiori JB, Athanasiadou S, & Thamsborg SM (2006). Use of plants in novel approaches for control of gastrointestinal helminths in livestock with emphasis on small ruminants. Vet Parasitol 139: 308-320.

Githiori JB, Hoglund J, & Waller PJ (2005). Ethnoveterinary plant preparations as livestock dewormers: practices, popular beliefs, pitfalls and prospects for the future. Anim Health Res Rev 6: 91-103.

Githiori JB, Hoglund J, Waller PJ, & Baker RL (2004). Evaluation of anthelmintic properties of some plants used as livestock dewormers against Haemonchus contortus infections in sheep. Parasitology 129: 245-253.

Gopalakrishnan M, Bertrand D, & Williams M (2007). Nicotinic acetylcholine receptors as therapeutic targets: emerging frontiers in basic research and clinical science. Biochem Pharmacol 74: 1091.

Gouy M, Guindon S, Gascuel O (2010). SeaView version 4: a multiplatform graphical user interface for sequence alignment and phylogenetic tree building. Mol Biol Evol 27: 221–224.

Greco WR, Faessel H, & Levasseur L (1996). The search for cytotoxic synergy between anticancer agents: a case of Dorothy and the ruby slippers? J Natl Cancer Inst 88: 699-700.

Greenberg RM (2014). Ion channels and drug transporters as targets for anthelmintics. Curr Clin Microbiol Rep 1: 51-60.

Guan B, Chen X, & Zhang H (2013). Two-electrode voltage clamp. Methods Mol Biol 998: 79-89.

Guest M, Bull K, Walker RJ, Amliwala K, O'Connor V, Harder A, *et al.* (2007). The calcium-activated potassium channel, SLO-1, is required for the action of the novel cyclo-octadepsipeptide anthelmintic, emodepside, in Caenorhabditis elegans. Int J Parasitol 37: 1577-1588.

Gurdon JB, Lane CD, Woodland HR, & Marbaix G (1971). Use of frog eggs and oocytes for the study of messenger RNA and its translation in living cells. Nature 233: 177-182.

Gustavsen K, Hopkins A, & Sauerbrey M (2011). Onchocerciasis in the Americas: from arrival to (near) elimination. Parasit Vectors 4: 205.

Gyapong JO, Kumaraswami V, Biswas G, & Ottesen EA (2005). Treatment strategies underpinning the global programme to eliminate lymphatic filariasis. Expert Opin Pharmacother 6: 179-200.

Gyapong M, Gyapong JO, Adjei S, Vlassoff C, & Weiss M (1996). Filariasis in northern Ghana: some cultural beliefs and practices and their implications for disease control. Soc Sci Med 43: 235-242.

Gyorkos TW, Maheu-Giroux M, Casapia M, Joseph SA, & Creed-Kanashiro H (2011). Stunting and helminth infection in early preschool-age children in a resource-poor community in the Amazon lowlands of Peru. Trans R Soc Trop Med Hyg 105: 204-208.

Halevi S, McKay J, Palfreyman M, Yassin L, Eshel M, Jorgensen E, *et al.* (2002). The C. elegans ric-3 gene is required for maturation of nicotinic acetylcholine receptors. EMBO J 21: 1012-1020.

Harder A, & von Samson-Himmelstjerna G (2001). Activity of the cyclic depsipeptide emodepside (BAY 44-4400) against larval and adult stages of nematodes in rodents and the influence on worm survival. Parasitol Res 87: 924-928.

Harder A, Holden-Dye L, Walker R, & Wunderlich F (2005). Mechanisms of action of emodepside. Parasitol Res 97 Suppl 1: S1-10.

Harder A, Schmitt-Wrede HP, Krucken J, Marinovski P, Wunderlich F, Willson J, *et al.* (2003). Cyclooctadepsipeptides--an anthelmintically active class of compounds exhibiting a novel mode of action. Int J Antimicrob Agents 22: 318-331.

Harnett W (2002). DNA-based detection of onchocerca volvulus. Trans R Soc Trop Med Hyg 96 Suppl 1: S231-234.

Harrison RA, Holt D, Pattison DJ, & Elton PJ (2004). Who and how many people are taking herbal supplements? A survey of 21,923 adults. Int J Vitam Nutr Res 74: 183-186.

Haswell-Elkins M, Elkins D, & Anderson RM (1989). The influence of individual, social group and household factors on the distribution of Ascaris lumbricoides within a community and implications for control strategies. Parasitology 98 (Pt 1): 125-134.

Haugstetter J, Blicher T, & Ellgaard L (2005). Identification and characterization of a novel thioredoxin-related transmembrane protein of the endoplasmic reticulum. J Biol Chem 280: 8371-8380.

Hewitson JP, Maizels RM (2014). Vaccination against helminth parasite infections. Expert Rev Vaccines 13: 473-487.

Hibbs RE, & Gouaux E (2011). Principles of activation and permeation in an anion-selective Cys-loop receptor. Nature 474: 54-60.

Hoenigl M, Valentin T, Zollner-Schwetz I, Salzer HJ, Raggam RB, Strenger V, *et al.* (2010). Pulmonary ascariasis: two cases in Austria and review of the literature. Wien Klin Wochenschr 122 Suppl 3: 94-96.

Hoerauf A, Adjei O, & Buttner DW (2002). Antibiotics for the treatment of onchocerciasis and other filarial infections. Curr Opin Investig Drugs 3: 533-537.

Hoerauf A, Mand S, Fischer K, Kruppa T, Marfo-Debrekyei Y, Debrah AY, *et al.* (2003). Doxycycline as a novel strategy against bancroftian filariasis-depletion of Wolbachia endosymbionts from Wuchereria bancrofti and stop of microfilaria production. Med Microbiol Immunol 192: 211-216.

Hoerauf A, Specht S, Buttner M, Pfarr K, Mand S, Fimmers R, *et al.* (2008). Wolbachia endobacteria depletion by doxycycline as antifilarial therapy has macrofilaricidal activity in onchocerciasis: a randomized placebo-controlled study. Med Microbiol Immunol 197: 295-311.

Hoerauf A, Specht S, Marfo-Debrekyei Y, Buttner M, Debrah AY, Mand S, *et al.* (2009). Efficacy of 5-week doxycycline treatment on adult Onchocerca volvulus. Parasitol Res 104: 437-447.

Hofmann K, & Stoffel W (1993). TMbase – a database of membrane spanning proteins segments. Biol Chem Hoppe Seyler 374: 166.

Holden-Dye L, & Walker RJ (1990). Avermectin and avermectin derivatives are antagonists at the 4-aminobutyric acid (GABA) receptor on the somatic muscle cells of Ascaris; is this the site of anthelmintic action? Parasitology 101 Pt 2: 265-271.

Holden-Dye L, & Walker RJ (2007). Anthelmintic drugs. WormBook: 1-13.

Holden-Dye L, Joyner M, O'Connor V, & Walker RJ (2013). Nicotinic acetylcholine receptors: a comparison of the nAChRs of Caenorhabditis elegans and parasitic nematodes. Parasitol Int 62: 606-615.

Holden-Dye L, O'Connor V, Hopper NA, Walker RJ, Harder A, Bull K, *et al.* (2007). SLO, SLO, quick, quick, slow: calcium-activated potassium channels as regulators of Caenorhabditis elegans behaviour and targets for anthelmintics. Invert Neurosci 7: 199-208.

Hollman A (1996). Drugs for atrial fibrillation. Digoxin comes from Digitalis lanata. BMJ 312: 912.

Hopkins AD (2005). Ivermectin and onchocerciasis: is it all solved? Eye (Lond) 19: 1057-1066.

Hopla CE, Durden LA, & Keirans JE (1994). Ectoparasites and classification. Rev Sci Tech 13: 985-1017.

Hotez P, Ottesen E, Fenwick A, & Molyneux D (2006). The neglected tropical diseases: the ancient afflictions of stigma and poverty and the prospects for their control and elimination. Adv Exp Med Biol 582: 23-33.

Hotez PJ (2007). Control of onchocerciasis--the next generation. Lancet 369: 1979-1980.

Hotez PJ, & Kamath A (2009). Neglected tropical diseases in sub-saharan Africa: review of their prevalence, distribution, and disease burden. PLoS Negl Trop Dis 3: e412.

Hotez PJ, Brindley PJ, Bethony JM, King CH, Pearce EJ, & Jacobson J (2008). Helminth infections: the great neglected tropical diseases. J Clin Invest 118: 1311-1321.

Hotez PJ, Fenwick A, Savioli L, & Molyneux DH (2009). Rescuing the bottom billion through control of neglected tropical diseases. Lancet 373: 1570-1575.

Hotez PJ, Molyneux DH, Fenwick A, Kumaresan J, Sachs SE, Sachs JD, *et al.* (2007). Control of neglected tropical diseases. N Engl J Med 357: 1018-1027.

Howes HL, Jr., & Lynch JE (1967). Anthelmintic studies with pyrantel. I. Therapeutic and prophylactic efficacy against the enteral stages of various helminths in mice and dogs. J Parasitol 53: 1085-1091.

Hu Y, Xiao SH, & Aroian RV (2009). The new anthelmintic tribendimidine is an L-type (levamisole and pyrantel) nicotinic acetylcholine receptor agonist. PLoS Negl Trop Dis 3: e499.

Hughes RG, Sharp DS, Hughes MC, Akau'ola S, Heinsbroek P, Velayudhan R, *et al.* (2004). Environmental influences on helminthiasis and nutritional status among Pacific schoolchildren. Int J Environ Health Res 14: 163-177.

Isah OA, Okunade SA, Aderinboye RY, & Olafadehan OA (2015). Effect of browse plant foliage supplementation on the performance of buckling goats fed threshed sorghum top basal diet. Trop Anim Health Prod 47: 1027-1032.

Jabbar A, Iqbal Z, Kerboeuf D, Muhammad G, Khan MN, & Afaq M (2006). Anthelmintic resistance: the state of play revisited. Life Sci 79: 2413-2431.

James CE, Hudson AL, & Davey MW (2009). Drug resistance mechanisms in helminths: is it survival of the fittest? Trends Parasitol 25: 328-335.

Jin T (2010). Near-infrared fluorescence detection of acetylcholine in aqueous solution using a complex of rhodamine 800 and p-sulfonatocalix[8]arene. Sensors (Basel) 10: 2438-2449.

Johnston KL, Ford L, & Taylor MJ (2014). Overcoming the challenges of drug discovery for neglected tropical diseases: the A.WOL experience. J Biomol Screen 19: 335-343.

Jones AK, Davis P, Hodgkin J, & Sattelle DB (2007). The nicotinic acetylcholine receptor gene family of the nematode Caenorhabditis elegans: an update on nomenclature. Invert Neurosci 7: 129-131.

Kalamida D, Poulas K, Avramopoulou V, Fostieri E, Lagoumintzis G, Lazaridis K, *et al.* (2007). Muscle and neuronal nicotinic acetylcholine receptors. Structure, function and pathogenicity. FEBS J 274: 3799-3845.

Kalappa BI, & Uteshev VV (2013). The dual effect of PNU-120596 on alpha7 nicotinic acetylcholine receptor channels. Eur J Pharmacol 718: 226-234.

Kale OO (1998). Onchocerciasis: the burden of disease. Ann Trop Med Parasitol 92 Suppl 1: S101-115.

Kaminsky R, Ducray P, Jung M, Clover R, Rufener L, Bouvier J, *et al.* (2008a). A new class of anthelmintics effective against drug-resistant nematodes. Nature 452: 176-180.

Kaminsky R, Gauvry N, Schorderet Weber S, Skripsky T, Bouvier J, Wenger A, *et al.* (2008b). Identification of the amino-acetonitrile derivative monepantel (AAD 1566) as a new anthelmintic drug development candidate. Parasitol Res 103: 931-939.

Kao PN, Dwork AJ, Kaldany RR, Silver ML, Wideman J, Stein S, *et al*. (1984). Identification of the alpha subunit half-cystine specifically labeled by an affinity reagent for the acetylcholine receptor binding site. J Biol Chem 259: 11662-11665.

Kaplan RM (2004). Drug resistance in nematodes of veterinary importance: a status report. Trends Parasitol 20: 477-481.

Kaplan RM, & Vidyashankar AN (2012). An inconvenient truth: global worming and anthelmintic resistance. Vet Parasitol 186: 70-78.

Karam M, & Ottesen E (2000). [The control of lymphatic filariasis]. Med Trop (Mars) 60: 291-296.

Karlin A (1993). Structure of nicotinic acetylcholine receptors. Curr Opin Neurobiol 3: 299-309.

Karlin A (2002). Emerging structure of the nicotinic acetylcholine receptors. Nat Rev Neurosci 3: 102-114.

Katabarwa MN, Eyamba A, Nwane P, Enyong P, Kamgno J, Kuete T, *et al.* (2013). Fifteen years of annual mass treatment of onchocerciasis with ivermectin have not interrupted transmission in the west region of cameroon. J Parasitol Res 2013: 420928.

Katabarwa MN, Eyamba A, Nwane P, Enyong P, Yaya S, Baldiagai J, *et al*. (2011). Seventeen years of annual distribution of ivermectin has not interrupted onchocerciasis transmission in North Region, Cameroon. Am J Trop Med Hyg 85: 1041-1049.

Kawashima K, & Fujii T (2008). Basic and clinical aspects of non-neuronal acetylcholine: overview of non-neuronal cholinergic systems and their biological significance. J Pharmacol Sci 106: 167-173.

Keiser J, Shu-Hua X, Chollet J, Tanner M, & Utzinger J (2007). Evaluation of the in vivo activity of tribendimidine against Schistosoma mansoni, Fasciola hepatica, Clonorchis sinensis, and Opisthorchis viverrini. Antimicrob Agents Chemother 51: 1096-1098.

Kerr KB, & Cavett JW (1952). A technic for initial evaluation of potential anthelmintics. *Exp Parasitol* 1: 161-167.

Kisangau DP, Hosea KM, Joseph CC, & Lyaruu HV (2007). In vitro antimicrobial assay of plants used in traditional medicine in Bukoba Rural district, Tanzania. Afr J Tradit Complement Altern Med 4: 510-523.

Kotze AC, Hunt PW, Skuce P, von Samson-Himmelstjerna G, Martin RJ, Sager H, *et al.* (2014). Recent advances in candidate-gene and whole-genome approaches to the discovery of anthelmintic resistance markers and the description of drug/receptor interactions. Int J Parasitol Drugs Drug Resist 4: 164-184.

Krause RM, Buisson B, Bertrand S, Corringer PJ, Galzi JL, Changeux JP, *et al.* (1998). Ivermectin: a positive allosteric effector of the alpha7 neuronal nicotinic acetylcholine receptor. Mol Pharmacol 53: 283-294.

Krucken J, Harder A, Jeschke P, Holden-Dye L, O'Connor V, Welz C, *et al.* (2012). Anthelmintic cyclcooctadepsipeptides: complex in structure and mode of action. Trends Parasitol 28: 385-394.

Krueger A, Fischer P, & Morales-Hojas R (2007). Molecular phylogeny of the filaria genus Onchocerca with special emphasis on Afrotropical human and bovine parasites. Acta Trop 101: 1-14.

Kulke D, Krucken J, Demeler J, Harder A, Mehlhorn H, & von Samson-Himmelstjerna G (2013a). In vitro efficacy of cyclooctadepsipepdtides and aminophenylamidines alone and in combination against third-stage larvae and adult worms of Nippostrongylus brasiliensis and first-stage larvae of Trichinella spiralis. Parasitol Res 112: 335-345.

Kulke D, Krucken J, Harder A, & von Samson-Himmelstjerna G (2014). Efficacy of cyclooctadepsipeptides and aminophenylamidines against larval, immature and mature adult stages of a parasitologically characterized trichurosis model in mice. PLoS Negl Trop Dis 8: e2698.

Kulke D, Krucken J, Harder A, Krebber R, Fraatz K, Mehlhorn H, *et al.* (2013b). In vivo efficacy of PF1022A and nicotinic acetylcholine receptor agonists alone and in combination against Nippostrongylus brasiliensis. Parasitology 140: 1252-1265.

Kulke D, Krucken J, Welz C, von Samson-Himmelstjerna G, & Harder A (2012). In vivo efficacy of the anthelmintic tribendimidine against the cestode Hymenolepis microstoma in a controlled laboratory trial. Acta Trop 123: 78-84.

Lacey E (1990). Mode of action of benzimidazoles. Parasitol Today 6: 112-115.

Lamorde M, Tabuti JR, Obua C, Kukunda-Byobona C, Lanyero H, Byakika-Kibwika P, *et al*. (2010). Medicinal plants used by traditional medicine practitioners for the treatment of HIV/AIDS and related conditions in Uganda. J Ethnopharmacol 130: 43-53.

Leathwick DM (2012). Modelling the benefits of a new class of anthelmintic in combination. Vet Parasitol 186: 93-100.

Leathwick DM, Hosking BC, Bisset SA, & McKay CH (2009). Managing anthelmintic resistance: is it feasible in New Zealand to delay the emergence of resistance to a new anthelmintic class? N Z Vet J 57: 181-192.

Lecova L, Stuchlikova L, Prchal L, & Skalova L (2014). Monepantel: the most studied new anthelmintic drug of recent years. Parasitology 141: 1686-1698.

Lee BH, Clothier MF, Dutton FE, Nelson SJ, Johnson SS, Thompson DP, *et al.* (2002). Marcfortine and paraherquamide class of anthelmintics: discovery of PNU-141962. Curr Top Med Chem 2: 779-793.

Lee DL (1996). Why do some nematode parasites of the alimentary tract secrete acetylcholinesterase? Int J Parasitol 26: 499-508.

Li SX, Huang S, Bren N, Noridomi K, Dellisanti CD, Sine SM, *et al*. (2011). Ligand-binding domain of an alpha7-nicotinic receptor chimera and its complex with agonist. *Nat Neurosci* 14: 1253-1259.

Li Z, Liu J, Zheng M, & Xu XZ (2014). Encoding of both analog- and digital-like behavioral outputs by one C. elegans interneuron. Cell 159: 751-765.

Liang JL, King JD, Ichimori K, Handzel T, Pa'au M, & Lammie PJ (2008). Impact of five annual rounds of mass drug administration with diethylcarbamazine and albendazole on Wuchereria bancrofti infection in American Samoa. Am J Trop Med Hyg 78: 924-928.

Lin-Moshier Y, & Marchant JS (2013). The Xenopus oocyte: a single-cell model for studying Ca2+ signaling. Cold Spring Harb Protoc 2013.

Little PR, Hodge A, Maeder SJ, Wirtherle NC, Nicholas DR, Cox GG, *et al.* (2011). Efficacy of a combined oral formulation of derquantel-abamectin against the adult and larval stages of nematodes in sheep, including anthelmintic-resistant strains. Vet Parasitol 181: 180-193.

Littleton JT, & Ganetzky B (2000). Ion channels and synaptic organization: analysis of the Drosophila genome. Neuron 26: 35-43.

Lloberas M, Alvarez L, Entrocasso C, Virkel G, Ballent M, Mate L, *et al.* (2013). Comparative tissue pharmacokinetics and efficacy of moxidectin, abamectin and ivermectin in lambs infected with resistant nematodes: Impact of drug treatments on parasite P-glycoprotein expression. Int J Parasitol Drugs Drug Resist 3: 20-27.

Luong TV (2003). De-worming school children and hygiene intervention. Int J Environ Health Res 13 Suppl 1: S153-159.

Lustigman S, & McCarter JP (2007). Ivermectin resistance in Onchocerca volvulus: toward a genetic basis. PLoS Negl Trop Dis 1: e76.

Mackenzie C, Geary T, Prichard R, & Boussinesq M (2007). Where next with Loa loa encephalopathy? Data are badly needed. Trends Parasitol 23: 237-238.

Mak JW (1987). Epidemiology of lymphatic filariasis. Ciba Found Symp 127: 5-14.

Makepeace BL, & Tanya VN (2016). 25 Years of the Onchocerca ochengi Model. Trends Parasitol 32: 966-978.

Malatt AE, & Taylor HR (1992). Onchocerciasis. Infect Dis Clin North Am 6: 963-977.

Marcellino C, Gut J, Lim KC, Singh R, McKerrow J, & Sakanari J (2012). WormAssay: a novel computer application for whole-plate motion-based screening of macroscopic parasites. PLoS Negl Trop Dis 6: e1494.

Markovich D (2008). Expression cloning and radiotracer uptakes in Xenopus laevis oocytes. Nat Protoc 3: 1975-1980.

Martin RJ (1997). Modes of action of anthelmintic drugs. Vet J 154: 11-34.

Martin RJ, & Kusel JR (1992). On the distribution of a fluorescent ivermectin probe (4" 5,7 dimethyl-bodipy proprionylivermectin) in Ascaris membranes. Parasitology 104 (Pt 3): 549-555.

Martin RJ, & Robertson AP (2007). Mode of action of levamisole and pyrantel, anthelmintic resistance, E153 and Q57. Parasitology 134: 1093-1104.

Martin RJ, & Robertson AP (2010). Control of nematode parasites with agents acting on neuro-musculature systems: lessons for neuropeptide ligand discovery. Adv Exp Med Biol 692: 138-154.

Martin RJ, Buxton SK, Neveu C, Charvet CL, & Robertson AP (2012a). Emodepside and SL0-1 potassium channels: a review. Exp Parasitol 132: 40-46.

Martin RJ, Clark CL, Trailovic SM, & Robertson AP (2004). Oxantel is an N-type (methyridine and nicotine) agonist not an L-type (levamisole and pyrantel) agonist: classification of cholinergic anthelmintics in Ascaris. Int J Parasitol 34: 1083-1090.

Martin RJ, Pennington AJ, Duittoz AH, Robertson S, & Kusel JR (1991). The physiology and pharmacology of neuromuscular transmission in the nematode parasite, Ascaris suum. Parasitology 102 Suppl: S41-58.

Martin RJ, Robertson AP, & Bjorn H (1997). Target sites of anthelmintics. Parasitology 114 Suppl: S111-124.

Martin RJ, Robertson AP, Buxton SK, Beech RN, Charvet CL, & Neveu C (2012b). Levamisole receptors: a second awakening. Trends Parasitol 28: 289-296.

Martin RJ, Verma S, Levandoski M, Clark CL, Qian H, Stewart M, *et al.* (2005). Drug resistance and neurotransmitter receptors of nematodes: recent studies on the mode of action of levamisole. Parasitology 131 Suppl: S71-84.

Martkoplishvili I, & Kvavadze E (2015). Some Popular Medicinal Plants and Diseases of the Upper Palaeolithic in Western Georgia. J Ethnopharmacol 166: 42-52.

McCormack TJ, Melis C, Colon J, Gay EA, Mike A, Karoly R, *et al*. (2010). Rapid desensitization of the rat alpha7 nAChR is facilitated by the presence of a proline residue in the outer beta-sheet. J Physiol 588 (Pt 22): 4415-4429.

McFarland JW, & Howes HL, Jr. (1972). Novel anthelmintic agents. 6. Pyrantel analogs with activity against whipworm. J Med Chem 15: 365-368.

McKay JP, Raizen DM, Gottschalk A, Schafer WR, & Avery L (2004). eat-2 and eat-18 are required for nicotinic neurotransmission in the Caenorhabditis elegans pharynx. Genetics 166: 161-169.

McKellar QA, & Benchaoui HA (1996). Avermectins and milbemycins. J Vet Pharmacol Ther 19: 331-351.

McKellar QA, & Scott EW (1990). The benzimidazole anthelmintic agents--a review. J Vet Pharmacol Ther 13: 223-247.

McKerrow JH (2005). Designing drugs for parasitic diseases of the developing world. PLoS Med 2: e210.

McMahon C, Bartley DJ, Edgar HW, Ellison SE, Barley JP, Malone FE *et al*. (2013). Anthelmintic resistance in Northern Ireland (I): prevalence of resistance in ovine gastrointestinal nematodes, as determined through faecal egg count reduction testing. Vet Parasitol 195: 122-130.

Melrose WD, Durrheim DD, & Burgess GW (2004). Update on immunological tests for lymphatic filariasis. Trends Parasitol 20: 255-257.

Miledi R, Parker I, & Sumikawa K (1982). Properties of acetylcholine receptors translated by cat muscle mRNA in Xenopus oocytes. EMBO J 1: 1307-1312.

Millar NS (2003). Assembly and subunit diversity of nicotinic acetylcholine receptors. Biochem Soc Trans 31: 869-874.

Millar NS, & Gotti C (2009). Diversity of vertebrate nicotinic acetylcholine receptors. Neuropharmacology 56: 237-246.

Miller AJ, & Zhou JJ (2000). Xenopus oocytes as an expression system for plant transporters. Biochim Biophys Acta 1465: 343-358.

Molyneux DH, Bradley M, Hoerauf A, Kyelem D, & Taylor MJ (2003). Mass drug treatment for lymphatic filariasis and onchocerciasis. Trends Parasitol 19: 516-522.

Mongan NP, Baylis HA, Adcock C, Smith GR, Sansom MS, & Sattelle DB (1998). An extensive and diverse gene family of nicotinic acetylcholine receptor alpha subunits in Caenorhabditis elegans. Receptors Channels 6: 213-228.

Mongan NP, Jones AK, Smith GR, Sansom MS, & Sattelle DB (2002). Novel alpha7-like nicotinic acetylcholine receptor subunits in the nematode Caenorhabditis elegans. Protein Sci 11: 1162-1171.

Morales-Hojas R, Cheke RA, & Post RJ (2006). Molecular systematics of five Onchocerca species (Nematoda: Filarioidea) including the human parasite, O. volvulus, suggest sympatric speciation. J Helminthol 80: 281-290.

Morgan S, Grootendorst P, Lexchin J, Cunningham C, & Greyson D (2011). The cost of drug development: a systematic review. Health Policy 100: 4-17.

Ndjonka D, Agyare C, Luersen K, Djafsia B, Achukwi D, Nukenine EN, *et al.* (2011). In vitro activity of Cameroonian and Ghanaian medicinal plants on parasitic (Onchocerca ochengi) and free-living (Caenorhabditis elegans) nematodes. J Helminthol 85: 304-312.

Nelson GS (1970). Onchocerciasis. Adv Parasitol 8: 173-224.

Nelson GS (1991). Human onchocerciasis: notes on the history, the parasite and the life cycle. Ann Trop Med Parasitol 85: 83-95.

Neveu C, Charvet CL, Fauvin A, Cortet J, Beech RN, & Cabaret J (2010). Genetic diversity of levamisole receptor subunits in parasitic nematode species and abbreviated transcripts associated with resistance. Pharmacogenet Genomics 20: 414-425.

Noordin R (2007). Lymphatic filariasis and the global elimination program. Malays J Med Sci 14: 1-3.

Norhayati M, Oothuman P, Azizi O, & Fatmah MS (1997). Efficacy of single dose albendazole on the prevalence and intensity of infection of soil-transmitted helminths in Orang Asli children in Malaysia. Southeast Asian J Trop Med Public Health 28: 563-569.

Nutman TB (2013). Insights into the pathogenesis of disease in human lymphatic filariasis. Lymphat Res Biol 11: 144-148.

Nwaka S, & Hudson A (2006). Innovative lead discovery strategies for tropical diseases. Nat Rev Drug Discov 5: 941-955.

Okulicz JF, Stibich AS, Elston DM, & Schwartz RA (2004). Cutaneous onchocercoma. Int J Dermatol 43: 170-172.

Okunade SA, Isah OA, Oyekunle MA, Olafadehan OA, & Makinde OJ (2016). Effects of supplementation of threshed sorghum top with selected browse plant foliage on haematology and serum biochemical parameters of Red Sokoto goats. Trop Anim Health Prod 48: 979-984.

Omura S (2008). Ivermectin: 25 years and still going strong. Int J Antimicrob Agents 31: 91-98.

Onwukaeme ND, Lot TY, & Udoh FV (1999a). Effects of Daniellia oliveri bark on isolated rat bladder. Phytother Res 13: 416-418.

Onwukaeme ND, Lot TY, & Udoh FV (1999b). Effects of Daniellia oliveri stem bark and leaf extracts on rat skeletal muscle. Phytother Res 13: 419-421.

Osei-Atweneboana MY, Awadzi K, Attah SK, Boakye DA, Gyapong JO, & Prichard RK (2011). Phenotypic evidence of emerging ivermectin resistance in Onchocerca volvulus. PLoS Negl Trop Dis 5: e998.

Ottesen EA, & Campbell WC (1994). Ivermectin in human medicine. J Antimicrob Chemother 34: 195-203.

Ottesen EA, Duke BO, Karam M, & Behbehani K (1997). Strategies and tools for the control/elimination of lymphatic filariasis. Bull World Health Organ 75: 491-503.

Palsson K, & Jaenson TG (1999a). Comparison of plant products and pyrethroid-treated bed nets for protection against mosquitoes (Diptera: Culicidae) in Guinea Bissau, West Africa. J Med Entomol 36: 144-148.

Palsson K, & Jaenson TG (1999b). Plant products used as mosquito repellents in Guinea Bissau, West Africa. Acta Trop 72: 39-52.

Palumbo E (2008). Filariasis: diagnosis, treatment and prevention. Acta Biomed 79: 106-109.

Papke RL, & Smith-Maxwell C (2009). High throughput electrophysiology with Xenopus oocytes. Comb Chem High Throughput Screen 12: 38-50.

Pennington AJ, & Martin RJ (1990). A patch-clamp study of acetylcholine-activated ion channels in Ascaris suum muscle. J Exp Biol 154: 201-221.

Permana PA, Ho DK, Cassady JM, & Snapka RM (1994). Mechanism of action of the antileukemic xanthone psorospermin: DNA strand breaks, abasic sites, and protein-DNA cross-links. Cancer Res 54: 3191-3195.

Petrovska BB (2012). Historical review of medicinal plants' usage. Pharmacogn Rev 6: 1-5.

Pink R, Hudson A, Mouries MA, & Bendig M (2005). Opportunities and challenges in antiparasitic drug discovery. Nat Rev Drug Discov 4: 727-740.

Polderman AM, Krepel HP, Baeta S, Blotkamp J, & Gigase P (1991). Oesophagostomiasis, a common infection of man in northern Togo and Ghana. Am J Trop Med Hyg 44: 336-344.

Posadas I, Lopez-Hernandez B, & Cena V (2013). Nicotinic receptors in neurodegeneration. Curr Neuropharmacol 11: 298-314.

Prichard RK (1970). Mode of action of the anthelminthic thiabendazole in Haemonchus contortus. Nature 228: 684-685.

Proskocil BJ, Sekhon HS, Jia Y, Savchenko V, Blakely RD, Lindstrom J, *et al*. (2004). Acetylcholine is an autocrine or paracrine hormone synthesized and secreted by airway bronchial epithelial cells. Endocrinology 145: 2498–2506.

Pullan RL, Smith JL, Jasrasaria R, & Brooker SJ (2014). Global numbers of infection and disease burden of soil transmitted helminth infections in 2010. Parasit Vectors 7: 37.

Puttachary S, Trailovic SM, Robertson AP, Thompson DP, Woods DJ, & Martin RJ (2013). Derquantel and abamectin: effects and interactions on isolated tissues of Ascaris suum. Mol Biochem Parasitol 188: 79-86.

Qato DM, Alexander GC, Conti RM, Johnson M, Schumm P, & Lindau ST (2008). Use of prescription and over-the-counter medications and dietary supplements among older adults in the United States. JAMA 300: 2867-2878.

Qian H, Martin RJ, & Robertson AP (2006). Pharmacology of N-, L-, and B-subtypes of nematode nAChR resolved at the single-channel level in Ascaris suum. FASEB J 20: 2606-2608.

Raeymaekers AH, Allewijn FT, Vandenberk J, Demoen PJ, Van Offenwert TT, & Janssen PA (1966). Novel broad-spectrum anthelmintics. Tetramisole and related derivatives of 6-arylimidazo[2,1-b]thiazole. J Med Chem 9: 545-551.

Raeymaekers AH, Roevens LF, & Janssen PA (1967). The absolute configurations of the optical isomers of the broad spectrum anthelmintic tetramisole. Tetrahedron Lett 16: 1467-1470.

Ramamoorthi R, Graef KM, & Dent J (2014a). WIPO Re:Search: Accelerating anthelmintic development through cross-sector partnerships. Int J Parasitol Drugs Drug Resist 4: 220-225.

Ramamoorthi R, Graef KM, Krattiger A, & Dent JC (2014b). WIPO re:search: catalyzing collaborations to accelerate product development for diseases of poverty. Chem Rev 114: 11272-11279.

Rayan P, Verghese S, & McDonnell PA (2010). Geographical location and age affects the incidence of parasitic infestations in school children. Indian J Pathol Microbiol 53: 498-502.

Rayes D, De Rosa MJ, Spitzmaul G, & Bouzat C (2001). The anthelmintic pyrantel acts as a low efficacious agonist and an open-channel blocker of mammalian acetylcholine receptors. Neuropharmacology 41: 238-245.

Raymond V, Mongan NP, & Sattelle DB (2000). Anthelmintic actions on homomer-forming nicotinic acetylcholine receptor subunits: chicken alpha7 and ACR-16 from the nematode Caenorhabditis elegans. Neuroscience 101: 785-791.

Ren HN, Cheng BZ, & Zhuang ZN (1987). [Experimental therapeutic efficacy of a new anti-hookworm drug, tribendimidin]. Zhongguo Ji Sheng Chong Xue Yu Ji Sheng Chong Bing Za Zhi 5: 262-264.

Renslo AR, & McKerrow JH (2006). Drug discovery and development for neglected parasitic diseases. Nat Chem Biol 2: 701-710.

Revah F, Bertrand D, Galzi JL, Devillers-Thiery A, Mulle C, Hussy N, *et al*. (1991). Mutations in the channel domain alter desensitization of a neuronal nicotinic receptor. Nature 353: 846–849.

Richard-Lenoble D, Chandenier J, & Gaxotte P (2003). Ivermectin and filariasis. Fundam Clin Pharmacol 17: 199-203.

Richards FO, Jr., Boatin B, Sauerbrey M, & Seketeli A (2001). Control of onchocerciasis today: status and challenges. Trends Parasitol 17: 558-563.

Richmond JE, & Jorgensen EM (1999). One GABA and two acetylcholine receptors function at the C. elegans neuromuscular junction. Nat Neurosci 2: 791-797.

Robertson AP, Bjorn HE, & Martin RJ (1999). Resistance to levamisole resolved at the single-channel level. FASEB J 13: 749-760.

Robertson AP, Clark CL, Burns TA, Thompson DP, Geary TG, Trailovic SM, *et al.* (2002). Paraherquamide and 2-deoxy-paraherquamide distinguish cholinergic receptor subtypes in Ascaris muscle. J Pharmacol Exp Ther 302: 853-860.

Robertson AP, Puttachary S, Buxton SK, & Martin RJ (2015). Tribendimidine: mode of action and nAChR subtype selectivity in Ascaris and Oesophagostomum. PLoS Negl Trop Dis 9: e0003495.

Robertson SJ, & Martin RJ (1993). Levamisole-activated single-channel currents from muscle of the nematode parasite Ascaris suum. Br J Pharmacol 108: 170-178.

Robertson SJ, Pennington AJ, Evans AM, & Martin RJ (1994). The action of pyrantel as an agonist and an open channel blocker at acetylcholine receptors in isolated Ascaris suum muscle vesicles. Eur J Pharmacol 271: 273-282.

Rosenbluth J (1965a). Ultrastructural organization of obliquely striated muscle fibers in Ascaris lumbricoides. J Cell Biol 25: 495-515.

Rosenbluth J (1965b). Ultrastructure of somatic muscle cells in Ascaris lumbricoides. II. Intermuscular junctions, neuromuscular junctions, and glycogen stores. J Cell Biol 26: 579-591.

Roses AD (2008). Pharmacogenetics in drug discovery and development: a translational perspective. Nat Rev Drug Discov 7: 807-817.

Rufener L, Baur R, Kaminsky R, Maser P, & Sigel E (2010). Monepantel allosterically activates DEG-3/DES-2 channels of the gastrointestinal nematode Haemonchus contortus. Mol Pharmacol 78: 895-902.

Rufener L, Bedoni N, Baur R, Rey S, Glauser DA, Bouvier J, *et al.* (2013). acr-23 Encodes a monepantel-sensitive channel in Caenorhabditis elegans. PLoS Pathog 9: e1003524.

Rufener L, Maser P, Roditi I, & Kaminsky R (2009). Haemonchus contortus acetylcholine receptors of the DEG-3 subfamily and their role in sensitivity to monepantel. PLoS Pathog 5: e1000380.

Saeger B, Schmitt-Wrede HP, Dehnhardt M, Benten WP, Krucken J, Harder A, *et al.* (2001). Latrophilin-like receptor from the parasitic nematode Haemonchus contortus as target for the anthelmintic depsipeptide PF1022A. FASEB J 15: 1332-1334.

Saint Andre A, Blackwell NM, Hall LR, Hoerauf A, Brattig NW, Volkmann L, *et al.* (2002). The role of endosymbiotic Wolbachia bacteria in the pathogenesis of river blindness. Science 295: 1892-1895.

Samje M, Metuge J, Mbah J, Nguesson B, & Cho-Ngwa F (2014). In vitro anti-Onchocerca ochengi activities of extracts and chromatographic fractions of Craterispermum laurinum and Morinda lucida. BMC Complement Altern Med 14: 325.

Sangster NC (1999). Anthelmintic resistance: past, present and future. Int J Parasitol 29: 115-124; discussion 137-118.

Sangster NC, & Gill J (1999). Pharmacology of anthelmintic resistance. Parasitol Today 15: 141-146.

Sasaki T, Takagi M, Yaguchi T, Miyadoh S, Okada T, & Koyama M (1992). A new anthelmintic cyclodepsipeptide, PF1022A. J Antibiot (Tokyo) 45: 692-697.

Sattelle DB, Buckingham SD, Akamatsu M, Matsuda K, Pienaar I, Jones AK, *et al.* (2009). Comparative pharmacology and computational modelling yield insights into allosteric modulation of human α7 nicotinic acetylcholine receptors. Biochem Pharmacol 78: 836–843.

Savioli L, & Albonico M (2004). Soil-transmitted helminthiasis. Nat Rev Microbiol 2: 618-619.

Schiff PL (1980). Pharmacognosy, 11th ed. By G. E. TREASE and W. C. EVANS. Cassell and Collier Macmillan Publishers Ltd., 35 Red Lion Square, London WC1R 49G, England. 1978. 784 pp. 16 × 23 cm. Price $32.50. Journal of Pharmaceutical Sciences 69: 619-620.

Schulz-Key H (1990). Observations on the reproductive biology of Onchocerca volvulus. Acta Leiden 59: 27-44.

Schulz-Key H, & Karam M (1986). Periodic reproduction of Onchocerca volvulus. Parasitol Today 2: 284-286.

Scott I, Pomroy WE, Kenyon PR, Smith G, Adlington B, & Moss A (2013). Lack of efficacy of monepantel against Teladorsagia circumcincta and Trichostrongylus colubriformis. Vet Parasitol 198: 166-171.

Séquéla P, Wadiche J, Dineley-Miller K, Dani JA, & Patrick JW (1993). Molecular cloning, functional properties, and distribution of rat brain alpha 7: a nicotinic cation channel highly permeable to calcium. J Neurosci 13: 596-604.

Shalaby HA (2013). Anthelmintics Resistance; How to Overcome it? Iran J Parasitol 8: 18-32.

Shan Q, Haddrill JL, & Lynch JW (2001). Ivermectin, an unconventional agonist of the glycine receptor chloride channel. J Biol Chem 276: 12556-12564.

Sharp NA (1927). Onchocerciasis. Proc R Soc Med 20: 927-937.

Shenoy RK (2008). Clinical and pathological aspects of filarial lymphedema and its management. Korean J Parasitol 46: 119-125.

Sievers F, Wilm A, Dineen D, Gibson TJ, Karplus K, Li W, *et al*. (2011). Fast, scalable generation of high-quality protein multiple sequence alignments using Clustal Omega. Mol Syst Biol 7: 539.

Sigel E (1990). Use of Xenopus oocytes for the functional expression of plasma membrane proteins. J Membr Biol 117: 201-221.

Somorin AO (1983). Onchocerciasis. Int J Dermatol 22: 182-188.

Southan C, Sharman JL, Benson HE, Faccenda E, Pawson AJ, Alexander SP, *et al*. (2016). The IUPHAR/BPS Guide to PHARMACOLOGY in 2016: towards curated quantitative interactions between 1300 protein targets and 6000 ligands. Nucl. Acids Res. 44: D1054-D1068.

Steinmann P, Zhou XN, Du ZW, Jiang JY, Xiao SH, Wu ZX, *et al.* (2008). Tribendimidine and albendazole for treating soil-transmitted helminths, Strongyloides stercoralis and Taenia spp.: open-label randomized trial. PLoS Negl Trop Dis 2: e322.

Stingl P (1987). [Onchocerciasis. Transmission--clinical aspects--diagnosis--treatment--immune relations]. Hautarzt 38: 709-715.

Stretton AO (1976). Anatomy and development of the somatic musculature of the nematode Ascaris. J Exp Biol 64: 773-788.

Stretton AO, Fishpool RM, Southgate E, Donmoyer JE, Walrond JP, Moses JE, *et al.* (1978). Structure and physiological activity of the motoneurons of the nematode Ascaris. Proc Natl Acad Sci U S A 75: 3493-3497.

Stuhmer W (1992). Electrophysiological recording from Xenopus oocytes. Methods Enzymol 207: 319-339.

Tagboto S, & Townson S (2001). Antiparasitic properties of medicinal plants and other naturally occurring products. Adv Parasitol 50: 199-295.

Takiguchi Y, Mishima H, Okuda M, Terao M, Aoki A, & Fukuda R (1980). Milbemycins, a new family of macrolide antibiotics: fermentation, isolation and physico-chemical properties. J Antibiot (Tokyo) 33: 1120-1127.

Takiguchi Y, Ono M, Muramatsu S, Ide J, Mishima H, & Terao M (1983). Milbemycins, a new family of macrolide antibiotics. Fermentation, isolation and physico-chemical properties of milbemycins D, E, F,G, and H. J Antibiot (Tokyo) 36: 502-508.

Taly A, Corringer PJ, Guedin D, Lestage P, & Changeux JP (2009). Nicotinic receptors: allosteric transitions and therapeutic targets in the nervous system. Nat Rev Drug Discov 8: 733-750.

Taman A, & Azab M (2014). Present-day anthelmintics and perspectives on future new targets. *Parasitol Res* 113: 2425-2433.

Tamarozzi F, Halliday A, Gentil K, Hoerauf A, Pearlman E, & Taylor MJ (2011). Onchocerciasis: the role of Wolbachia bacterial endosymbionts in parasite biology, disease pathogenesis, and treatment. Clin Microbiol Rev 24: 459-468.

Tapia L, Kuryatov A, & Lindstrom J (2007). Ca2+ permeability of the (alpha4)3(beta2)2 stoichiometry greatly exceeds that of (alpha4)2(beta2)3 human acetylcholine receptors. Mol Pharmacol 71: 769-776.

Taylor HR (1990). Onchocerciasis. Int Ophthalmol 14: 189-194.

Taylor MJ, Bandi C, Hoerauf AM, & Lazdins J (2000). Wolbachia bacteria of filarial nematodes: a target for control? Parasitol Today 16: 179-180.

Tejada P, Sanchez-Moreno M, Monteoliva M, & Gomez-Banqueri H (1987). Inhibition of malate dehydrogenase enzymes by benzimidazole anthelmintics. Vet Parasitol 24: 269-274.

Theodoulou FL, & Miller AJ (1995). Xenopus oocytes as a heterologous expression system. Methods Mol Biol 49: 317-340.

Thienpont D, Brugmans J, Abadi K, & Tanamal S (1969). Tetramisole in the treatment of nematode infections in man. Am J Trop Med Hyg 18: 520-525.

Thienpont D, Vanparijs OF, Raeymaekers AH, Vandenberk J, Demoen JA, Allewijn FT, *et al.* (1966). Tetramisole (R 8299), a new, potent broad spectrum anthelmintic. Nature 209: 1084-1086.

Thomsen EK, Sanuku N, Baea M, Satofan S, Maki E, Lombore B, *et al.* (2016). Efficacy, Safety, and Pharmacokinetics of Coadministered Diethylcarbamazine, Albendazole, and Ivermectin for Treatment of Bancroftian Filariasis. Clin Infect Dis 62: 334-341.

Thylefors B, Negrel AD, Pararajasegaram R, & Dadzie KY (1995). Global data on blindness. Bull World Health Organ 73: 115-121.

Touroutine D, Fox RM, Von Stetina SE, Burdina A, Miller DM, 3rd, & Richmond JE (2005). acr-16 encodes an essential subunit of the levamisole-resistant nicotinic receptor at the Caenorhabditis elegans neuromuscular junction. J Biol Chem 280: 27013-27021.

Trees AJ, Graham SP, Renz A, Bianco AE, & Tanya V (2000). Onchocerca ochengi infections in cattle as a model for human onchocerciasis: recent developments. Parasitology 120 Suppl: S133-142.

Trees AJ, Wood VL, Bronsvoort M, Renz A, & Tanya VN (1998). Animal models--Onchocerca ochengi and the development of chemotherapeutic and chemoprophylactic agents for onchocerciasis. Ann Trop Med Parasitol 92 Suppl 1: S175-179.

Treinin M, Gillo B, Liebman L, & Chalfie M (1998). Two functionally dependent acetylcholine subunits are encoded in a single Caenorhabditis elegans operon. Proc Natl Acad Sci U S A 95: 15492-15495.

Trent C, Tsuing N, & Horvitz HR (1983). Egg-laying defective mutants of the nematode Caenorhabditis elegans. Genetics 104: 619-647.

Trouiller P, & Olliaro PL (1998). Drug development output from 1975 to 1996: what proportion for tropical diseases? Int J Infect Dis 3: 61-63.

Trouiller P, & Olliaro PL (1999). Drug development output: what proportion for tropical diseases? Lancet 354: 164.

Trouiller P, Olliaro P, Torreele E, Orbinski J, Laing R, & Ford N (2002). Drug development for neglected diseases: a deficient market and a public-health policy failure. Lancet 359: 2188-2194.

Tsaffack M, Nguemeving JR, Kuete V, Ndejouong Tchize Ble S, Mkounga P, Penlap Beng V, *et al.* (2009). Two new antimicrobial dimeric compounds: febrifuquinone, a vismione-anthraquinone coupled pigment and adamabianthrone, from two Psorospermum species. Chem Pharm Bull (Tokyo) 57: 1113-1118.

Turner JD, Tendongfor N, Esum M, Johnston KL, Langley RS, Ford L, *et al.* (2010). Macrofilaricidal activity after doxycycline only treatment of Onchocerca volvulus in an area of Loa loa co-endemicity: a randomized controlled trial. PLoS Negl Trop Dis 4: e660.

Udall DN (2007). Recent updates on onchocerciasis: diagnosis and treatment. Clin Infect Dis 44: 53-60.

Unwin N (2005). Refined structure of the nicotinic acetylcholine receptor at 4A resolution. J Mol Biol 346: 967-989.

Vallejo R, Barkin RL, & Wang VC (2011). Pharmacology of opioids in the treatment of chronic pain syndromes. Pain Physician 14: E343-360.

Van den Bossche H, & Janssen PA (1967). The biochemical mechanism of action of the anthelmintic drug tetramisole. Life Sci 6: 1781-1792.

Vlassoff C, Weiss M, Ovuga EB, Eneanya C, Nwel PT, Babalola SS, *et al.* (2000). Gender and the stigma of onchocercal skin disease in Africa. Soc Sci Med 50: 1353-1368.

von Samson-Himmelstjerna G, Harder A, Sangster NC, & Coles GC (2005). Efficacy of two cyclooctadepsipeptides, PF1022A and emodepside, against anthelmintic-resistant nematodes in sheep and cattle. Parasitology 130: 343-347.

Wachtel-Galor S, & Benzie IFF (2011). Herbal Medicine: An Introduction to Its History, Usage, Regulation, Current Trends, and Research Needs. In Herbal Medicine: Biomolecular and Clinical Aspects. eds Benzie I.F.F., & Wachtel-Galor S.: Boca Raton (FL).

Wagner CA, Friedrich B, Setiawan I, Lang F, & Broer S (2000). The use of Xenopus laevis oocytes for the functional characterization of heterologously expressed membrane proteins. Cell Physiol Biochem 10: 1-12.

Wahl G, Ekale D, & Schmitz A (1998a). Onchocerca ochengi: assessment of the Simulium vectors in north Cameroon. Parasitology 116 (Pt 4): 327-336.

Wahl G, Enyong P, Ngosso A, Schibel JM, Moyou R, Tubbesing H, *et al.* (1998b). Onchocerca ochengi: epidemiological evidence of cross-protection against Onchocerca volvulus in man. Parasitology 116 (Pt 4): 349-362.

Waller PJ (1997). Anthelmintic resistance. Vet Parasitol 72: 391-405; discussion 405-312.

Waller PJ, Bernes G, Thamsborg SM, Sukura A, Richter SH, Ingebrigtsen K, *et al.* (2001). Plants as de-worming agents of livestock in the Nordic countries: historical perspective, popular beliefs and prospects for the future. Acta Vet Scand 42: 31-44.

Wang GX, Han J, Zhao LW, Jiang DX, Liu YT, & Liu XL (2010a). Anthelmintic activity of steroidal saponins from Paris polyphylla. Phytomedicine 17: 1102-1105.

Wang GX, Zhou Z, Jiang DX, Han J, Wang JF, Zhao LW, *et al.* (2010b). In vivo anthelmintic activity of five alkaloids from Macleaya microcarpa (Maxim) Fedde against Dactylogyrus intermedius in Carassius auratus. Vet Parasitol 171: 305-313.

Wang LJ, Cao Y, & Shi HN (2008). Helminth infections and intestinal inflammation. World J Gastroenterol 14: 5125-5132.

Wanji S, Tendongfor N, Nji T, Esum M, Che JN, Nkwescheu A, *et al.* (2009). Community-directed delivery of doxycycline for the treatment of onchocerciasis in areas of co-endemicity with loiasis in Cameroon. Parasit Vectors 2: 39.

Weil GJ, & Ramzy RM (2007). Diagnostic tools for filariasis elimination programs. Trends Parasitol 23: 78-82.

Weiss MG (2008). Stigma and the social burden of neglected tropical diseases. PLoS Negl Trop Dis 2: e237.

Wessler I, & Kirkpatrick CJ (2008). Acetylcholine beyond neurons: the non-neuronal cholinergic system in humans. Br J Pharmacol 154: 1558-1571.

Willcox M (2009). Artemisia species: From traditional medicines to modern antimalarials--and back again. J Altern Complement Med 15: 101-109.

Williams DK, Wang J, & Papke RL (2011). Positive allosteric modulators as an approach to nicotinic acetylcholine receptor-targeted therapeutics: advantages and limitations. Biochem Pharmacol 82: 915-930.

Williamson SM, Robertson AP, Brown L, Williams T, Woods DJ, Martin RJ, *et al.* (2009). The nicotinic acetylcholine receptors of the parasitic nematode Ascaris suum: formation of two distinct drug targets by varying the relative expression levels of two subunits. PLoS Pathog 5: e1000517.

Willson J, Amliwala K, Davis A, Cook A, Cuttle MF, Kriek N, *et al.* (2004). Latrotoxin receptor signaling engages the UNC-13-dependent vesicle-priming pathway in C. elegans. Curr Biol 14: 1374-1379.

Winthrop KL, Furtado JM, Silva JC, Resnikoff S, & Lansingh VC (2011). River blindness: an old disease on the brink of elimination and control. J Glob Infect Dis 3: 151-155.

Wolstenholme AJ (2011). Ion channels and receptor as targets for the control of parasitic nematodes. Int J Parasitol Drugs Drug Resist 1: 2-13.

Wolstenholme AJ, & Martin RJ (2014). Anthelmintics - from discovery to resistance. Int J Parasitol Drugs Drug Resist 4: 218-219.

Wolstenholme AJ, & Rogers AT (2005). Glutamate-gated chloride channels and the mode of action of the avermectin/milbemycin anthelmintics. Parasitology 131 Suppl: S85-95.

Wolstenholme AJ, Fairweather I, Prichard R, von Samson-Himmelstjerna G, & Sangster NC (2004). Drug resistance in veterinary helminths. Trends Parasitol 20: 469-476.

Wu ZX, Fang YY, & Liu YS (2006). [Effect of a novel drug--enteric coated tribendimidine in the treatment of intestinal nematode infections]. Zhongguo Ji Sheng Chong Xue Yu Ji Sheng Chong Bing Za Zhi 24: 23-26.

Wynd S, Melrose WD, Durrheim DN, Carron J, & Gyapong M (2007). Understanding the community impact of lymphatic filariasis: a review of the sociocultural literature. Bull World Health Organ 85: 493-498.

Xiao SH, Hui-Ming W, Tanner M, Utzinger J, & Chong W (2005). Tribendimidine: a promising, safe and broad-spectrum anthelmintic agent from China. Acta Trop 94: 1-14.

Xiao SH, Utzinger J, Tanner M, Keiser J, & Xue J (2013). Advances with the Chinese anthelminthic drug tribendimidine in clinical trials and laboratory investigations. Acta Trop 126: 115-126.

Xiao SH, Xue J, Xu LL, Zheng Q, Qiang HQ, & Zhang YN (2009). The in vitro and in vivo effect of tribendimidine and its metabolites against Clonorchis sinensis. Parasitol Res 105: 1497-1507.

Xu LL, Jiang B, Duan JH, Zhuang SF, Liu YC, Zhu SQ, *et al.* (2014). Efficacy and safety of praziquantel, tribendimidine and mebendazole in patients with co-infection of Clonorchis sinensis and other helminths. PLoS Negl Trop Dis 8: e3046.

Yassin L, Gillo B, Kahan T, Halevi S, Eshel M, & Treinin M (2001). Characterization of the deg-3/des-2 receptor: a nicotinic acetylcholine receptor that mutates to cause neuronal degeneration. Mol Cell Neurosci 17: 589-599.

Zahner H, Taubert A, Harder A, & von Samson-Himmelstjerna G (2001a). Effects of Bay 44-4400, a new cyclodepsipeptide, on developing stages of filariae (Acanthocheilonema viteae, Brugia malayi, Litomosoides sigmodontis) in the rodent Mastomys coucha. Acta Trop 80: 19-28.

Zahner H, Taubert A, Harder A, & von Samson-Himmelstjerna G (2001b). Filaricidal efficacy of anthelmintically active cyclodepsipeptides. Int J Parasitol 31: 1515-1522.

Zhang ZQ (2013). Animal biodiversity: An outline of higher-level classification and survey of taxonomic richness (Addenda 2013). Zootaxa 3703: 1-82.

Zhao L, Kuo YP, George AA, Peng JH, Purandare MS, Schroederv L, *et al*. (2003). Functional properties of homomeric, human alpha 7-nicotinic acetylcholine receptors heterologously expressed in the SH-EP1 human epithelial cell line. J Pharmacol Exp Ther 305: 1132-1141.

Zimmerman PA, Guderian RH, Aruajo E, Elson L, Phadke P, Kubofcik J, *et al.* (1994). Polymerase chain reaction-based diagnosis of Onchocerca volvulus infection: improved detection of patients with onchocerciasis. J Infect Dis 169: 686-689.

APPENDIX A. INVESTIGATION OF ACETYLCHOLINE RECEPTOR DIVERSITY IN A NEMATODE PARASITE LEADS TO CHARACTERIZATION OF TRIBENDIMIDINE- AND DERQUANTEL-SENSITIVE nAChRs

A paper published in *PLoS Pathogens* (2014)[1]

Samuel K. Buxton[2,3], Claude L. Charvet[3,4], Cédric Neveu[3,4], Jacques Cabaret[3,4], Jacques Cortet[3,4], Nicolas Peineau[5], Melanie Abongwa[2], Elise Courtot[3], Alan P. Robertson[2], Richard J. Martin[2*]

[1] Reprinted with permission of *PLoS Pathog* (2016), **10**(1): e1003870
[2] Department of Biomedical Sciences, College of Veterinary Medicine, Iowa State University, Ames, Iowa, United States of America
[3] INRA, UR1282 Infectiologie Animale et Santé Publique, Nouzilly, France
[4] Université François Rabelais de Tours, UMR1282 Infectiologie et Santé Publique, Tours, France
[5] Université François Rabelais de Tours, Département de Physiologie Animale, Tours, France
[*] Corresponding author and Distinguished Professor, Department of Biomedical Sciences, Iowa State University

A1.0 Abstract

Nicotinic acetylcholine receptors (nAChRs) of parasitic nematodes are required for body movement and are targets of important "classical" anthelmintics like levamisole and pyrantel, as well as "novel" anthelmintics like tribendimidine and derquantel. Four biophysical subtypes of nAChR have been observed electrophysiologically in body muscle of the nematode parasite *Oesophagostomum dentatum*, but their molecular basis was not understood. Additionally, loss of one of these subtypes (G 35 pS) was found to be associated with levamisole resistance. In the present study, we identified and expressed in *Xenopus* oocytes, four *O. dentatum* nAChR subunit genes, *Ode-unc-38, Ode-unc-63, Ode-unc-29 and Ode-acr-8,* to explore the origin of the receptor diversity. When different combinations of subunits were injected in *Xenopus* oocytes, we reconstituted and characterized four

pharmacologically different types of nAChRs with different sensitivities to the cholinergic anthelmintics. Moreover, we demonstrate that the receptor diversity may be affected by the stoichiometric arrangement of the subunits. We show, for the first time, different combinations of subunits from a parasitic nematode that make up receptors sensitive to tribendimidine and derquantel. In addition, we report that the recombinant levamisole-sensitive receptor made up of Ode-UNC-29, Ode-UNC-63, Ode-UNC-38 and Ode-ACR-8 subunits has the same single-channel conductance, 35 pS and 2.4 ms mean open-time properties, as the levamisole-AChR (G35) subtype previously identified *in vivo*. These data highlight the flexible arrangements of the receptor subunits and their effects on sensitivity and resistance to the cholinergic anthelmintics; pyrantel, tribendimidine and/or derquantel may still be effective on levamisole-resistant worms.

A2.0 Author Summary

Parasitic nematode infections of humans and animals are world-wide. In humans, they cause disease and perpetuate a cycle of poverty. In animals, the parasites cause welfare problems and production loss. In developing countries, the debilitating effect of nematode parasites in school children limits their education, and in adults reduces productivity. These two factors, along with the production loss associated with nematode infections of animals that affects human nutrition, sustain poverty. Treatment and prophylaxis of these parasites requires the use of anthelmintic drugs. Here, we employ the *Xenopus* oocyte expression system to investigate the diversity of anthelmintic receptors in the parasitic nematode *Oesophagostomum dentatum*. We demonstrate effects of the 'novel' anthelmintics tribendimidine and derquantel on these reconstituted receptors, revealing, for the first time, the subunits that make up a tribendimidine- and derquantel-sensitive receptor from a parasitic

nematode. We show that the receptor structure and pharmacology can be plastic, and depends on subunit composition and stoichiometry. The factors that affect the diversity of the receptor may contribute to anthelmintic resistance. Our results demonstrate the presence of acetylcholine receptor subtypes that may serve as anthelmintic targets and suggest that pyrantel, tribendimidine and/or derquantel may still be effective on levamisole-resistant worms.

A3.0 Introduction

Human nematode parasite infections are of public health concern in many developing countries where over a billion people are infected [1], [2]. Also very important for human nutrition are infections of livestock which cause significant production loss [3]. Treatment and prophylaxis for these nematode infections requires the use of anthelmintic drugs because sanitation is limited and vaccines are not available. Disturbingly, the regular use of anthelmintics has now been associated with treatment failures and gives rise to concerns about the development of resistance. Resistance has been seen, for example, against levamisole and pyrantel in animals [4]. These two 'classic' anthelmintics work by selectively opening ligand-gated nicotinic acetylcholine (nAChR) ion-channels of nematode muscle to produce depolarization, entry of calcium, contraction and spastic paralysis [5]. The nAChR is composed of 5 transmembrane subunits which surround the cation permeable channel pore. The importance of nAChRs has increased recently because of the introduction of novel cholinergic anthelmintics including: the agonist tribendimidine, which has been approved for human use in China [6]; the allosteric modulator monepantel [7], [8]; and the antagonist derquantel [9]. Tribendimidine is a symmetrical diamidine derivative of amidantel effective against *Ascaris*, hookworms, *Strongyloides stercolaris*, trematodes and tapeworms [10].

Molecular experiments using the free-living model nematode *C. elegans* suggest that tribendimidine acts as a cholinergic agonist like levamisole and pyrantel [11]. Derquantel is a 2-desoxo derivative of paraherquamide in the spiroindole drug class effective against various species of parasitic nematodes, particularly the trichostrongylid nematodes [12]. Derquantel is a selective competitive antagonist of nematode muscle nAChRs especially on the *B*-subtype nAChR from *Ascaris suum* [13]. In contrast to levamisole and pyrantel sensitive-nAChRs [14], [15], [16], the molecular basis for the action of tribendimidine and derquantel in parasitic nematodes are still not known. The chemical structures of the cholinergic anthelmintics are different and resistance to one of the cholinergic anthelmintics sometimes does not give rise to cross-resistance to other cholinergic anthelmintics [17]. These observations imply that the nAChR subtypes in nematode parasites may represent distinct pharmacological targets sensitive to different cholinergic anthelmintics. Therefore, in the present work, we have investigated mechanistic explanations for the variability and diversity of the cholinergic receptors of parasitic nematodes and their therapeutic significance.

The model nematode, *C. elegans*, possesses two muscle nAChR types: one sensitive to levamisole and one sensitive to nicotine [18]. The levamisole AChR type is composed of the five subunits, Cel-UNC-29, Cel-UNC-38, Cel-UNC-63, Cel-LEV-1 and Cel-LEV-8 [18], [19], [20], [21], [22]. The nicotine-AChR type is a homopentamer composed of Cel-ACR-16 subunits [23]. In *Ascaris suum*, there are three pharmacologically separate nAChR types on the body muscle: the *N*-type that is preferentially activated by nicotine; the *L*-type that is preferentially activated by levamisole and; the *B*-type that is preferentially activated by bephenium [13]. In *Oesophagostomum dentatum* there are four muscle nAChRs which are defined by their single-channel conductances: G 25 pS, G 35 pS, G 40 pS and G 45 pS. The

G 35 pS receptor type of *O. dentatum* is reduced in a levamisole-resistant isolate [24] but not in a pyrantel-resistant isolate [25]. Interestingly, the G 35 pS type of *O. dentatum* has a similar channel conductance to the *L*-type from the distantly related species, *A. suum* [13].

However, the precise molecular mechanisms of levamisole and pyrantel resistance occurring in *O. dentatum* isolates are still unknown because the *O. dentatum* genes encoding muscle nAChR subunits have not yet been identified. In order to determine a mechanistic explanation for the variability and pharmacological diversity of the muscle nAChR types in parasitic nematodes like *Oesophagostomum dentatum*, we took advantage of the *Xenopus* oocyte expression system [14], [26], [27].

In this study our first objective was to clone the four putative subunit genes *Ode-unc-38*, *Ode-unc-29 Ode-unc-63* and *Ode-acr-8*, which are homologues of the *C. elegans* levamisole muscle receptor genes [15], [16] and express them in *Xenopus laevis* oocytes to recapitulate the levamisole-sensitive AChRs of *O. dentatum*. In a previous study on *H. contortus* which is closely related to *O. dentatum*, we have reported that co-expression of four AChR subunits (Hco-UNC-38, Hco-UNC-63, Hco-UNC-29 and Hco-ACR-8) in *Xenopus* oocytes resulted in the robust expression of a levamisole sensitive nAChR [16]. In the present work we have identified and cloned the homologs of the corresponding genes in O. dentatum (*Ode-unc-38*, *Ode-unc-63*, *Ode-unc-29* and *Ode-acr8*) and express them in Xenopus oocytes. Of particular note is the evidence that these receptor subtypes are pharmacological targets of the new anthelmintic tribendimidine. Moreover, we demonstrate that the nAChR reconstituted with all four subunits is more sensitive to levamisole than pyrantel and has a single channel conductance of 35 pS, corresponding to the *L-type* previously observed *in vivo* in *O. dentatum* and *A. suum*. Another receptor type, made of 3

subunits, was more sensitive to pyrantel and the new anthelmintic derquantel had a selective effect against receptors activated by pyrantel rather than levamisole, providing the first insight of its molecular target composition in any parasitic nematode. These results provide a basis for understanding the greater diversity of the nAChR repertoire from parasitic nematodes and for deciphering the physiological role of nAChR subtypes targeted by distinct cholinergic anthelmintics. This study will facilitate more rational use of cholinergic agonists/antagonists for the sustainable control of parasitic nematodes impacting both human and animal health.

A4.0 Results

A4.1 Identification of *unc-29, acr-8, unc-38* and *unc-63* homologues from *O. dentatum* and phylogenetic comparison to related nematode species

Taking advantage of the phylogenetic closeness of *O. dentatum*, *C. elegans* and *H. contortus* in clade V of the nematode phylum, we used a candidate gene approach to identify full-length subunit cDNAs from *O. dentatum* of *unc-63*, *unc-29* and *acr-8* homologues. The previously available *O. dentatum unc-38*-like full-length cDNA sequence (Accession number GU256648) allowed the rapid cloning of the *Ode-unc-38* subunit cDNA. The UNC-38 and UNC-63 subunits being closely related in the UNC-38 "core" group [28], multi-alignment of *unc-63* and *unc-38* cDNA sequences from different nematode species allowed the design of degenerate primers that were able to specifically amplify the *unc-63* homologue from *O. dentatum*. To identify the *unc-29* homologue from *O. dentatum*, degenerate primers from the *H. contortus* and *C. elegans unc-29* sequences were used to amplify a partial 288 bp cDNA sequence, providing specific information to get the full-length cDNA by RACE-PCR standard procedures. To identify the *acr-8* homologue from *O. dentatum*, a partial cDNA of

861 bp was cloned using primers from *H. contortus acr-8*, allowing subsequent identification of the full-length cDNA encoding Ode-ACR-8 subunit. The four *O. dentatum* subunit transcripts were trans-spliced at their 5′end with the splice leader 1 (SL1). The predicted nAChR proteins displayed typical features of LGIC subunits including a secretion signal peptide, a cys-loop domain consisting of 2 cysteines separated by 13 amino acid residues and four transmembrane domains (TM1-4) (supplemental figure S1A–D). The Ode-UNC-38, Ode-UNC-63 and Ode-ACR-8 subunits contained in their N-terminal part the Yx(x)CC motif characteristic of the α-type subunits whereas the Ode-UNC-29 subunit sequence lacked these vicinal di-cysteines. The different nAChR subunit sequences, accession numbers, characteristics and closest levamisole subunit homologues of *C. elegans* and *H. contortus* are presented in Table 1. Alignment of the deduced amino acid sequences of the four *O. dentatum* nAChR subunits revealed 66 to 92% identity with their respective homologues from *C. elegans* and *H. contortus* (Table 1 and supplemental Fig. S1A–D), indicating that even in closely related species some interspecies polymorphisms could impact the nAChR subunit composition and pharmacological properties. The phylogenies shown in Fig. 1 (maximum likelihood tree) and supplemental Fig. S2 (distance tree) identify a single ortholog each for the *unc-38*, *unc-63*, *acr-8*, and *unc-29* subunits in *O. dentatum*. The branching topology is consistent, in each case, with a taxonomic position of *O. dentatum* with strongylida and outside the trichstrongyloidea [29]. Interestingly, this topology places the speciation of *O. dentatum* significantly before the previously identified trichostrongylid specific *unc-29* diversification event [15]. As such, these duplications cannot be shared with *O. dentatum*, although it is not possible to rule out other independent *unc-29* duplication events in *O. dentatum*. Clearly, further studies that include analysis of *unc-29* homolog

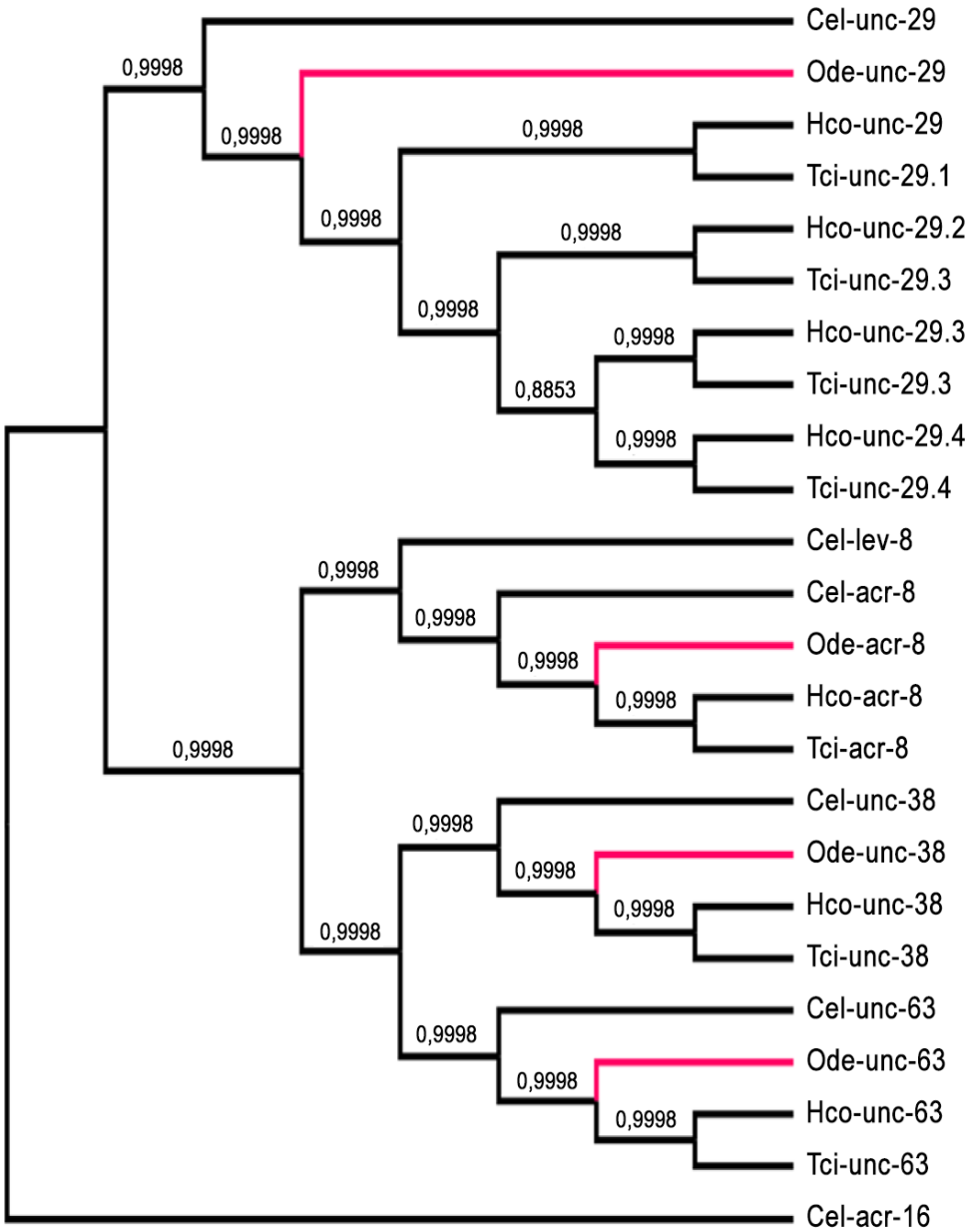

Figure 1. Maximum likelihood tree showing relationships of acetylcholine receptor (nAChR) subunit cDNA sequences in *Oesophagostomum dentatum* (Ode, highlighted in red), *Caenorhabditis elegans* (Cel), *Haemonchus contortus* (Hco) and *Teladorsagia circumcincta* (Tci). The *C. elegans acr-16* nAChR subunit sequence was used as an outgroup. Branch support was evaluated using the chi2 option of PhyML and values more than 0.9 were considered reliable.

Table 1. Comparison of *O. dentatum* AChR subunits with the homologs of *C. elegans* and *H. contortus*.

Gene name	Accession number	Full-length cDNA size (bp)	Deduced protein seq. length	% nucleotide identity		% amino acid identity/similarity	
				C. elegans	*H. contortus*	*C. elegans*	*H. contortus*
Ode-unc-29	JX429919	1637	497	66	73	78/87	85/90
Ode-unc-38[a]	JX429920	1681	507	66	70	72/77	83/87
Ode-unc-63	HQ162136	2265	507	67	80	77/84	92/95
Ode-acr-8	JX429921	1851	538	62	77	66/93	80/97

[a]Similar to complete cDNA sequence GU256648.
doi:10.1371/journal.ppat.1003870.t001

sequences in a wide range of nematode species are required to understand the evolutionary impact of such duplication events.

A4.2 Expression of *Ode(29-63)*, the *Pyr-nAChR* and stoichiometry effect on pharmacological properties

Our investigation of *O. dentatum* receptor expression determined the minimum number of subunits that is required to reconstitute a functional muscle nAChR. Previous expression studies of *C. elegans* and *H. contortus* functional nAChRs in *Xenopus* oocytes required the use of ancillary proteins [16], [26]. Hence, the *H. contortus* ancillary factors *Hco-ric-3*, *Hco-unc-50* and *Hco-unc-74* were also injected to facilitate the expression of *O. dentatum* functional receptors in *Xenopus* oocytes. In control experiments we observed that oocytes injected with ancillary protein cRNAs did not produce current responses to 100 µM acetylcholine or other cholinergic anthelmintics. We then injected different combinations of pairs of cRNAs (1:1) of: *Ode-unc-29*, *Ode-unc-38*, *Ode-unc-63* and *Ode-acr-8*.

Only those oocytes injected with 1:1 *Ode-unc29:Ode-unc-63* cRNA, regularly produced currents of >50 nA in response to 100 µM acetylcholine or cholinergic anthelmintics, indicating that the two subunits could form functional receptors (Fig. 2). We

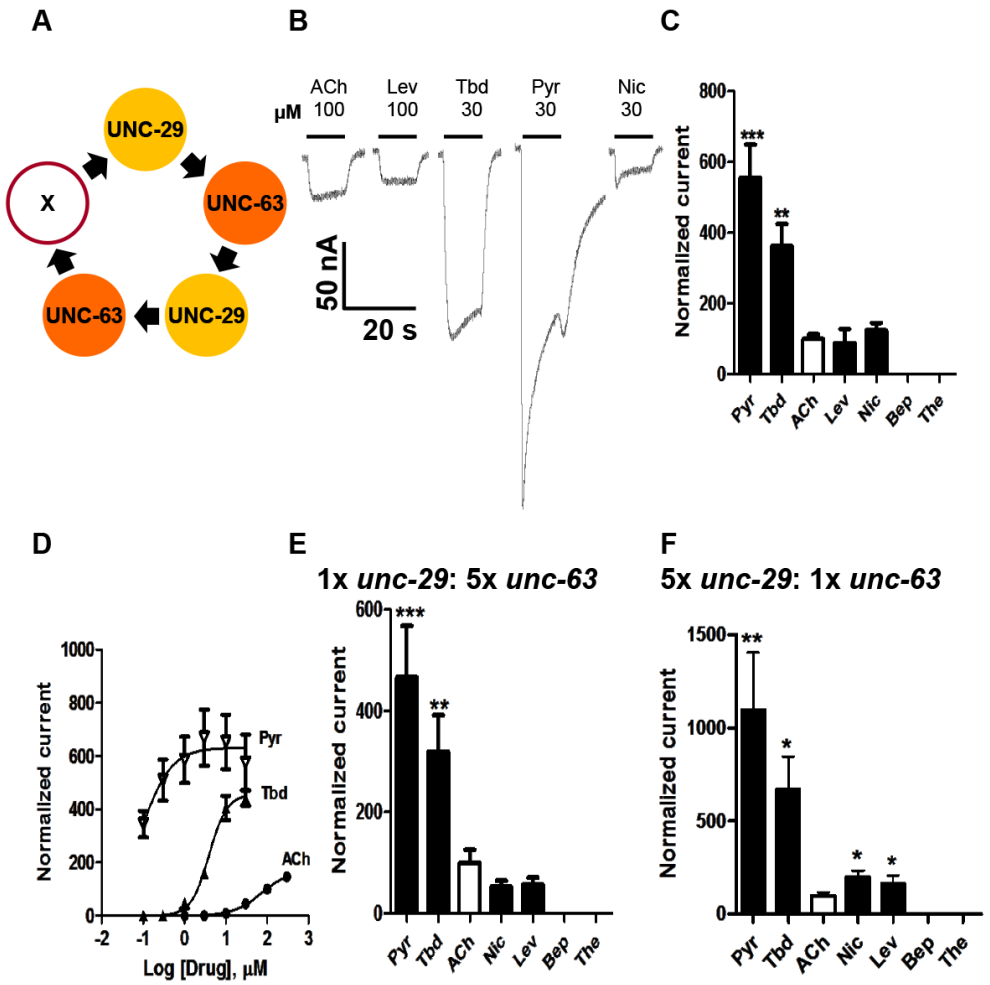

Figure 2. Voltage-clamp of oocytes injected with *O. dentatum Ode-unc-29* and *Ode-unc-63* nAChR subunits. (A) Diagram of possible subunit arrangements of *Ode-unc-29* and *Ode-unc-63*. X represents either UNC-63 or UNC-29 subunit. PyR, pyrantel; Tbd, tribendimidine, ACh, acetylcholine; Nic, nicotine; Bep, bephenium; The, thenium. (B) Representative traces showing the inward currents in oocytes injected with 1:1 *Ode-unc-29* and *Ode-unc-63*. (C) Bar chart (mean ± se) of agonists-elicited currents in the *Ode-*(*29 - 63*) Pyr-nAChR, (p*aired t-test*, **p<0.01, ***p<0.001). All agonist responses have been normalized to the average 100 µM ACh currents. (D) Dose-response relationships for Pyr (inverted Δ, n=6), Tbd (▲, n=5) and ACh (•, n=6) in the *Ode-*(*29 - 63*) Pyr-nAChR, (n=number of oocytes). (E) Bar chart (mean ± se) of normalized currents elicited by different agonists in 1:5 *Ode-unc-29:Ode-unc-63* injected oocytes. Currents have been normalized to and compared with 100 µM ACh currents (*paired t-test*, **p<0.01, ***p<0.001). (F) Bar chart (mean ± se) of normalized currents elicited by different agonists in oocytes injected with 5:1 *Ode-unc-29:Ode-unc-63*. Currents normalized to and compared with 100 µM ACh currents (*paired t-test*, *p<0.05, **p<0.01).

found that no other paired combination produced currents. Without both subunits in any of our subsequent injected mixes, no functional receptor could be reconstituted, demonstrating that Ode-UNC-29 and Ode-UNC-63 are essential *O. dentatum* levamisole receptor subunits. Injection of each of these subunits alone did not form receptors that responded to the agonists we tested, demonstrating that these subunits do not form homopentamers.

More than 75% of injected oocytes responded to acetylcholine. For our standard test concentrations, except for 100 µM acetylcholine and 100 µM levamisole, we used 30 µM drug concentrations of different important anthelmintics to limit effects of open-channel block. Interestingly, the novel anthelmintic tribendimidine elicited currents when perfused on oocytes expressing Ode-UNC-29 and Ode-UNC-63. The potency series of the agonists (anthelmintics) based on the normalized currents, Fig. 2C, was: 30 µM pyrantel >30 µM tribendimidine >30 µM nicotine ≈100 µM levamisole ≈100 µM acetylcholine. Neither 30 µM bephenium, nor 30 µM thenium, were active. Even at 30 µM, pyrantel produced currents bigger than 100 µM acetylcholine (Fig. 2C). We refer to this receptor type as: *Ode*(*29–63*), or the *Pyr-nAChR*.

We determined the concentration current-response plot for pyrantel, tribendimidine and acetylcholine, Fig. 2D for *Ode*(*29–63*). The EC_{50} values for pyrantel and tribendimidine were less than the EC_{50} for acetylcholine but the I_{max} values were larger for pyrantel and tribendimidine (Table 2). Thus the anthelmintics pyrantel and tribendimidine were much more potent and produced a greater maximum response than the natural ligand, acetylcholine and levamisole on this type of receptor. To date, this result represents the first characterization of a nematode tribendimidine-sensitive nAChR.

Table 2. Properties of the four main receptor subtypes obtained from dose-response relationships.

		Ode(29-63)	*Ode(29-63-38)*	*Ode(29-63-8)*	*Ode(29-63-8-38)*
Acetylcholine	EC_{50}	72.4±13.3	13.2±0.8	3.5±0.2	4.2±0.2
	I_{max}	100.0	100.0	100.0	100.0
	nH	1.28±0.31	1.10±0.044	1.18±0.055	0.77±0.06
Levamisole	EC_{50}	*	*	2.2±0.2	3.1±2.2
	I_{max}	*	*	73.0±2.4	119.0±3.7
	nH	*	*	1.36±0.18	0.87±0.10
Pyrantel	EC_{50}	0.09±0.005	0.4±0.1	ND	ND
	I_{max}	632.0±55.8	172.0±10.4	ND	ND
	nH	1.20±0.95	0.88±0.18	ND	ND
Tribendimidine	EC_{50}	3.9±0.8	2.2±0.5	0.8±0.1	0.3±0.6
	I_{max}	458.0±28.8	155.0±8.8	75.0±6.2	69.0±5.0
	nH	1.98±0.46	1.17±0.18	0.94±0.22	0.50±0.09

ND: Not determined.
*Dose-response measurements not possible due to the small size of currents elicited by the agonists on these receptor subtypes.
doi:10.1371/journal.ppat.1003870.t002

We were interested to see if there was evidence of pharmacological changes associated with variation in stoichiometry of the *Ode*(*29-63*) receptor. When we injected a 1:5 ratio of *Ode-unc-29:Ode-unc-63* cRNA with the same 1:1:1 ratio of ancillary proteins, the mean amplitudes of the pyrantel and tribendimidine currents were significantly increased (pyrantel: 6-fold increase from a mean of 104 nA to 653 nA, $p<0.01$; tribendimidine: 7-fold increase from a mean of 68 nA to a mean of 447 nA, $p<0.01$). The large increase in the size of the currents with increased *Ode-unc-63* cRNA suggests that increased UNC-63 favors expression of receptors with a stoichiometry of $(UNC\text{-}63)_3$: $(UNC\text{-}29)_2$ [14]. Also, when we injected 5:1 *Ode-29:Ode-63* cRNA, the normalized currents of 30 µM nicotine and 100 µM levamisole became significantly bigger than 100 µM acetylcholine (Fig. 2C, E &F) suggesting increased expression of $(UNC\text{-}63)_2$: $(UNC\text{-}29)_3$. The increase in currents with the 1:5 and 5:1 *Ode-29:Ode-63* cRNA was not due to variability in currents with different

batches of oocytes because we observed the same effects when we injected 1:1, 1:5 and 5:1 *Ode-29*:*Ode-63* cRNA in the same batch of oocytes.

A4.3 Expression of *Ode(29-63-38)*, the *Pyr/Tbd-nAChR*

We subsequently added *unc-38* and injected *Ode-unc-29*:*Ode-unc-63*:*Ode-unc-38* cRNAs in the ratio 1:1:1, along with the three *H. contortus* ancillary factors. Oocytes injected with this mix responded with larger currents of around 250 nA to 100 μM acetylcholine and to all the other agonists tested except bephenium and thenium (Fig. 3A–D). Pyrantel was the most potent agonist but with this receptor type, pyrantel and tribendimidine produced the same amplitude of current at 30 μM. We termed this receptor the *Ode*(*29–63–38*), or the *Pyr/Tbd-nAChR*. The potency series of the agonists based on the normalized currents was 30 μM pyrantel ≈30 μM tribendimidine >100 μM acetylcholine >30 μM nicotine ≈100 μM levamisole (Fig. 3 C). The dose-response curves for pyrantel, tribendimidine and acetylcholine are shown in Fig. 3D. The EC_{50} for pyrantel was less than the EC_{50} for tribendimidine and acetylcholine (Table 2). The Hill slopes for tribendimidine and acetylcholine were both close to 1.0 (Table 2), showing little co-operativity between agonist concentration and response. Again interestingly, the two anthelmintics, pyrantel and tribendimidine were more potent than the natural ligand and the anthelmintic levamisole, but with this receptor type, the currents were larger than with the *Ode*(*29–63*) receptor.

A4.4 Expression of *Ode(29-63-8)*, the *ACh-nAChR*

When we added *Ode-acr-8* and injected *Ode-unc-29*:*Ode-unc-63*:*Ode-acr-8* cRNA in the ratio 1:1:1 along with the three *H. contortus* ancillary factors into the oocytes, we observed even bigger receptor responses to 100 μM acetylcholine. We also observed responses to all the agonists we tested, including bephenium and thenium (Fig. 3E–H), which

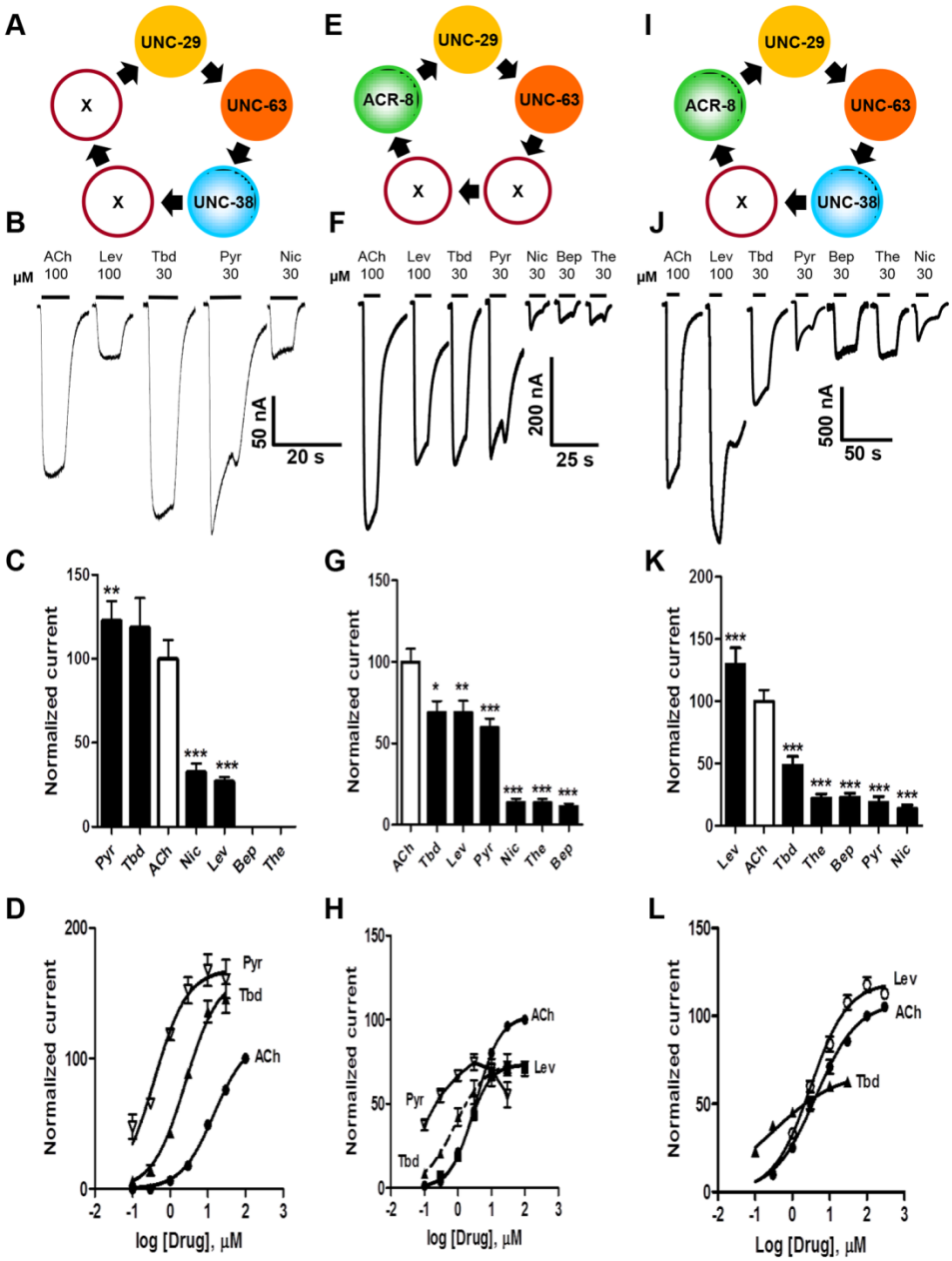

Figure 3. Voltage-clamp of oocytes injected with different combinations of the four *O. dentatum* nAChR subunits. (A) Depiction of a possible arrangement of *O. dentatum* UNC-29, UNC-63 & UNC-38. 'X' represents any of the subunits. PyR, pyrantel; Tbd, tribendimidine, ACh, acetylcholine; Nic, nicotine; Bep, bephenium; The, thenium. (B) Representative traces of inward currents elicited by the various agonists in oocytes injected with 1:1:1 *Ode-unc-29:Ode-unc-63:Ode-unc-38*. Pyr & Tbd were the most potent agonists on this receptor subtype. (C) Bar chart (mean ± se) of currents elicited by the different agonists in the *Ode-*(*29 - 38 - 63*) Pyr/Tbd-nAChR (*paired t-test*, **p<0.01, ***p<0.001). (D) Dose-response of normalized currents *vs* log concentration for Pyr (inverted Δ, n=6), Tbd (▲, n=6) and ACh (•, n=5) in the Pyr/Tbd-nAChR. (E) Diagrammatic representation of the three subunits, *unc-29*,

unc-63 and *acr-8* injected into oocytes. 'X' could be any of the three subunits. (F) Representative traces of inward currents produced by the different agonists in oocytes injected with 1:1:1 *Ode-unc-29*:*Ode-unc-63*:*Ode-acr-8*. (G) Bar chart (mean ± se) of normalized currents elicited by the different agonists in the *Ode*(*29-63-8*) receptor subtype. All currents normalized to 100 µM ACh currents; comparisons made with the ACh currents (*paired t-test*, *p<0.05, **p<0.01, ***p<0.001). (H) Dose-response plot of normalized currents vs log. Concentration of Pyr (inverted Δ, n=6), Tbd (▲, n=6), ACh (•, n=6) and Lev (▪, n=6). (I) Representation of a possible arrangement of the four *O. dentatum* subunits injected into *Xenopus* oocytes. (J) Representative traces of inward currents elicited by the different agonists on the *Ode*(*29–63–38–8)* or Lev-nAChR. (K) Bar chart (mean ± se) of normalized currents elicited by the different agonists on the Lev-nAChR subtype. Comparisons were made with 100 µM ACh currents, which was used for the normalization (*paired t-test*, ***p<0.001). (L) Dose-response plot of normalized currents against log of Tbd (▲, n=6), ACh (•, n=18) and Lev (○, n=5) concentrations.

suggests that *Ode-acr-8* introduces bephenium and thenium binding sites. 100 µM acetylcholine produced the largest current responses, always greater than 800 nA and sometimes greater than 1 µA. We termed this receptor type: *Ode*(*29–63–8*), or the ACh-nAChR.

For the *Ode*(*29–63–8*) receptor, the potency series of the agonists (anthelmintics) based on the normalized currents, was 100 µM acetylcholine >30 µM tribendimidine ≈100 µM levamisole ≈30 µM pyrantel >30 µM nicotine ≈30 µM thenium ≈30 µM bephenium (Fig. 3G). Here, the least potent agonists were nicotine, bephenium and thenium with average currents <20% of the acetylcholine currents. The dose-response curves (Fig. 3H) show that at the highest concentrations tested, levamisole and tribendimidine current responses were less than that of acetylcholine. Despite this, the EC_{50} values of both tribendimidine and levamisole were lower than acetylcholine on this receptor type. The EC_{50} values are summarized in Table 2. The levels of co-operativity (slope) were similar for these three agonists, but I_{max} for acetylcholine (100.0%) was bigger than I_{max} for tribendimidine (75.0±6.2%) and levamisole (73.0±2.4%).

Two characteristic features of the response of the *Ode*(*29–63–8*) receptor to pyrantel suggest the presence of open-channel block which is more pronounced with *Ode*(*29–63–8*) than with the other types. Firstly, the maintained application of 30 µM pyrantel produced a response that declined rapidly despite the concentration being maintained, and secondly, on wash-out of pyrantel the response 'rebounded' or increased temporally before declining. Pronounced open-channel block with pyrantel has been observed at the single-channel level [30]. Altogether, these results highlight for the first time the reconstitution of a new functional receptor with distinct pharmacological profile made of the UNC-29, UNC-63 and ACR-8 subunits.

A4.5 Expression of *Ode(29-63-8-38)*, the *Lev-nAChR*

Finally, we injected all our subunits in a mix of *Ode-unc-29*:*Ode-unc-63*:*Ode-acr-8*:*Ode-unc-38* cRNA in the ratio 1:1:1:1 along with the three *H. contortus* ancillary factors. These subunits reconstituted a receptor type on which 100 µM levamisole produced the biggest responses of >1.5 µA, sometimes reaching >4.5 µA, Fig. 3I–L. We termed this receptor type: *Ode*(*29–63–8–38*) or the *Lev-nAChR*. The potency series of the agonists based on the normalized currents, was 100 µM levamisole >100 µM acetylcholine >30 µM tribendimidine >30 µM thenium ≈30 µM bephenium ≈30 µM pyrantel >30 µM nicotine (Fig. 3K). Here, the least potent agonists were thenium, bephenium, pyrantel and nicotine with average currents <25% of the acetylcholine currents. The EC_{50} for tribendimidine was less than the EC_{50} for levamisole and acetylcholine (Table 2). The dose-response curves were rather shallow with Hill slopes less than one for acetylcholine, levamisole and tribendimidine (Table 2). We have shown that expression of Ode-UNC-29, Ode-UNC-63 Ode-ACR-8 and Ode-UNC-38 produced large currents, and that the receptor, *Ode(29–63–8–38)*, was most

sensitive to levamisole. It is clear from the observations above that each of the four subunits: Ode-UNC-29, Ode-UNC-63 Ode-ACR-8, and Ode-UNC-38 may combine and be adjacent to different subunits as they form different pentameric nAChRs.

A4.6 Antagonistic effects of derquantel

We tested the antagonist effects of derquantel on the levamisole and pyrantel concentration-response plots of *Ode (29-63-38-8)* and *Ode (39-63-38)*, Fig. 4A–D. Recall that levamisole is more potent as an agonist on *Ode(29–63–8–*38) and pyrantel is more potent on *Ode(39-63-38)*. Fig. 4A shows that derquantel behaves like a potent competitive antagonist of levamisole, with 0.1 µM producing a right shift in EC_{50} dose-ratio of 1.7 (the antagonist negative log dissociation constant from the Schild equation, pK_B, was 6.8±0.1). When we tested the antagonist effects of derquantel on *Ode(29–63–8–38)* using pyrantel as the agonist, we saw mixed non-competitive and competitive antagonism: there was a right-shift in the EC_{50} and a reduction to 41% of the maximum response by 0.1 µM derquantel, Fig. 4 B. One explanation for these mixed effects of derquantel is that co-expression of UNC-29, UNC-63, UNC-38, ACR-8 subunits produces a mixture of receptors: mostly *Ode(39-63-38-8)* receptors that are preferentially activated by levamisole and which are competitively antagonized by derquantel and; a smaller number of receptors like *Ode(39-63-38)* that are preferentially activated by pyrantel and antagonized non-competitively by derquantel. To test this further we examined the antagonist effects of derquantel on pyrantel and levamisole activation of *Ode (39-63-38)*. Derquantel antagonized both agonists non-competitively, Fig. 4 C & D. We interpret these observations to suggest that expression of *Ode(39-63-38-8)* receptors can give rise to expression of a smaller number of other receptors

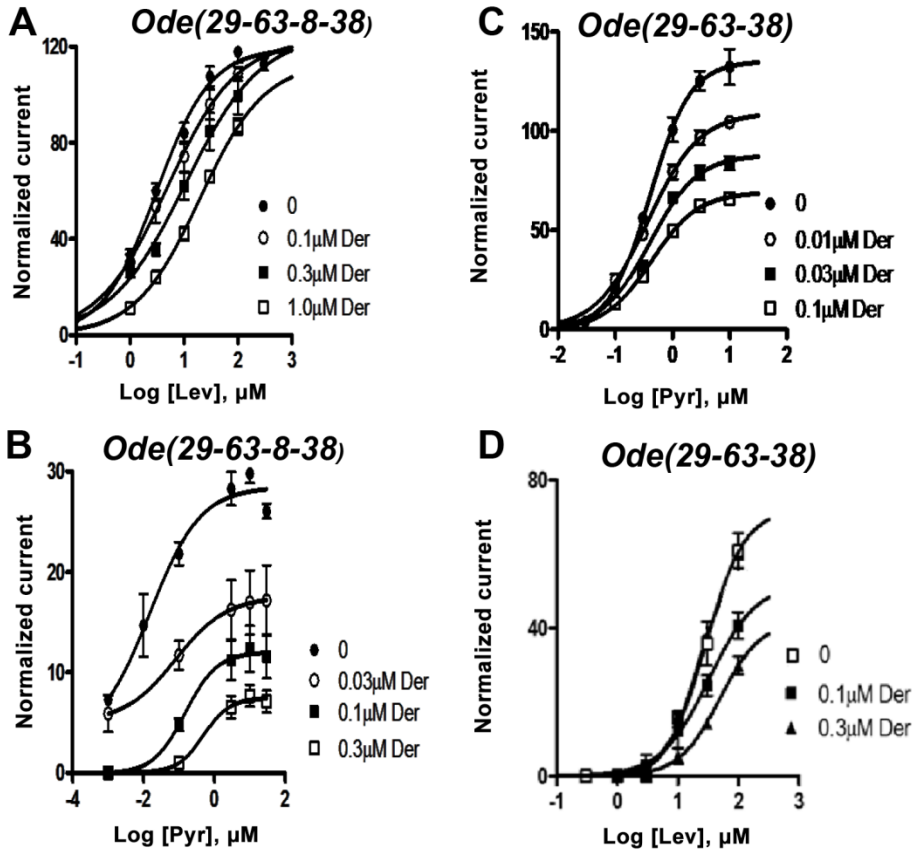

Figure 4. Effects of derquantel on levamisole-activated and pyrantel-activated expressed *Ode(29-63-8-38), the Lev-nAChR*, and on pyrantel-activated and levamisole-activated *Ode(29-63-38), the PyR/Trbd-nAChR* subtypes. Der: derquantel; Lev: levamisole; Pyr: pyrantel. (A) Antagonistic effects of varying derquantel concentrations on levamisole currents of *Ode(29-63-8-38).* Levamisole evokes supramaximal normalized currents and derquantel competitively inhibited levamisole currents. (B) Derquantel antagonism of pyrantel currents of *Ode(29-63-8-38).* Here, derquantel produced mixed non-competitively competitive antagonism. Pyrantel did not activate supramaximal currents. (C) Antagonism of pyrantel by derquantel on the *Ode(29-63-38*), Pyr/Tbd-nAChR. Derquantel is a potent non-competitive antagonist. (D) Derquantel non-competitively antagonized levamisole responses on the *Ode(29-63-38*) receptor.

including *Ode(39-63-38)*. We comment further on these observations in our discussion. Nonetheless, the competitive and non-competitive antagonism of derquantel when levamisole is used on the two different receptor subtypes, Fig. 4 A & D, illustrates that derquantel effects are subtype selective.

A4.7 The receptor types have different calcium permeabilities

The EC_{50} concentrations of acetylcholine for the different expressed receptors varied (Table 2), suggesting that there are different physiological functions for the different nAChR types. One physiological difference may be the permeability to the second messenger, calcium. To examine this we measured the relative permeability of calcium in *Ode*(*29–63–38*), *Ode*(*29–63–8*) and *Ode(29–63–8–38)*, receptors which produced large enough currents to determine reversal potentials.

We observed two different effects of increasing calcium from 1 mM to 10 mM on the acetylcholine currents. One effect was potentiation of the current amplitudes, an effect that was voltage-dependent (Fig. 5A, B & C). The voltage-dependent increases in acetylcholine currents was prominent in *Ode(29–63–8–38)*, and less in the other two receptor types. The potentiating effect of calcium on the acetylcholine currents indicates the presence of positive allosteric binding sites on one or more subunits of the pentameric nAChR [31]. The second effect was a positive shift to the right of the current-voltage plot indicating that the channels are permeable to calcium [32]. A shift in reversal potential of 1.7 mV was recorded for the *Ode*(*29–63–8*) (Fig. 5A). Using the Goldman Hodgkin Katz constant field equation (Text S1 Legend), we calculated this change in reversal potential corresponds to a relative calcium permeability ratio, P_{Ca}/P_{Na} of 0.5. The reversal potential shift for *Ode*(*29–63–38*) was similar, 1.3 mV, also giving a permeability ratio P_{Ca}/P_{Na} of 0.4 (Fig. 5B). For *Ode(29–63–8–38)*, the shift was 16.0 mV (Fig. 5C), corresponding to a calcium permeability ratio, P_{Ca}/P_{Na}, of 10.3. The *Ode(29–63–8–38)* receptor, was therefore much more permeable to extracellular calcium and positively allosterically [31] modulated by extracellular calcium than the other two receptor types, a physiologically significant observation.

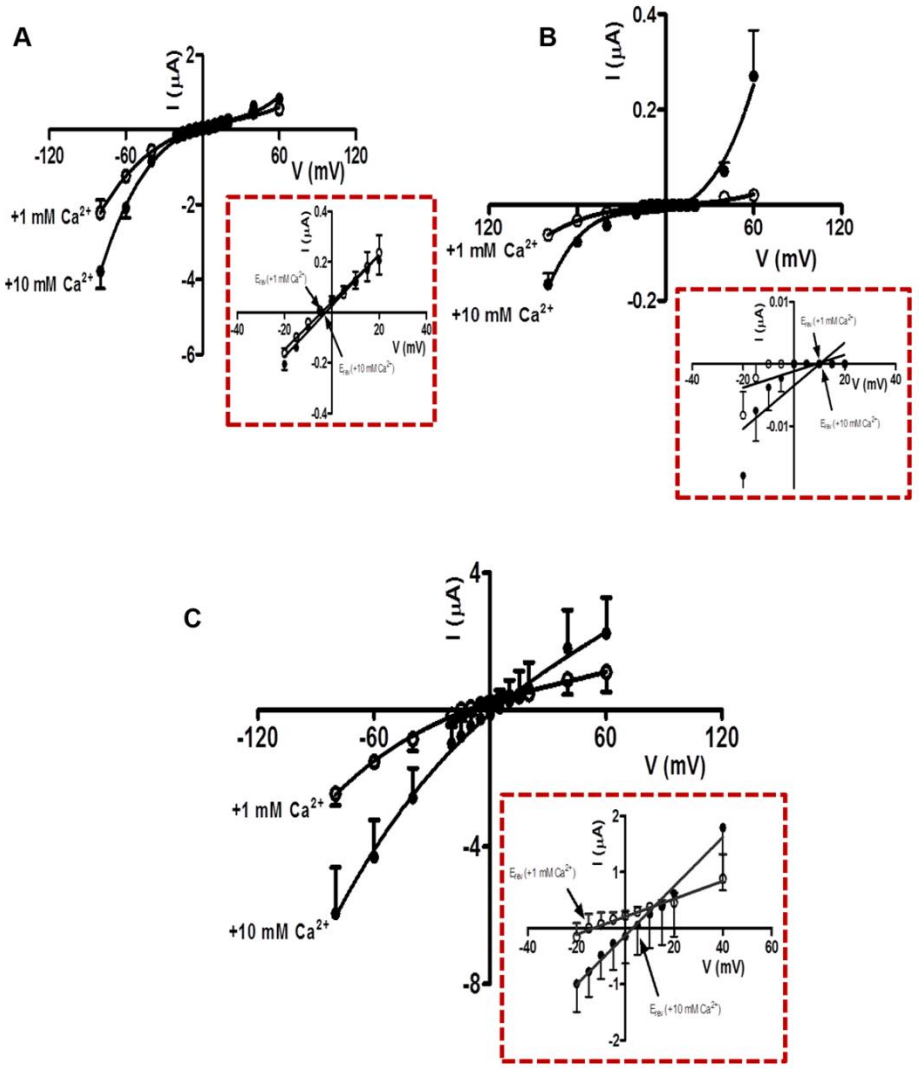

Figure 5. Ca^{2+} permeability of the *O. dentatum* receptor subtypes with large ACh currents. (A) Current-Voltage plot for oocytes injected with *Ode*(*29–63–8)*, showing the change in current with voltage in 1 mM and 10 mM Ca^{2+} recording solutions. *Insert:* Magnified view of current-voltage plot from −20 mV to +40 mV showing the E_{rev} in 1 mM and 10 mM extracellular Ca^{2+}. (B) Current-Voltage plot for oocytes injected with *Ode*(*29–63–38)* showing the current changes in 1 mM and 10 mM Ca^{2+} recording solution under different voltages. *Insert:* Magnified view of current-voltage plot from −20 mV to +40 mV showing the E_{rev} in 1 mM and 10 mM extracellular Ca^{2+}. (C) Current-Voltage plot for oocytes injected with *Ode*(*29–63–38–8)* in 1 mM and 10 mM Ca^{2+} recording solutions. *Insert:* Magnified view of current-voltage plot from −20 mV to +40 mV showing the E_{rev} in 1 mM and 10 mM extracellular Ca^{2+}. The calcium permeability was calculated using the GHK equation (Text S1 Legend).

A4.8 *Ode(29-63-8-38), Lev-nAChR* channels have a mean conductance of 35 pS

Single-channel studies in *Oesophagostomum dentatum* body muscle have demonstrated the presence of different nAChR types with conductances of 25, 35, 40 and 45 pS, showing the presence of four or more receptor types. We have shown in experiments here, that combinations of four nAChR subunits from this parasite can produce four pharmacologically different receptor types. We found that the expressed *Ode*(*29–63–38–8*) *Lev-nAChR* type was most sensitive to levamisole and had a high permeability to calcium and hypothesized that this type may be the G35 type. Accordingly we investigated the single-channel properties of this type under patch-clamp using 10 μM levamisole as the agonist. In control oocytes injected with only the ancillary proteins, we recorded no nAChR-like channel currents in 4 oocytes. We found however, that in patches from oocytes expressing the *Ode(29–63–8–38)* type, that more than 90% of patches contained active, recognizable nAChR channels with one main conductance level. Fig. 6A shows representative channel currents from one of these patches and its current-voltage plots which had a conductance of 36.6±0.5 pS (mean ± SE). The mean conductance of channel from patches made from five different oocytes was 35.1±2.4 pS. We did not test the effects of different cholinergic anthelmintics on channel conductance. The reversal potentials of all plots were close to 0 mV, an indication that the channel was nonselective and permeable to Cs^+ (reversal potential of 0 mV).

We measured the mean open times, τ, at the different potentials and observed values of 2.4±0.4 ms at +100 mV and 2.9±0.5 ms at −100 mV (Fig. 6B). The mean open times are comparable to the mean open times recorded *in vivo* in *O. dentatum* with the same concentration of levamisole.

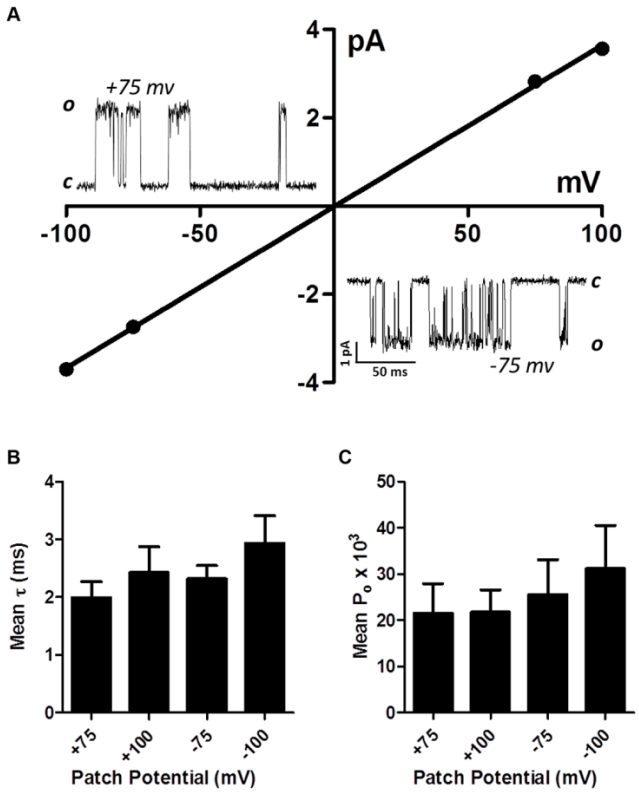

Figure 6. Single-channel properties of the *Lev-nAChR* subtype. (A) Representative current-voltage plot from oocyte-attached patch with 10 µM levamisole. Inserts are representative channel openings at +75 mV and −75 mV membrane potentials. Even with 10 µM levamisole, we sometimes observed 'flickering' channel block events; note the 'flickering' channel block shown by openings at −75 mV. (B) Bar chart (mean ± se) of the mean open times (τ) at the different patch potentials. (C) Bar chart (mean ± se) of the probability of channel opening, P_o, at the different patch potentials.

A4.9 The three ancillary proteins affect expression levels

We tested the requirements for the ancillary proteins, RIC-3, UNC-50 and UNC-74, by removing each of the ancillary proteins in turn when expressing the *Ode(29–63–8–38)* receptor. We found that the requirement for all the ancillary proteins was not essential and that each protein, when absent reduced currents produced by the expressed receptors (Fig. S3). When all the ancillary factors were removed, we observed no measurable currents in response to acetylcholine. Here, we have observed that unlike in *C. elegans*, robust

functional *O. dentatum* receptors can be reconstituted when one of these three ancillary factors is omitted and that the ancillary proteins can affect the balance of the pharmacology of the receptors expressed (Fig. S3)

A5.0 Discussion

A5.1 The origin of diverse nAChR types in parasitic nematodes

We have shown previously in the parasitic nematodes, *O. dentatum* [24] and *A. suum* [13], that there are diverse types of nAChR on body muscle of parasitic nematodes which may be activated by cholinergic anthelmintics. In *A. suum* we found that these types have different sensitivities to different cholinergic anthelmintics like levamisole and derquantel. In *O. dentatum* there are four types that can be distinguished by their single-channel conductance, with reduced numbers of the G 35 pS type in levamisole resistant isolates. Here we explored and tested the hypothesis that the receptor subtypes may be due to different combinations of subunits. We found that four main pharmacology types could be produced and separated by expressing in *Xenopus* oocytes different combinations of the α-subunits Ode-UNC-38, Ode-UNC-63 and Ode-ACR-8 together with the non-α subunit Ode-UNC-29. The types could be separated on the basis of their EC_{50} and amplitude of response to the natural ligand acetylcholine, permeability to calcium and anthelmintic profiles (rank order potency and/or concentration-response relationships). We have not tested the possibility that post-translational modification may serve as an additional mechanism to produce different receptor types.

A5.2 The different AChR types have different functional properties

Ode(*29–63–38–8*), *Ode(29–63–8)* and *Ode*(*29–63–38*) produce the largest current responses to acetylcholine. On the basis of the larger size of the currents responses to

acetylcholine and the smaller currents of *Ode*(*29–63*) mixture, we speculate that the other three receptor types have more important physiological roles in the worm. *Ode*(*29–63–38*) was the most sensitive type to acetylcholine with an EC_{50} of 3.5±0.2 µM but it had a lower calcium permeability, P_{Ca}/P_{Na} of 0.5, than *Ode*(*29–63–38–8*) that had an acetylcholine EC_{50} of 4.2±0.2 µM. However, *Ode*(*29–63–38–8*) had greater responses to levamisole and a calcium permeability, P_{Ca}/P_{Na} of 10.4. Thus the addition of ACR-8 is responsible for increasing the calcium permeability and the response to levamisole. Since the *Ode*(*29–63–38–8*) receptor produced the biggest current to levamisole and had a single-channel conductance of 35.1±2.4 pS, close to the *in vivo* G 35 pS type that is reduced with levamisole resistance, we suggest that *Ode*(*29–63–38–8*) subunit combinations give rise to the *in vivo* G 35 pS channel in *O. dentatum*. There may also be pH regulatory effects on channel activity of *Ode*(*29–63–38–8*). The presence of histidine (*pKa* 6.0) in the ACR-8 (Fig. S1D, position 282) channel pore entrance on TM2 region is predicted to produce a pH sensitive channel that is less permeable to cations and calcium at pH 6.0 than 7.5. ACR-8 may provide a functional mechanism of reducing depolarization and muscle contraction at low pHs that can occur in an anaerobic environment. It would also have been of interest to look at the single-channel properties of the other receptor types when activated with levamisole to compare with the *in vivo* channel properties. Unfortunately, the smaller size of the levamisole currents due to the presence of fewer receptors on the oocytes, made single-channel recording less tractable than for *Ode*(*29–63–38–8*).

A5.3 Different nAChR types and sensitivities to levamisole, pyrantel, tribendimidine and derquantel

The different nAChR types have different sensitivities to cholinergic anthelmintics: for example *Ode*(*29–63–38–8*) produces the biggest response to levamisole, while *Ode*(*29–63–38*) produces the biggest response to pyrantel. If these two types of receptors exist together in the nematode parasite, our observations suggest that combinations of levamisole and pyrantel will produce a bigger therapeutic response than either of the two anthelmintics given alone and that combination therapy may be advantageous. However, very few reports of combining levamisole and pyrantel for treatment are available. In one report [33] using *T. muris* infected mice, combination of levamisole and pyrantel treatment produced antagonism but these authors did not determine the EC_{50} dose for pyrantel pamoate and used a very high dose of 300 mg/Kg dose, above the normal therapeutic dose. At this level we anticipate the presence of open-channel block limiting the effects of the therapeutic combination [32].

We tested the effects of derquantel on the *Ode*(*29–63–38–8*), the *Lev-nAChR*, and on *Ode(29-63-38*), the *Pyr/Trbd-nAChR*. Interestingly, the mode of action of derquantel varied (competitive or non-competitive) with the receptor subtypes when activated by the same agonist, levamisole. The difference in the mode of action will relate to the preferred non-equivalent binding sites of derquantel, of levamisole and of pyrantel on the receptor subtypes. The competitive antagonism of levamisole suggests a common binding site for derquantel on the *Ode*(*29–63–38–8*) receptor; the non-competitive antagonism of pyrantel and levamisole by derquantel on *Ode*(*29–63–38*) suggests negative allosteric modulation and different non-equivalent binding sites for derquantel and the agonists, levamisole and derquantel, on this receptor. Interestingly the loss of the ACR-8 subunit, which reduces the

levamisole sensitivity of the *Ode(29-63-38)* receptor, changes the antagonism of levamisole from competitive to non-competitive. Thus ACR-8 may contribute to a high affinity binding site of levamisole and a competitive site of derquantel. When ACR-8 was not present derquantel behaved non-competitively. We have interpreted the mixed non-competitive competitive antagonism of pyrantel by derquantel on *Ode*(*29–63–38–8*) to be due to a mixed expression of receptor subtypes with mostly the levamisole sensitive *Ode*(*29–63–38–8*) receptors being present and a smaller proportion of other receptors like *Ode(29-63-38)* being present. This is certainly possible because, as we have shown, the subunits can and do combine in different ways to form 4 types of receptor. Although less likely, it may be that: 1) expression of *Ode(29-63-38-8)* produces only one receptor type, 2) levamisole and pyrantel bind to separate sites on this receptor, 3) derquantel acts competitively, binding at the levamisole site but; 4) derquantel acts as a negative allosteric modulator when pyrantel binds to its receptor. Further study is required to elucidate details of binding sites on the different receptor types. Despite these possibilities we have seen potent antagonist effects of derquantel on both the *Ode*(*29–63–38-8*) and the *Ode*(*29–63–38*) subtypes suggesting that derquantel could still be active against levamisole resistance associated with reduced ACR-8 expression.

We were also interested in the effects of the novel cholinergic anthelmintics tribendimidine [6] and to compare their effect with the other anthelmintics. We found that tribendimidine was a potent cholinergic anthelmintic on the *Ode*(*29–63–38*), *Ode*(*29–63–8*) and *Ode*(*29–63–38–8*) types. Thus tribendimidine could remain an effective anthelmintic if levamisole resistance in parasites were associated with null mutants or decreased expression of *acr-8* and/or *unc-38*.

A5.4 Regulation of AChR type expression

The different functional properties of the nAChR types indicate that each type may have different physiological roles to play in the parasite and the proportion of the different types present at the membrane surface is likely to be regulated. This regulation could allow changes in calcium permeability, desensitization, receptor location, receptor number and anthelmintic sensitivity. The control is expected to include dynamic physiological processes and developmental process that take place over different time scales. An adaptable and diverse receptor population may allow changes, even during exposure to cholinergic anthelmintics. We know little about these processes, their time-scales and how they may be involved in anthelmintic resistance in parasitic nematodes but some information is available from *C. elegans*.

In *C. elegans* there are a number of genes involved in processing and assembly of the subunits of AChR; specific examples include *Cel-ric-3*, *Cel-unc-74* and *Cel-unc-50* [34], [35], [36]. Cel-RIC-3 is a small transmembrane protein, which is a chaperone promoting nAChR folding in the endoplasmic reticulum [37]. The gene *Cel-unc-74* encodes a thioredoxin-related protein required for the expression of levamisole AChR subunits [38]. The gene *Cel-unc-50* encodes a transmembrane protein in the Golgi apparatus [35]. In *Cel-unc-50* mutants, levamisole nAChR subunits are directed to lysosomes for degradation. We found that acetylcholine currents and pharmacological profile of the receptors were sensitive to the presence of the accessory proteins, RIC-3, UNC-74 & UNC-50, suggesting the possibility that the expression level of these proteins could contribute to anthelmintic resistance in parasitic nematodes.

A5.5 Species differences

We show here that four *O. dentatum* receptor subunits can be used to reconstitute different functional levamisole receptor types and that levamisole is a full agonist in one of the main types. All of the four main *O. dentatum* receptor types responded to nicotine, which supports our use of the term nAChR. In contrast, in the expressed levamisole-sensitive AChRs of *C. elegans*, levamisole is a partial agonist, requires five subunits (Cel-UNC-38:Cel-UNC-29:Cel-UNC-63:Cel-LEV-1:Cel-LEV-8) and does not respond to nicotine. The *C. elegans* nicotine-sensitive muscle receptor is a separate homopentamer of ACR-16 [39]. We also saw differences between the expressed receptors of *O. dentatum* and the expressed AChR of *H. contortus* [16]: only two types of AChRs were produced in *Xenopus* oocytes expressing *H. contortus* subunits. Furthermore, we saw differences and similarities between the expressed *O. dentatum* receptors and the expressed *A. suum* receptors [14]. Only two subunits were used to reconstitute the *A. suum* AChR, such that varying the amounts of the subunit cRNAs injected changed the pharmacology of the expressed receptors. This is similar to the *Ode(29–63)*, in that only two subunits were used to reconstitute a *Pyr-nAChR* and varying the amount of injected subunit cRNAs affected the pharmacology of the receptor. Whereas no ancillary factors were used to reconstitute the *A. suum* nAChRs, we observed that the three ancillary factors were required to reconstitute the *O. dentatum* receptors. Another observation is that the amounts of cRNA we injected to reconstitute the *O. dentatum* receptors were far less than what was injected to reconstitute the *A. suum* receptors. These demonstrate differences between the expressed receptors of nematodes in the same clade (*O. dentatum*, *C. elegans* and *H. contortus*) and/or in different clades (*O. dentatum* and *A. suum*). In addition we have also demonstrated tribendimidine's effect on all four *O. dentatum*

receptor types and in two of the receptor types, the EC_{50} values show tribendimidine was more potent than the other agonists across the types. We found that pyrantel was the most potent agonist of two types of *O. dentatum* receptors but it is only most potent in one of the types of *H. contortus*. The real and significant differences between the effects of pharmacological agents on the model nematode *C. elegans* and on the parasitic nematode *O. dentatum*, both Clade V nematodes, shows that species variation requires that effects of anthelmintics on the relevant nematode parasite are tested as a vital reality check.

A6.0 Materials and Methods

A6.1 Ethical Concerns

All animal care and experimental procedures in this study were in strict accordance with guidelines of good animal practice defined by the Center France-Limousin ethical committee (France). The vertebrate animals (pig) studies were performed under the specific national (French) guidelines set out in the Charte Nationle portant sur l'ethique de l'experimentation animal of the Ministere De Lensiengnement Superieur et de la Recherch and Ministere De L'Agriculture et de la Peche experimental agreement 6623 approved by the Veterinary Services (Direction des Services Vétérinaires) of Indre et Loire (France).

A6.2 Nematode isolates

These studies were carried out on the levamisole-sensitive (SENS) isolate of *O. dentatum* as previously described [40]. Large pigs were experimentally infected with 1000 infective larvae (L3s) and infection was monitored 40 days later by fecal egg counts every 3 days. The pigs were slaughtered after 80 days at the French National Institute for Agricultural Research (Nouzilly) abattoir and adult nematodes (males and females) were collected from the large intestine and stored in RNA later (Qiagen®) at −80°C.

A6.3 Molecular biology

Ten adult males from *O. dentatum* SENS isolate were used for total RNA preparation using TRIzol (Invitrogen) according to the manufacturer's instructions. First-strand cDNA synthesis on resuspended and DNase-treated total RNA was carried out with the oligo (dT) RACER primer and superscript III reverse transcriptase (Invitrogen, Carlsbad, CA, USA) as previously described [16]. To identify full-length cDNA sequences of *O. dentatum unc-29*, *unc-63* and *acr-8* homologues, 5′- and 3′- rapid amplification of complementary ends (RACE) polymerase chain reactions (PCR) were performed using the splice leader sequence primer (SL1) with internal reverse primers and internal forward specific primers with reverse transcription 3′-site adapter primers, respectively. PCR products were cloned into the pGEM-T vector (Promega). Positive identifications were made by BLAST analysis against all *Haemonchus contortus* entries in the *H. contortus* information resource data base. Primers designed on *unc-29* sequence from *H. contortus* and *C. elegans* (unc-29-F0 GGACGAGAAAGATCAAGTTATGCA, unc-29-XR2 TCATCAAATGGGAAGAAYTCGACG) allowed PCR amplification of a 288 bp fragment corresponding to partial *O. dentatum unc-29* homologue. New gene specific primer sets were designed on this sequence for the 5′- and 3′-RACE-PCR providing the full-length cDNA sequence of *Ode-unc-29*. To identify the *unc-63* homologue from *O. dentatum*, degenerate primers were designed based on the *Ode-unc-38* mRNA sequence (accession number GU256648) and the *unc-63* and *unc-38* sequences of cDNAs available from multiple nematode species (Ode-unc-63-F1 GCGAATCGCGAYGCGAATCGKCT, F2 AARAGYATGTGYCAAATWGAYGT, R3 ATATCCCAYTCGACRCTGGGATA, R4 TAYTTCCAATCYTCRATSACCTG). An 861 bp partial coding sequence of *Ode-acr-8*

cDNA was amplified using a sense primer (Hco-acr-8-FT1 TATGGTTAGAGATGCAATGGTT) and an antisense primer (Hco-acr-8-RE8 GTGTTTCGATGAAGACAGCTT) from *H. contortus Hco-acr-8*. The product of this reaction was cloned and sequenced, and the data were used to design primers to get the 5′ and the 3′ ends of the target transcript. To amplify the full-length coding sequence of *Ode-unc-38*, *Ode-unc-63*, *Ode-unc-29* and *Ode-acr-8*, we used the Phusion DNA polymerase (Finnzymes) and gene specific primer pairs containing *Hind*III or *Xho*I and *Apa*I restriction enzyme sites (Table S1 in Text S1) to facilitate directional cloning into the pTB-207 expression vector that is suitable for *in vitro* transcription. PCR products were then digested with XhoI and ApaI restriction enzymes (except *Ode-unc-29*, digested with HindIII and ApaI), purified using the NucleoSpin Gel and PCR Clean-up kit (Macherey-Nagel), ligated into the respective corresponding sites of the pTB-207 expression vector with T4 DNA Ligase (New England Biolabs), and resulting constructs were transformed into *E. coli* DG1 cells (Eurogentec) [26]. Three clones of each gene were sequenced using the standard primers T7 and polyT-V. Each of the reported sequences in supplementary figures S1A–D is from one of the nearly identical clones. The mMessage mMachine T7 transcription kit (Ambion) was used for *in vitro* cRNA synthesis from linearized plasmid DNA templates. The cRNAs were precipitated by lithium chloride, resuspended in RNAse-free water and stored at −80°C.

A6.4 Sequence analysis and accession numbers

Database searches, prediction of conserved motifs and phylogenetic analyses for the cDNAs were carried out as already described [16]. Maximum likelihood analysis was performed on full-length AChR subunit cDNA sequences as follows: sequences were aligned

with Geneious 6.1.6 (Biomatters Ltd) using the translation align MAFFT plugin [41] that aligns the nucleotide sequences as codons based on amino acid sequences. The resulting nucleotide alignment was used to generate phylogenetic trees with the PhyML plugin for Geneious [42]. The HK85 substitution matrix was selected in order to optimize the tree topology and branch lengths. Branch support was evaluated using the chi2 option of PhyML. The accession numbers for cDNA and protein sequences mentioned in this article are *C. elegans*: UNC-29 NM_059998, UNC-38 NM_059071, UNC-63 NM_059132, ACR-8 JF416644; *H. contortus*: *Hco-unc-29.1* GU060980, *Hco-unc-38* GU060984, *Hco-unc-63a* GU060985, *Hco-acr-8* EU006785, *Hco-unc-50* HQ116822, *Hco-unc-74* HQ116821, *Hco-ric-3.1* HQ116823; *O. dentatum*: *Ode-unc-29* JX429919, *Ode-unc-38* JX429920, *Ode-unc-63* HQ162136, *Ode-acr-8* JX429921.

A6.5 Voltage-clamp studies in oocytes

Xenopus laevis ovaries were obtained from NASCO (Fort Atkinson, Wisconsin, USA) and defolliculated using 1–2 mg/ml collagenase type II and Ca^{2+}-free OR2 (mM: NaCl 100, KCl 2.5, HEPES 5, pH 7.5 with NaOH). Alternatively, defolliculated oocytes were purchased from Ecocyte Bioscience (Austin, Texas, USA). Oocytes (animal pole) were microinjected with ~36 nL of a cRNA injection mix containing 50 ng/μL of each subunit cRNA, as described in [26]. Equal amounts of the *H. contortus* ancillary factors *ric-3, unc-50* and *unc-74* were added to each mix. Microinjected oocytes were incubated at 19°C for 2–5 days. The oocytes were incubated in 200 μL of 100 μM BAPTA-AM for ~3 hours prior to recordings, unless stated otherwise. In control experiments, we recorded from un-injected oocytes. Recording and incubation solutions used are reported in [26]. Incubation solution was supplemented with Na pyruvate 2.5 mM, penicillin 100 U/mL and streptomycin 100

µg/ml. All drugs applied, except tribendimidine and derquantel, were purchased from Sigma Aldrich (St Louis, MO, USA). Oocytes were voltage-clamped at −60 mV with an Axoclamp 2B amplifier; all data were acquired on a desktop computer with Clampex 9.2.

A6.6 Single-channel studies

Oocyte-attached (outside-out) patch-clamp procedure was used to obtain all recordings at room temperature (20°C–25°C). Oocytes were prepared for the recordings by removal of the vitelline membrane with forceps after placing in hypertonic solution, as already described [43]. The oocytes were transferred to the recording chamber and bathed in a high Cs solution with no added Ca^{2+} (composition in mM: CsCl 140, $MgCl_2$ 2, HEPES 10, EGTA 1, pH 7.3) to reduce K^+ currents and lower opening of Ca^{2+}-activated Cl^- channels. Patch electrodes were pulled from thin-walled capillary glass tubing (Warner Instruments, Hamden, CT), coated close to the tip with sylgard and fire-polished. The electrodes were filled with a high pipette solution {composition in mM: CsCl 35, CsAc 105, $CaCl_2$ 1, HEPES 10} containing 10 µM levamisole. Axopatch 200B amplifier (Axon Instruments, Union City, CA) was used to amplify currents which were sampled at 25 kHz with Digidata 1320A (Axon Instruments) and filtered at 1.5 kHz (3-pole Bessel). The linear least squares regression was used to estimate the conductances of the channels since the slopes were linear and did not show rectification.

A6.7 Data analysis

Acquired data were analyzed with Clampfit 9.2 (Molecular Devices, Sunnyvale, CA, USA) and Graphpad Prism 5.0 software (San Diego, CA, USA). The peak of currents in BAPTA-soaked oocytes was measured. The response to 100 µM ACh was normalized to 100% and the responses to the other agonists normalized to that of ACh. For all dose-

response relationships, the mean ± s.e of the responses is plotted. Dose-response data points were fitted with the Hill equation as described previously [26]. To calculate the pK_B values, the graphs were fitted with the Gaddum/Schild EC_{50} shift and the bottom of the curves were set to zero.

A7.0 Supporting Information

A7.1 Supplementary figures

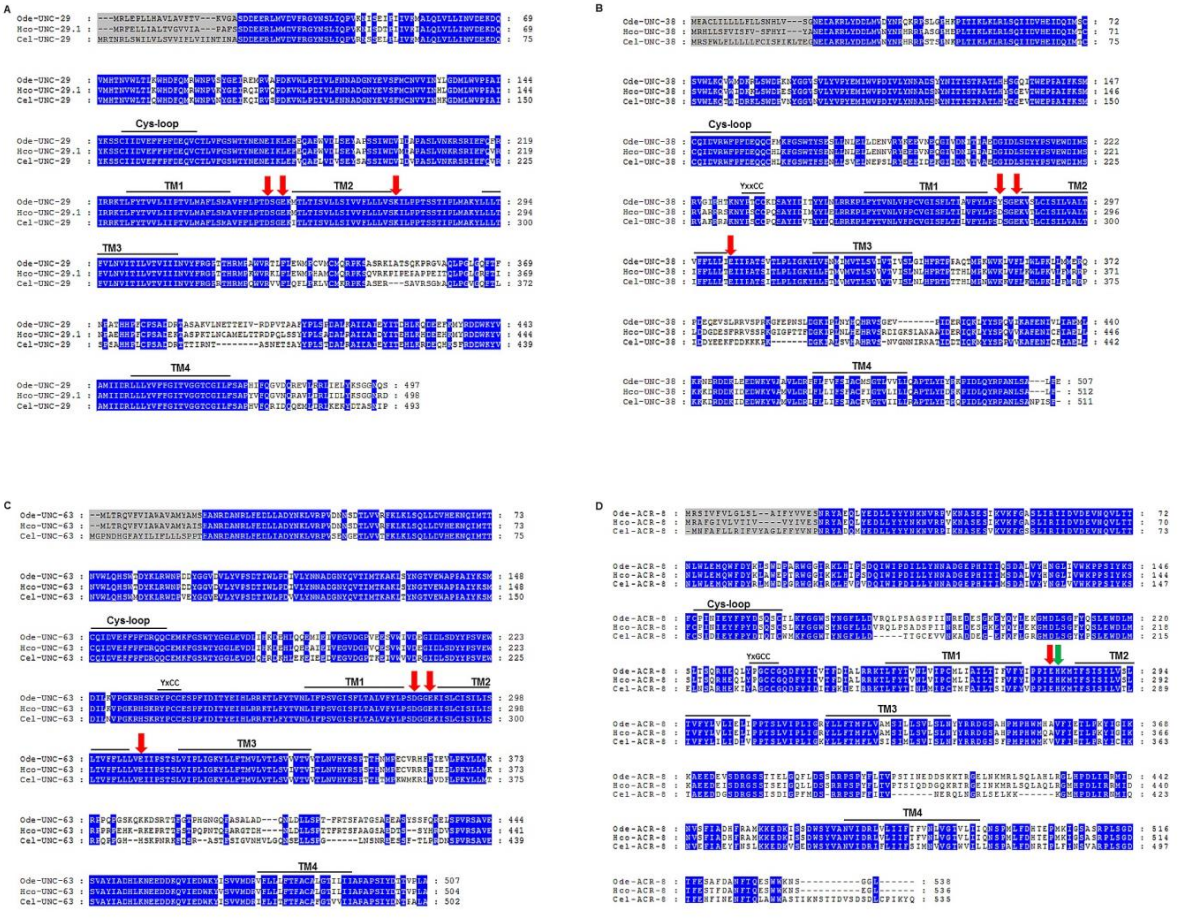

Supplementary **Figure S1.** A–D. Amino acid alignments of the four *O. dentatum* nAChR subunits with the *H. contortus* and *C. elegans* homologues. The sequences were aligned with the MUSCLE algorithm [44] and processed further with GeneDoc. Shaded in grey are the predicted signal peptides and in blue are the amino acids conserved between all three species. Noted above the aligned sequences are the cys-loop, Yx(x)CC motif and transmembrane domains. Noted with red arrows (S1 A–C) are the amino acids, on either side of the transmembrane region (TM2) that are predicted to contribute to the permeability of the channel to calcium [45], [46]. Green arrow in S1 D shows a histidine which implies pH sensitivity around pH 6.5 to channel permeability.

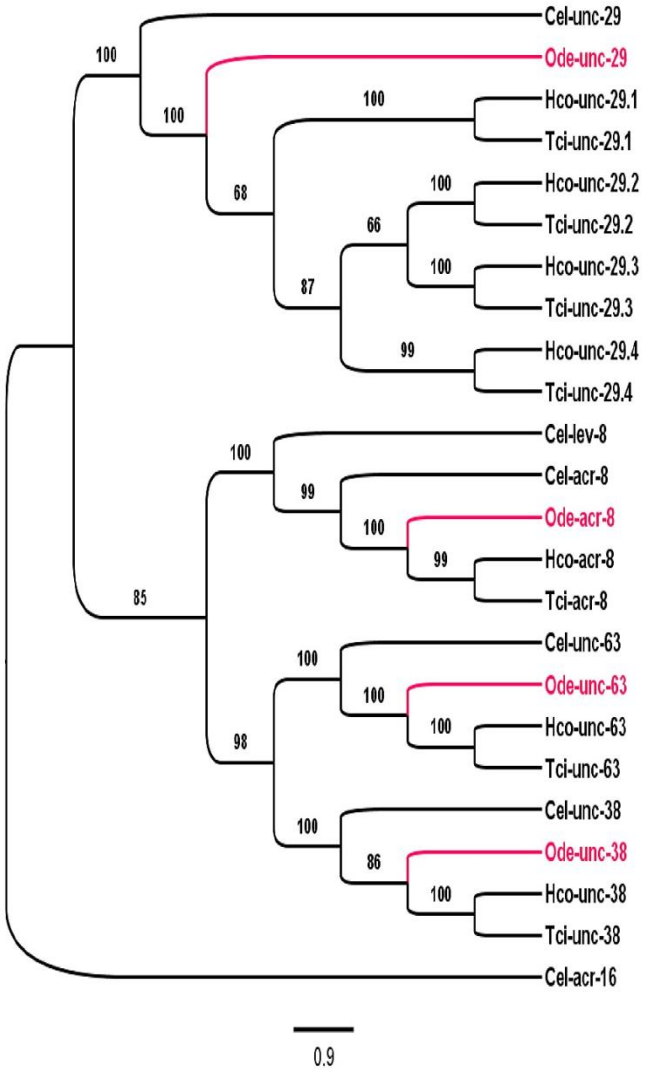

Supplementary **Figure S2.** Distance tree showing relationships of nicotinic acetylcholine receptors (nAChR) subunit sequences in *Oesophagostomum dentatum* (Ode, highlighted in red), *Caenorhabditis elegans* (Cel), *Haemonchus contortus* (Hco) and *Teladorsagia circumcincta* (Tci). Numbers at each branch indicate percentage boostrap values corresponding to 1000 replicates. The scale bar represents substitutions per site. The *C. elegans acr-16* nAChR subunit was used as an outgroup. Distance analyses were performed on full-length cDNA sequences. Multiple alignment was performed using Muscle program with standard parameters [47]. Relationships between sequences were determined using the neighbor-joining method and the HKY substitution model [48]. One thousand bootstrap replicates were performed to test the support of nodes.

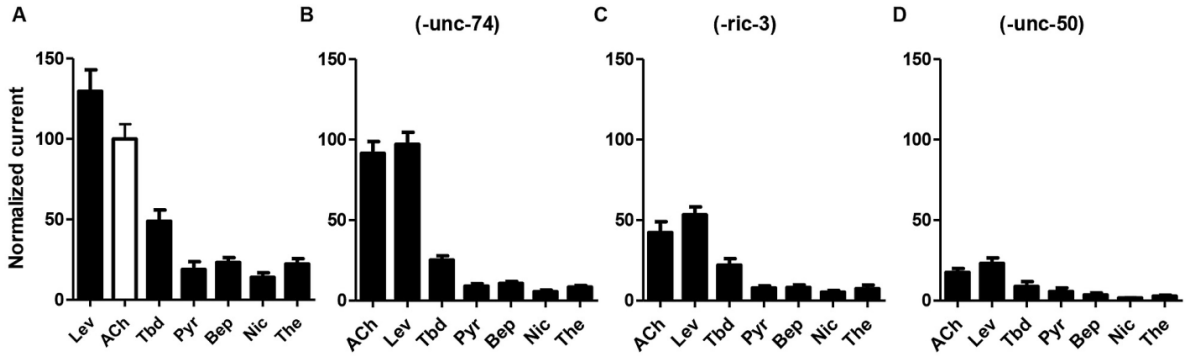

Supplementary **Figure S3.** Effect of the ancillary proteins on receptor reconstitution. (A) Bar chart (mean ± se) of agonist-elicited currents in the *Ode*(*29–63–38–8*) or Lev-nAChR subtype. This receptor subtype was used to test the effect of sequentially removing the ancillary proteins on the reconstitution. All responses were normalized to control 100 µM ACh (unfilled bar) currents in oocytes expressing this receptor subtype with all the ancillary proteins (A). (B) Effect of removing *unc-74* from the mix on the *Ode*(*29–63–38–8)*/Lev-nAChR subtype. Note the relative change in ACh and Lev responses. (C) Effect of removing *ric-3* on the *Ode*(*29–63–38–8*) : Lev-nAChR subtype. The ACh current responses were reduced to <50% of the control. (D) Effect of removing *unc-50* on the *Ode*(*29–63–38–8*) or Lev-nAChR subtype. Note the dramatic decrease in currents elicited by all agonists.

A7.2 Supplementary Results

A7.2.1 Supplementary results S1. UNC-74 is a gene that encodes a transmembrane thioredoxin that can affect expression of nAChRs [26]. When we expressed the *Ode(29–63–8–38)* receptor with RIC-3 and UNC-50 but without UNC-74, the oocytes responded with acetylcholine currents that were only slightly reduced (mean 9%, S2-B). However, the order of the agonist potency series changed from 100 µM acetylcholine > 100 µM levamisole to 100 µM acetylcholine ≈ 100 µM levamisole (S2-A, B). We tested the agonist potency series of all the anthelmintic agonists and found that their normalized responses were significantly different ($p < 0.0001$, F-test). Thus, UNC-74 was not an absolute requirement for expression of *Ode(29–63–8–38)* but affected the pharmacological profile of the expressed receptors suggesting that it changed the balance of the receptor subtypes types present. RIC-3 is an

endoplasmic reticulum resident protein that acts as a nAChR chaperone. RIC-3 enhances functional expression of some nAChRs, whilst inhibiting expression of other nAChRs [49,50,51]. RIC-3 stabilizes receptor intermediates and promotes maturation of receptors through subunit-specific interactions with nAChR subunits [52]. When we removed just RIC-3 from the mix, the acetylcholine and levamisole currents were reduced to < 60 % of control (S2-A, C). When we compared the acetylcholine-normalized responses of all the agonists we found that they were significantly different ($p< 0.0001$, F-test) suggesting that the balance of the receptor types present had changed.

The most striking decrease in current amplitude was obtained when just UNC-50 was removed. The acetylcholine current amplitudes obtained were < 20 % of control (S2-D). UNC-50 is a Golgi resident protein that is required to prevent some nAChR types from being trafficked to and degraded by the lysosomal system [53]. In the absence of UNC-50, it is reasonable to postulate that only a few synthesized receptors make it to the cell membrane. When we compared the acetylcholine-normalized responses of all the anthelmintic agonists to the control, we again found that they were significantly different ($p< 0.0001$, F-test), suggesting that the balance of the receptor types expressed was changed.

A7.3 Supplementary text

A7.3.1 Text S1 Materials and Methods: Ca^{2+}-permeability measurements. For these set of experiments, we increased external Ca2+ in the recording solution from 1 mM to 10 mM without changing the concentration of the other ions. We used the GHK equation to calculate the permeability ratio, *PCa/PNa*. Due to BAPTA treatment before recordings, we assumed the internal [Ca2+] to be negligible; we also assumed permeability to Na and K, *PNa* and *PK*, are equal. Ionic activities were used for the calculations (activity coefficients:

0.56 for Ca2+ and 0.72 for Na+ and K+). Below is the GHK equation used to calculate the calcium permeability ratio, with the activity coefficients for Na+, K+ and Ca2+ inserted:

Erev = RT/F

*In{(PNa*0.72[Na]o+PK*0.72[K]o+4P'*0.56[Ca]o)/{PNa*0.72[Na]i+PK*0.72[K]i)}*.

Where R is the universal gas constant (8.314 JK-1mol-1); F is Faraday's constant (96485 Cmol-1); T is the temperature (room temperature, 298 K); and *P' = PCa/PNa{1/(1+eFErev/RT)}*.

A7.3.2 Table S1.0 Primers used for the PCR and cloning of *O. dentatum* AChR subunits

Gene name	Primer name	Primer sequence
Ode-unc-29	F-Hind3	AAAAAGCTTATGCGTCTCGAACCGTTACTTC
	R-Apa1	TTTGGGCCCTAAACCCGTACAGTCATAAAACAAT
Ode-unc-38	F-Xho1	AAACTCGAGATAGCTGGTTGCAAGTGCGTATT
	R-Apa1	TTTGGGCCCTCTCAACAAAATTGGCCTAATATAC
Ode-unc-63	F-Xho1	AAACTCGAGATGCTGACGCGACAAGTGTTC
	R-Apa1	TTTGGGCCCTACCCAGCCGGCTGCTCGC
Ode-acr-8	F-Hind3	AAACTCGAGCTTGGCTAGCTTAAAACTAAGATT
	R-Apa1	TTTGGGCCCAACCATAATACTATACATATCTCAGA

A8.0 Acknowledgements

We are grateful to Debra J Woods, Zoetis Animal Health, Kalamazoo, MI for the generous supply of derquantel. We would like to thank Prof. Shu Hua Xiao, National Institute of Parasitic Diseases, Shanghai, Peoples' Republic of China for the gift of tribendimidine. The authors would like to thank Dr. Robin Beech, McGill University, Canada for his help and comments concerning the phylogenetic analysis. We particularly thank Elise Courtot, INRA, Nouzilly, France and Dr. Jeff Beetham, Department of Vet Pathology, Iowa State University for assistance cloning the receptor subunits.

A9.0 Author Contributions

Conceived and designed the experiments: SKB CLC CN APR RJM. Performed the experiments: SKB CLC JCo MA APR. Analyzed the data: SKB CLC CN APR RJM. Contributed reagents/materials/analysis tools: CLC CN NP APR RJM EC. Wrote the paper: SKB CLC CN JCa APR NP RJM.

APPENDIX B. ANTHELMINTICS: THE BEST WAY TO PREDICT THE FUTURE IS TO CREATE IT

A paper published in *Veterinary Parasitology* (2015)[1]

Richard J. Martin[2*], Saurabh Verma[2], Shivani Choudhary[2], Sudhanva Kashyap[2], Melanie Abongwa[2], Fudan Zheng[2], Alan P. Robertson[2]

[1] Reprinted with permission of *Vet Parasitol* (2015), **212**(1-2): 18–24
[2] Department of Biomedical Sciences, Iowa State University, Ames, IA 50011, USA
[*] Corresponding author and Distinguished Professor, Department Biomedical Sciences, Iowa State University

B1.0 Abstract

'The best way to predict the future is to create it.' When we look at drugs that are used to control parasites, we see that new knowledge has been created (discovered) about their modes of action. This knowledge will allow us to predict combinations of drugs which can be used together rationally to increase the spectrum of action and to slow the development of anthelmintic resistance. In this paper we comment on some recent observations of ours on the modes of action of emodepside, diethylcarbamazine and tribendimidine. Emodepside increases the activation of a SLO-1 K^+ current inhibiting movement, and diethylcarbamazine has a synergistic effect on the effect of emodepside on the SLO-1 K^+ current, increasing the size of the response. The combination may be considered for further testing for therapeutic use. Tribendimidine is a selective cholinergic nematode B-subtype nAChR agonist, producing muscle depolarization and contraction. It has different subtype selectivity to levamisole and may be effective in the presence of some types of levamisole resistance. The new information about the modes of action may aid the design

of rational drug combinations designed to slow the development of resistance or increase the spectrum of action.

B1.1 Keywords

Anthelmintic; mode of action; tribendimidine; emodepside; diethylcarbamazine

B2.0 Introduction

'The best way to predict the future is to create it.' This quote is usually ascribed to Abraham Lincoln and leads to some interesting thoughts when applied to different research fields including our own field of study, that is, anthelmintics. What are we creating and what can we see for the future for anti-parasitic drugs? We are creating new techniques for the screening of anthelmintic drugs, we are creating new methods for studying the modes of actions of anthelmintics and we are creating new ways for detecting anthelmintic resistance (Gilleard and Beech, 2007 and Lanusse et al., 2014). We are also creating better awareness of the 'neglected tropical diseases' (Hotez et al., 2008) of humans which include ascariasis, hookworm and trichuriasis and better awareness of the link between human and animal medicine, the 'One Health' concept. Our western economic system has also produced a more favorable economic environment for the development of animal anthelmintics, than anthelmintics for humans. Currently, we limit the damage done by nematode parasites of animals with pasture management, and improved targeted metaphylactic and therapeutic use of anthelmintics; for humans, clean water and sanitation are limiting factors (like clean pasture for animals) while mass drug administration (MDA) has similarities to the regular metaphylactic use of anthelmintics for animals. Vaccinations against parasites for both humans and animals are very desirable but so far they have limited efficacy.

The advances and creations listed above lead to a number of logical predictions for the future use and development of anthelmintics. We are confident that the development and better understanding of anthelmintic properties will continue, at a steady but modest pace, driven by economic, human and animal needs. We think that the economic pressures associated with animal medicine will remain greater than for human medicine and focused on the development of novel 'resistance-busting' anthelmintics. Success in research can be limited by funding as was said by the father of modern drug development, Paul Ehrlich, Fig. 1 (1854–1915), who recognized success required the four Gs: *Gluck, Geduld, Geshcick und Geld* (luck, patience, skill and money, (Perutz, 1988). The 'money' for animal anthelmintics comes from the market for anti-parasitic drugs and chemicals for small animals and livestock which was estimated at $11 billion (Evans and Chapple, 2002). This contrasts with the market for human anthelmintics which is only $0.5 billion despite some 2 billion humans being infected in developing countries, around 25 cents per person annually! Given that the out of pocket costs of new human drugs may be $403 million (at year 2000 valuations (DiMasi et al., 2003) or more, we can see that the commercial development of human anthelmintic drugs is not favorable. It seems more likely that the economics of animal health will drive the development and advance of the knowledge base of animal anthelmintics and that these developments will be applied and adapted for human use (ivermectin and perhaps emodepside) unless private charities, governments and foundations overcome the financial limitations. In addition to the gradual development of resistance-busting anthelmintics we see: developments in our understanding of the modes of action of anthelmintics; we see more logical combinations of anthelmintics to slow down or counter the development of resistance and; also new methods for detecting anthelmintic resistance.

Fig. 1. Paul Erlich in his Frankfurt office, *circa* 1900, the father of modern chemotherapy, who worked on trypanosome diseases and popularized the concept of the 'magic bullet' (magische Kugel, the perfect therapeutic agent).

Our lab has focused on understanding of the modes of action of anthelmintics and in this paper we illustrate some of our recent observations and developments in our understanding of the actions of emodepside, diethylcarbamazine and tribendimidine. The mode of action of these anthelmintics involves effects on membrane ion-channels and has required us to use electrophysiological techniques for their study (Martin et al., 1996b). We think that better knowledge of the mode of action of these compounds will allow rational combination with other anthelmintics to increase potency, spectra and allow a slowing of the speed of development of resistance in animal and human parasites. This paper is based on a lecture given to the World Association for the Advancement of Veterinary Parasitology (WAAVP) in Liverpool, 2015 and covers: (1) emodepside, an anthelmintic used for small animals, which has the potential for being used for human use to control filarial parasites; (2)

diethylcarbamazine, a long serving anthelmintic still used for the control of filariasis in humans and; (3) tribendimidine, a recent anthelmintic developed by China for human use.

B3.0 Emodepside

Emodepside is a cyclooctadepsipeptide developed by Bayer, Fig. 2, which is related to its parent compound, PF1022A (Martin et al., 1996a) which has broad-spectrum anthelmintic activity. Emodepside has an inhibitory effect on locomotion that allowed (Guest et al., 2007) to use a *C. elegans* mutagenesis screen to find that *slo-1* (a Ca^{2+}-dependent K^+ channel) mutant alleles were resistant to the inhibitory effects of emodepside. (Crisford et al., 2011) also described transgenic experiments in which *C. elegans* SLO-1a channels were swapped for KCNMA1, the human orthologue of SLO-1 channels. These studies found that the sensitivity to emodepside in the rescues depended upon the origin of the SLO-1 channel: the human KCNMA1 channel was 10–100 times less sensitive to emodepside than the rescues expressing *C. elegans* SLO-1a channel. These experiments suggested that SLO-1Ca^{2+}-dependent K^+ channels of nematodes are a major part of the target site of emodepside. Expression of *C. elegans* SLO-1a channels in *Xenopus* oocytes have revealed that emodepside can directly open these channels (Kulke et al., 2014) and that emodepside action on this splice variant of the channel does not require the presence of additional receptors like the latrophilin receptors for an emodepside effect (Willson et al., 2004). It does not however, rule out a contribution of latrophilin receptors to the overall mode of action of emodepside in parasites as indicated by the interaction of Lat-1 and emodepside (Saeger et al., 2001).

SLO-1 K^+ channels have large (~200 pS) single-channel conductances and are also known as ‘big’ potassium (BK) channels. These channels serve to clamp the membrane potential near the potassium reversal potential and inhibit electrical excitability. The SLO-1 K^+ channel, has a different function to the high conductance Ca^{2+}-dependent Cl^- channel

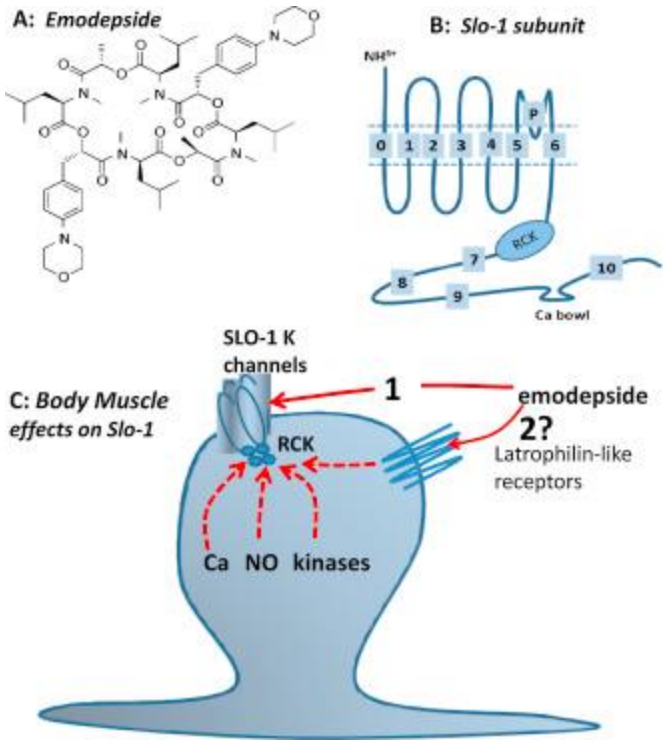

Fig. 2. Summary diagrams of emodepside structure, Slo-1 subunit and a model of the mode action of emodepside on nematode body muscle. A: Emodepside. B: Line diagram of structure of one SLO-1 subunit; each SLO-1 K^+ channel is made up of 4 of these subunits. C. Putative mode of action of emodepside on SLO-1K^+ channels in the muscle: act directly (1) or indirectly by stimulating latrophilin-like receptors (2) and signaling cascades that may involve NO, protein Kinase C and/or calcium. It is unlikely that emodepside acts at the extracellular surface of the SLO-1 K^+ channel because of the slow time course of its action. It is very lipophilic and could act in the lipid membrane phase on the SLO-1 K^+ channel or move into the cytoplasm and act intracellularly. A SLO-1 K^+ channel (C) is shown composed of 4 subunits along with the 'RCK' cytoplasmic regulatory region of the channel. (Martin et al., 2012).

(Thorn and Martin, 1987) which is associated with the transport of carboxylic acids from anaerobic metabolism of glucose (Valkanov and Martin, 1995). Subunits homologous to the vertebrate SLO-1 K^+ channels are found in *C. elegans* and *Ascaris suum* (Buxton et al., 2011). The SLO-1 K^+ channels are composed of 4 α-subunits; α-subunits have seven (S0–S6) transmembrane regions, a P-loop between S5 and S6, a large intracellular domain (S7-S-10) and a well conserved 'calcium bowl' between domains S9 and S10, Fig. 2. In addition, the regulator of the K^+ channel conductance (RCK) domains (S7, S8) contains high and low affinity calcium binding sites. The SLO-1 α-subunits show alternative splicing, producing

channels with different calcium sensitivities; in *C. elegans* there are up to 15 splice variants (including SLO-1a, SLO-1b and SLO-1c (Kulke et al., 2014 and Wang et al., 2001)). Each α-subunit of the channel has at least two high affinity calcium binding sites and one low affinity calcium/magnesium binding site. The channel also combines with secondary, regulatory β-subunits in vertebrates (Knaus et al., 1994) but these subunits have not yet been identified in *C. elegans*. However, *Drosophila,* which also lacks β subunits, has Slob proteins, which appear to carry out similar functions to the vertebrate β-subunits and these may be present in nematodes (Claridge-Chang et al., 2001).

The suggested function of the SLO-1 K^+ channels is that they adjust the resting membrane potential of electrically excitable cells and adjust the level of excitability, up or down, and so affect the response to other inputs. The opening of the SLO-1 K^+ channel, Fig. 2, is regulated by at least ten factors including: (1) membrane potential; (2) calcium; (3) magnesium; (4) NO; (5) CO; (6) arachidonic acid; (7) propagandist; (8) phosphorylation by cAMP-dependent protein kinase A; (9) phosphorylation by diacylgycerol/Ca^{2+}-dependent protein kinase C; and (10) phosphorylation by cGMP-dependent protein kinase G (Salkoff et al., 2006). The kinases allow SLO-1 to be coupled to multiple and quite diverse signaling cascades permitting different ways of adjusting the excitability of the cells. The different nematode neuropeptides could affect cAMP and cGMP levels (e.g., AF1, AP2, and PF1 and PF2) could then affect SLO-1 channels (Muhlfeld et al., 2009, Verma et al., 2007 and Verma et al., 2009). A selective agonist for the PF1 and/or a selective antagonist of the AF1 receptor would activate a SLO-1 K^+-like current and increase the efficacy of emodepside. The neuropeptides AF1, AF10 and PF2 also bind with low affinity to the latrophilin-like receptor, HC110-R of *Haemonchus contortus,* suggesting that emodepside could also have an indirect

mode of action on SLO-1 K^+ channels through these latrophilin-like receptors (Fig. 2) that are neuropeptide receptors (Muhlfeld et al., 2009).

We found (Buxton et al., 2011 and Martin et al., 2012 that *Asu-slo-1* is an evolutionarily conserved homologue of the *slo-1* genes, expressed in adult *A. suum* body muscle flaps. Using a two-micro-electrode current-clamp and voltage-clamp technique, Fig. 3A, we found in the nematode parasite *A. suum*, that emodepside activates SLO-1-like K^+ channels to produce hyperpolarization under current-clamp, Fig. 3B1, and an outward current when under voltage-clamp, Fig. 3B2. We also found that emodepside increased voltage-activated K^+ currents, Fig. 3C and D, in a time dependent manner. Emodepside, Fig. 3C, unlike PF1 did not decrease calcium currents and so emodepside does not work by releasing PF1 as has been hypothesized. We found that the effects of emodepside on the voltage-activated K^+ channels is Ca^{2+}-dependent and were inhibited by 5 mM 4-aminopyridine, Fig. 4A. The membrane hyperpolarization and increase in voltage-activated K^+ current produced by emodepside, Fig. 3B, are very slow in onset and increase over a period of more than 10 min (Buxton et al., 2011); the slow onset effect of emodepside might be due to its very lipophilic nature and a membrane partitioning effect. It may also be because the effects of emodepside are indirect and produced by activation of a slow signaling cascade. Fig. 4B and C shows that the effects of emodepside are potentiated by sodium nitroprusside (a NO donor), antagonized by iNOS inhibitors (NNLA), and inhibited by 1 μM staurosporine, an inhibitor of protein kinase (Buxton et al., 2011). Interestingly, these signaling molecules are known as activators of SLO-1 in other cells (Bolotina et al., 1994b, Holden-Dye et al., 2007,
C shows that the effects of emodepside are potentiated by sodium nitroprusside (a NO donor), antagonized by iNOS inhibitors (NNLA), and inhibited by 1 μM staurosporine, an

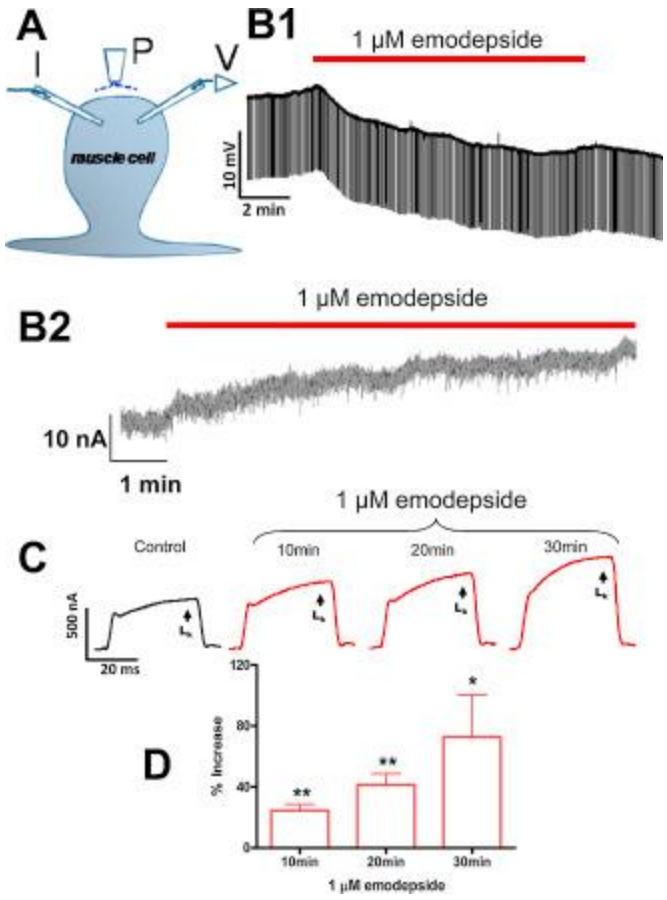

Fig. 3. Electrophysiological techniques (two micropipette current-clamp and voltage-clamps) for recording from *Ascaris suum*. A: *A. suum* muscle bag showing the current (I) and voltage (V) micropipettes in the bag, and the perfusion needle (P). B1: Representative current-clamp trace showing the slow hyperpolarizing membrane potential during and after 10 min application of 1 µM emodepside. B2: Outward current response to 1 µM emodepside at higher time resolution. Holding potential −35 mV. Notice that emodepside produces a gradually increasing current after a delay of some 30 seconds. The response does not plateau in the time period of this recording. C: Voltage-clamp traces of control K^+ current and the time-dependent effects of 1 µM emodepside on the K^+ currents, all to a step potential of 0 mV from a holding potential of −35 mV. D: Bar chart (mean ± S.E.) of 1 µM emodepside effect on steady state(LK) currents. Comparison was made between the control 0 mV step current at 30−40 ms and the corresponding current increased by emodepside at 10, 20 and 30 min. Emodepside increased LK currents at 10 min ($p < 0.01$, $n = 4$, paired *t*-test), 20 min ($p < 0.01$, $n = 4$, paired *t*-test) and 30 min ($p < 0.05$, $n = 4$, paired *t*-test). (Martin et al., 2012).

inhibitor of protein kinase (Buxton et al., 2011). Interestingly, these signaling molecules are known as activators of SLO-1 in other cells (Bolotina et al., 1994b, Holden-Dye et al., 2007, Mistry and Garland, 1998 and Wang et al., 1999) and therefore encourage the view that emodepside could act through either or both of these signaling cascades and the signaling

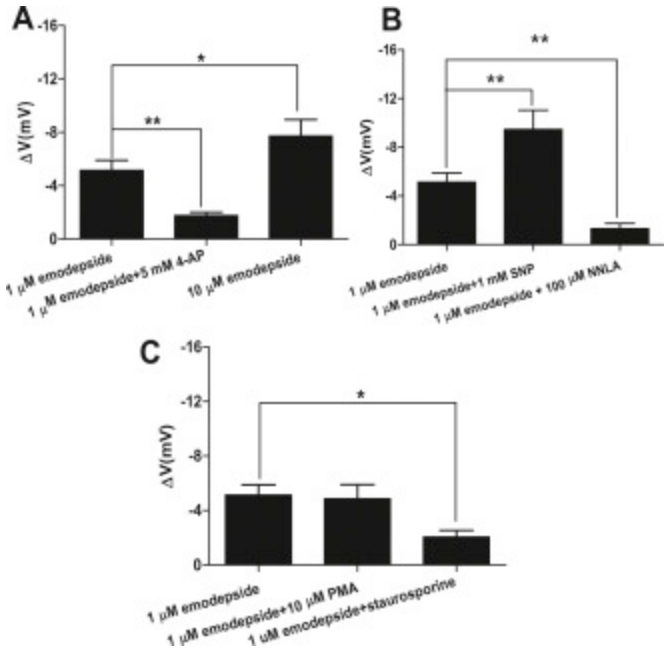

Fig. 4. Effect of 1 μM emodepside on membrane potential. A: Comparison was made between membrane potential before and during emodepside application. 1 μM emodepside caused a significant membrane hyperpolarization ($p < 0.001$, $n = 10$, paired *t*-test) which was reduced in the presence of 5 mM 4-aminopyridine ($p < 0.01$, $n = 8$, unpaired *t*-test). 10 μM emodepside caused an increased hyperpolarization in comparison to 1 μM emodepside ($p < 0.05$, unpaired *t*-test). B: Bar chart (mean ± s.e) of NO influence on emodepside-induced hyperpolarization. In the presence of 1 mM SNP, 1 μM emodepside caused an increased hyperpolarization ($p < 0.01$, $n = 4$, paired *t*-test). 100 μM NNLA decreased the hyperpolarization caused by 1 μM emodepside ($p < 0.01$, unpaired *t*-test). C: Bar chart (mean ± s.e) of effect of protein kinase modulators on emodepside-induced hyperpolarization. 10 μM PMA had no significant effects on the hyperpolarization caused by 1 μM emodepside. However, 1 μM staurosporine decreased the hyperpolarization caused by 1 μM emodepside ($p < 0.05$, unpaired *t*-test). (Martin et al., 2012).

cascades may be in series or parallel, Fig. 2C. A number of studies on the mammalian orthologues of SLO-1 show that they are directly and alternately regulated by complex, multiple signaling cascades, involving NO and diacylglycerol or PKC activation (Ghatta et al., 2006 and Salkoff et al., 2006). It is pointed out that NO signaling pathways in mammals may not be conserved in all species of nematode.

Thus emodepside appears to selectively activate the SLO-1 K^+ current that is present in nematodes but has less effect on the SLO-1 K^+ currents of vertebrates. This can explain the selective toxicity of the drug. The existence and mechanisms of resistance to emodepside

in nematode parasites remain to be studied but could involve several different mechanisms including changes in the splice forms of the SLO-1 K^+ channel or its regulation by different signaling cascades. However, such resistance, depending on the specific mechanism, might be countered (Verma et al., 2007 and Verma et al., 2009) by a selective agonist for the FMRFamide PF1 receptor and/or a selective antagonist of the FMRFamide AF1 receptor which would activate a SLO-1 K^+-like current and increase the efficacy of emodepside. An increased knowledge of the physiology of target site of emodepside provides a new way of designing drug combinations. The complex nature of SLO-1 K^+ regulation suggests that if there were resistance to emodepside it would be complex in nature and therefore likely to be polygenic involving multiple mechanisms.

B4.0 Diethylcarbamazine

Diethylcarbamazine, Fig. 5A, is an antifilarial drug that has been used since 1947 against lymphatic filariasis and loiasis. It is still an important and effective antifilarial drug but its mode of action is not fully described. Diethylcarbamazine has been suggested to have an indirect, host mediated mode of action: it appears to alter host arachidonic acid, nitric oxide metabolic pathways and inhibits NF-κB, which together in an unknown way leads to immobilization and sequestration of the microfilariae (Maizels and Denham, 1992 and Peixoto and Silva, 2014). Diethylcarbamazine activity against *B. malayi* microfilariae is abolished in inducible nitric oxide synthase knockout mice ($iNOS^{-/-}$), suggesting that diethylcarbamazine activity is dependent on host inducible nitric oxide synthase (iNOS) and nitric oxide (McGarry et al., 2005).

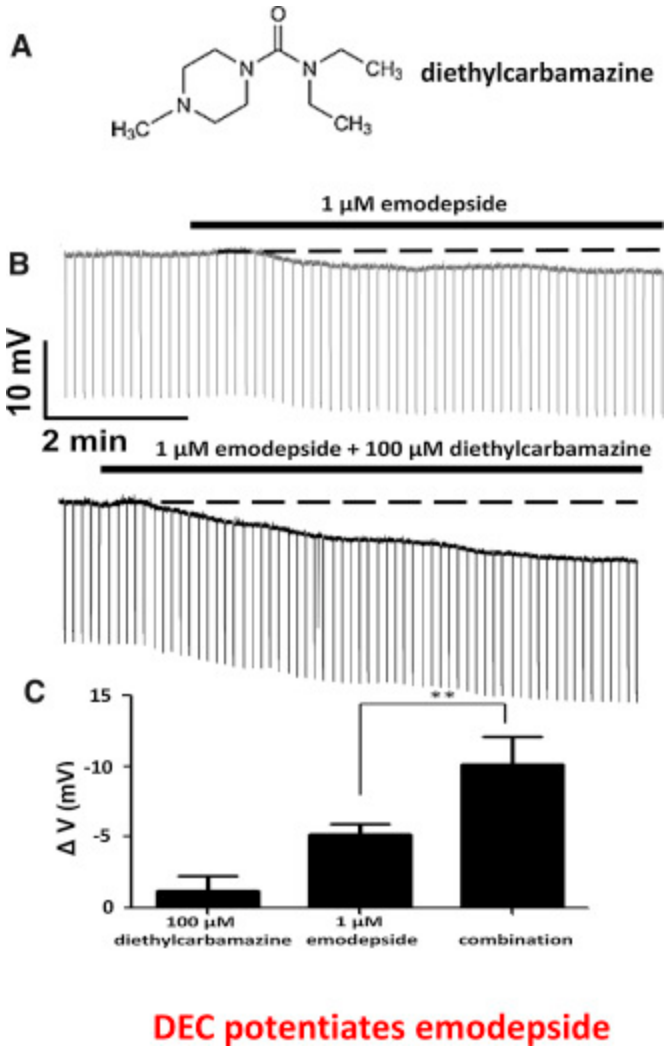

Fig 5. The combined effect of emodepside and diethylcarbamazine is greater than the effect of emodepside alone on *A. suum* membrane potential. A: Chemical structure of diethylcarbamazine. B: Representative current-clamp traces showing the membrane potential before, during 1 µM emodepside application (top trace) and during application of 1 µM emodepside plus 100 µM diethylcarbamazine (lower trace). The time delay between the end of the application of 100 µM diethylcarbamazine and 1 µM emodepside plus 100 µM diethylcarbamazine was 10 min. The change in membrane potential between the beginning of the 100 µM diethylcarbamazine and application of 1 µM emodepside plus 100 µM diethylcarbamazine was a hyperpolarization of 1.5 mV. C: Bar chart (mean ± i.e.) of diethylcarbamazine effect on emodepside-induced hyperpolarization. 100 µM diethylcarbamazine increased the hyperpolarization caused by 1 µM emodepside ($p < 0.01$, $n = 5$, unpaired *t*-test. (Buxton et al., 2014a).

We were interested to determine how diethylcarbamazine would affect calcium-dependent SLO-1 K^+ currents in isolated *A. suum* muscle flap preparations, and how diethylcarbamazine interacts with emodepside. The interest was prompted by observations in vertebrates (Bolotina et al., 1994a) which show that nitric oxide activates SLO-1 K^+ channels and observations on *A. suum* indicating the presence of nitric oxide synthase and of SLO-1 K^+ channels which show positive modulation by a nitric oxide pathway (Buxton et al., 2011). We hypothesized that diethylcarbamazine, with effects on arachidonic acid and nitric oxide pathways, would increase activation of SLO-1 K^+ currents in *A. suum* muscle and potentiate effects of emodepside on membrane potential (Buxton et al., 2014a). We conducted current-clamp and voltage-clamp electrophysiological experiments, using *A. suum* body muscle in the presence of sufficient calcium to allow activation of the SLO-1 K^+ currents. We found that indeed diethylcarbamazine, by itself, can increase activation of SLO-1 K^+ currents and potentiate the hyperpolarizing effects of emodepside. This to us was very interesting since it showed that diethylcarbamazine has a direct effect on the nematode parasite and its effects are not exclusively mediated via the host as has been suggest by earlier experiments. It seems likely that the effects of diethylcarbamazine may involve effects on NO or arachidonic acid metabolites both in the host and in the parasite. Although the mechanism of action of diethylcarbamazine remains to be further defined, the synergistic effect of emodepside and diethylcarbamazine suggests that the combination of the two drugs could be considered for therapeutic use for the treatment of filarial nematode infections.

B5.0 Tribendimidine

Tribendimidine, Fig. 6, is a symmetrical diamidine derivative, of amidantel which was developed in China for use in humans in the mid-1980s. It is a broad-spectrum

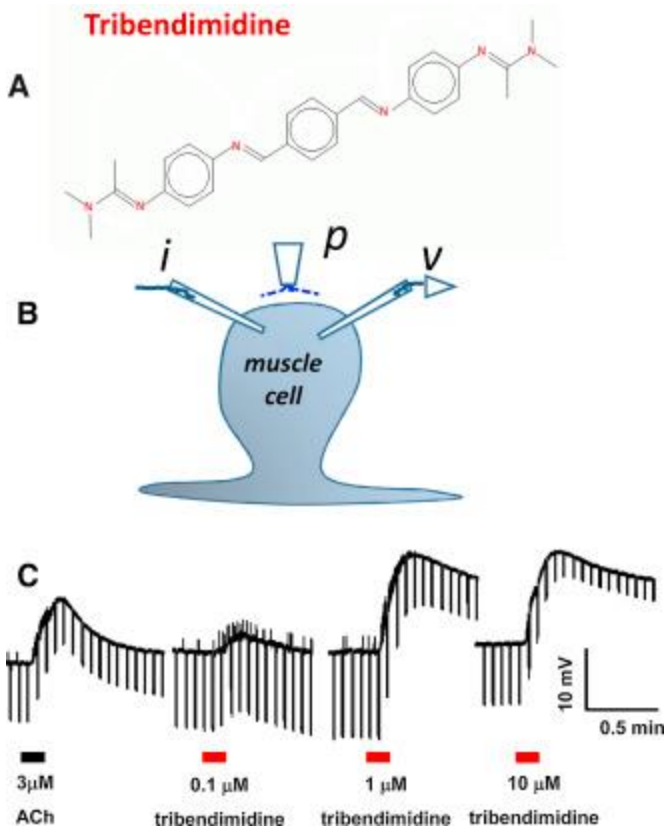

Fig. 6. A: Chemical structure of tribendimidine. B: Diagram of the two-micropipette current-clamp technique used to record the membrane potential (*v*) and to inject 40 nA hyperpolarizing 500 ms current pulses (i) at 0.3 Hz. *p* is the microperfusion pipette used to apply and wash off the drugs. C: Application of 3 μM acetylcholine and then 0.1, 1 and 10 μM tribendimidine to the same preparation. 1 μM tribendimidine produces a bigger depolarization response (upward movement) and conductance increase (reduction in the voltage responses to current injection, producing a narrowing of the width of the trace) than 3 μM acetylcholine (Robertson et al., 2015).

anthelmintic effective against soil-transmitted helminthiasis including hookworm, pinworms, roundworms, *Strongyloides* and flatworms (Xiao et al., 2005 and Xu et al., 2014) of humans. Molecular studies (Hu et al., 2009) on *C. elegans* using null-mutants of the levamisole receptor subunits strongly suggested that tribendimidine is a cholinergic agonist that is selective for the same nematode muscle nAChR as levamisole. When we looked at these studies we found that there are no direct electrophysiological observations in nematode parasites that had been made to test this hypothesis and we were aware that sometimes

observations on the model Clade V nematode were not always the same in parasitic nematodes, particularly for the parasites from a different Clade. We were also interested in trying to explain why tribendimidine is effective against some nematode parasites when levamisole is not.

We tested the effects of tribendimidine on the electrophysiology, Fig. 6, and contraction of *A. suum* muscle (Robertson et al., 2015) and found that tribendimidine produces a dose-dependent depolarization associated with an increase in the conductance of the muscle membrane as the nicotinic receptors (nAChRs) open, Fig. 6. We found that tribendimidine was more potent than acetylcholine and had an EC_{50} of 0.8 μM. We also tested the effects of the nicotinic antagonist mecamylamine, a potent antagonist of muscle nAChRs of parasitic nematodes and found that 3 μM was potent against tribendimidine; the antagonist effects of mecamylamine confirmed the cholinergic action of tribendimidine on the nAChRs of the parasite *A. suum.*

We characterized the pharmacological profile of tribendimidine using our *Ascaris* muscle contraction assay systems (Qian et al., 2006 and Robertson et al., 2002) with tribendimidine as the agonist and methyllycaconitine, paraherquamide and derquantel as antagonists to calculate the potency, pA_2, of the antagonists and the subtype of the selectivity of tribendimidine. We found that tribendimidine was more selective for the **B**-subytpe (bephenium preferring) nAChRs than the **L**-subtype (levamisole preferring) or the **N**-subtype (nicotine preferring). These observations showed the selectivity for the different groups of nAChRs present on the *Ascaris* muscle was not the same as levamisole and it was possible that levamisole-resistant parasites would remain sensitive to tribendimidine. To test this we used, *Oesophagostomum dentatum* L_3 larval migration inhibition assays with levamisole-

sensitive isolates and levamisole-resistant isolates and tested the effects of tribendimidine on motility. Levamisole was less effective ($p < 0.001$, *F*-test) in inhibiting migration of levamisole-resistant larvae than the migration of levamisole-sensitive larvae. We tested the effects of tribendimidine to the limits of its solubility, ~30 μM, and found that tribendimidine was actually more potent on the levamisole-resistant isolate than on the levamisole-sensitive isolates ($p < 0.001$, *F*-test). The larger effect of tribendimidine on the levamisole-resistant, than the levamisole-sensitive isolates at lower tribendimidine concentrations, supports the view that levamisole and tribendimidine do not activate identical nAChR receptor subtypes. The higher efficacy of tribendimidine on the levamisole resistant O. dentatum isolate might indicate a case of negative cross resistance (Miltsch et al., 2013)

We have been able to express, in *Xenopus* oocytes a range of different nAChR receptor subtypes derived from anthelmintic sensitive *Oesophagostomum dentatum* clones of their nAChR receptor subunits (Buxton et al., 2014b). Fig. 7 shows a diagram of the subunit composition of two nAChR subtypes expressed in oocytes, one composed of Ode-UNC-29:Ode-UNC-63:Ode-UNC-38, the other composed of Ode-UNC-29:Ode-UNC-63:Ode-UNC-38:Ode-ACR-8 subunits. The Ode-UNC-29:Ode-UNC-63:Ode-UNC-38 receptor was more sensitive to tribendimidine and pyrantel but not to levamisole or nicotine. We can see that the receptor subunit arrangements affect their pharmacology and that not all cholinergic anthelmintics have the same selectivity.

Our understanding to date is that there are a range of pharmacologically different nAChR subtypes present in parasitic nematodes and the pharmacology of the receptor subtypes varies with the subunit composition of the receptor which varies with the tissue and

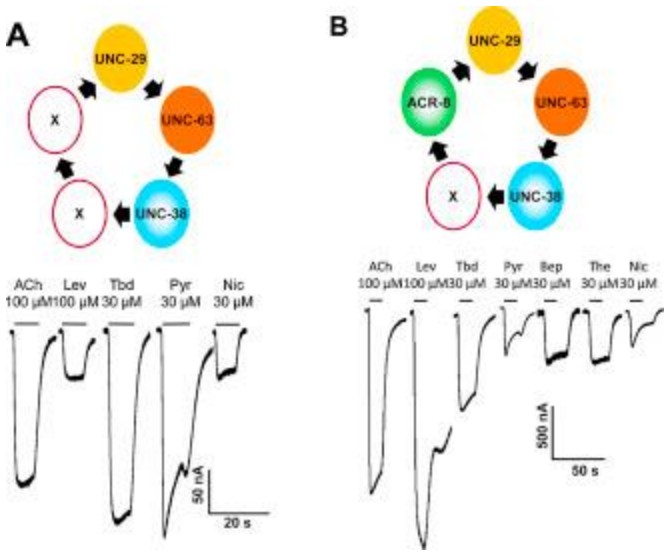

Fig. 7. Tribendimidine as an agonistof Ode-(29 – 8 – 38 – 63) and Ode-(29-63-38) receptors expressed in oocytes, currents recorded under voltage-clamp at −60 mV (Buxton et al., 2014b) A: Tribendimidine and pyrantel at 100 µM is more potent than levamisole on the Ode(29 – 38 – 63) receptor. B: Levamisole at 100 µM is more potent than acetylcholine tribendimidine, pyrantel and nicotine on the expressed Ode(29 – 8 – 38 – 63) receptor. Note that derquantel produces competitive antagonism of the effects of levamisole but a non-competitive antagonism of pyrantel, suggesting that the mode of action of levamisole and pyrantel are not identical.

species of the nematode parasite. There will therefore be cholinergic anthelmintics that act on different nAChR subtypes and it is therefore possible that there will not always be cross-resistance between the cholinergic anthelmintics.

B6.0 Discussion

Diethylcarbamazine is used mostly for treatment of filariasis in humans but has effects against hookworm and ascariasis, intestinal nematode parasites (Meyrowitsch and Simonsen, 2001). In addition to the treatment of filariasis, diethylcarbamazine, as a single dose treatment, has modest effects on intestinal nematode parasite infections including ascariasis and trichuriasis but is more effective when combined with ivermectin or albendazole (Belizario et al., 2003). We have seen in our experiments that emodepside increases a Slo-1 K^+ current in the parasite and that diethylcarbamazine can potentiate the

effect of emodepside. Both of these compounds have been used separately as single anthelmintics but we do not have data on their therapeutic effect when used in combination. This information is desirable to obtain and if therapeutic combination of emodepside and diethylcarbamazine is safe and more potent than either compound in isolation, such synergism could slow the development of resistance and extend the spectrum of action of the therapy.

Levamisole and tribendimidine have different selectivities for nAChR subtypes. In *Ascaris* tribendimidine is more selective for the B-subtype rather than the L-subtype of nAChR. Tribendimidine is more potent on expressed *O. dentatum* receptor subtypes composed of Ode-UNC-29:Ode-UNC-63:Ode-UNC-38 subunits, than on subtypes composed of Ode-UNC-29:Ode-UNC-63:Ode-UNC-38:Ode-ACR-8 subunits (Buxton et al., 2014b). The difference in selectivity suggests that tribendimidine has the potential to be effective against nematode parasites that are not sensitive to levamisole, including those parasites that have developed resistance. A careful combination of different cholinergic anthelmintics has the potential to extend the spectrum of action of the drug treatment. Tribendimidine has an interesting and promising pharmacology and has the potential for single-dose MDA with its broad-spectrum of action. Although tribendimidine appears safe and has broad-spectrum activity, a large-scale clinical study is advocated to further verify human safety.

B7.0 Conclusion

We have been excited by our discovery of further details of the modes of action of the different anthelmintics that we work on and believe that the information will be useful for defining mechanisms of resistance to the anthelmintic drugs that we have studied. We also think that the improved understanding of their mechanisms of action will lead to better use of

these compounds and logical design of synergistic combinations. We do not look back, but ***forward***, to the future.

B8.0 Funding

The research project culminating in this paper was funded by the National Institute of Allergy and Infectious Diseases (NIH) grant R01 A1047194 to RJM and R21 AI092185 to APR. The funders had no role in study design, data collection and analysis, decision to publish, or preparation of the manuscript.

APPENDIX C. THE *ASCARIS SUUM* NICOTINIC RECEPTOR, ACR-16, AS A DRUG TARGET: FOUR NOVEL NEGATIVE ALLOSTERIC MODULATORS FROM VIRTUAL SCREENING

A paper published in *International Journal for Parasitology: Drugs and Drug Resistance* (2016)[1]

Fudan Zheng[2], Alan P. Robertson[3], Melanie Abongwa[3], Edward W. Yu[2,4], Richard J Martin[3*]

[1] Reprinted with permission of *Int J Parasitol Drugs Drug Resist* (2016), **6**(1): 60–73
[2] Department of Chemistry, College of Liberal Arts and Sciences, Iowa State University, Ames, IA 50011, USA
[3] Department of Biomedical Sciences, College of Veterinary Medicine, Iowa State University, Ames, IA 50011, USA
[4] Department of Physics and Astronomy, College of Liberal Arts and Sciences, Iowa State University, Ames, IA 50011, USA
[*] Corresponding author and Distinguished Professor, Department of Biomedical Sciences, Iowa State University
[3] Performed some of the experiments

C1.0 Abstract

Soil-transmitted helminth infections in humans and livestock cause significant debility, reduced productivity and economic losses globally. There are a limited number of effective anthelmintic drugs available for treating helminths infections, and their frequent use has led to the development of resistance in many parasite species. There is an urgent need for novel therapeutic drugs for treating these parasites. We have chosen the ACR-16 nicotinic acetylcholine receptor of *Ascaris suum* (Asu-ACR-16), as a drug target and have developed three-dimensional models of this transmembrane protein receptor to facilitate the search for new bioactive compounds. Using the human α7 nAChR chimeras and *Torpedo marmorata* nAChR for homology modeling, we defined orthosteric and allosteric binding sites on the Asu-ACR-16 receptor for virtual screening. We identified four ligands that bind to sites on

Asu-ACR-16 and tested their activity using electrophysiological recording from Asu-ACR-16 receptors expressed in *Xenopus* oocytes. The four ligands were acetylcholine inhibitors (SB-277011-A, IC_{50}, 3.12 ± 1.29 μM; (+)-butaclamol Cl, IC_{50}, 9.85 ± 2.37 μM; fmoc-1, IC_{50}, 10.00 ± 1.38 μM; fmoc-2, IC_{50}, 16.67 ± 1.95 μM) that behaved like negative allosteric modulators. Our work illustrates a structure-based in silico screening method for seeking anthelmintic hits, which can then be tested electrophysiologically for further characterization.

C1.1 Keywords

Asu-ACR-16; Structure-based drug discovery; Homology modeling; Orthosteric site; Allosteric modulator; *Xenopus* expression

C1.2 Abbreviations

ECD, extracellular domain; TID, transmembrane and intracellular domain; (+), principal subunit; (−), complementary subunit; NAM, negative allosteric modulator; nAChR, nicotinic acetylcholine receptor; AChBP, acetylcholine-binding protein

C2.0 Introduction

Soil-transmitted gastrointestinal nematodes, namely roundworms, whipworms and hookworms, infect approximately two billion people worldwide and pose a significant health challenge to humans and animals (de Silva et al., 2003 and Bethony et al., 2006). The infections with the soil-transmitted helminths can cause malnutrition, iron-deficiency anemia and impaired cognitive performance (Crompton, 2000 and Hotez et al., 2007). Currently, there are no effective vaccines available (Hewitson and Maizels, 2014), and sanitation is not adequate in many countries. The World Health Organization (WHO) recommends four anthelmintics for treatment and prophylaxis of soil-transmitted nematode infections: albendazole, mebendazole, levamisole and pyrantel (Keiser and Utzinger, 2008). The

repeated use of a limited number of anthelmintic drugs has led to an increase in drug resistance in animals and there are similar concerns for humans. It is therefore important to identify novel therapeutic compounds that selectively target receptors of parasitic nematodes so that we maintain effective therapeutics.

The nicotinic acetylcholine receptors (nAChRs) are pentameric ligand-gated ion channels that mediate synaptic transmission at neuromuscular junctions of vertebrates and invertebrates (Changeux and Edelstein, 1998). The neurotransmitter, acetylcholine, activates nAChRs by binding to orthosteric binding sites on the extracellular domain of the receptor and triggers the opening of the channel pore in the transmembrane domain. The opening of the nicotinic receptors leads to an influx of sodium and calcium depending on the receptor subtypes, as well as an output of potassium ions, followed by membrane depolarization and muscle contraction.

Nicotinic anthelmintics are selective agonists of nematode muscle nAChRs which cause spastic paralysis of the parasites (Martin and Robertson, 2010 and Buxton et al., 2014). There are three different pharmacological subtypes of nAChRs present on muscle of *Ascaris suum*. The anthelmintics, levamisole and pyrantel are selective agonists of L-subtypes of nAChRs in *A. suum* (Martin et al., 2012). Bephenium selectively activates B-subtypes of nAChRs. Nicotine and oxantel selectively activate N-subtypes of nAChRs in *A. suum* (Qian et al., 2006). The anthelmintic monepantel activates nAChRs which are composed of DEG-3-like subunits (*Haemonchus. contortus* MPTL-1, *Caenorhabditis. elegans* ACR-20 and *H. contortus* ACR-23 subunits (Rufener et al., 2010 and Buxton et al., 2014). We have selected the N-subtype of nAChR that is composed of ACR-16 subunits (Ballivet et al., 1996 and Polli et al., 2015) for a drug target, because it is pharmacologically different to the

other nicotinic receptor subtypes (Raymond et al., 2000), for further study. Asu-ACR-16 transcript has been found in *A. suum* muscle and may be involved in locomotion.

The ACR-16 nicotinic acetylcholine receptor of *A. suum* (Asu-ACR-16) is a homomeric receptor made up of five identical α subunits. Homomeric nAChRs have five identical orthosteric binding sites where agonists and competitive antagonists bind at the interface of two adjacent subunits. The orthosteric site is in the extracellular domain and is formed by the loops A, B & C of the principal subunit and by the loops D, E & F on the complementary subunit (Galzi et al., 1991 and Arias, 2000). In addition, three allosteric binding sites close to the orthosteric binding sites in the extracellular domain have been observed in the α7 nAChR-AChBP chimera (Spurny et al., 2015). In the transmembrane domain, an intrasubunit allosteric binding site has been found in *Rattus. norvegicus* α7 nAChR (Young et al., 2008), while an intersubunit allosteric binding site has been found in C. elegans glutamate-gated chloride channel (GluCl) (Hibbs and Gouaux, 2011). These well-studied binding sites in nAChRs or other Cys-loop receptors provided our framework for characterizing putative orthosteric and allosteric sites in Asu-ACR-16.

Because of the lack of a crystal structure for Asu-ACR-16, we used homology modeling to predict the protein structure, based on the observations that proteins with similar sequences usually have similar structures (Cavasotto and Phatak, 2009). In this study, we used homology modeling to predict the three-dimensional structure of Asu-ACR-16, based on the observed experimental structures of the human α7 nAChR chimeras and the *Torpedo marmorata* nAChR as templates. Virtual screening was performed for the ACR-16 orthosteric binding sites, using the predicted structure to identify the potential candidates of agonists and competitive antagonists. Allosteric binding sites were also used to examine the

binding properties of the virtual screening hits. Subsequently, we tested the pharmacological profiles of virtual screening hits on Asu-ACR-16 receptors expressed in *Xenopus laevis* oocytes, using a two-electrode voltage clamp to test the activity of the hits on the receptors.

C3.0 Materials and methods

C3.1 Identification of template structures

We selected the extracellular domain of Asu-ACR-16 (ECD-Asu-ACR-16) because it forms a homologomer that allows homology modeling. In addition, many of the agonists that activate Asu-ACR-16, acetylcholine, nicotine, cytisine, epibatidine (Abongwa et al., 2016), are also known to bind to the orthosteric binding sites of extracellular domain of *Lymnaea stagnalis* AChBP or *A. california* AChBP (Celie et al., 2004, Li et al., 2011, Rucktooa et al., 2012 and Olsen et al., 2014a). In addition to the orthosteric binding site, three separate allosteric binding sites in the extracellular domain of α7 nAChR are now recognized (Bertrand et al., 2008, Pan et al., 2012 and Spurny et al., 2015), increasing the possibility of identifying allosteric modulators.

The amino acid sequence of Asu-ACR-16 (Fig. 1) was obtained from the UniProtKB/SwissProt database with the accession number F1KYJ9 (Wang et al., 2011). Structural templates were identified by using BLASTP on NCBI network service (Altschul et al., 1997) and PSI-BLAST on the ProtMod server (Rychlewski et al., 2000) by searching in the Protein Data Bank (Berman et al., 2000). Three crystal structures of human α7 nAChR chimeras with different co–crystal ligands in orthosteric binding site were used: epibatidine bound (PDB code: 3SQ6; Li et al., 2011), no ligand (PDB code: 3SQ9; Li et al., 2011), and α-bungarotoxin bound (PDB code: 4HQP; Huang et al., 2013). These structures were selected as the templates for three different bound-forms of the ECD-Asu-ACR-16. The three

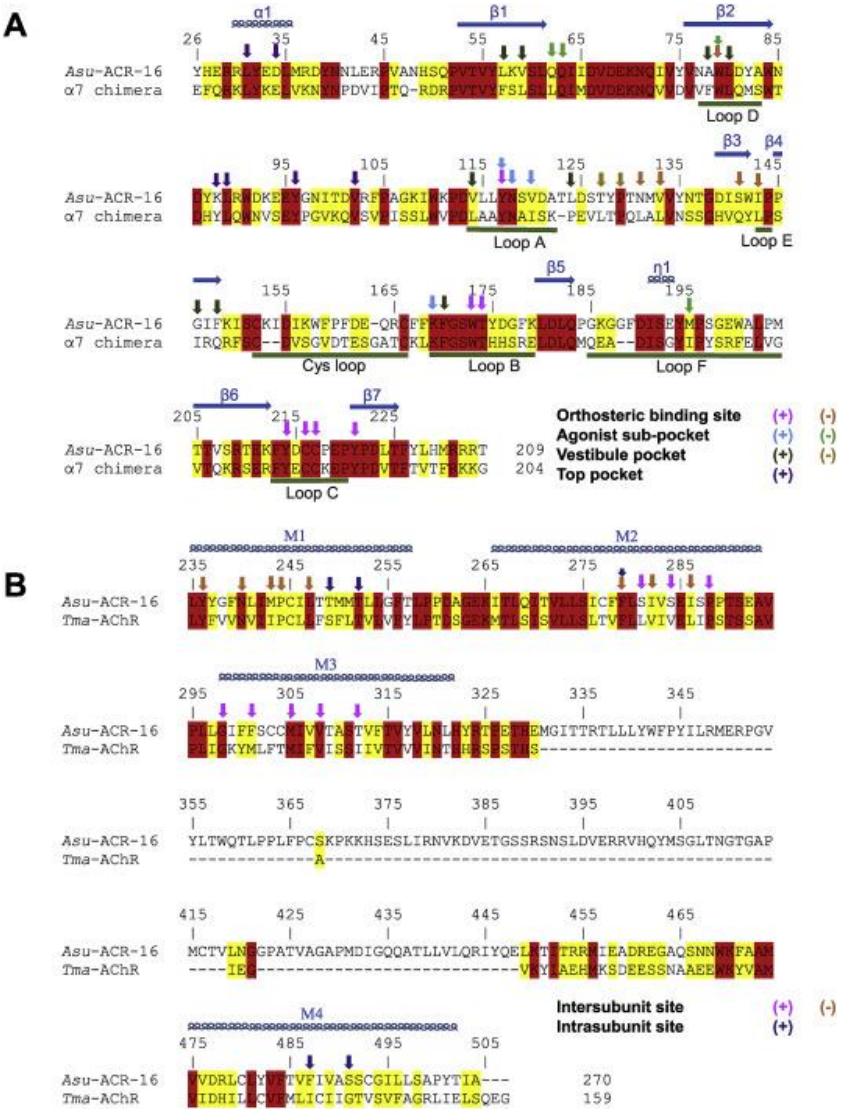

Fig. 1. (A) Sequence and numbering of the ECD-Asu-ACR-16 and its alignment with the template, human α_7 nAChR chimera subunit. Completely conserved residues (red background) and partially conserved residues (yellow background) are indicated. Secondary structures are shown schematically above the sequences. α_1 represents α helix. $\beta_{1\text{-}7}$ represent β sheet. η_1 represents α helix. The Cysteine loop and loops A - F are labeled by dark green bars. Residues in the orthosteric binding site are indicated by arrows (principal subunit, pink; complementary subunit, orange). Residues in three allosteric binding pockets are highlighted by arrows (principal subunit of agonist sub-pocket, turquoise; complementary subunit of agonist sub-pocket, green; principal subunit of vestibule pocket, dark green; complementary subunit of vestibule pocket, gold; principal subunit of top pocket, purple). (B) Sequence and numbering of the TID-Asu-ACR-16 and its alignment with the template TID-Tma-AChR subunit A. Completely conserved residues (red background) and partially conserved residues (yellow background) are indicated. Four transmembrane α helixes (M1, M2, M3 and M4) are shown schematically above the sequences. Residues in the allosteric binding pocket are indicated by arrows (principal subunit, pink; complementary subunit, orange). (For interpretation of the references to colour in this figure legend, the reader is referred to the web version of this article.)

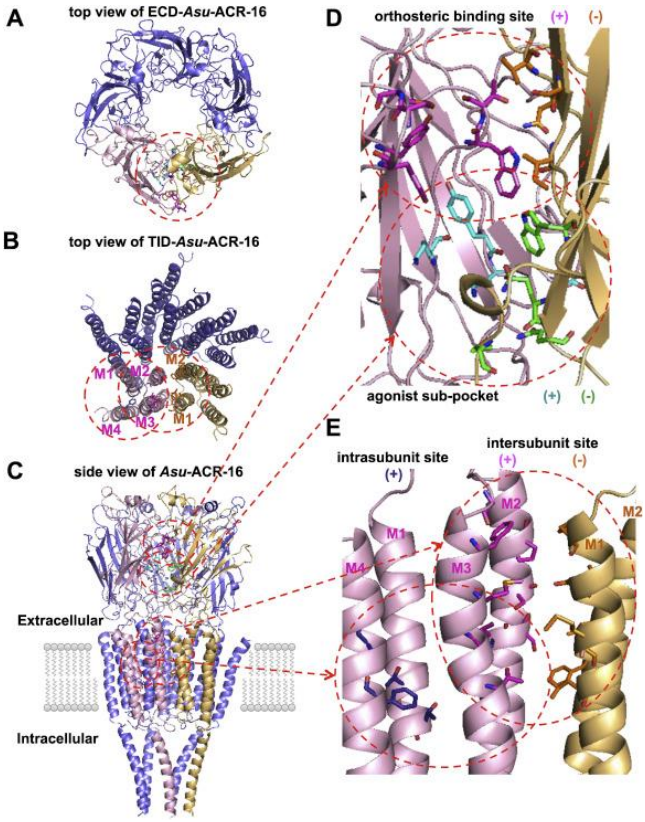

Fig. 2. (A) Ribbon diagram of the antagonist-bound model of ECD-Asu-ACR-16 viewed from the synaptic cleft, showing the location of the orthosteric binding site and agonist sub-pocket. For clarity, only the front two subunits are highlighted (principal subunit, light pink; complementary subunit, yellow). The residues that contribute to the orthosteric binding site (principal side, pink; complementary side, orange) and the agonist sub-pocket (principal side, turquoise; complementary side, green) are represented by sticks and highlighted inside the red dotted circle. (B) Ribbon diagram of the antagonist-bound model of TID-Asu-ACR-16 viewed above the membrane, showing the location of two transmembrane allosteric binding sites. For clarity, only the front two subunits are highlighted (principal subunit, light pink; complementary subunit, yellow). The residues that contribute to the intersubunit site (principal side, pink; complementary side, orange) and intrasubunit site (principal side, purpleblue) are represented by sticks and highlighted inside the red dotted circle. (C) Ribbon diagram of the antagonist-bound model of full-length Asu-ACR-16 viewed parallel to the membrane plane, showing the location of the orthosteric binding site and the agonist sub-pocket in the extracellular domain, the intersubunit and intrasubunit binding sites in the transmembrane domain. For clarity, only the front two subunits are highlighted (principal subunit, light pink; complementary subunit, yellow). The residues that contribute to the ligand binding sites are represented by sticks (orthosteric site: (+), pink; (−), orange; agonist sub-pocket: (+), turquoise; (−), green; intersubunit transmembrane site: (+), pink; (−), orange; intrasubunit transmembrane site: purpleblue) and highlighted inside the red dotted circle. (D) Detailed view of the orthosteric binding site and agonist sub-pocket in the antagonist-bound model of ECD-Asu-ACR-16. The principal subunit is colored light pink, whereas the complementary subunit is colored yellow. The residues that contribute to the orthosteric binding site (principal side, pink; complementary side, orange) and the agonist sub-pocket (principal side, turquoise; complementary side, green) are represented by sticks and highlighted inside the red dotted circle. Carbon is in either turquoise or green. Nitrogen is in blue. Oxygen is in red. (E) Detailed view of the transmembrane allosteric binding sites in the antagonist-bound model of TID-Asu-ACR-16. The principal subunit is colored light pink, whereas the complementary subunit is colored yellow. The residues that contribute to intersubunit site (principal side, pink; complementary side, orange) and intrasubunit site (principal side, purpleblue) are represented by sticks and highlighted inside the red dotted circle. Carbon is in either pink or orange or purpleblue. Nitrogen is in blue. Oxygen is in red. Sulfur is in yellow. (For interpretation of the references to colour in this figure legend, the reader is referred to the web version of this article.)

models were: the agonist-bound form ECD-Asu-ACR-16; the apo form ECD-Asu-ACR-16 and; the antagonist-bound form ECD-Asu-ACR-16 (Fig. 2A).

We modeled the transmembrane and intracellular domains of Asu-ACR-16 (TID-Asu-ACR-16, Fig. 2B) because of the presence of an intrasubunit allosteric binding site that is found in α7 nAChR and an intersubunit allosteric binding site that is demonstrated in a Cys-loop receptor, GluCl crystal structure in complex with ivermectin (Young et al., 2008, Bertrand et al., 2008 and Hibbs and Gouaux, 2011). Ivermectin is a known allosteric modulator of α7 nAChRs (Krause et al., 1998). The *T. marmorata* nAChR (PDB code: 2BG9 chain A; Unwin, 2005) is the only pentameric nAChR structure with the transmembrane domains and partial intracellular domains determined. Therefore, the transmembrane and intracellular domains of *T. marmorata* nAChR (TID-Tma-nAChR) were selected as the template for our TID-Asu-ACR-16 model.

The sequence of the ECD-Asu-ACR-16 and the human α7 nAChR chimera (SwissProt ID: P36544; Peng et al., 1994) were aligned using CLUSTALW multiple alignment (Thompson et al., 1994). The sequence of the TID-Asu-ACR-16 and TID-Tma-nAChR (SwissProt ID: P02711; Devillers-Thiery et al., 1983 and Devillers-Thiery et al., 1984) were aligned using CLUSTALW.

C3.2 Homology modeling of *Asu*-ACR-16

We used Modeller (Eswar et al., 2007) to build a three-dimensional model of ECD-Asu-ACR-16 and used JACKAL (http://wiki.c2b2.columbia.edu/honiglab_public/index.php/Software:Jackal) to build the model of TID-Asu-ACR-16 for each of the five subunits. These five subunits were then assembled to generate the pentamer using COOT software (Emsley and Cowtan, 2004). The

model geometry was first refined manually, and then optimized by PHENIX software (Adams et al., 2010). Each of the TID-Asu-ACR-16 subunits were then merged into the ECD-Asu-ACR-16 model by using COOT to edit and alter the C_α coordinates of residues around the outer membrane regions. The final optimized pentameric model was then visualized using the program PyMol (The PyMOL Molecular Graphics System, Version 1.7.4, Schrödinger, and LLC., Figs. 2C & S1).

C3.3 Structure-based virtual screening

Smiles strings of ligands were downloaded from the lead-like subset of commercially available compounds in the ZINC Database (Irwin et al., 2012) and were converted initially to PDB formats using the PHENIX-eLBOW program (Moriarty et al., 2009). The ligand and receptor input files were then prepared in PDBQT format for AutoDock Vina by using the AutoDock Tools package (Morris et al., 2009). For initial screening, a docking area was defined visually around the orthosteric binding site of ECD-Asu-ACR-16 (Fig. 2D S2A & S2B) by a grid box of 40 Å × 40 Å × 40 Å using 0.375 Å grid point spacing in AutoGrid. The conformations of ligands in the binding sites of the receptor were searched with GALS (Genetic Algorithm with Local Search; Morris et al., 1998). The binding free energies between the ligands and receptor were calculated by the combination of the knowledge-based and empirical scoring function in AutoDock Vina (Trott and Olson, 2010). The best nine binding modes of the ligand based on the binding affinities on the three bound-forms of ECD-Asu-ACR-16 models were implemented by AutoDock 20 runs for each ligand. Each docked ligand was then ranked by its highest binding affinity to the orthosteric binding site of the apo, agonist-bound, or antagonist-bound model. From the 60,000 screened molecules, we selected the top 9 ligands (0.015%) with the highest predicted affinities that had

appropriate binding modes within the ligand-binding pockets for further study. We rejected those compounds without a cationic nitrogen in their structure and that were known to be: acutely toxic, or carcinogenic, or respiratory depressants, caused dermatitis or conjunctivitis or to be significant environmental hazards as recorded on the compound Safety Data Sheets available from Sigma Aldrich (http://www.sigmaaldrich.com/safety-center.html).

The four virtual screen hits (Table 1) out of the top 9 selected ligands (44%) were also specifically docked into five allosteric binding pockets: the agonist sub-pocket (Fig. S2C & S2D); the vestibule pocket (Fig. S2E & S2F); the top pocket (Fig. S2G & S2H); the intersubunit and; the intrasubunit transmembrane sites (Fig. 2E S2I S2J). The docking area was defined visually around each allosteric binding pockets of Asu-ACR-16 by a grid box of 40 Å × 40 Å × 40 Å using 0.375 Å grid point spacing in AutoGrid. The docking was performed by AutoDock Vina (Fig. 3).

Table 1
Physicochemical properties and chemical structures of four virtual screen hits. The four hits are: fmoc-4-(naphthalen-2-yl)-piperidine-4-carboxylic acid (fmoc-2), SB-277011-A hydrochloride hydrate (SB-277011-A), fmoc-4-(naphthalen-1-yl)-piperidine-4-carboxylic acid (fmoc-1), (+)-butaclamol hydrochloride ((+)-butaclamol Cl). The molecular mass (Mol. Mass), number of hydrogen bondonors, number of hydrogen bond acceptors, number of rotatable bonds and partition coefficient (xlogP) are listed for each hits.

ZINC ID	44122512	26574567	44122502	02008410
Hits	fmoc-2	SB-277011-A	fmoc-1	(+)-butaclamol Cl
Structure	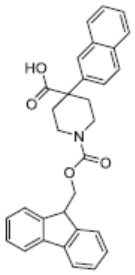	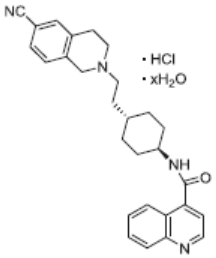	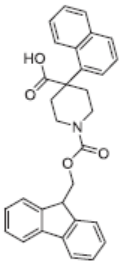	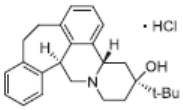
Mol. Mass	478	475	478	363
H-bondonors	0	1	0	2
H-bond acceptors	5	5	5	2
Rotatable bonds	5	5	5	1
XlogP	6.04	4.27	6.02	4.96

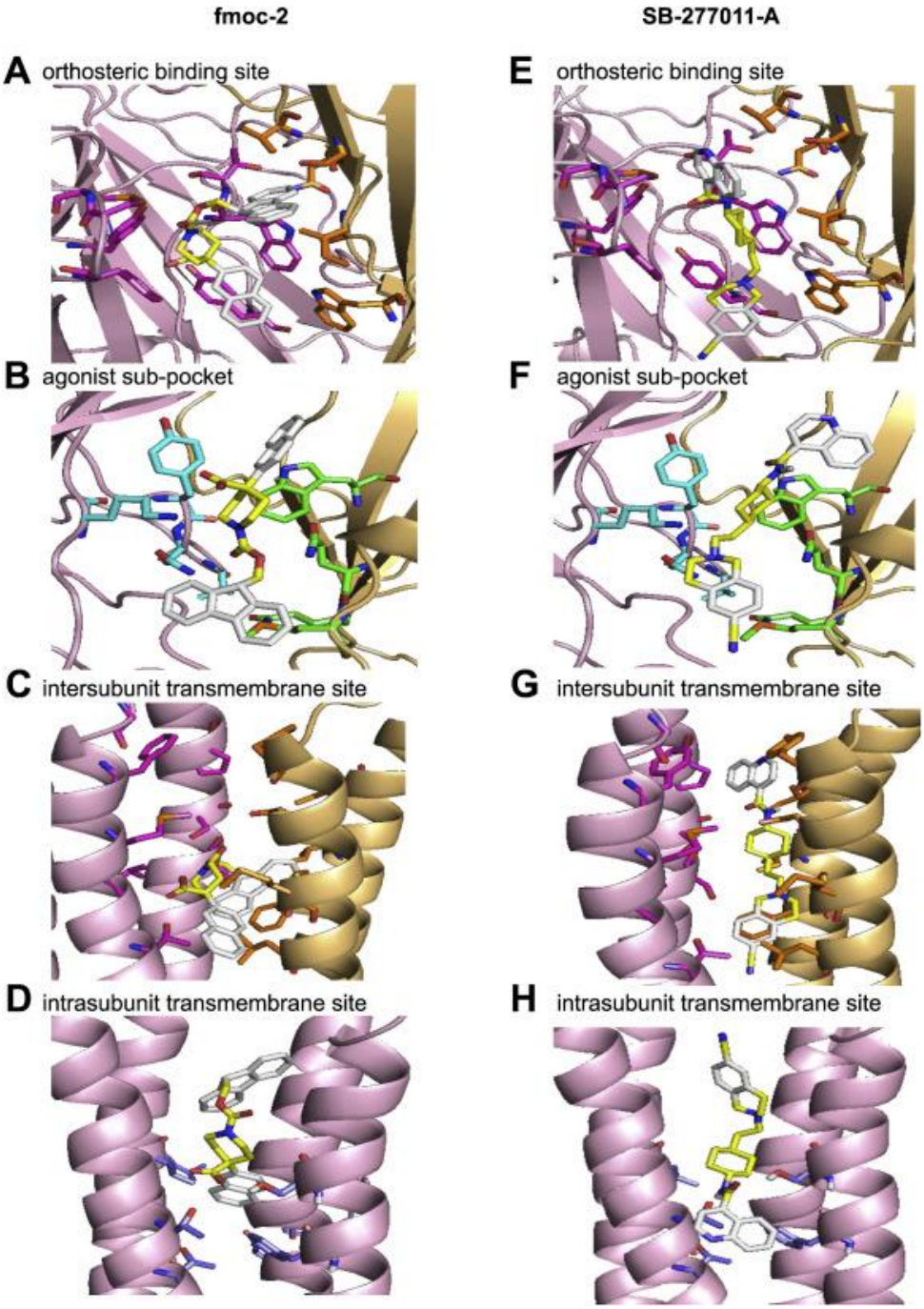

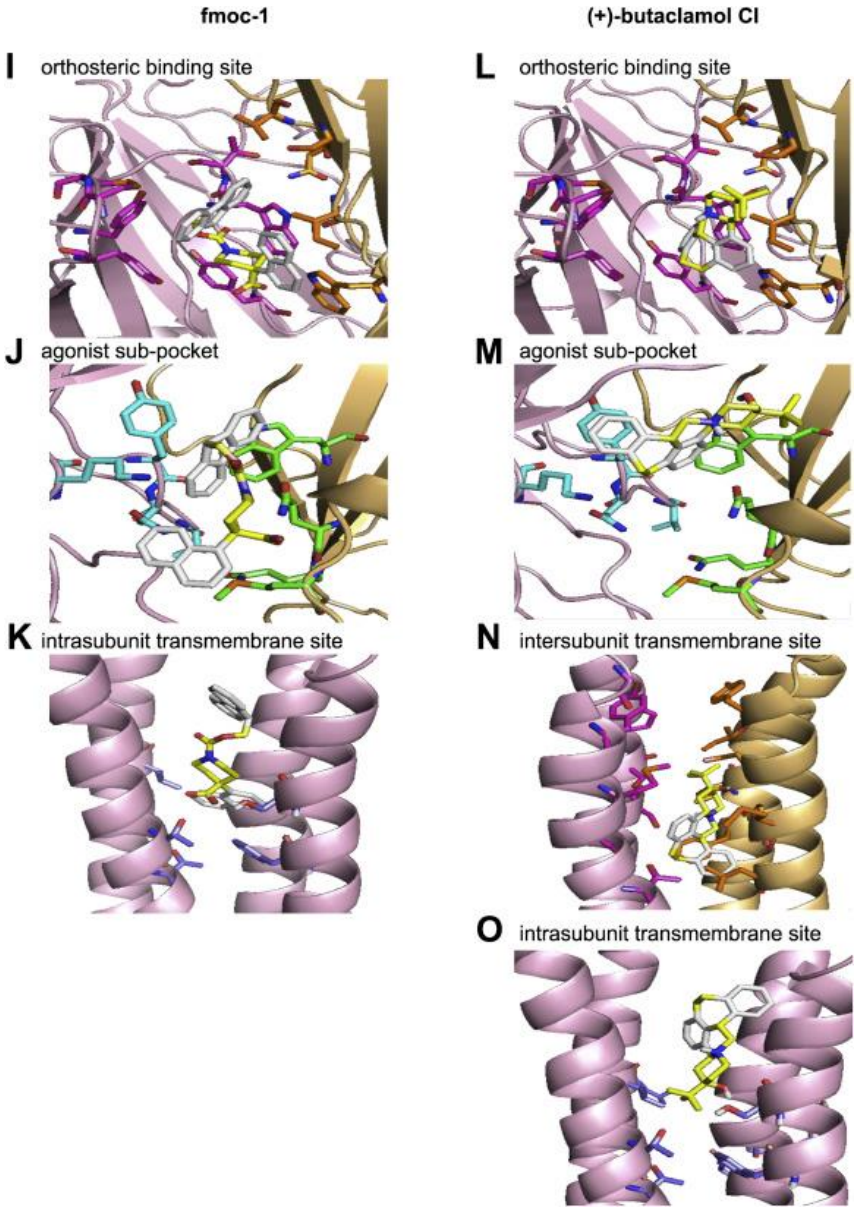

Fig. 3. Binding modes of four virtual screening hits in the orthosteric binding site, the agonist sub-pocket, the intersubunit and intrasubunit transmembrane allosteric binding pockets of the antagonist-bound model of Asu-ACR-16: (A), (B), (C), (D) fomc-2; (E), (F), (G), (H) SB-277011-A; (I), (J), (K) fomc-1; (L), (M), (N), (O) (+)-butaclamol Cl. Hits docked into the binding pockets are represented by sticks (carbon in yellow; ring in white; nitrogen in blue; oxygen in red). (A), (E), (I) and (L) show the four hits bound in the orthosteric binding site of the antagonist-bound model of ECD-Asu-ACR-16. The front two subunits are highlighted (principal subunit, light pink; complementary subunit, yellow). The residues in the orthosteric binding site are labeled (principal side, pink; complementary side, orange) to show the location of the orthosteric binding site. (B), (F), (J) and (M) show the four hits bound in the agonist sub-pocket of the antagonist-bound model of ECD-Asu-ACR-16. The front two subunits are highlighted. The residues in the agonist sub-pocket are labeled (principal side, turquoise; complementary side, green) to show the location of the agonist sub-pocket. (C), (G) and (N) show the four hits bound in the intersubunit transmembrane site of the antagonist-bound model of TID-Asu-ACR-16. The front two subunits are highlighted. The residues in the intersubunit transmembrane site are labeled (principal side, pink; complementary side, orange) to show the location of the intersubunit transmembrane binding site. (D), (H), (K) and (O) show the four hits bound in the intrasubunit transmembrane site of the antagonist-bound model of TID-Asu-ACR-16. The residues in the intrasubunit transmembrane site are labeled (purpleblue) to show the location of the intersubunit transmembrane binding site. (For interpretation of the references to colour in this figure legend, the reader is referred to the web version of this article.)

C3.4 *In vitro* synthesis of cRNA and microinjection into *Xenopus laevis* oocytes

We used TRIzol (Invitrogen™) to extract the total RNA samples from a 1 cm muscle flap and dissected the whole pharynx of *A. suum*. The first-strand of cDNA was synthesized with oligo RACER primer, Random Hexamer and superscript III reverse transcriptase (Invitrogen, Carlsbad, CA, USA) from total RNA in the muscle and pharynx by reverse transcription polymerase chain reaction (RT-PCR). Full-length Asu-acr-16 cDNA was amplified with the forward primer TTGATGTAGTGGCGTCGTGT, ATCACGCATTACGGTTGATG and the reverse primer GCATTGATGTTCCCTCACCT, ATTAGCGTCCCAAGTGGTTG (Boulin et al., 2011). The XhoI and ApaI restriction enzymes were used to digest the amplified product, which was then cloned into pTB207 expression vector (Boulin et al., 2008) and linearized by NheI. We used the mMessage mMachine T7 kit (Ambion) to in vitro transcribe the linearized cDNA to cRNA, which was then precipitated with lithium chloride, re-suspended in RNase-free water, aliquoted and stored at −80 °C.

The ancillary protein RIC-3 is required for the expression of ACR-16 in Xenopus oocytes (Halevi et al., 2003). A 50 nL cRNA mixture was prepared with 25 ng Asu-acr-16 cRNA, 5 ng Asu-ric-3 cRNA (SwissProt ID: F1L1D9; Wang et al., 2011) dissolved in RNAse-free water. The nanoject II microinjector (Drummond Scientific, PA, USA) was used to injected the cRNA mixture into the animal pole of the de-folliculated *X. laevis* oocyte (Ecocyte Bioscience, Austin, TX, USA).

The injected oocytes were separated into 96-well culture plates and incubated in the incubation solution (pH 7.5), which is composed of 100 mM NaCl, 2 mM KCl, 1.8 mM $CaCl_2 \cdot 2H_2O$, 1 mM $MgCl_2 \cdot 6H_2O$, 5 mM HEPES, 2.5 mM Na pyruvate, 100 U/mL penicillin,

100 μg/mL streptomycin and changed daily. The injected oocytes were stored at 19 °C for 4–8 days to allow the receptor to be expressed.

C3.5 Two-electrode voltage-clamp oocyte recording

We used two-electrode voltage-clamp electrophysiology to record the inward current generated by the activated Asu-ACR-16 receptors expressed in *X. laevis* oocytes. 100 μM BAPTA-AM (final concentration) was added into the oocyte incubation solution 4 h prior to recording, to prevent the current produced by the endogenous calcium-activated chloride channels during recording. An Axoclamp 2B amplifier (Molecular Devices, CA, USA) was used for recording and oocytes were held at −60 mV. A PC computer with software Clampex 9.2 (Molecular Devices, CA, USA) was used to acquire the recording data. The microelectrodes used to measure current in oocytes were pulled on a Flaming/Brown horizontal electrode puller (Model P-97, Sutter Instruments), filled with 3M KCl and had resistances of 20–30 MΩ. The microelectrode tips were broken back carefully with Kimwipes (Wilmington, NC, USA) to reduce the resistance to 2–5 MΩ. The recording solution was: 100 mM NaCl, 2.5 mM KCl, 1 mM $CaCl_2 \cdot 2H_2O$ and 5 mM HEPES, pH 7.3 (Buxton et al., 2014). Oocytes were placed into a tiny groove of the narrow oocyte recording chamber. The Digidata 1322A (Molecular Devices, CA, USA) was used to control the switches that controlled the perfusion of the chamber at a speed of 4–6 ml/min.

100 μM acetylcholine was applied initially for 10 s as a control to check the viability of the oocytes and Asu-ACR-16 expression for all the recordings. Recording solution was then used to wash out the drug from the oocytes for 2–3 min before next application of drug perfusion.

C3.6 Drugs

Table 1 lists the compounds used, their chemical properties and structures. Fmoc-4-(naphthalen-2-yl)-piperidine-4-carboxylic acid (fmoc-2), SB-277011-A hydrochloride hydrate (SB-277011-A), fmoc-4-(naphthalen-1-yl)-piperidine-4-carboxylic acid (fmoc-1) and (+)-butaclamol hydrochloride (+)-butaclamol Cl), acetylcholine chloride (ach), methyllycaconitine citrate salt (mla) were purchased from Sigma–Aldrich (St Louis, MO, USA). Levamisole hydrochloride (levamisole) was purchased from MP Biomedicals (Santa Ana, CA, USA). With the exception of ach and mla which were dissolved in the recording solution, the rest of chemicals were dissolved in dimethyl sulfoxide (DMSO) to make stock solutions. Stock solutions of 100 mM were prepared, except for SB-277011-A where a stock solution of 10 mM was prepared due to the solubility; stock solutions were frozen until required. Working solutions were then prepared by dilution on the day of the experiment.

C3.7 Pharmacological characterization of molecules selected by virtual screening

To characterize the four hits (Table 1) selected by our virtual screening, each drug was applied for 10 s to the oocytes expressing Asu-ACR-16 to test if the drugs were agonists. They were then tested as antagonists against ach.

To characterize the antagonistic properties of the four hits, the following protocol was used: a) 10 s of 100 μM ach alone; b) then 10 s of 100 μM ach + hit and then; c) 10 s of 100 μM ach alone. This test procedure was repeated with increasing concentrations of the four hits (Fig. 4A–D), to determine the inhibitory dose–response relationships and IC_{50} by fitting Hill equations to the inhibitory dose–response curves using GraphPad Prism 5.0 (Graphpad Software Inc., CA, USA). As a further study of the antagonism, each of the four hits was applied before and during 10 s test applications of increasing concentrations of ach (Fig. S4).

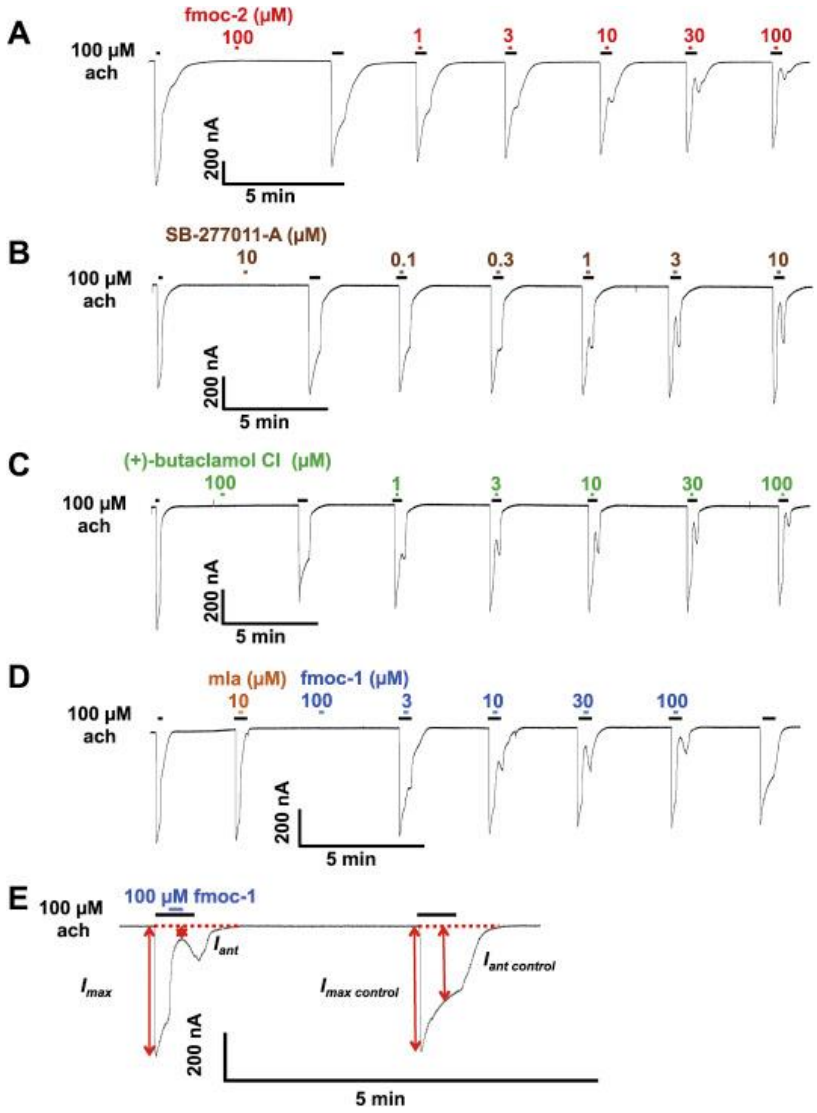

Fig. 4. Effects of four virtual screening hits on Asu-ACR-16 mediated ach responses. Sample traces for: (A) fmoc-2, (B) SB-277011, (C) (+)-butaclamol Cl, (D) fmoc-1 concentration-inhibition relationships on Asu-ACR-16. Mla in (D), which stands for methyllycaconitine citrate salt, was used as an antagonist control of Asu-ACR-16. All four hits did not induce the current response by themselves, while produced the concentration-depended inhibition of ach current response. (E) is the magnified figure of part of (D) as an example to show the four parameters needed to measure the inhibition percentage. $I_{max\ control}$ was the peak current of the control 30 s application of 100 μM ach. I_{max} was the peak current of the 100 μM ach that preceded the 10 s co-application of ach and antagonist. I_{ant} was the minimal current during the co-application of 100 μM ach and antagonist. $I_{ant\ control}$ was the current at the same time point from the beginning of the 30 s application as I_{ant} during the control 30 s application of 100 μM ach.

C3.8 Data analysis

The data from electrophysiological recordings were analyzed using Clampfit 9.2 (Molecular Devices, CA, and USA) and GraphPad Prism 5.0 (Graphpad Software Inc., CA, USA). In all recordings, the peak currents in response to applied drugs were measured, which were later normalized to the control 100 μM ach response, and expressed as mean ± S.E.M. The mean % inhibition of currents elicited by 100 μM ach ± S.E.M. was used to determine the inhibition percentage, which was quantified using the following equation:

$$Inhibition(\%) = \left(1 - \frac{I_{ant}}{\frac{I_{ant\ control}}{I_{max control}} \times I_{max}}\right) \times 100\%$$

where $I_{max\ control}$ was the peak current of the control 30 s application of 100 μM ach, I_{max} was the peak current of the 100 μM ach that preceded the 10 s co-application of ach and antagonist. I_{ant} was the minimal current during the co-application of 100 μM ach and antagonist. $I_{ant\ control}$ was the current at the same point from the beginning of the 30 s application as I_{ant} during the control 30 s application of 100 μM ach (Fig. 4E). Concentration-response relationships or concentration-inhibition (%) relationships were analyzed by fitting data points into the Hill equation, with at least four replicates of each experiment set.

C3.9 Drug treatment of *C. elegans*

The wild-type *C. elegans* strain N2 were obtained from the Caenorhabditis Genetics Center (University of Minnesota, MN, USA). We grew *C. elegans* at 20 °C on nematode growth media (NGM, 3 g/l NaCl, 17 g/l agar, 2.5 g/l peptone, 1 mM $CaCl_2$, 5 mg/l cholesterol, 1 mM $MgSO_4$, 25 mM KPO_4 buffer) agar plates, seeded with *Escherichia. coli* OP50 lawn under standard conditions (Brenner, 1974). Ten larvae at L4 stage with active thrashing movement (defined as “normal”) were transferred from NGM plates into M9 buffer

(3 g/l KH_2PO_4, 6 g/l Na_2HPO_4, 5 g/l NaCl, 1 mM $MgSO_4$) in 24-wall plates for each treatment. We counted the number of worms with normal motility in M9 buffer with diluted drugs from the stock solutions (≤1% DMSO) at 0, 5, 10, 15 and 20 min. Five replicates were applied for each treatment. Motility between negative control (1% DMSO, final concentration) and drug treated worms were compared at each time point using student t-test.

C4.0 Results

C4.1 Sequence alignment of *Asu*-ACR-16 and template homologue proteins

The full-length protein sequence of Asu-ACR-16 (504 residues) was retrieved from the SwissProt database, of which the ECD-Asu-ACR-16 accounts for 234 residues. The first 25 resides of Asu-ACR-16 were excluded from alignment with the full length human nAChR α7 chimera (204 residues) because of the shorter length of the template protein sequence. The human α7 nAChR chimera shows 37.6% sequence identity and 72.9% sequence similarity with the ECD-Asu-ACR-16, based on the alignment generated by CLUSTALW (Fig. 1A, job ID: 65782ad6ad6d). The TID-Tma-nAChR subunit A shows 22.0% sequence identity and 45.4% sequence similarity with TID-Asu-ACR-16, aligned by CLUSTALW (Fig. 1B, job ID: 644888f4f30e). The residues involved in the putative orthosteric and the allosteric binding sites are highlighted in amino acids sequence of Asu-ACR-16.

C4.2 Models of the *Asu*-ACR-16 pentamer

The model of the antagonist-bound form of the ECD-Asu-ACR-16 subunit starts from an N-terminal α helix followed by seven β strands that comprise an immunoglobulin fold. Loop A (Val114 – Ala122), loop B (Lys169 – Lys179), loop C (Phe213 – Pro220) from the principal subunit, and loop D (Ala78 – Ala83), loop E (Ile143 – Pro144), loop F (Gly185 – Met204) from the complementary subunit are involved in forming the orthosteric binding

site. A disulphide bond between Cys152 and Cys166 contributes to the characteristic component of Cys-loop receptors. The C-terminal continues into the transmembrane domain (Fig. S1A).

The transmembrane domains of the Asu-ACR-16 model are made of four α-helices (M1, M2, M3 and M4). M1 links to the β7 sheet of the extracellular domain and extends down into the membrane and is followed by the M2 and the M3 helixes as the membrane-spanning portions. The MA cytoplasmic loop (helix) connects between M3 and M4. The region between M3 and MA is not modeled due to the poorly defined intracellular domain of the template structure. The C-terminal follows the M4 helix and faces toward the extracellular surface (Fig. S1B).

The pentameric model of Asu-ACR-16 has a five-fold symmetric around the channel pore. The average pairwise Root Mean Square Deviation (RMSD) fit of the C_α coordinates of the antagonist-bound ECD-Asu-ACR-16 pentameric model and human α7 nAChR chimera pentamer (PDB code: 4HQP) was 0.9 Å, which indicates a strong structural conservation between the model and the template structures (Fig. S1C). The C_α-RMSD between the TID-Asu-ACR-16 pentamer and the TID-Tma-AChR pentamer was 1.5 Å, which shows the TID fit is still good but not as good as the ECD fit. The membrane-spanning domains are arranged symmetrically. The M2 helix lines the channel pore, while M1, M3 and M4 do not contribute to the channel pore and are arranged peripherally (Fig. S1D).

Since no binding site data of Asu-ACR-16 is available to date, we used the published orthosteric binding site and allosteric binding sites in nAChRs or other Cys-loop receptors to predict the putative binding sites in Asu-ACR-16 (Galzi et al., 1991, Arias, 2000, Young et al., 2008, Hibbs and Gouaux, 2011 and Spurny et al., 2015). The orthosteric binding site is

at the interface between the principal site and the complementary site in two adjacent subunits of the ECD-Asu-ACR-16 pentamer (Fig. 2S2A & S2B). The principal subunit (+) has vicinal cysteines (Cys216, Cys217) that contributes to the loop C of the binding site. The complementary subunit (−) does not use vicinal cysteines as part of the binding pocket and the residues are more variable when nAChRs are compared. The agonist sub-pocket, which we argue is a less significant allosteric binding site in ECD-Asu-ACR-16, is located right below the orthosteric binding site in the extracellular domain (Fig. 2S2C & S2D). The vestibule pocket (Fig. S2E & S2F) and the top pocket (Fig. S2G & S2H) were not high affinity binding sites for the ligands and are not discussed further in this manuscript. The intersubunit allosteric binding sites in TID-Asu-ACR-16 are at the interface region between M2(+), M3(+), M1(−) and M2(−) (Fig. 2S2I & S2J). The intrasubunit allosteric binding sites are at the center of the four transmembrane helixes (M1, M2, M3 and M4) in each of the five subunits.

C4.3 Binding properties of virtual screening hits

We carried out virtual screening of the ZINC ligand-database by using the three different bound forms of the ECD-Asu-ACR-16 models. Four molecules were selected as hits based on their high binding affinities and appropriate binding modes within the ligand-binding sites. The 9-fluorenylmethoxycarbonyl group (FMOC) was observed in twelve out of top forty hits ranked by binding affinities and exists in the two out of four hits, which suggests that FMOC could be necessary for the ligand recognition by the receptor. The FMOC group has a low predicted bioavailability due to the biphenyl scaffold, which limits aqueous solubility and may affect distribution to the *A. suum* parasite. Table 1 lists the physicochemical characteristics of four hits. They have relatively high molecular weights and

are more hydrophobic compared to known Asu-ACR-16 agonists. However, they do follow the Lipinski's rule of five, which suggests that these molecules may be orally actively (Lipinski et al., 2001 and Lipinski, 2004).

The atomic structure predicts the partition-coefficients (XlogP) of the four hits to be between 4.27 and 6.04 (Table 1). The XlogPs suggest that the four hits are 10,000–1,000,000 times more concentrated in the lipophilic phase of the lipid bilayer than the aqueous phase of the extracellular domain (Cheng et al., 2007). The four hydrophobic hits are, therefore, more likely to bind into the transmembrane allosteric binding pockets rather than to the extracellular ligand binding sites. The four hits which bind in the transmembrane allosteric binding pockets are therefore predicted to be allosteric modulators of the Asu-ACR-16 receptor that alter the activity of the agonists or competitive antagonists that bind to orthosteric binding site. SB-277011-A is known to be a potent and selective dopamine D_3 receptor antagonist with high oral availability (Stemp et al., 2000). (+)-butaclamol Cl is a non-selective dopamine receptor antagonist and a potent antipsychotic agent (Chrzanowski et al., 1985). No paper reporting on the activities of fmoc-2 and fmoc-1 has been published to date.

The four hits (Table 1) were tested for docking into the orthosteric binding sites of the three forms of ECD-Asu-ACR-16 models and the five allosteric binding pockets in the antagonist-bound form of full-length Asu-ACR-16 models. All four hits bound to the orthosteric binding sites of three ECD-Asu-ACR-16 models, but only bound to the three allosteric binding sites out of five: the intersubunit and intrasubunit transmembrane pockets and the agonist sub-pocket (Fig. 3) with high binding affinities.

In the intersubunit transmembrane site of TID-Asu-ACR-16 model, M243 (M1, (−)), L247 (M1, (−)) make hydrophobic interactions with naphthalene of fmoc-2. T312 (M3, (+)), S284 (M2, (+)) form hydrogen bonds with carboxylic acids of fmoc-2. F279 (M2, (−)), I282 (M2, (−)) and make hydrophobic contacts with fluorene of fmoc-2. F279 (M2, (−)), P244 (M1, (−)) make hydrophobic interactions with tetrahydroisoquinoline of SB-277011-A. N240 (M1, (−)) forms a hydrogen bond with carboxamide of SB-277011-A. P288 (M2, (+)) has hydrophobic interactions with quinoline of SB-277011-A. L247 (M1, (−)), F279 (M2, (−)) and makes hydrophobic contacts with dibenzocycloheptene of (+)-butaclamol Cl.

Ach, the natural agonist of Asu-ACR-16 was docked into the ligand binding sites of three forms of Asu-ACR-16 models for comparison. As expected, ach bound to the orthosteric binding site of the agonist-bound Asu-ACR-16 with an affinity (−4.3 kcal/mol), which was higher than the affinities at the other binding sites. The binding pose of ach docked in the orthosteric binding site of the agonist-bound Asu-ACR-16 model was in agreement with the binding pose of ach in the *L. stagnalis* AChBP cocrystal structure (PDB code: 3WIP; Olsen et al., 2014b). The quaternary ammonium of ach faces the basal side of the binding cavity and make cation-π interaction with five aromatic residues from the Asu-ACR-16 ((+): Y89, W143, Y185, Y192; (−): W53), while the carbonyl oxygen of ach faces toward the apical side of the binding cavity. The binding affinities of the selected four compounds were higher than −8.0 kcal/mol in the three different bound forms of Asu-ACR-16, while the binding affinities of ach were lower than −4.5 kcal/mol in three states of Asu-ACR-16 (Table 2).

Table 2
Binding affinities (kcal/mol) of the four hits and ach in the orthosteric binding sites of the three different bound models of ECD-Asu-ACR-16 and three allosteric binding sites of the antagonist-bound model of full-length Asu-ACR-16.

Hits	Binding affinities (kcal/mol)					
	Apo	Agonist-bound	Antagonist-bound		Transmembrane site	
	Orthosteric binding site	Orthosteric binding site	Orthosteric binding site	Agonist sub-pocket	Inter-subunit	Intra-subunit
fmoc-2	−10.4	−13.0	−10.2	−8.5	−11.4	−10.8
SB-277011-A	−9.8	−12.3	−9.2	−9.5	−10.8	−9.7
fmoc-1	−10.6	−12.3	−10.3	−8.9	NA	−11.0
(+)-butaclamol Cl	−9.5	−11.8	−8.2	−9.2	−10.8	−9.0
ach	−4.2	−4.3	−3.9	−4.0	−3.7	NA

C4.4 Pharmacological properties of virtual screening hits

We tested the effects of the putative allosteric modulators on Asu-ACR-16 receptors expressed in Xenopus oocyte using two-electrode voltage clamp to observe the currents that flow through Asu-ACR-16 receptors. Representative traces showing the inhibitory dose–response relationships are shown in Fig. 4. Their IC_{50} (Fig. 5A and B) and maximum inhibition (Fig. S3) were determined as described in the methods (Table 3). The most potent antagonist among them was SB-277011-A, which had an IC_{50} of 3.12 ± 1.29 μM and maximum inhibition effect of 96.07 ± 10.66% (n = 4).

The ach concentration-response plots in the presence of 3 μM of each putative allosteric modulator (Fig. S4 & Fig. 5C), show the reduced maximum current responses with little shift in EC_{50} of ach (Fig. 5Dand E & Table 4), and that the hits were non-competitive antagonists and negative allosteric modulators.

At 10 μM, SB-277011-A, showed evidence of a mixed competitive and non-competitive antagonism (Fig. S5), characterized by a reduced maximum current response and a right-shift in the EC_{50} of ach (Fig. 5D and E). Thus, 10 μM SB-277011-A appears to act at more than one binding site which may include the orthosteric binding sites and additional allosteric binding sites.

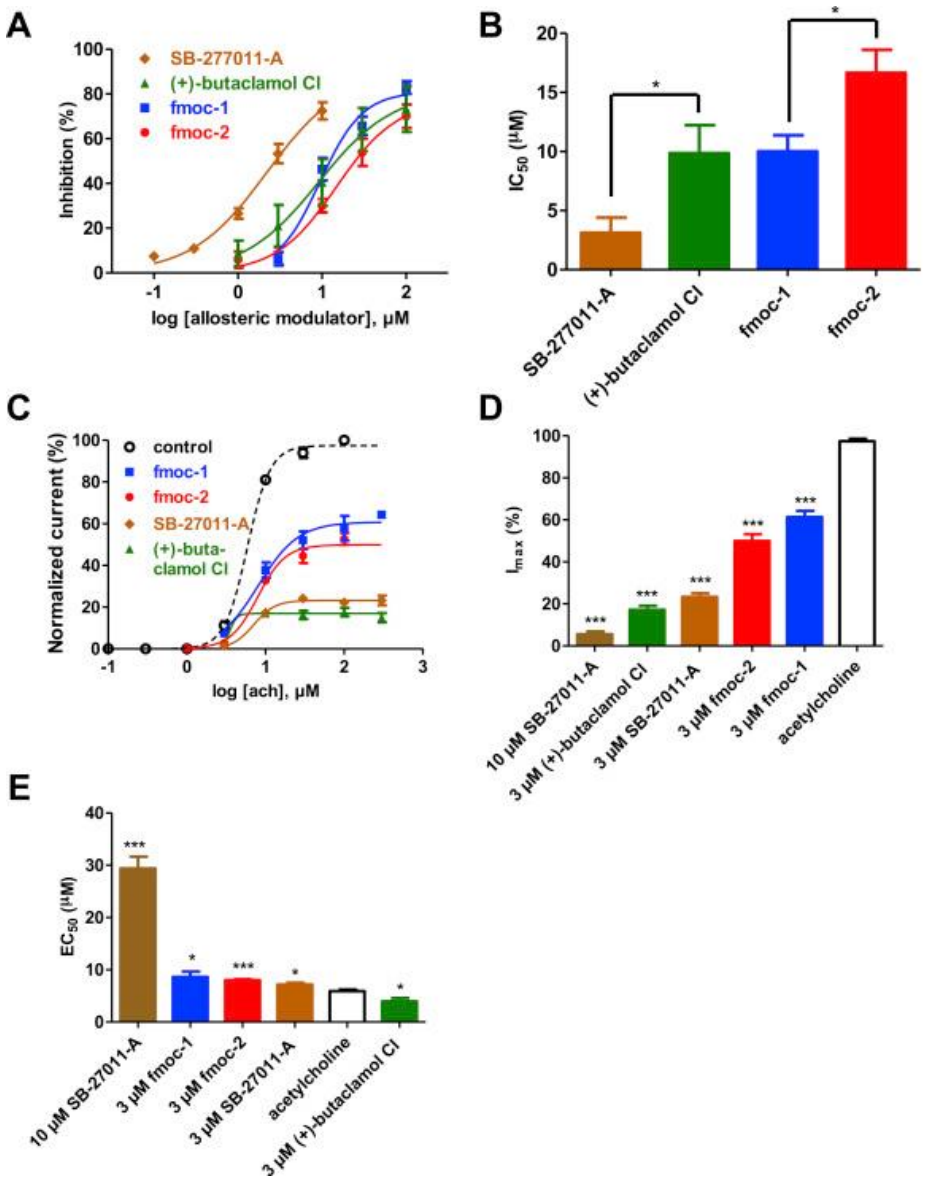

Fig. 5. (A) Effects of four virtual screening hits on Asu-ACR-16 mediated ach responses. Fmoc-2, fmoc-1, (+)-butaclamol Cl and SB-277011-A concentration-inhibition curves for Asu-ACR-16. Results were expressed as mean % inhibition of currents elicited by 100 µM ach ± S.E.M. (B) Bar chart representing the IC50 (mean ± S.E.M, µM) of each plots in (A). The rank order series of inhibition based on IC50 for four hits is: SB-277011-A (3.12 ± 1.29 µM, n = 4) < (+)-butaclamol Cl (9.85 ± 2.37 µM, n = 4) ≈ fmoc-1 (10.00 ± 1.38 µM, n = 4) < fmoc-2 (16.67 ± 1.95 µM, n = 4). * represents $p < 0.05$ (unpaired t-test). (C) Ach concentration-response plots for Asu-ACR-16 in the absence of hits as a control (ach) and in the continual presence of four hits identified in (A). Ach concentration-response curves for Asu-ACR-16 in the presence of 3 µM of four hits: fmoc-1, fmoc-2, SB-27011-A and (+)-butaclamol Cl. (D) Bar chart (mean ± S.E.M, %) representing the reduced maximum current response of ach concentration-response curves in (C). The series of reduced maximum response of each hits compared to that of ach by unpaired t-test is: 10 µM SB-27011-A (5.51 ± 1.38%, n = 4), 3 µM (+)-butaclamol Cl (17.22 ± 1.94%, n = 4), 3 µM SB-27011-A (23.25 ± 1.80%, n = 5), 3 µM fmoc-2 (49.92 ± 3.27%, n = 4), 3 µM fmoc-1 (61.25 ± 3.08%, n = 4) and ach (97.45 ± 1.19%, n = 4). * represents $p < 0.05$, ** represents $p < 0.01$, *** represents $p < 0.001$. All four hits significantly inhibited the maximum current response induced by ach. (E) Bar chart (mean ± S.E.M, µM) displaying the EC50 of ach concentration-response curves in (C). The series of variable EC50 of each hits compared to that of ach by unpaired t-test is: 10 µM SB-27011-A (29.40 ± 2.27 µM, n = 4), 3 µM fmoc-1 (8.62 ± 1.04 µM, n = 4), 3 µM fmoc-2 (8.01 ± 0.18 µM, n = 4), 3 µM SB-27011-A (7.17 ± 0.33 µM, n = 5), ach (5.92 ± 0.29 µM, n = 4) and 3 µM (+)-butaclamol Cl (3.94 ± 0.66 µM, n = 4). The EC50 of all four hits obviously shift away from the control when applied.

Table 3
Pharmacological profiles of the inhibitory effects of four hits on Asu-ACR-16 mediated ach responses. Results (mean ± S.E.M.) were expressed as IC_{50} (μM), Hill slope (n_H), maximum inhibition (%) and the number of repeats (N) of each experiment.

Hits	IC_{50} (μM)	nH	Inhibition max (%)	N
fmoc-2	16.67 ± 1.95	1.22 ± 0.17	80.34 ± 10.32	4
SB-277011-A	3.12 ± 1.29	0.99 ± 0.11	96.07 ± 10.66	4
fmoc-1	10.00 ± 1.38	1.97 ± 0.37	82.49 ± 4.74	4
(+)-butaclamol Cl	9.85 ± 2.37	1.34 ± 0.29	79.53 ± 12.41	4

Table 4
Pharmacological profiles of EC_{50} shifts and maximum current reductions of Asu-ACR-16 mediated ach responses in the presence and absence of four hits. Results (mean ± S.E.M.) were expressed as EC_{50} (μM), Hill slope (nH) and maximum response (%) and the number of repeats (N) of each experiment.

Hits	EC_{50} (μM)	nH	Imax (%)	N
control	5.92 ± 0.29	3.05 ± 0.07	97.45 ± 1.19	4
3 μM fmoc-2	8.01 ± 0.18	2.54 ± 0.18	49.92 ± 3.27	5
1 μM SB-277011-A	9.85 ± 4.80	2.60 ± 0.71	75.96 ± 4.40	4
3 μM SB-277011-A	7.17 ± 0.33	3.37 ± 0.28	23.25 ± 1.80	5
10 μM SB-277011-A	29.40 ± 2.27	7.43 ± 3.30	5.51 ± 1.38	4
3 μM fmoc-1	8.62 ± 1.04	1.76 ± 0.21	61.25 ± 3.08	4
1 μM (+)-butaclamol Cl	4.54 ± 0.92	9.64 ± 4.14	30.34 ± 4.03	4
3 μM (+)-butaclamol Cl	3.94 ± 0.66	12.75 ± 3.63	17.22 ± 1.94	4

C4.5 SB-277011-A reversibly inhibits locomotion in *C. elegans*

We tested the effects of each allosteric modulator on the locomotion of *C. elegans* L4 larvae. The number of normal worms with thrashing-like movement dropped by 60% in 5 min after exposed to 30 μM SB-277011-A ($p < 0.01$, $n = 5$, t-test). Paralysis-like movement was observed in the rest of the worms. Interestingly, the number of worms with motility that appeared normal recovered to 50% ($p < 0.05$, $n = 5$, t-test) in 10 min, 85% in 15 min ($p > 0.05$, $n = 5$, t-test) and returned to near negative control values after 20 min (Fig. S6). The recovery may relate to the desensitization properties of the ACR-16 receptor. The reversible inhibition of motility in worms was also observed in 100 μM (+)-butaclamol Cl, but no significant difference between the number of normal treated worms and negative

control was observed at any time point. No visual effects of 100 μM fmoc-2 or 100 μM fmoc-1 were found on the locomotion of worms.

C5.0 Discussion

C5.1 *Asu*-ACR-16 models

We have built up three-dimensional models of full-length structures of Asu-ACR-16 at the atomic level for the first time. We used homology modeling based on X-ray crystal structures of human α7 nAChR chimeras and the electron microscopic structure of the *T. marmorata* nAChR as templates for different domains. The quality of our homology models are dependent on the sequence identity of the templates (human α7 nAChR chimeras and *T. marmorata* nAChR) and the target sequence (Asu-ACR-16) and the resolutions of template structures (Hillisch et al., 2004 and Cavasotto and Phatak, 2009). Our three ECD-Asu-ACR-16 models are likely to be reliable for virtual screening because they have high sequence identities (37.6% identity and 72.9% similarity) with high resolution (<4 Å) templates. More errors might be expected in the TID-Asu-ACR-16 model, because of the missing loop between M3 and MA in the template structure which reduces sequence identity with the target protein. The missing loop does not include an allosteric binding site, so we can assume that the TID-Tma-nAChR structure is similar to the TID-Asu-ACR-16 structure (Bertrand et al., 2008). The overall secondary structures of our models are also consistent with published nAChRs structures (Finer-Moore and Stroud, 1984, Miyazawa et al., 2003 and Unwin, 2005).

We developed the apo, the agonist-bound and the antagonist-bound models of the ECD-Asu-ACR-16 on the assumption that these three states of the Asu-ACR-16 receptor most closely represent the receptor conformations in the presence and absence of agonists or

antagonists. To produce a realistic dynamic model would require more extensive work (Cavasotto and Orry, 2007 and Spyrakis et al., 2011) and is beyond the scope of this study.

C5.2 Virtual screening

Our structure-based virtual screening approach identified four novel and potent negative allosteric modulators of Asu-ACR-16, which were validated by our electrophysiological studies. The putative ligands were initially selected based on the virtual screening using the orthosteric binding site of the receptor. It was possible that these ligands could have been agonists or competitive antagonists that bind within the orthosteric binding site. In contrast, the pharmacological characterization of the four virtual screening hits shows that they behave as negative allosteric modulators and bind to allosteric sites. This outcome may be due to the hydrophobic properties of the four compounds that impedes their interactions with the orthosteric site in the extracellular domain of the receptor. The high lipid solubility of these compounds increases their concentration in the membrane lipid phase, in the region of the transmembrane allosteric sites.

The binding affinities calculated in the scoring function of AutoDock Vina software usually increase with the number of non-hydrogen atoms, which may be due to the neglect of desolvation in the scoring function (Shoichet et al., 1999, Kuntz et al., 1999 and Park et al., 2006). This leads to a bias of virtual screening methods towards big molecules which are more hydrophobic, concentrated in the lipid bilayer, and less likely to interact with the binding sites in the extracellular domains (Hopkins et al., 2004). It is also pointed out that the simplified force fields used to estimate the binding free energies are unable to evaluate the conformational entropies and other contributions to the free energies (Cosconati et al., 2010). Thus, the success rate of identifying bioactive hits (44%) would be enhanced if we are able to

include these additional parameters into a scoring function for virtual screening. Another approach, which we did not follow here, to enhance the success rate of identifying bio-active hits, is to use the known agonists or antagonists as scaffolds. This would facilitate the identification of low molecular-weight and more hydrophilic agonists or antagonists, and allow further study of the quantitative structure-activity relationships (Sun, 2008).

C5.3 Four negative allosteric modulators of *Asu*-ACR-16

We evaluated the potency of inhibition for the four negative allosteric modulators in our electrophysiology studies on *Xenopus* oocytes: SB-277011-A (IC_{50} 3.12 ± 1.29 μM) < (+)-butaclamol Cl (IC_{50} 9.85 ± 2.37 μM) ≈ fmoc-1 (IC_{50} 10.00 ± 1.38 μM) < fmoc-2 (IC_{50} 16.67 ± 1.95 μM). This rank of inhibition agrees with the level of effects of the four modulators in the motility of *C. elegans*. The most potent modulator SB-277011-A was shown to decrease the motility of *C. elegans* larvae for a duration of about 10 min, yet less effective on adult *C. elegans*. Desensitization of the ACR-16 or other nAChRs in *C. elegans* body muscle may be a reason for the reduced effects of SB-277011-A on worms (Hernando et al., 2012). Treating the acr-16-null mutant of *C. elegans* with SB-277011-A can help us to investigate the mode of action of SB-277011-A on *C. elegans* as genetic models to understand SB-277011-A action on the parasitic nematode *A. suum* (Ward, 2015).

C5.4 Allosteric binding sites may offer a better opportunity for drugs that can discriminate between the parasite *Asu*-ACR-16 and mammalian host α7 nAChR

Asu-ACR-16 shows 42.5% sequence identity and 71.2% sequence similarity with the human α7 nAChR (SwissProt ID: P36544) based on the alignment generated by CLUSTALW (Fig. S7, CLUSTALW job ID: cfed4f821eaf). The residues constituting the

orthosteric binding site (pink and orange arrows in Fig. S7) are highly conserved between Asu-ACR-16 and human α7 nAChR, which shows 66.7% identity and 100% similarity (Fig. S8). In contrast, the residues of the four allosteric binding sites have much greater differences (variance) between the nematode parasite and the equivalent sites on the α7 receptor (identities: 62.5%, 45.5%, 66.7%, 62.5% and 40.0% and; similarities: 87.5%, 81.8%, 83.3, 93.8% and 100%). The sequence divergence in the allosteric binding sites between Asu-ACR-16 and host human α7 nAChR indicates that drugs targeted at these sites may be more selective than drugs targeted at orthosteric binding sites. Virtual screening specifically targeting the allosteric binding sites is predicted to offer a better opportunity for development of drugs with much greater receptor subtype selectivity (Nussinov and Tsai, 2013 and Iturriaga-Vasquez et al., 2015).

C5.5 Conclusion

We have developed a structure-based in silico screening approach to search for the bioactive hits that target at a parasitic nematode receptor. This approach allowed us to identify four negative allosteric modulators that were validated using our electrophysiological studies. These four compounds may be useful leads for anthelminthic drug discovery. We point out however, that we have not yet made the structural models for the host human α7 nAChR or other receptors, which would help to distinguish compounds that are active only on the nematode receptors, thereby reducing potential toxicity. It would also be desirable to perform virtual screening for toxicity on a range of host receptors, some structures of which have already been determined and others need to be modeled.

C6.0 Statement of conflict of interest

None identified.

C7.0 Acknowledgements

We would like to thank Tsung-Han Chou for the help and advice in modeling and docking. The research funding was by The Hatch Act, State of Iowa, and by NIH grants R01 AI047194 (to RJM) and AI114629 (to EWY) of the National Institute of Allergy and Infectious Diseases. The funding agencies had no role in the design, execution or publication of this study. The content is solely the responsibility of the authors and does not necessarily represent the official views of the National Institute of Allergy and Infectious Disases.

C8.0 Supplementary data

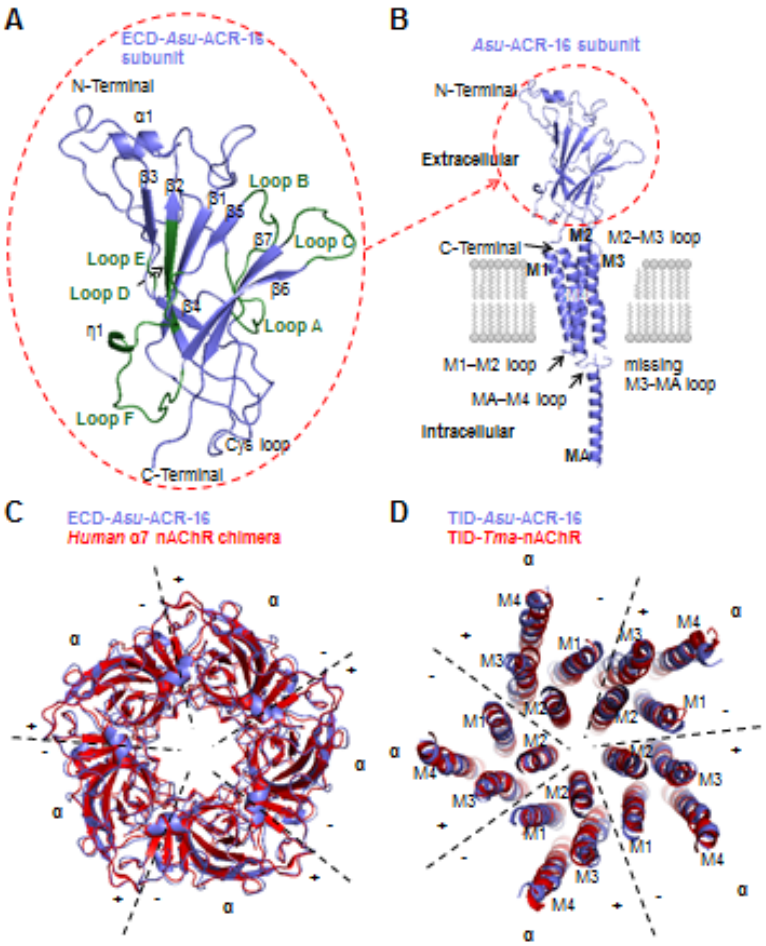

Supplementary Figure S1. (A) Ribbon representation of the ECD-Asu-ACR-16 monomer. Secondary elements are indicated. Loop A, B, C in the principal subunit and loop D, E, F in the complementary subunit which mainly contribute to the orthosteric binding site are labeled by dark green. In the complete structure, the C-terminal would enter the membrane at the bottom and link to M1 helix in the transmembrane domain. (B) Ribbon representation of the full-length Asu-ACR-16 monomer, as viewed parallel to the membrane plane. Four α helixes (M1, M2, M3 and M4) that contribute to transmembrane domain and one MA helix that makes up the intracellular domain are indicated. The functionally important M1-M2, M2-M3 and MA-M4 loops are labeled. (C) Superposition of antagonist-bound model of ECD-Asu-ACR-16 pentamer (purple blue) and template human α7 nAChR chimera (red; PDB code: 4HQP, ligands removed for clarity) viewed from the synaptic cleft. Five homomeric α-subunits are labeled. The interfaces between two vicinal α-subunits are marked by dotted lines. Five orthosteric binding sites are at each interface between the principal side (+) and the complementary side (−) from two vicinal subunits. (D) Superposition of TID-Asu-ACR-16 pentamer (purple blue) and template TID-Tma-AChR (red; PDB code: 2BG9) viewed above the membrane. Five homomeric α-subunits are labeled. The interfaces between two vicinal α-subunits are marked by dotted lines. Five allosteric binding sites are at each interface among the M2, M3 in the principal side (+) and the M1 in the complementary side (−) from two vicinal subunits.

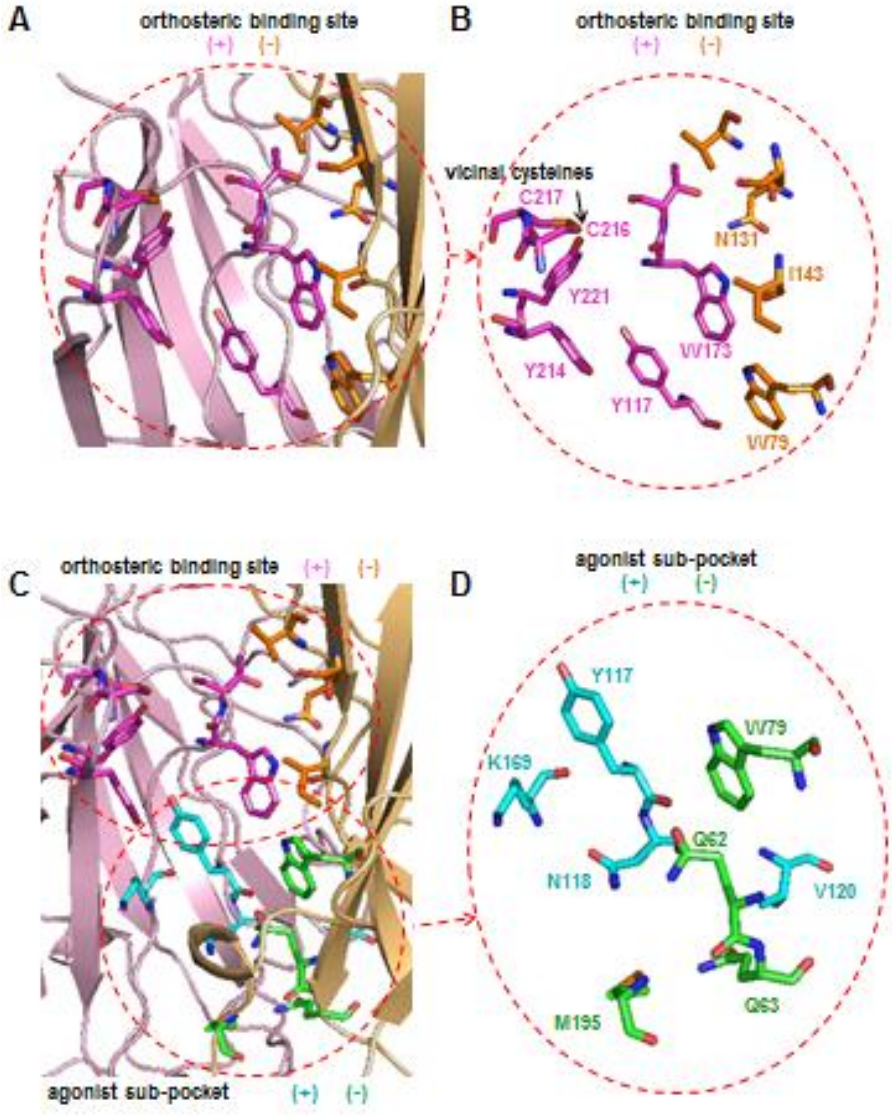

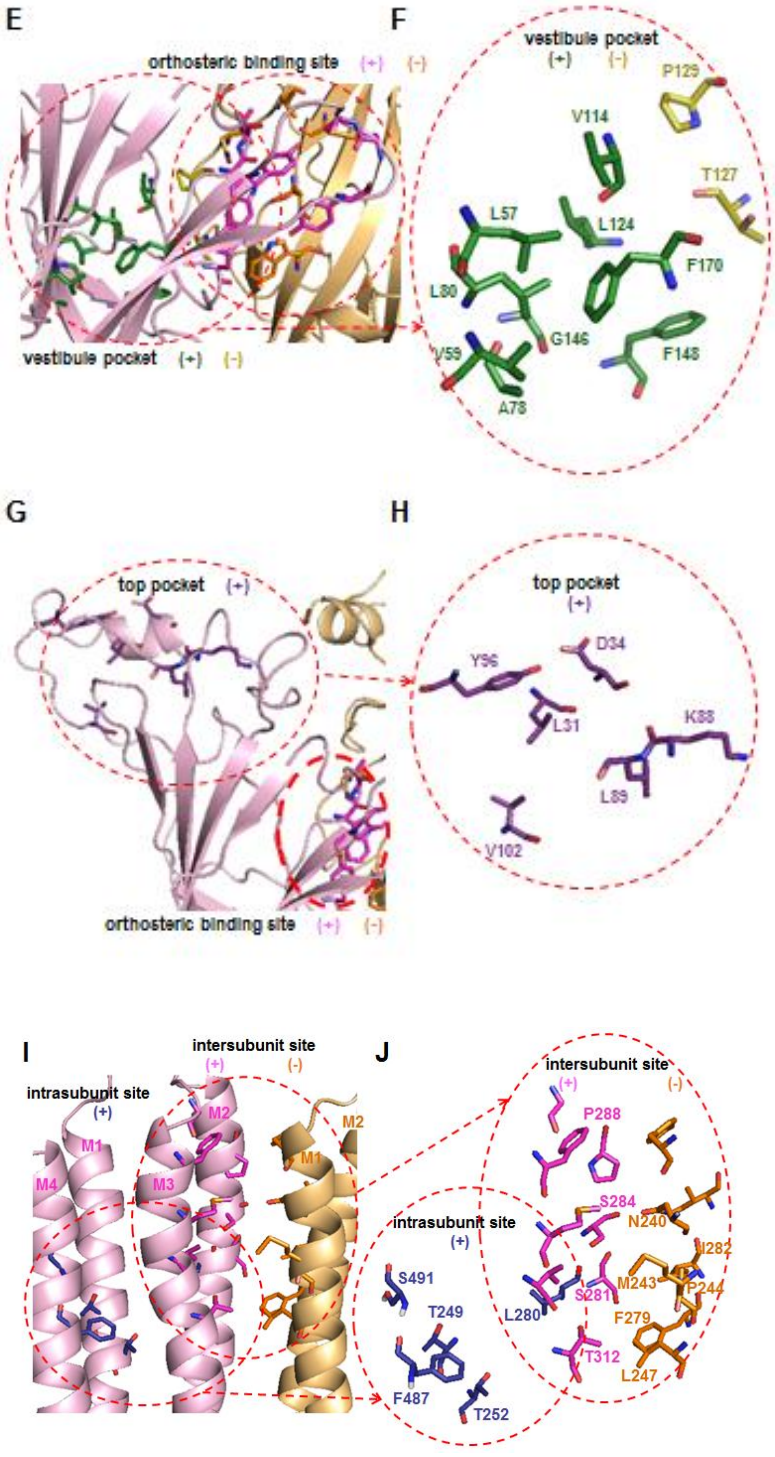

Supplementary Figure S2. (A) Detailed view of the orthosteric binding site in the antagonist-bound model of ECD-Asu-ACR-16. Principal subunit is colored light pink, whereas the complementary subunit is colored yellow. The residues that contribute to the orthosteric binding site are represented by sticks (principal side (+), pink; complementary side (−), orange) and highlighted inside the red dotted circle. Carbon is in either pink or orange. Nitrogen is in blue. Oxygen is in red. Sulfur is in yellow. (B) Detailed view of the residues involving in the orthosteric binding site in the antagonist-bound model of ECD-Asu-ACR-16. Functionally important amino acids which interact with the ligands bound in this region are labeled. (C) Detailed view of the agonist sub-pocket relative to the location of the orthosteric binding site in the antagonist-bound model of ECD-Asu-ACR-16. Principal subunit is colored light pink, whereas the complementary subunit is colored yellow. The residues that contribute to the agonist sub-pocket are represented by sticks (principal side (+), turquoise; complementary side (−), green) and highlighted inside the red dotted circle at the bottom. Carbon is in either turquoise or green. Nitrogen is in blue. Oxygen is in red. (D) Detailed view of the residues involving in the agonist sub-pocket in the antagonist-bound model of ECD-Asu-ACR-16. Functionally important amino acids which interact with the allosteric modulators bound in this region are labeled. (E) Detailed view of the vestibule pocket relative to the location of the orthosteric binding site in the antagonist-bound model of ECD-Asu-ACR-16. Principal subunit is colored light pink, whereas the complementary subunit is colored yellow. The residues that contribute to the vestibule pocket are represented by sticks (principal side (+), dark green; complementary side (−), gold) and highlighted inside the red dotted circle on the left. Carbon is in either dark green or gold. Nitrogen is in blue. Oxygen is in red. (F) Detailed view of the residues involving in the vestibule pocket in the antagonist-bound model of ECD-Asu-ACR-16. Functionally important amino acids which interact with the allosteric modulators bound in this region are labeled. (G) Detailed view of the top pocket relative to the location of the orthosteric binding site in the antagonist-bound model of ECD-Asu-ACR-16. Principal subunit is colored light pink, whereas the complementary subunit is colored yellow. The residues that contribute to the vestibule pocket are represented by sticks (principal side (+), purple) and highlighted inside the red dotted circle at the top. Carbon is in purple. Nitrogen is in blue. Oxygen is in red. (H) Detailed view of the residues involving in the top pocket in the antagonist-bound model of ECD-Asu-ACR-16. Functionally important amino acids which interact with the allosteric modulators bound in this region are labeled. (I) Detailed view of the two transmembrane allosteric binding sites in the antagonist-bound model of TID-Asu-ACR-16. Principal subunit is colored light pink, whereas the complementary subunit is colored yellow. The residues that contribute to the intersubunit site (principal side, pink; complementary side, orange) and intrasubunit site (principal side, purpleblue) are represented by sticks and highlighted inside the red dotted circle. Carbon is in either pink or orange or purpleblue. Nitrogen is in blue. Oxygen is in red. Sulfur is in yellow. (J) Detailed view of the residues involving in the two transmembrane allosteric binding sites in the antagonist-bound model of TID-Asu-ACR-16. Functionally important amino acids which interact with the allosteric modulators bound in this region are labeled.

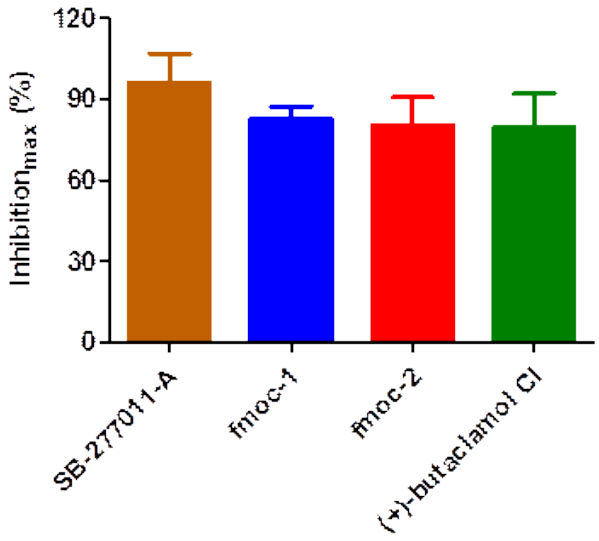

Supplementary Figure S3. Bar chart showing effects of the four hits on Asu-ACR-16. Results are expressed as maximum inhibition (mean ± S.E.M, %) of each plots in (Fig. 5A). The rank order series of inhibition based on maximum inhibition percentage for four hits is: SB-277011-A (96.07 ± 10.66%, n = 4) ≈ fmoc-1 (82.49 ± 4.74%, n = 4) ≈ fmoc-2 (80.34 ± 10.32%, n = 4) ≈ (+)-butaclamol Cl (79.53 ± 12.41%, n = 4) using unpaired t-test.

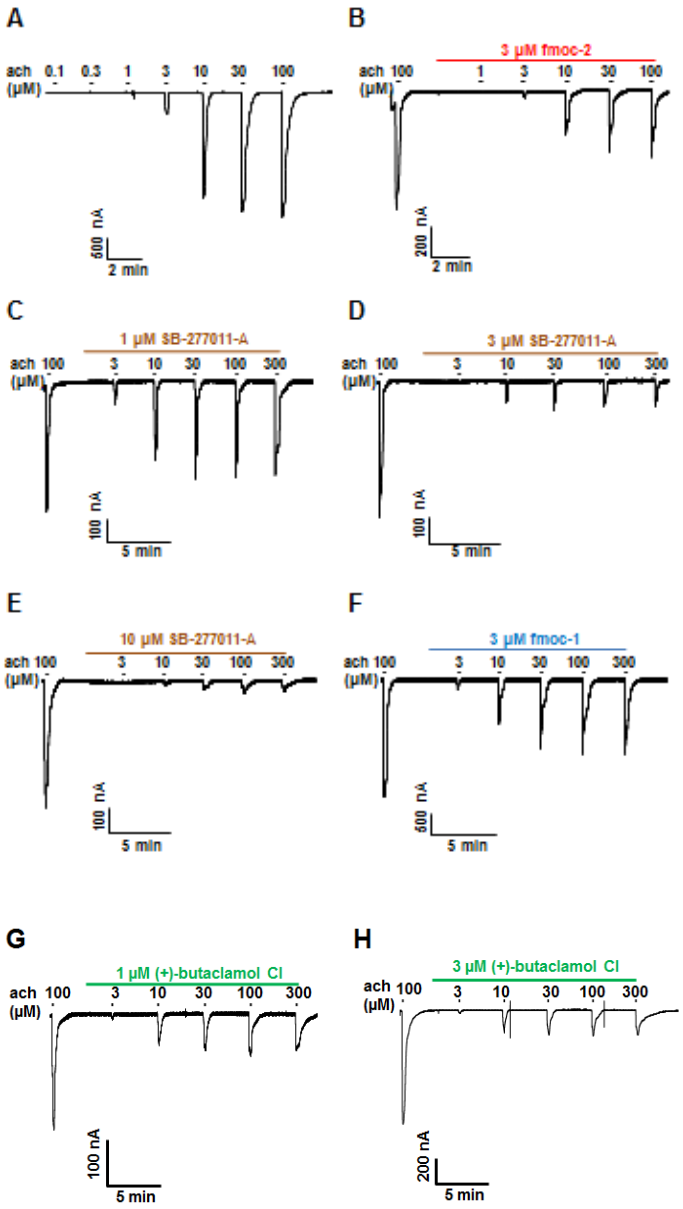

Supplementary Figure S4. Sample traces showing the effects of four hits on the acetylcholine concentration-response relationships for Asu-ACR-16. Sample trace of acetylcholine concentration-response relationships in the absence of hits is depicted in (A) as a control. 3 μM of each of four hits are applied: (B) fmoc-2, (D) SB-277011, (F) fmoc-1, (H) (+)-butaclamol Cl, to compare the EC50 shifts and the maximum response reduction for four hits. 1 μM SB-277011-A (C), 1 μM (+)-butaclamol Cl (G) and 10 μM SB-277011-A (E) were tested to study the concentration effects on the mode of inhibition.

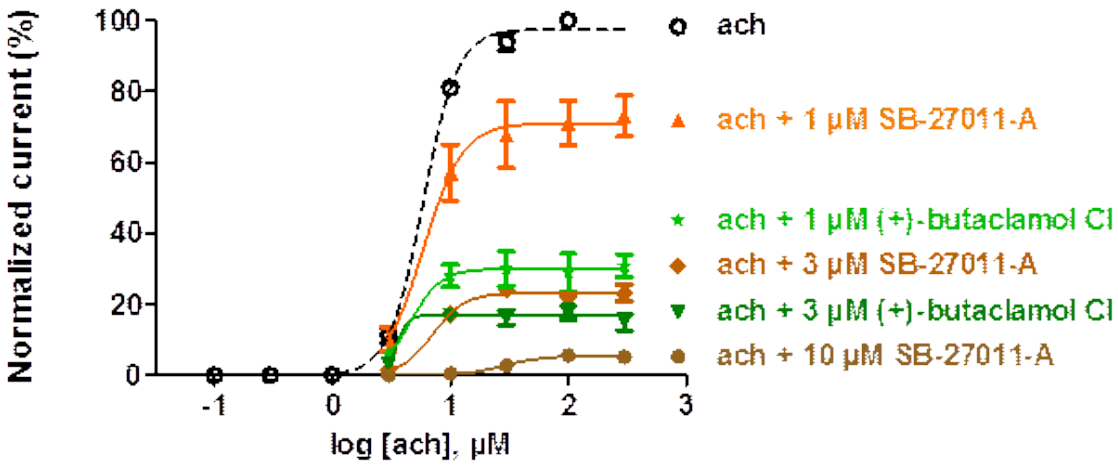

Figure S5. Ach concentration-response curves for Asu-ACR-16 in the absence of hits as a control (ach) and in the continual presence of 1 µM, 3 µM, 10 µM SB-277011-A, 1 µM, 3 µM (+)-butaclamol Cl.

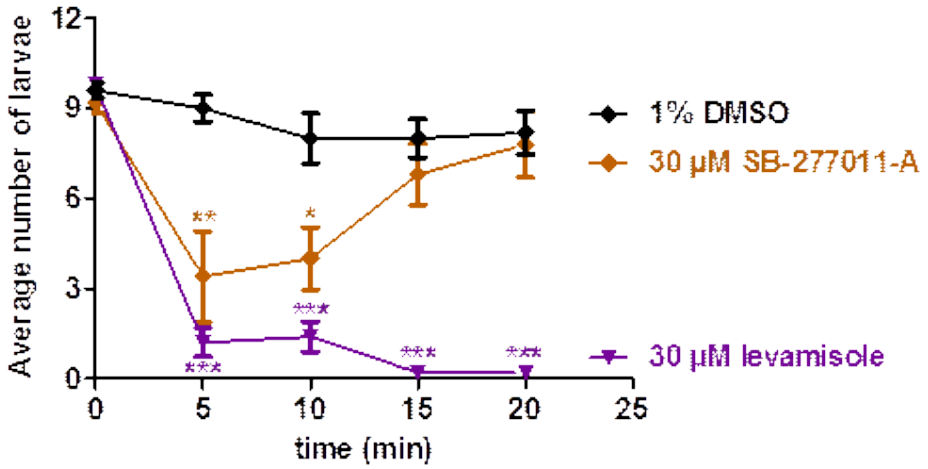

Supplementary Figure S6. Plot of average number of L4 C. elegans larvae with normal motility (A) vs. time (min) in the absence of drug (1% DMSO, control), presence of 30 µM SB-277011-A and 30 µM levamisole. Ten worms were used for each treatment, which was replicated by five times. Comparisons of locomotion were made between control and treated worms at each time point. *p < 0.05, **p < 0.01, ***p < 0.001. The recovery of normal motility was observed only in the larvae treated with 30 µM SB-277011-A within 20 min, but not in the larvae treated with 30 µM levamisole within 24 h.

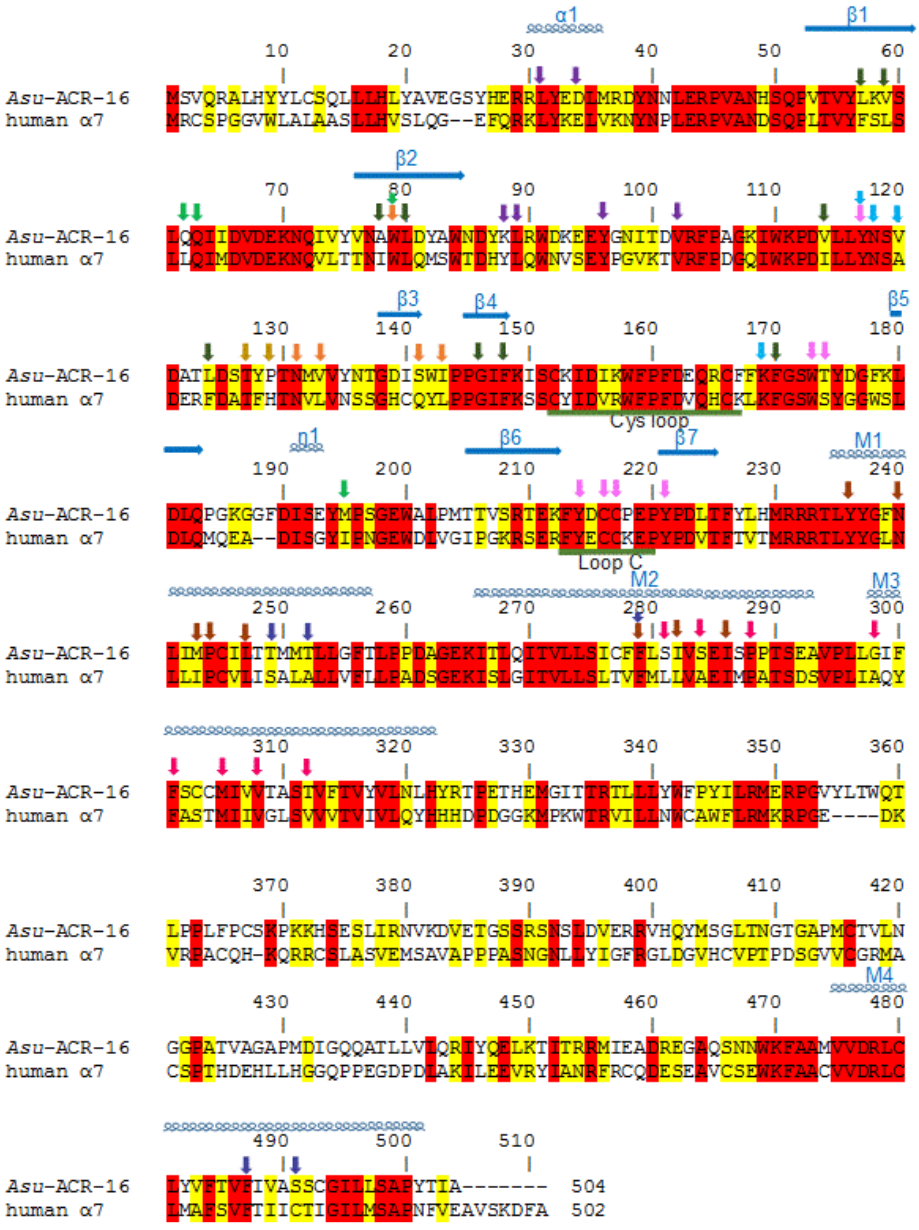

Supplementary Figure S7. Sequence and numbering of the full-length Asu-ACR-16 and its alignment with the human α7 nAChR subunit. Completely conserved residues (red background) and partially conserved residues (yellow background) are indicated. Secondary structures are shown schematically above the sequences. α1 represents α helix. β1-7 represent β strand. η1 represents 310 helix. The Cysteine loop labeled by green bars. Four transmembrane α helixes (M1, M2, M3 and M4) are labeled by blue coils. Residues in the orthosteric binding site are indicated by arrows (principal subunit, pink; complementary subunit, orange). Residues in four allosteric binding sites are highlighted by arrows (principal subunit of agonist sub-pocket, turquoise; complementary subunit of agonist sub-pocket, green; principal subunit of vestibule pocket, dark green; complementary subunit of vestibule pocket, gold; principal subunit of top pocket, purple; principal subunit of intersubunit transmembrane site: bright pink; complementary subunit of intersubunit site: brown; principal subunit of intrasubunit site: purpleblue).

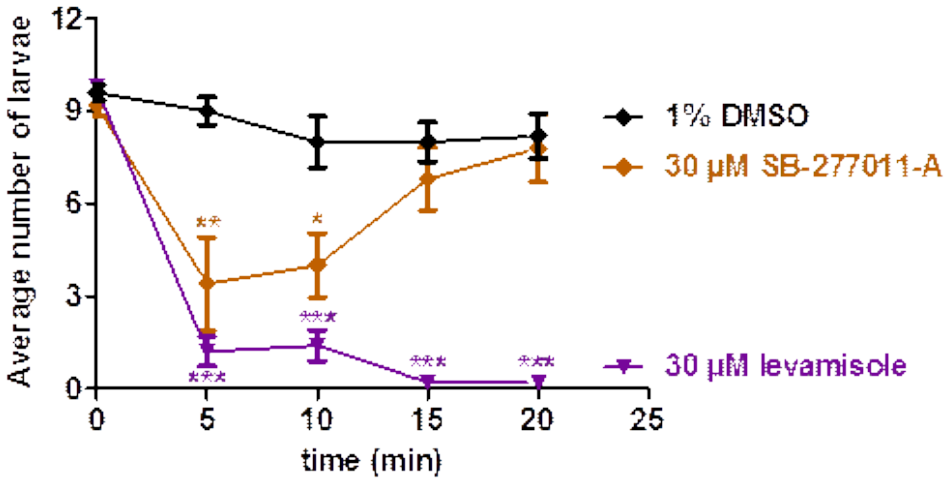

Supplementary Figure S8. Comparison of residues in the orthosteric binding site and five allosteric binding sites between Asu-ACR-16 and human α7 nAChR.

APPENDIX D. THE CHOLINOMIMETIC MORANTEL AS AN OPEN CHANNEL BLOCKER OF THE *ASCARIS SUUM* ACR-16 nAChR

A paper published in *Invertebrate Neuroscience* (2016)[1]

Melanie Abongwa[2], Katherine E. Baber[2], Richard J. Martin[2], Alan P. Robertson[2*]

[1] Reprinted with permission of *Invert Neurosci* (2016), **16**: 10
[2] Department of Biomedical Sciences, College of Veterinary Medicine, Iowa State University, Ames, IA, USA
[*] Corresponding author and Associate Professor, Department of Biomedical Sciences, Iowa State University

D1.0 Abstract

Nematode parasite infections pose a significant threat in human and veterinary medicine. At least a third of the world's population is at risk from nematode parasite infections. These infections not only cause health problems, but also cause loss of livestock production and hence, economic losses. Anthelmintic drugs are the mainstay by which control of nematode parasite infections is achieved. Many of the currently available anthelmintics act on nicotinic acetylcholine receptors (nAChRs). However, the detailed mode of action (MOA) of these anthelmintics is not clearly understood. Elucidation of the MOA of anthelmintics is highly desirable; an in-depth knowledge of the MOA will better inform on mechanisms of resistance development and on ways to slow down or overcome resistance. The cholinomimetic anthelmintic, morantel, has a complex MOA involving the activation and block of levamisole-sensitive single nAChR channels (L-type nAChR or L-nAChR). More recently, morantel has been demonstrated to activate *Haemonchus contortus* and *Parascaris equorum* ACR-26/ACR-27 nAChRs expressed in *Xenopus laevis* oocytes. Previous studies in our laboratory, however, have shown morantel does not activate the

nicotine-sensitive nAChR (N-type nAChR or N-nAChR), *Ascaris suum* ACR-16 (*Asu*-ACR-16). In this study, we used two-electrode voltage-clamp (TEVC) electrophysiology to investigate the inhibitory effects of morantel, on expressed *Asu*-ACR-16 nAChRs in *X. laevis* oocytes. Our results show that morantel acts as a non-competitive antagonist on *Asu*-ACR-16. This non-competitive antagonism by morantel was further demonstrated to be voltage-sensitive. We conclude based on our findings that morantel is a non-competitive voltage-sensitive open channel blocker of *Asu*-ACR-16.

D1.1 Keywords

Ascaris suum ACR-16nAChRElectrophysiologyMorantelOpen channel block

D1.2 Abbreviations

nAChR	Nicotinic acetylcholine receptor
MOA	Mode of action
TEVC	Two-electrode voltage-clamp
BAPTA-AM	1,2-Bis(2-aminophenoxy)ethane-N,N,N′,N′-tetra-acetic acid tetrakis (acetoxymethylester)
HEPES	4-(2-Hydroxyethyl)piperazine-1-ethanesulfonic acid
ach	Acetylcholine
mor	Morantel
DMSO	Dimethyl sulfoxide

D2.0 Introduction

Nematode parasite infections are a significant threat in both human and veterinary medicine, affecting about one-third of the human population and causing significant animal production losses (Bethony et al. 2006; de Silva et al. 2003; Hotez et al. 2006, 2008). The major control strategy for nematode parasite infections involves use of anthelmintic drugs, which are selectively toxic to the parasites (Brooker et al. 2006). Although the mode of action (MOA) of many anthelmintics is not fully understood, some of their sites of action and

biochemical mechanisms are well known. Many of the currently available anthelmintics target nicotinic acetylcholine receptors (nAChRs), which are involved in neuromuscular coordination (Martin et al. 1997; Wolstenholme 2011). Other anthelmintics exhibit their pharmacological effect by interfering with the parasite cell integrity, feeding, or some protective mechanisms against the host which may cause starvation, paralysis and expulsion, or digestion of the parasite (Holden-Dye and Walker 2007, 2014; Lustigman et al. 2014; Morel et al. 2014).

Nematode muscle nAChRs are of significant interest because they are targets for many anthelmintics. nAChRs are pentameric ligand-gated ion channels which mediate rapid synaptic transmission at the neuromuscular and nerve–nerve junctions of vertebrates and invertebrates (Karlin 2002; Zouridakis et al. 2009). The cholinergic anthelmintic agonist, morantel, is a classic example of an anthelmintic that acts on nematode muscle nAChRs (Martin 1997). The published MOA of morantel is that it selectively opens nAChRs present on nematode parasite muscle cells to cause muscle contraction and hence, spastic paralysis and expulsion of the parasite (Martin et al. 1996). However, the agonist effect of morantel has been demonstrated in the levamisole-sensitive nAChRs (L-nAChRs) which are insensitive to nicotine and are heteropentameric, comprising more than one subunit type (Rayes et al. 2007). Morantel has also been shown to cause block of L-nAChRs in addition to its agonist effect on these receptor types (Evans and Martin 1996). At the single-channel level, L-nAChRs have a conductance (G) of 35 pS in *A. suum* (Qian et al. 2006), a Clade III nematode. A similar channel conductance was observed in *Oesophagostomum dentatum* (Buxton et al. 2014), a Clade V nematode.

More recently, morantel was shown to activate the nAChRs, *Haemonchus contortus* ACR-26/ACR-27 (*Hco*-26/27) and *Parascaris equorum* ACR-26/ACR-27 (*Peq*-26/27) expressed in *Xenopus laevis* oocytes, and the sensitivity of *Caenorhabditis elegans* to morantel was increased when these receptors were expressed in body wall muscles (Courtot et al. 2015). The nicotine-sensitive nAChRs (N-nAChRs) which are insensitive to levamisole and are homopentameric, comprising of one subunit type, are not activated by morantel (Raymond et al. 2000). In agreement with this observation, previous studies in our laboratory involving the pharmacological characterization of the N-nAChR, *A. suum* ACR-16 (*Asu*-ACR-16), showed ACR-16 to be insensitive to morantel, in addition to other cholinergic anthelmintic agonists including levamisole, methyridine, thenium, bephenium, tribendimidine, and pyrantel (Abongwa et al. 2016a). In an effort to further elucidate the MOA of morantel, we used the two-electrode voltage-clamp electrophysiology technique to characterize morantel's antagonistic effects on *Asu*-ACR-16 expressed in *X. laevis* oocytes.

D3.0 Materials and methods

D3.1 cRNA preparation

Preparation of the *Asu-acr-16* and *Asu-ric-3* cRNA used in this study has been previously reported (Abongwa et al. 2016a).

D3.2 Expression of *Asu*-ACR-16 in *Xenopus laevis* oocytes

Expression of *Asu*-ACR-16 in *X. laevis* oocytes has been described previously (Abongwa et al. 2016a). Briefly, defolliculated *X. laevis* oocytes obtained from Ecocyte Bioscience (Austin, Texas, USA) were injected with 25 ng *Asu-acr-16* cRNA in combination with 5 ng of the required ancillary factor, *Asu-ric-3* cRNA, in a total volume of 50 nL. Once injected, individual oocytes were transferred to a 96-well culture plate containing 200 μL of

incubation solution (100 mM NaCl, 2 mM KCl, 1.8 mM $CaCl_2 \cdot 2H_2O$, 1 mM $MgCl_2 \cdot 6H_2O$, 5 mM HEPES, 2.5 mM Na pyruvate, 100 U/mL penicillin, and 100 µg/mL streptomycin, pH 7.5). Oocytes were then incubated at 19 °C for 5–7 days, with incubation solution changed daily, to allow for protein functional expression.

D3.3 Two-electrode voltage-clamp (TEVC) electrophysiology

At least 2 h prior to recording, 100 µM BAPTA-AM was added to the incubation solution to prevent activation of endogenous calcium-activated chloride channels. Current responses to drug applications were recorded using TEVC electrophysiology (Abongwa et al. 2016b; Robertson et al. 2008). An Axoclamp 2B amplifier (Warner Instruments, USA) was used to record currents from oocytes voltage-clamped at −90, −60, or −30 mV. The data were acquired on a computer with Clampex 9.2 software (Molecular Devices, CA, USA). Microelectrodes (standard wall borosilicate glass with filament, o.d. 1.5 mm, i.d. 0.86 mm) (G150F-6, Warner Instruments, USA) for impaling oocytes were pulled using a Flaming/Brown horizontal electrode puller (Model P-97, Sutter Instruments). The microelectrodes were then filled with 3 M KCl, and the tips carefully broken with a piece of tissue paper to achieve a resistance of 2–5 MΩ in recording solution (100 mM NaCl, 2.5 mM KCl, 1 mM $CaCl_2 \cdot 2H_2O$, and 5 mM HEPES, pH 7.3).

D3.4 Drugs

The drugs used for this study, acetylcholine (ach) and morantel (mor), were purchased from Sigma-Aldrich (St Louis, MO, USA). BAPTA-AM, an intracellular calcium chelator, was also purchased from Sigma-Aldrich (St Louis, MO, USA). Acetylcholine and morantel stock solutions were prepared in recording solution and dimethyl sulfoxide

(DMSO), respectively. The final working DMSO concentration did not exceed 0.1% in all experiments.

D3.5 Drug applications

Oocytes were perfused with drugs by a system controlled by eight valves (VC-8 valve controller) (Warner Instruments, USA) at a flow rate of 4 ml/min. Except otherwise indicated, each concentration of acetylcholine in the absence or presence of morantel was applied for 10 s, followed by a 2-min wash with recording solution in between drug applications. The oocytes were voltage-clamped at −60 mV, except for the voltage sensitivity experiments where the oocytes were voltage-clamped at −90, −60, and −30 mV. Acetylcholine concentration–response relationships in the absence of morantel were generated by applying acetylcholine at concentrations of 0.1–300 μM, at semilog intervals. Morantel antagonism was estimated by first applying 100 μM acetylcholine for 30 s as a control, followed by a 2-min wash with recording solution. Thereafter, a test 100 μM acetylcholine was applied for 10 s, followed by a 10-s co-application of 100 μM acetylcholine in the presence of either 0.3, 1, 3, 10, 30 or 100 μM morantel, and then a final 10-s application of 100 μM acetylcholine. For subsequent experiments, morantel was used at 1 and 3 μM. Acetylcholine concentration–response relationships in the presence of 1 and 3 μM morantel were generated by first applying a control 100 μM acetylcholine for 10 s, followed by a 2-min application of morantel, and 10-s applications of 3, 10, 30, 100 and 300 μM acetylcholine in the continued presence of morantel. Voltage sensitivity experiments were conducted by holding the membrane potential at −90, −60, or −30 mV, and applying a control 100 μM acetylcholine for 10 s, followed by a 10-s application of 100 μM acetylcholine in the presence of 3 μM morantel, at each holding potential.

D3.6 Data analysis

Data acquired from the TEVC electrophysiological recordings were analyzed with Clampfit 9.2 (Molecular Devices, CA, USA) and GraphPad Prism 5.0 software (GraphPad Software Inc., CA, USA). Unless otherwise indicated, peak currents in response to applied drugs were measured and normalized to the 100 μM acetylcholine control response and expressed as mean ± S.E.M. The concentration–response relationships were analyzed by fitting data points with the Hill equation as previously described (Martin et al. 2004). Initial experiments to measure morantel inhibition of acetylcholine responses used a brief (10 s) application of morantel during a longer (30 s) application of acetylcholine (Fig. 2a). In these experiments, inhibition was calculated by measuring the smallest current during the morantel application and the largest current induced by acetylcholine after morantel wash-off began. Percent inhibition was calculated as: (acetylcholine current − morantel current)/acetylcholine current × 100. In subsequent experiments where morantel was present for sustained period of time, the peak currents in the presence of morantel were used and normalized to acetylcholine currents in the absence of the drug (Figs. 3a, 4a). The voltage-sensitive block effects of morantel were estimated as $1/\tau$, where τ was the mean of a single exponential decay fit to the acetylcholine-induced currents in the presence of morantel:

$$f(t) = \sum_{i=1}^{n} A_i e^{-t/\tau_i} + C$$

where n = number of components, A = amplitude, t = time, τ = time constant, and C = constant y-offset for each i component.

Statistical comparisons were done using unpaired Student's t test or one-way ANOVA. A p value < 0.05 was considered significant.

D4.0 Results

D4.1 *Asu*-ACR-16 is activated by acetylcholine in a concentration-dependent manner

Figure 1a, b, respectively, show the sample traces (inward currents) and concentration–response relationship for acetylcholine. *Asu*-ACR-16 was not activated by 0.1, 0.3, and 1 μM acetylcholine, but was activated by acetylcholine concentrations ≥3 μM. As previously observed, current responses increased with increasing acetylcholine concentrations, demonstrating activation of the *Asu*-ACR-16 nAChR by acetylcholine is concentration dependent (Abongwa et al. 2016a; Zheng et al. 2016). The EC_{50} for acetylcholine was 6.1 ± 0.2 μM, R_{max} 99.4 ± 0.6%, and Hill slope (n_H) 3.4 ± 0.1 (n = 5).

D4.2 Morantel is a non-competitive antagonist of the *Asu*-ACR-16 nAChR

We tested the antagonistic effects of morantel on the *Asu*-ACR-16 nAChR by varying the concentration of morantel from 0.3 to 100 μM, while repeatedly applying a constant acetylcholine concentration of 100 μM. The morantel inhibition plot is shown in Fig. 2, with sample traces (a) shown above the plot (b). Inhibition of *Asu*-ACR-16 acetylcholine responses was seen to increase with increasing morantel concentration. Morantel was a potent antagonist of *Asu*-ACR-16 as reflected by its observed IC_{50} value of 5.6 ± 1.8 μM (n = 4), n_H 0.9 ± 0.1 (n = 4).

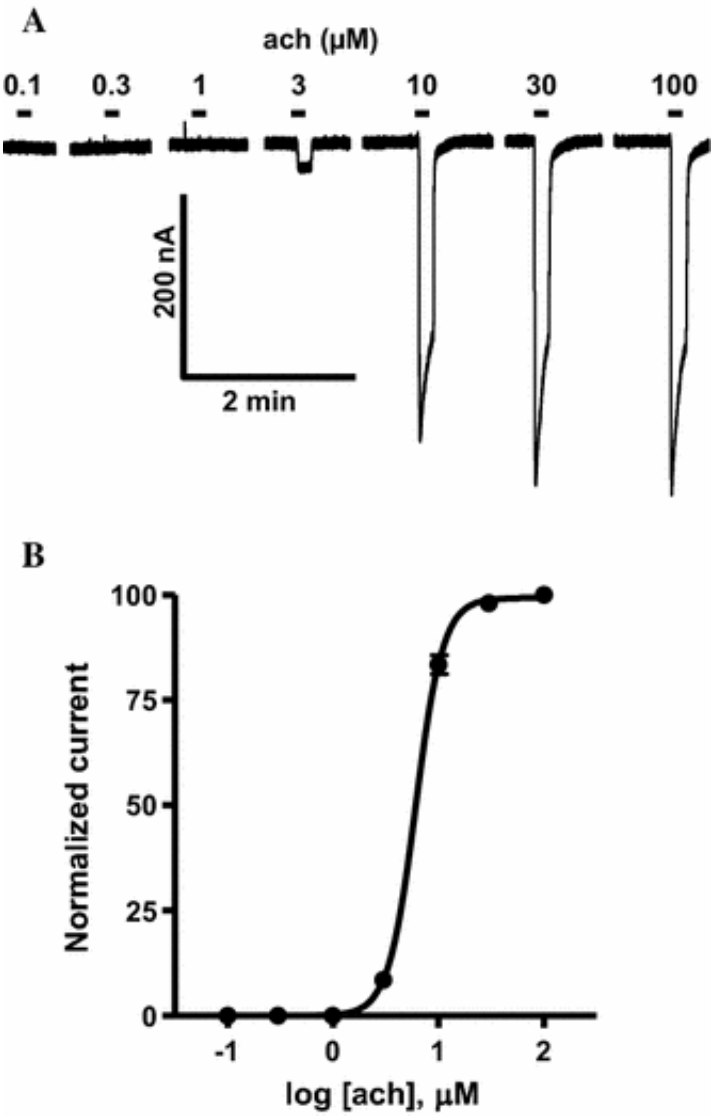

Fig. 1 Acetylcholine concentration–response relationship for *A. suum* ACR-16. **a** Sample traces showing *inward currents* in response to 0.1–100 μM acetylcholine. **b** Acetylcholine concentration–response plot for *A. suum* ACR-16. EC_{50} for acetylcholine was 6.1 ± 0.2 μM, R_{max} 99.4 ± 0.6%, and Hill slope (n_H) 3.4 ± 0.1 (n = 5).

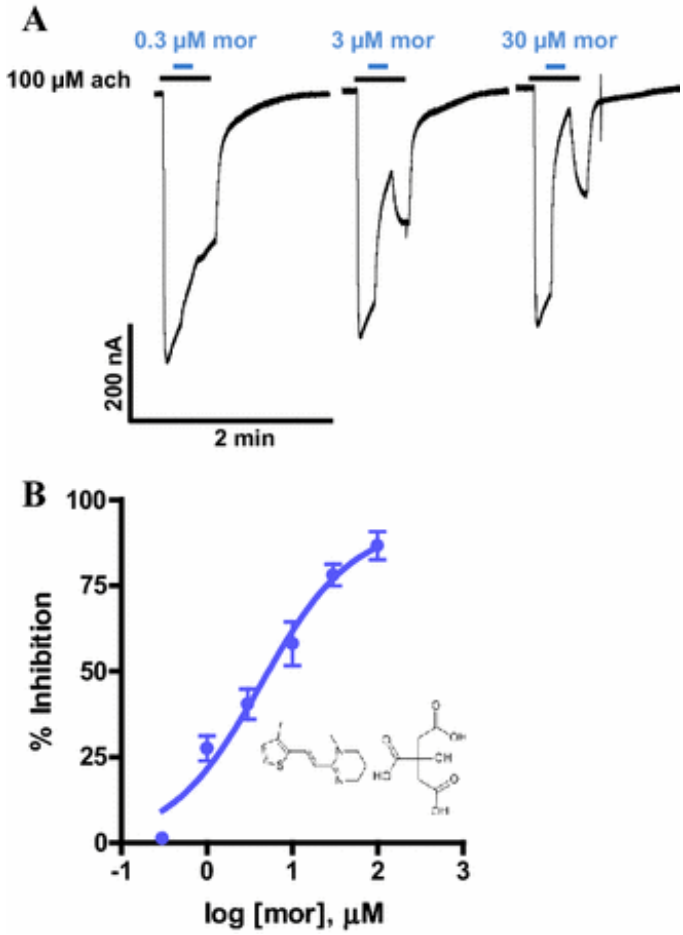

Fig. 2 Inhibition of *A. suum* ACR-16 responses to 100 µM acetylcholine by 0.3–100 µM morantel. **a** Sample traces (*inward currents*) showing a concentration-dependent inhibition of acetylcholine responses by morantel. **b** Concentration–response plot showing percent inhibition of 100 µM acetylcholine by 0.3–100 µM morantel. IC_{50} morantel was 5.6 ± 1.8 µM (n = 4), n_H 0.9 ± 0.1 (n = 4)

To elucidate the type of antagonism produced by morantel, we first applied 0.3, 1, 3, 10, 30, 100, and 300 μM acetylcholine in the absence of morantel, which served as the control. This was followed by a different set of experiments where we applied 3, 10, 30, 100, and 300 μM acetylcholine in the presence of 1 and 3 μM morantel. Sample traces for these recordings are shown in Fig. 3a. The concentration–response relationships for acetylcholine in the absence and presence of 1 and 3 μM morantel are shown in Fig. 3b. The EC_{50} and R_{max} values were 4.5 ± 0.1 μM and 98.2 ± 0.1% (n = 3) for acetylcholine, 4.5 ± 0.3 μM and 82.6 ± 3.0% (n = 4) in 1 μM morantel, and 4.0 ± 0.5 μM and 39.4 ± 1.6% (n = 4) in 3 μM morantel. Morantel showed a concentration-dependent significant reduction of R_{max} ($p < 0.01$ for 1 μM morantel; $p < 0.001$ for 3 μM morantel), with no change in EC_{50} ($p > 0.05$), which are characteristics of non-competitive antagonism. These results indicate that morantel is a non-competitive antagonist of the *Asu*-ACR-16 nAChR.

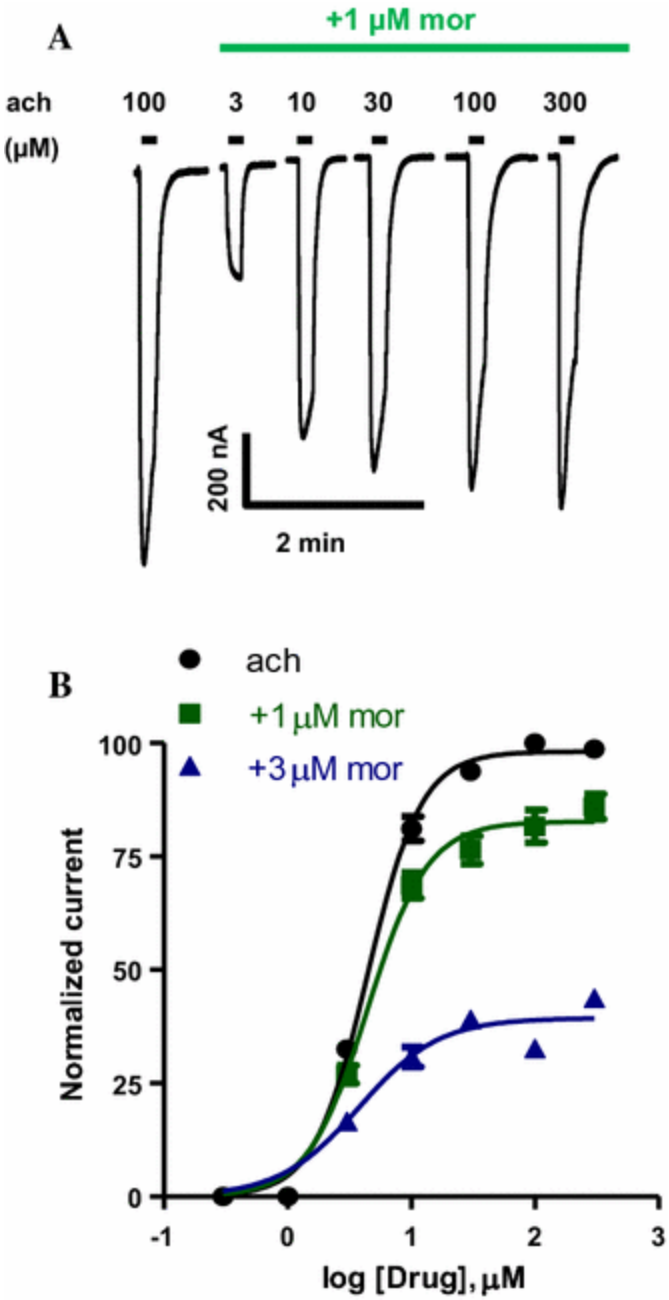

Fig. 3 Concentration–response relationships for acetylcholine in the absence and presence of morantel. **a** Sample traces showing *inward currents* in response to acetylcholine in the presence of 1 µM morantel. **b** Concentration–response plots for acetylcholine alone (*black curve*), acetylcholine in the presence of 1 µM morantel (*green curve*), and acetylcholine in the presence of 3 µM morantel (*blue curve*). EC_{50} and R_{max} values were 4.5 ± 0.1 µM and 98.2 ± 0.1% (n = 3) for acetylcholine, 4.5 ± 0.3 µM and 82.6 ± 3.0% (n = 4) in 1 µM morantel, and 4.0 ± 0.5 µM and 39.4 ± 1.6% (n = 4) in 3 µM morantel.

D4.3 Morantel acts as an open channel blocker to produce antagonism

Voltage sensitivity experiments were performed to further elucidate the mechanism of morantel's non-competitive antagonism. Figure 4a shows sample traces of the effect of morantel on acetylcholine responses at different holding potentials. Figure 4b shows a plot of $1/\tau$ against membrane potential (−90, −60 and −30 mV). One-way ANOVA revealed a significant effect of voltage on morantel's blocking actions ($p < 0.05$); showing morantel's blocking action is voltage-sensitive. In whole-cell recordings, $1/\tau$ is representative of the mean open time of the channel. The reduction in $1/\tau$ (and therefore mean open-time of the channel) as the holding potential becomes more negative is consistent with the drug acting as an open channel blocker.

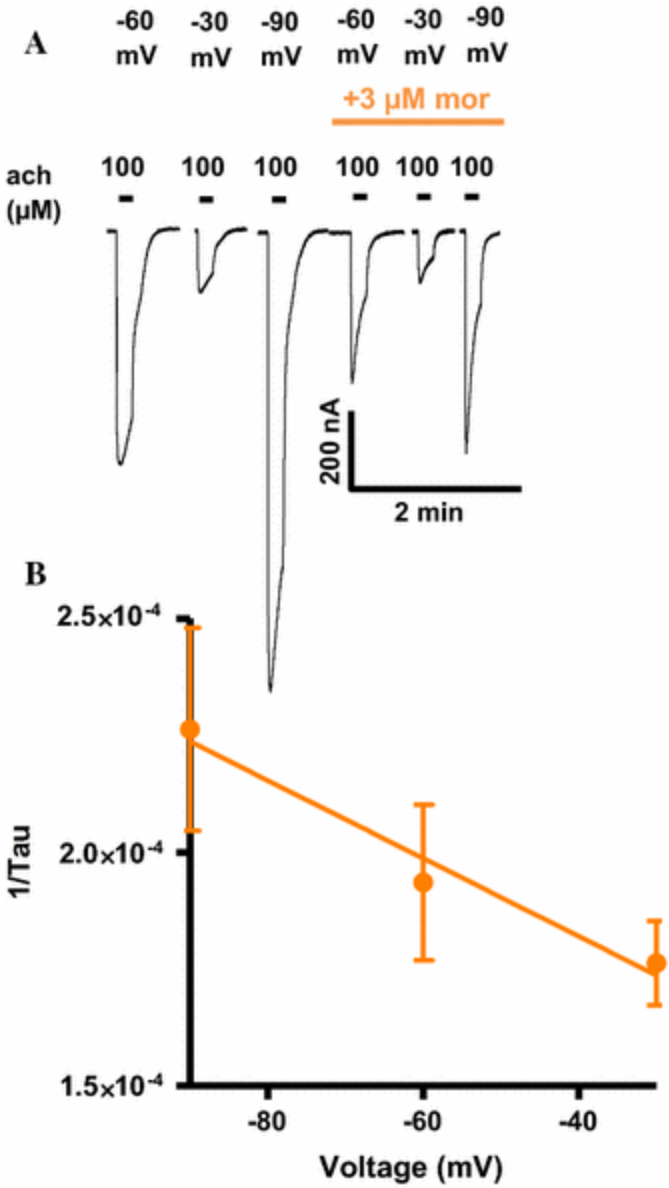

Fig. 4 Voltage sensitivity of morantel's inhibitory effects on *A. suum* ACR-16 responses to acetylcholine. **a** Sample traces (*inward currents*) showing acetylcholine responses in the absence and presence of 3 µM morantel at different holding membrane potentials (−90, −60, −30 mV). **b** $1/\tau$ versus holding potential (mV) showing *line of best fit* by linear regression. Notice morantel's inhibitory effects were higher at more negative membrane potentials, indicating morantel's blocking action is voltage-sensitive.

D5.0 Discussion

The goal of this study was to provide an understanding of the MOA of morantel on the recently characterized *Asu*-ACR-16 nAChR. Like *C. elegans* ACR-16 (*Cel*-ACR-16),

Asu-ACR-16 is a member of the N-type nAChRs that are preferentially activated by nicotine (Abongwa et al. 2016a; Ballivet et al. 1996). It is noteworthy that the characterization of the N-type nAChRs is not as extensive as the L-type channels preferentially activated by levamisole. Furthermore, N-type nAChRs are not activated by the currently used cholinergic anthelmintic agonists (Abongwa et al. 2016a; Raymond et al. 2000). As such, the N-type nAChRs are not well exploited for anthelmintic drug discovery, compared to the L-type. Raymond et al. (2000) showed morantel did not activate *C. elegans* ACR-16 or chicken α7 receptors expressed in *X. laevis* oocytes, voltage-clamped at −100 mV. Rather, morantel inhibited current responses to 1 mM acetylcholine in a dose-dependent manner, with pIC_{50} values of, respectively, 5.7 and 5.6 for *C. elegans* ACR-16 and chicken α7, which approximates to IC_{50} values of 2 µM for *C. elegans* ACR-16 and 2.5 µM for chicken α7 (Raymond et al. 2000) versus our observed IC_{50} of 5.6 ± 1.8 µM for expressed *Asu*-ACR-16 in oocytes voltage-clamped at −60 mV. Notice the IC_{50} values for *C. elegans* ACR-16 and chicken α7 are lower than that for *Asu*-ACR-16, and this is likely due to more negative holding potential (−100 mV) used in oocytes expressing *C. elegans* ACR-16 or chicken α7, whereas in our experiments, oocytes expressing *Asu*-ACR-16 were held at −60 mV.

By taking advantage of the *X. laevis* oocyte expression system, we have demonstrated using TEVC electrophysiology that morantel acts as a non-competitive antagonist of the *Asu*-ACR-16 nAChR and that the mechanism by which morantel produces its inhibitory effects is consistent with open channel block. This provides new information for the MOA of morantel on the N-type nAChR, *Asu*-ACR-16, in addition to its known agonistic and blocking effects on levamisole receptors (Evans and Martin 1996; Rayes et al. 2007). In our study, however, we found morantel to be more potent on the expressed *Asu*-ACR-16 (IC_{50} 5.6 ± 1.8 µM,

n = 4) compared to the IC_{50} of 10 µM observed in *A. suum* muscle cells at the single-channel level (Evans and Martin 1996). The Hill slope for morantel concentration–response curve in our study (n_H 0.9 ± 0.1, n = 4) was also less than that reported by Evans and Martin (n_H 1.6). The conductance of *A. suum* muscle nAChRs (32–40 pS, depending on the polarity of the holding potential) reported by Evans and Martin (1996) indicate that they were investigating L-type channels, as described by Qian et al. (2006) rather than the N-type investigated in this study. It is also possible that the study by Evans and Martin (1996) included examples of channels formed by ACR-26/ACR-27 subunits (Courtot et al. 2015) that have not been characterized at the single-channel level to date. According to Raymond et al. (2000), morantel IC_{50} and n_H values for *C. elegans* ACR-16 (2 µM and −0.9) and chicken α7 (2.5 µM and −1.1) were also less than those reported by Evans and Martin (1996) for *A. suum* muscle nAChRs (10 µM and 1.6), implying morantel is also more potent on expressed *C. elegans* ACR-16 and chicken α7 receptors than in *A. suum* muscle cells. Therefore, morantel appears to have different effects on the nicotine and levamisole receptor types.

Multiple sites of action for an anthelmintic are desirable (Martin et al. 1998). Morantel is believed to cause spastic paralysis of the nematode by its action as an L-nAChR agonist. L-nAChRs are involved in muscle contraction; however, ACR-16 may have a paracrine function given its wide distribution in *A. suum* body tissues (Abongwa et al. 2016a). Hence, ACR-16 may not have a distinct role in fast signal transduction at the neuromuscular junction of nematodes, and just as in *C. elegans*, inhibition of *Asu*-ACR16 may have no obvious effect on motility (Touroutine et al. 2005). Therefore, although the inhibition of ACR-16 may be deleterious to the parasite, this anthelmintic effect is uncertain. Regardless, it may not be desirable to use morantel with compounds that act as agonists of

ACR-16. That notwithstanding, a detailed knowledge of drug effects on multiple receptors will inform the selection of compounds to be used in combination therapy, an approach that is increasing in popularity due to its potential for slowing the development of drug resistance, in addition to the obvious potential increase in spectrum of action.

D6.0 Author's contribution

MA, RJM and APR conceived and designed the research study. MA and KEB performed the research. MA, KEB and APR analyzed the data. RJM and APR contributed to reagents/materials/analysis tools. MA, RJM and APR wrote the paper.

D7.0 Funding

This research was funded by the National Institute of Allergy and Infectious Diseases of the National Institutes of Health under Award Number R01AI047194 to RJM, R21AI121831-01 to APR and the Schlumberger Foundation to MA.

D8.0 Compliance with ethical standards

D8.1 Conflict of interest

The authors declare that they have no conflict of interest.

D8.2 Ethical approval

No vertebrate animals were directly used in this study. Adult female *A. suum* worms and defolliculated *Xenopus laevis* oocytes used in this study were obtained from Marshalltown Pork Plant, Marshalltown, Iowa, and Ecocyte Bioscience (Austin, TX, USA), respectively.

APPENDIX E. LIST OF ALL CONFERENCE ABSTRACTS, AWARDS AND FUNDING

CONFERENCE ABSTRACTS

Melanie Abongwa, Fidelis Cho-Ngwa, Godfred Ayimele, Moses Samje, Smith B. Babiaka, Judy Sakanari, Eman Mostafa, Adrian J. Wolstenholme, Richard J. Martin, Alan P. Robertson. "Activity of crude extracts and chromatographic fractions of *Daniellia oliveri* and *Psorospermum febrifugum* against adult *Brugia pahangi*". American Society of Tropical Medicine and Hygiene (ASTMH) 65th Annual Meeting, held at Atlanta Marriott Marquis and Hilton Atlanta, Atlanta, Georgia, USA, November 13-17, 2016.

Melanie Abongwa, Fidelis Cho-Ngwa, Godfred Ayimele, Moses Samje, Smith B. Babiaka, Ann Perera, Eman Mostafa, Adrian J. Wolstenholme, Richard J. Martin, Alan P. Robertson. "Filaricidal activities of extracts of *Daniellia oliveri* and *Psorospermum febrifugum*". International Symposium on Anthelmintics: From Discovery to Resistance II, held at the Marina Village Center, San Diego, California, USA, February 9-12, 2016.

Richard J. Martin, Fudan Zheng, Alan P. Robertson, **Melanie Abongwa** and Edward W. Yu. "The *Ascaris suum* nicotinic receptor, ACR-16, as a drug target: four novel negative allosteric modulators from virtual screening". International Symposium on Anthelmintics: From Discovery to Resistance II, held at the Marina Village Center, San Diego, California, USA, February 9-12, 2016.

Sasa Trailovic, Djorje Marianovic, James G. Tipton, **Melanie Abongwa**, Fudan Zheng, Shivani Choudhary, Richard J. Martin and Alan P. Robertson. "Effects of monepantel on nicotinic acetylcholine receptors from *Ascaris suum* and *Oesophagostomum dentatum*". International Symposium on Anthelmintics: From Discovery to Resistance II, held at the Marina Village Center, San Diego, California, USA, February 9-12, 2016.

Mark McHugh, Saurabh Verma, Shivani Choudhary, **Melanie Abongwa**, Sudhanva Kashyap, JoAnne Powell- Coffman, Alan Robertson, Richard Martin. "Differential expression of four nicotinic acetylcholine receptor subunits (nAChRs) in *Ascaris suum* tissues". International Symposium on Anthelmintics: From Discovery to Resistance II, held at the Marina Village Center, San Diego, California, USA, February 9-12, 2016.

Melanie Abongwa, Fidelis Cho-Ngwa, Godfred Ayimele, Moses Samje, Smith B. Babiaka, Ann Perera, Adrian J. Wolstenholme, Richard J. Martin, Alan P. Robertson. *In vitro* antifilarial activities and metabolomic profiling of extracts of *Daniellia oliveri* and *Psorospermum febrifugum*. American Society of Tropical Medicine and Hygiene (ASTMH) 64th Annual Meeting, held at Philadelphia Marriott Downtown, Philadelphia, Pennsylvania, USA, October 25-29, 2015.

Melanie Abongwa, Alan P. Robertson, Richard J. Martin. "Not just GluCls (Glutamate-gated Chloride channels): Abamectin has potent effects on nicotinic acetylcholine receptors of nematode parasites". 25th International Conference of the World Association for the Advancement of Veterinary Parasitology (WAAVP), held at The Arena and Convention Centre, Liverpool, UK, August 16-20, 2015.

Melanie Abongwa, Fidelis Cho-Ngwa, Godfred A. Ayimele, Moses Samje, Smith B. Babiaka, Ann Perera, Richard J. Martin, Alan P. Robertson. "Anthelmintic activity and metabolomic profiling of extracts of *Daniellia oliveri* and *Psorospermum febrifugum*". 25th International Conference of the World Association for the Advancement of Veterinary Parasitology (WAAVP), held at The Arena and Convention Centre, Liverpool, UK, August 16-20, 2015.

Melanie Abongwa, Fudan Zheng, Samuel K Buxton, Elise Courtot, Claude Charvet, Cédric Neveu, Ciaran J McCoy, Saurabh Verma, Alan P Robertson and Richard J Martin. "*Asu*-ACR-16: a homomeric nAChR widely distributed in Ascaris tissues". 25th International Conference of the World Association for the Advancement of Veterinary Parasitology (WAAVP), held at The Arena and Convention Centre, Liverpool, UK, August 16-20, 2015.

Melanie Abongwa, Fidelis Cho-Ngwa, Godfred A. Ayimele, Moses Samje, Smith B. Babiaka, Richard J. Martin, Alan P. Robertson. "*In vitro* filaricidal activity, cytotoxicity and phytochemical analysis of crude extracts of *Daniellia oliveri* and *Psorospermum febrifugum*". Society of Toxicology (SOT) 54th Annual Meeting & ToxExpo™, San Diego Convention Center, San Diego, California, USA, March 21-26, 2015.

Claude L Charvet, Samuel K Buxton, Cédric Neveu, Jacques Cabaret, Nicolas Peineau, **Melanie Abongwa**, Elise Courtot, Alan P Robertson, Richard J Martin. "Nematode nicotinic acetylcholine receptor diversity: expression of tribendimidine- & derquantel-sensitive receptors in Xenopus oocytes". Joint Meeting of the 16th Drug Design & Development Seminar (DDDS 2015) and WG4 of COST Action CM1307, held at the Robert Koch Institute, Berlin, Germany, March 16-18, 2015.

R. J. Martin, **M. Abongwa**, A. P. Robertson. "Not just GluCls (Glutamate-gated Chloride channels): abamectin has potent effects on nicotinic acetylcholine receptors of nematode parasites". Proceedings of the 59th Annual Meeting of the American Association of Veterinary Parasitologists (AAVP), held at The Curtis Hotel, Denver, Colorado, USA, July 26-29, 2014. pp81. Published as an Oral Communication in *Journal of Veterinary Pharmacology and Therapeutics* (2015), **38**: 42-43.

Alan Robertson, **Melanie Abongwa**, Samuel Buxton, Elise Courtot, Claude Charvet, Cedric Neveu, Richard Martin. "Characterization of a homomeric nicotinic acetylcholine receptor, *Ascaris suum* ACR-16, in *Xenopus laevis* oocytes". Proceedings of the 59th Annual Meeting of the American Association of Veterinary Parasitologists (AAVP), held at The Curtis Hotel, Denver, Colorado, USA, July 26-29, 2014. p. 82.

Shivani Choudhary, **Melanie Abongwa**, Samuel K. Buxton, Ciaran J. McCoy, Alan P. Robertson, Saurabh Verma, Richard J. Martin. "*Ascaris suum* ACR-21 forms a homomeric nicotinic acetylcholine receptor with novel pharmacology". Proceedings of the 59th Annual Meeting of the American Association of Veterinary Parasitologists (AAVP), held at The Curtis Hotel, Denver, Colorado, USA, July 26-29, 2014. p. 54.

Charvet, C., Buxton, S. K., Neveu, C., Cabaret, J., Cortet, J., Peineau, N., **Abongwa, M**., Robertson, A. P., Martin, R. J. (2014). "Nicotinic acetylcholine receptors: expression in oocytes and functional diversity in parasitic nematodes". Presented at NemaTours: Bringing worms together, Tours, FRA (2014-07-17 - 2014-07-18). [http://prodinra.inra.fr/record/276369].

M. Abongwa, S. K. Buxton, S. Verma, A. P. Robertson and R. J. Martin. "Pharmacological and electrophysiological characterization of *Ascaris suum* homopentameric nicotinic acetylcholine receptors in *Xenopus laevis* oocytes". Society of Toxicology (SOT) 53rd Annual Meeting & ToxExpo™, Phoenix Convention Center, Phoenix, Arizona, USA, March 23-27, 2014.

M. Abongwa, S. K. Buxton, C. L. Charvet, C. Neveu, A. P. Robertson and R. J. Martin "Characterization of the *Ascaris suum* homomeric nicotinic acetylcholine receptor, ACR-16, in *Xenopus laevis* oocytes". International Symposium on Anthelmintics: From Discovery to Resistance, held at the Fort Mason Conference Center, San Francisco, California, USA, February 5-7, 2014. p. 27.

R. J. Martin, **M. Abongwa**, S. K. Buxton and A. P. Robertson "Effects of paraherquamide, derquantel, and the macrocyclic lactone, abamectin, on native and expressed receptors of nematode parasites". International Symposium on Anthelmintics: From Discovery to Resistance, held at the Fort Mason Conference Center, San Francisco, California, USA, February 5-7, 2014. 7A.

Alan P Robertson **Melanie Abongwa**, Samuel K Buxton, Sreekanth Puttachary, Nathan Romine, Saurabh Verma, Adrian J Wolstenholme, and Richard J Martin "Cholinergic receptors on the *Ascaris suum* pharynx". International Symposium on Anthelmintics: From Discovery to Resistance, held at the Fort Mason Conference Center, San Francisco, California, USA, February 5-7, 2014. 6D.

M. Abongwa, S. K. Buxton, S. Verma, A. P. Robertson and R. J. Martin "Pharmacological and electrophysiological characterization of *Ascaris suum* homopentameric nicotinic acetylcholine receptors in *Xenopus laevis* oocytes". Central States Regional Chapter Of The Society of Toxicology (CS-SOT) Annual Fall Meeting, held at the Gateway Center and Hotel, Ames, Iowa, USA, October 10-11, 2013. p. 33.

AWARDS

2017 (i) Iowa State University Graduate College, Research Excellence Award, Spring 2017.

(ii) Iowa State University Interdepartmental Toxicology High Impact Publication Award for the academic year 2016 – 2017 (Publication: **Melanie Abongwa**, Samuel K Buxton, Elise Courtot, Claude L Charvet, Cédric Neveu, Ciaran J McCoy, Saurabh Verma, Alan P Robertson and Richard J Martin (2016) "Pharmacological profile of Asu-ACR-16, a new homomeric nAChR widely distributed in Ascaris tissues" British Journal of Pharmacology 173(16): 2463-77. doi: 10.1111/bph.13524).

2016 (i) Schlumberger Foundation Faculty for the Future PhD Fellowship Renewal for the academic year 2016 – 2017 (Amount Awarded: $36,000).

(ii) Iowa State University Graduate and Professional Student Senate (GPSS) Research Award.

(iii) Iowa State University Graduate and Professional Student Senate (GPSS) Professional Advancement Grant (PAG) Award.

2015 (i) Schlumberger Foundation Faculty for the Future PhD Fellowship Renewal for the academic year 2015 – 2016 (Amount Awarded: $43,000).

(ii) American Society of Tropical Medicine and Hygiene (ASTMH) Young Investigator Award – 1st Place Winner for Poster and Oral Presentations.

(iii) Society of Toxicology (SOT) – Drug Discovery Toxicology Specialty Section (DDTSS) Emil A. Pfitzer Award – 3rd Place Student Poster Contest.

(iv) Burroughs Wellcome Fund Collaborative Research Travel Award – University of California San Francisco, January 10 – February 14, 2016.

(v) Iowa State University College of Veterinary Medicine (CVM) Travel Award.

(vi) Iowa State University Graduate and Professional Student Senate (GPSS) Professional Advancement Grant (PAG) Award.

2014 (i) Schlumberger Foundation Faculty for the Future PhD Fellowship for the academic year 2014 – 2015 (Amount Awarded: $22,684).

(ii) Toxicologists of African Origin (TAO) Graduate Student Travel Award to attend the Society of Toxicology (SOT) 53rd Annual Meeting in Phoenix, Arizona, USA.

2012: Three-year Miller Fellowship, Iowa State University, Ames, USA.

FUNDING

2016-2017	Schlumberger Foundation Faculty for the Future Program. Amount Awarded $36,000.
2015-2016	Schlumberger Foundation Faculty for the Future Program. Amount Awarded $43,000.
2014-2015	Schlumberger Foundation Faculty for the Future Program. Amount Awarded $22,684.
2015	Burroughs Wellcome Fund Collaborative Research Travel Award. Amount Awarded $1,500.
TOTAL	**$103,184**